Caged Phosphopeptides and Phosphoproteins: Agents in Unraveling Complex Biological Pathways

by

Deborah Maria Rothman

S. B., Biochemistry, University of Chicago, 2000
A. B., Biology, University of Chicago, 2000

Submitted to the Department of Chemistry
in Partial Fulfillment of the Requirements for the
Degree of Doctor of Philosophy

at the

Massachusetts Institute of Technology

June 2005

Signature of Author: _____

Department of Chemistry
May 9, 2005

Certified by: _____

Barbara Imperiali
Class of 1922 Professor of Chemistry and Professor of Biology
Thesis Supervisor

Accepted by: _____

Robert W. Field
Haslam and Dewey Professor of Chemistry
Chairman, Departmental Committee on Graduate Students

This doctoral thesis has been examined by a committee of the Department of Chemistry as follows:

Timothy F. Jamison _____
Chairman
Professor of Chemistry

Barbara Imperiali _____
Thesis Supervisor
Class of 1922 Professor of Chemistry and Professor of Biology

Douglas A. Lauffenburger _____
Whitaker Professor of Biological Engineering, Professor of Chemical Engineering and Biology

Caged Phosphopeptides and Phosphoproteins: Agents in Unraveling Complex Biological Pathways

by

Deborah Maria Rothman

Submitted to the Department of Chemistry
on May 9, 2005 in Partial Fulfillment of the
Requirements for the Degree of Doctor of Philosophy

ABSTRACT

Within cellular signaling, protein phosphorylation is the post-translational modification most frequently used to regulate protein activity. Protein kinases and phosphoprotein phosphatases generate and terminate these phosphoryl signals, respectively. Chemical approaches for studying protein phosphorylation and the roles of phosphoproteins include photolabile caged analogs of bioactive species. Caged compounds are ideal chemical probes for studying cellular signaling because they afford researchers spatial and temporal control over the release of targeted effector molecules. Ligands or proteins involved in signal transduction can be chemically caged and subsequently irradiated to release a concentration burst of a specific species, allowing the downstream effects to be monitored without disrupting other aspects of the system.

The syntheses and applications of caged phosphopeptides and phosphoproteins have been developed and detailed within this thesis. Two methods to synthesize 1-(2-nitrophenyl)ethyl caged phosphopeptides were developed. These peptides demonstrated good quantum yields of uncaging as compared to literature values of other *ortho*-nitrobenzyl derived caged compounds. A study in which these caged phosphopeptide tools yielded seminal information about the 14-3-3 protein family's involvement in cell cycle control successfully demonstrated the unique utility of these probes. Furthermore, the synthesis that allowed the extension of the nonsense codon suppression methodology to include caged phosphoproteins was developed. The three most commonly phosphorylated amino acids (serine, threonine, and tyrosine) were each incorporated into a test protein in their caged phosphorylated form. Toward studying cell motility, caged phosphoserine was incorporated into position 153 of mVASP for use in live cell assays.

Thesis Advisor: Barbara Imperiali
Title: Class of 1922 Professor of Chemistry and Professor of Biology

Acknowledgements

"I'm gonna tell you a story; I'm gonna tell you about my town
I'm gonna tell you a big bad story, baby; Aww, it's all about my town..."

First and foremost, I thank Barbara Imperiali for being nothing less than a wonderful Ph. D. advisor. Thank you for welcoming me to the lab, giving me a place to learn chemistry and science as a whole, teaching me to discover the answers to my many questions, and trusting me to establish a project within the group. It has been a challenging adventure that knowing what I know now, I would choose to do all over again. Also, thank you for being so extremely supportive throughout the post-graduate search.

The Imperiali lab is an incredibly encouraging learning environment; the spectrum of skills members have and their enthusiasm for science and life have turned all the inevitable rough patches of research into learning experiences I won't soon forget. I've seen the lab turnover quite a bit, and I hope I can acknowledge everyone appropriately. From day one, I thank Kathy Franz for introducing me to the lab and getting me started on my first peptide- of course, it was insoluble. I thank Harm Brummerhop for introducing me to the wonderful world of synthetic chemistry, rainbow colored columns, and turning a dark bay into a techno-dance party, liquid nitrogen and all. For answering my thousands of first-year questions, I thank Kevin McDonnell, Dierdre Pierce, Jen Ottessen, Rob Dempski, Mayssam Ali, Mike Torrice, Mark Nitz, and Vladimir Goncharov. I thank Carlos Bosques and Maria Ufret for their senior wisdom and other pieces of fun I can't forget: the mad cow on Eugenio's desk, the "laser," and so much time in the dark HPLC room. For creating a lab community that is as good as it gets, I thank the more current lab members: Eranthie Weerapana for being my "twin" all these years; Seungjib Choi for keeping everyone safe; Mary O'Reilly for her ability to wow everyone with her Irish genes; Christina Carrigan for her energy and empathy for bad backs; Jebrell Glover for all the biochemical tips and all the song lyrics; Guofeng Zhang for great political discussions; Elvedin Luckovic for being a fabulous dancing buddy; Langdon Martin for his creative slides and Red Sox spirit; Galen Loving for his genuine curiosity; Christian Hackenberger for all the great chocolate; Bianca Sculimbrene for her eagerness to learn biology, her Red Sox spirit, and her contagious laugh; Matthieu Sainlos for warming up to the crazy Americans in the lab; Dorra Carrico for always bringing a smile to the lab; Debby Pheasant for great lunchroom conversations and a fabulous first name; Ryu Yoshida for his dedication to the lab and learning; Becca Maglathlin for being wise and fun beyond her years. To Mark Chen and Andrew Dutton, best of luck to you newbies. Our lab would not function well if it wasn't for Elizabeth Fong; thank you for answering all the inevitable questions that did not have much to do with chemistry and always sharing a warm smile.

In the realms of Chemistry and Biology labwork, I have been fortunate to have some great collaborators. Thanks to Professor Michael Yaffe for a collaboration that not only provided proof-of-concept for our new tools, but also allowed us to make some new discoveries about the 14-3-3 family. Thank you, Justine Stehn, for being so excited about working on the project and constantly pushing it forward. Thank you, Cokey Nguyen, for taking over from Justine and working with my precious peptide samples, and also being a friend outside the lab. Thanks to Professor Dennis Dougherty and his entire group who welcomed me to CalTech to learn about nonsense codon suppression techniques. A special thanks to James Petersson who worked with me in the trenches to get caged phosphoserine into protein, especially since it seemed to be during the apocalypse. Thanks to Professor Frank Gertler for starting a collaboration with mVASP; I hope that the project continues until cells are walking under the control of light. Also thanks to Melanie Barzik for answering many questions along the way. Of course, I'd like to thank my thesis committee members, Professor Timothy Jamison and Professor Douglas Lauffenburger, for being here on this significant day. A special thank you to Tim for following my progress through the years, and for offering advice when I needed it most.

"Yeah, down by the river; Down by the banks of the river Charles (aw, that's what's happenin' baby)
That's where you'll find me; Along with lovers, fuggers, and thieves (aw, but they're cool people)
Well I love that dirty water; Oh, Boston, you're my home (oh, you're the Number One place)..."

I have been extremeley privaleged to meet three people that have blurred the line between lab-mate and great friend. Eugenio Vázquez, thank you for being a partner on the caging project, but more than that, thank you for being like a big brother to me. Thanks for always supporting me and encouraging me in lab and

in life, and for telling me stories that maybe I did not need to hear, but always made me smile. Beth Vogel, thank you for being so patient when learning from me, working with me on the caging project, and being a genuinely happy person. I've had so much fun running into lab to talk about the "Sox last night," among many other things. Thanks for being yourself, a definite bright spot in the group. And to my last partner in crime in the lab, thank you, Melissa Shults, for being my comrade in everything else. Thank you for talking world politics, Red Sox, the Beatles and music in general, food and wine, and of course chemistry shop. I can't imagine what the past years would have been like without you. Best of luck on the left coast!

"Frustrated women (I mean they're frustrated); Have to be in by twelve o'clock (oh, that's a shame)
But I'm wishin' and a-hopin, oh; That just once those doors weren't locked (I like to save time for my baby to walk around); Well I love that dirty water; Oh, Boston, you're my home (oh, yeah)..."

Before I started calling Boston my home, there was Bethesda and Chicago. Thank you, mom and dad, for supporting me throughout the years. From Bradley Hills to Whitman to Chicago and to M. I. T., thanks for allowing me to figure out what I wanted to pursue, and supporting me in every way that you could; I love you. Thank you, Ari, for making the wonderful analogy between chemistry and laundry, but even more for being my big brother when I needed it most. Momom and Popop, if you were still here, I know you would be proud; thank you for your enthusiasm about everything I ever did. Thank you Aunt Mary, Aunt Sis, and of course the other resident scientist in the family, Uncle Albert, for your devotion and support through all the years.

From Maryland to Boston and a few places in between, I thank Katie Straus who has been a great friend for so many years. Thanks for always being there at the most important times, no matter how different our "languages" are and how many miles apart we may have been. Here in Boston, I thank the girls of the BAB for the five fun and crazy years we have had. A special thanks to Erika Swanson for understanding me and being a great friend through all the tough times and the great times. I can't wait to see you in my old stomping ground, Chicago! From my days in Chicago, I thank Rachel Knipe, Clara Park, and Meredith Fishbane for being great friends in college and beyond. And a gigantic thank you to Barbara Blank who is the definition of a loyal friend. Thank you for being my "bickering sister" since college and thank you for being a huge support system even from hundreds of miles away for the past five years. All my best to you and JJ, and I hope our visits are more frequent in the coming years.

"Because I love that dirty water; Oh, oh, Boston, you're my home (oh, yeah)..."

I didn't think it was possible to fall in love with a city, but that was my gut reaction to Boston when I hopped on the T at the old Airport station five years ago. "This is where I want to be." So, thank you, Boston, for surpassing my expectations for an amazing city. I plan to be running the bridge loops for years to come. Within Boston, I thank the Red Sox teams through 2003 who taught me what it felt to be a traditional Red Sox fan, and the 2004 team that made the most unbelievable comeback in sports history to then win the World Series while causing massive sleep deprivation throughout Boston proper. Along the sports theme, another thank you to the Patriots and Tom Brady for roping me into football. I may have starting watching for one reason, but now I can say I watch for the game... sort of. In any case, Boston is a great city for many reasons, and I think the Standells sum it up well:

"Well, I love that dirty water (I love it, baby); I love that dirty water (I love Baw-stun)
I love that dirty water (Have you heard about the Strangler?); I love that dirty water (I'm the man, I'm the man); I love that dirty water (Owww!); I love that dirty water (Come on, come on)"

- Dirty Water
THE STANDELLS

Table of Contents

List of Figures

Chapter 1

Chapter 2

Chapter 3

Chapter 4

Chapter 5

List of Schemes

List of Tables

Abbreviations/Nomenclature

Standard one and three letter codes are used for the naturally occurring amino acids. Standard one-letter codes are used for nucleotides.

Abbreviation	Definition
4PO-	4-pentenoyl
6XHis-tag	Protein purification tag comprising 6 histidine residues
ahx	Aminohexanoic acid
AM-PS	Aminomethyl-polystyrene
cp	Caged phospho-
C-terminus	The carboxylic acid end of a polypeptide chain or protein
DNA	Deoxyribonucleic acid
ESI-TOF MS	Electrospray ionization time of flight mass spectrometry
FACS	Fluorescence-activated cell sorting
FITC	Fluorescein-5-isothiocyanate
Fmoc	N^{α}-fluorenylmethoxycarbonyl
G1 phase	First growth phase in the cell cycle
G2 phase	Second, shorter growth phase in the cell cycle
GST	Glutathione S-transferase
HPLC	High performance/pressure liquid chromatography
In vitro	Performed outside the context of the cell; lit: in glass
In vivo	Performed in the context of living cells; lit: in life
ITC	Isothermal calorimetry
M phase	Mitosis; cell phase in which two identical daughter cells divide from one parent cell
MALDI-TOF MS	Matrix assisted laser desorption ionization time of flight mass spectrometry
MAS-NMR	Magic angle spinning nuclear magnetic resonance
mRNA	Messenger RNA
mVASP	Murine vasodilator stimulated phosphoprotein
nAChR-α	Nicotine acetylcholine receptor α-subunit

N-terminus	The amino end of a polypeptide chain or protein
NVOC	6-nitroveratryloxy carbamate
RNA	Ribonucleic acid
S phase	Synthesis phase; cell cycle phase in which DNA is copied
SDS-PAGE	Sodium dodecyl-sulfate polyacrylamide gel electrophoresis
SPPS	Solid phase peptide synthesis
tRNA	Transfer RNA
UV-A	Ultraviolet A irradiation, 320 nm ≥ λ ≥ 400 nm
UV-B	Ultraviolet B irradiation, 280 nm ≥ λ ≥ 320 nm
Φ	Quantum yield of uncaging

List of Spectra

Chapter 2

Chapter 4

Chapter 1
Introduction

Portions of this chapter have been submitted for publication to *Trends in Cell Biology.*

1-1. General Introduction

Cellular signaling pathways integrate the actions of a myriad of ligands, substrates and proteins that comprise extremely complex networks of forward signals, feedback loops, and modulatory actions. Defining the spatial and temporal roles of the participants in the signaling cascades of living systems is a major challenge in cell biology. Since signaling molecules are in a constant state of flux, experimental approaches that afford information on the temporal and spatial dynamics of the components are extremely desirable. In this context, chemically-driven strategies including small molecule inhibitors and activators as well as biotic and abiotic chemosensors provide a powerful complement to the robust genetics-based methods that have enabled the identification of numerous pathways in living cells.[1] Chemical probes for the study of signal transduction networks can be of either exogenous or endogenous origin. Endogenous probes, including designed sensors based on the *Aequoria victoria* fluorescent proteins (AFPs), are expressed and used within cells, while exogenous probes are prepared *ex vivo* and may be introduced into living cells *via* microinjection, transfection, or through utilization of protein transduction domains.

Within cellular signaling, protein phosphorylation is the most abundant post-translational modification for the regulation of protein activity.[2, 3] Protein kinases and phosphoprotein phosphatases generate and terminate these phosphoryl signals, respectively.[4] Chemical approaches for studying protein phosphorylation and the roles of phosphoproteins include photolabile caged analogs of bioactive species (Figure 1.1).

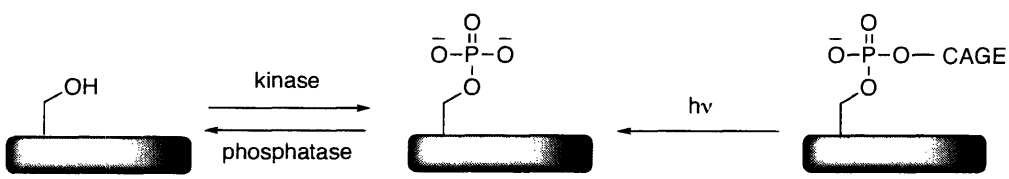

Figure 1.1. Phosphoregulation of proteins. Kinases append phosphoryl groups to hydroxyl side chains, while phosphatases remove them. Alternatively, a caging group on a phosphate can be removed with light to reveal the phosphoprotein.

Caged compounds are ideal chemical probes for studying cellular signaling because they afford researchers spatial and temporal control over the release of targeted effector molecules. Ligands or proteins involved in signal transduction can be chemically caged and subsequently irradiated to release a concentration burst of the specific species, allowing the downstream effects to be monitored without disrupting other aspects of the system. For a brief discussion of caging and the history of the technique, please see Section 1-7. The most frequently implemented caging groups in biological experiments are derived from the *ortho*-nitrobenzyl protecting group, discussed in further detail below (Section 1-8). Other caging groups used in biological studies include hydroxyphenacyl derivatives, coumarins, and cinammic acid derivatives.[5-9] Several examples of recently developed caged signaling molecules are discussed here with an emphasis on those used for studying phosphorylation in signal transduction.

1-2. Caged Small Molecules, Peptides, and Proteins

More than two decades have passed since the original caging experiments of ATP and divalent cations were published.[10-12] Currently, multiple reports of caged neurotransmitters, peptides and full-length proteins are present in the literature. These studies revealed information in space and time domains inaccessible by other methods.[13-17]

Both caged L-glutamic acid[18] and caged D-aspartic acid[19] have been synthesized and used to study the effects of each stimulant on its cognate receptor. The molecular mechanism of the high affinity glutamate transport process is difficult to study with traditional rapid solution exchange techniques due to poor time resolution. It was found that L-glutamic acid caged on the γ-carboxylate with the α-carboxynitrobenzyl moiety had desirable photochemical properties with a half-life of 21 μs and quantum yield of 0.14.[18] Taken together, these parameters allowed the time-resolved study of the activation of glutamate receptors, which have a lifetime for the "open" species on the 1 ms timescale. In a further example of caged neurotransmitters, D-aspartic acid was caged in order to study the effect of D-aspartic acid on glutamate transport, which is a highly pH dependent process. The rate and quantum yield of uncaging is also dependent on pH. An α-carboxynitrobenzyl caged D-aspartic acid was synthesized that had good uncaging kinetics at various pH values which was valuable for further synaptic studies.[19]

Caged peptides can be used as masked inhibitors of protein functions that are regulated by phosphorylation. After introduction of a caged inhibitory peptide, the steady state of the

system is not perturbed; therefore, the immediate downstream effects of sequestering a targeted protein can be monitored upon uncaging. In a study on eosinophil cell motility two caged tyrosine peptide inhibitors of myosin light chain kinase (MLCK) were employed to reveal that MLCK is globally central to whole cell movement.[20] Flash photolysis allowed the peptides to rapidly sequester the MLCK in the system, and it was observed that cell motility significantly decreased, thus demonstrating that MLCK is essential in cell migration signaling. Whereas former studies had been performed on the minute to hour timescale, the observations described were made in the previously inaccessible time domain of seconds.

Several amino acid side chains in full-length protein have been caged using various methods. Approaches range from non-specific labeling of nucleophilic residues to cysteine scanning-mutagenesis trials to site-specific incorporation of caged amino acids (see reviews 13, 14, 16, 17). In a more recent study, thymosin β4 (Tβ4) was non-specifically caged on lysine residues, and observations from studies with its use were compiled to formulate a mechanical model of cell turning in locomoting keratocytes (Figure 1.2).[21] Computer simulations predicted the concentration of locally uncaged Tβ4 necessary within a locomoting cell to cause a biological response without loss of effect due to diffusion. Indeed, upon local photolytic release of Tβ4, cell movement changed dramatically and appeared temporarily imbalanced relative to control cells. Using caged Tβ4 allowed both spatial and temporal release of the protein, yielding new information about its functional role in motile cells.

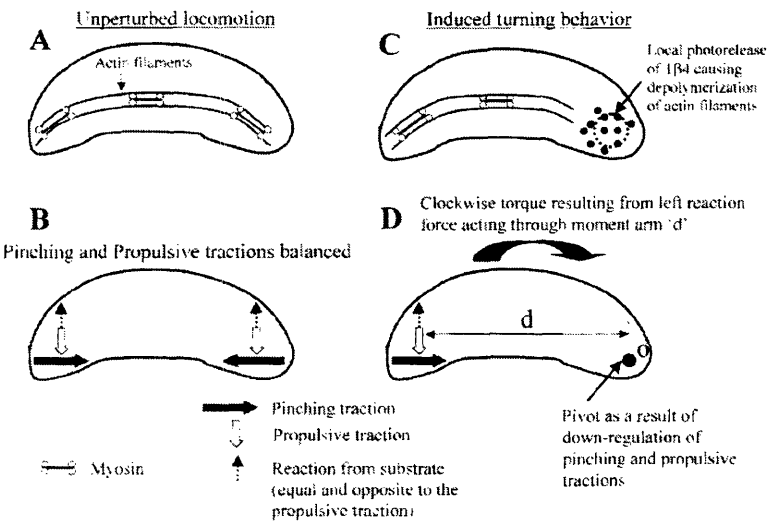

Figure 1.2. Schematic of the mechanical consequences of local photorelease of Tβ4 (**C**, **D**) compared to unperturbed locomotion (**A**, **B**). Proposed model for the turning of keratocytes in response to photoreleased Tb4 at the wing. Cell turning is the result of a clockwise torque generated by substrate reaction to unbalanced propulsive traction. See reference 21.

1-3. Caged Phosphopeptides

As mentioned above, essential early studies demonstrated that simple caged peptides allow phenotypic observations to be made in the previously inaccessible time domain of seconds.[13, 20] More recently, methods to synthesize caged phosphopeptides have been developed for the purpose of studying phosphopeptide-binding domains (Chapter 2).[22, 23] With these new chemical tools, the global temporal function of the entire 14-3-3 family on cell cycle regulation was examined (Chapter 3).[24] Photoliberation of a phosphopeptide designed to bind to all isoforms of 14-3-3 caused synchronized cells to exhibit several unique characteristics compared to control cells: increase in programmed cell death, loss of G2/M-phase progression, and loss of S-phase checkpoint function (in cells with DNA damage) (Figure 1.3). The temporally controlled release of the caged phosphopeptide enabled the observation that 14-3-3 is necessary for mitotic entry of normally cycling cells and it is essential for S-phase checkpoint function in cells with DNA damage.

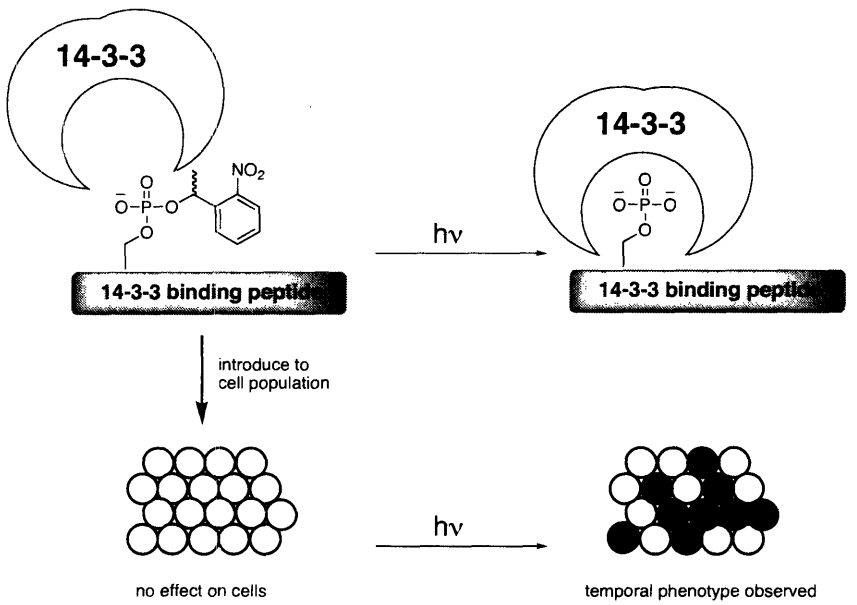

Figure 1.3. Caged phosphopeptide allows temporal control over the release of an inhibitory peptide. Before photolysis, the peptide cannot bind 14-3-3. After brief irradiation, the peptide binds all 14-3-3 and downstream signaling events are observed *in vivo*.

1-4. Caged Constitutively Active Kinase Substrate

Some kinase substrates are inactivated by phosphorylation and activated by dephosphorylation. The LIM-kinase substrate cofilin is one such protein: in the unphosphorylated form, cofilin binds to F-actin and severs the filaments to create barbed ends and modulate cell motility. LIM-kinase phosphorylates serine-3 of cofilin to render the protein inactive.[25] Recently, a constitutively active mutant, cofilin Ser3Cys, was prepared and it was demonstrated that exposure of this mutant to F-actin caused filament severing and

depolymerization *in vitro*. In order to regulate the cofilin activity, the mutant protein was caged *via* selective chemical modification with the α-carboxynitrobenzyl group at the unique cysteine at position 3. In these studies, the α-carboxylate substituent in the caging moiety enhanced the efficiency of uncaging while simultaneously mimicking the inactive phosphorylated cofilin (Figure 1.4). In the presence of caged cofilin Ser3Cys, F-actin was as stable as in the control system. However, upon irradiation, 80% of severance activity was restored to cofilin Ser3Cys. This caged mutant protein was further evaluated in live cells and the studies revealed that active cofilin is essential for many aspects of cell motility.[26] Cofilin aided in G-actin polymerization *in vivo*: global uncaging of cofilin Ser3Cys increased free barbed ends, F-actin content, and cell locomotion, while local uncaging generated lamellipodia and determined the direction of cell migration. Since LIM-kinase cannot phosphorylate the Ser3Cys mutant, the effect of cofilin persisted for the duration of the cell monitoring. For these studies, this effect was advantageous since the active species is the unphosphorylated protein. However, for situations in which the phosphorylated species is the active form of the protein, it is desirable to have access to the caged phosphoprotein.

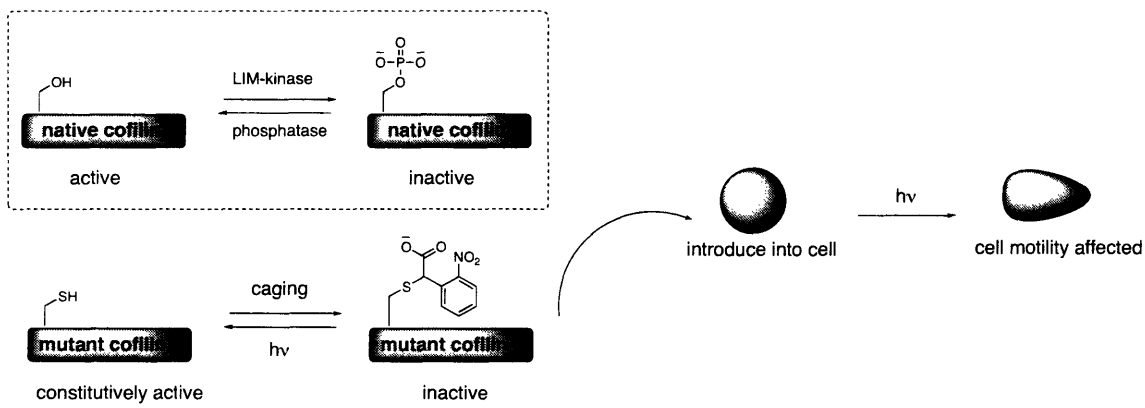

Figure 1.4. Caged mutant cofilin (Ser3Cys) reveals a role for cofilin during cell motility.

1-5. Caged Phosphothioproteins

Thiophosphoryl derivatives of serine, threonine and tyrosine can act as phospho-amino acid analogs in biological studies of protein phosphorylation. Thiophosphoryl groups demonstrate distinct properties in cellular systems: they are more nucleophilic and more resistant to hydrolysis by phosphatases compared with native phosphoryl groups.[27] Recent work has extended the strategy for caging thiophosphopeptides to the preparation of full-length caged

thiophosphoproteins.[6, 7, 28] The semi-synthetic approach involves thiophosphorylation of a serine, threonine, or tyrosine residue using an appropriate kinase in the presence of ATP(γ)S and a thiophilic divalent cation, such as Co^{2+} (Figure 1.5).[7] The caging group is then introduced by taking advantage of the nucleophilicity of the thiophosphate sulfur to displace bromide from the electrophile. In these studies, it was found that the hydroxyphenacyl caging group had superior photosensitivity (Box 2) to the *o*-nitrobenzyl group on thiophosphate.[7] At the protein level, a caged thiophosphothreonine-197 variant of PKA was prepared by semi-synthesis and then activated via UV irradiation.[6] Upon uncaging, 85–90% of protein activity was restored, corresponding to a ~15-fold increase in activity over the caged precursor, which is significant for potential biological studies. Caged thiophosphoproteins are useful reagents for studying signal transduction due to the stability of the thiophosphates towards endogenous phosphatases. However, the enzyme-catalyzed thiophosphorylation reaction is not general and multiple kinases and divalent cations must be screened for the semi-synthesis of each new caged peptide or protein target.

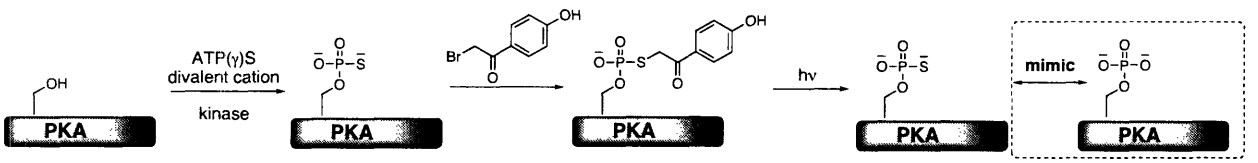

Figure 1.5. Caged thiophosphoproteins mimic phosphoproteins upon uncaging.

1-6. Caged Phosphoproteins

Recently, expressed protein ligation and semi-synthesis has been used to prepare the caged phosphoprotein Smad2, which was caged on two phosphoserines at the C-terminus (Ser 465 and Ser 467) (Figure 1.6).[29] Under native conditions, transforming growth factor β (TGF-β) phosphorylates two serine residues on Smad2, which then causes disengagement from the cytosolic retention factor SARA and allows homotrimerization of Smad2 and nuclear uptake. The caged phospho-Smad2 binds to SARA and cannot homotrimerize. However, upon brief and intense irradiation, the phospho-Smad2 is uncaged and released from SARA thereby initiating homotrimerization and nuclear localization.[29] These experiments demonstrate the application of native chemical ligation for the preparation of caged phosphoproteins that are amenable to semi-synthetic strategies.

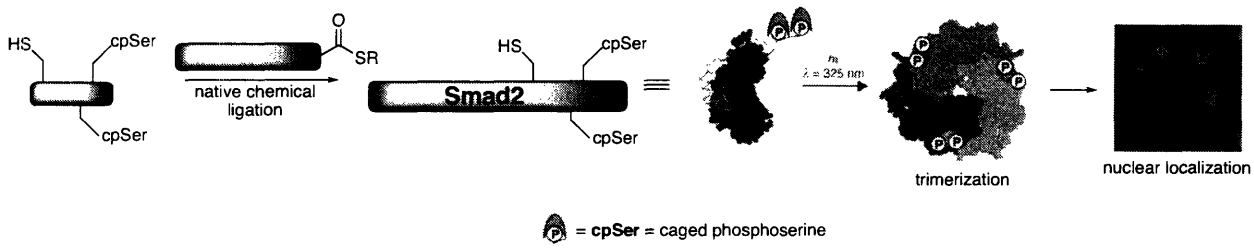

Figure 1.6. Caged phospho-Smad2 acts like native phospho-Smad2 after UV-irradiation. See reference 29.

An alternative general approach for the synthesis of caged phosphoproteins has recently been introduced which allows for the replacement of a single residue in native proteins with a caged phospho-amino acid (Chapter 4).[30] A novel phosphitylation reagent enabled the chemical synthesis of an appropriately protected amino acid derivative for the generation of an amino-acyl tRNA charged with the caged phospho-amino acid. Incorporation of the unnatural amino acid into proteins was then accomplished *via* the nonsense codon suppression methodology using an *in vitro* translation system. This strategy was used for the semi-synthesis of the cell motility protein mVASP with caged phosphoserine at position 153 (Chapter 5). Gel shift analysis demonstrated that the caged phosphoprotein behaves as the unphosphorylated protein, and upon UV irradiation the uncaged protein migrates adjacent to the phosphorylated control. This directed approach should allow for the substitution of any serine, threonine, or tyrosine residue in full-length proteins with caged phosphorylated analogs provided that the *in vitro* translation efficiency is acceptable.[30] The recent developments in the availability of full-length caged phosphoproteins, in addition to the aforementioned caged analogs, should further advance studies exploiting the caging technology in the realm of signal transduction.

1-7. History and Requirements of Caging Groups

Caged compounds are molecules that include a photolabile mask on an essential functional group. With UV irradiation the mask is removed and the liberated molecule can exert its effect on the system.[10] Photolabile protecting groups have been in use in organic synthesis for many years.[31] Due to the hydrophobicity of photolabile groups, they were first used in biological systems to aid in cell membrane permeation of caged nucleotide analogs which could subsequently be uncaged in living cells.[32] The term "caging" was coined when a photolabile protecting group was placed on the γ-phosphate of ATP. The ability of the caged compound to

release ATP upon irradiation (be "uncaged") was characterized by Na,K-ATPase consumption and Na^+ efflux from cells via the Na:K pump.[10] The caged ATP could not be hydrolyzed by the Na,K-ATPase until after illumination to remove the caging group. Additionally, caged ATP had no effect on the Na:K pump in cells until after photolytic removal of the caging group. This study set the precedent for the future of caging in biological studies. In addition to control over the release of the effector molecule, caged compounds enable complete intracellular distribution of the target compound,[14] thus allowing each cell to serve as its own control (before and after photolysis).[20] Use of caged compounds circumvents genetic compensation effects often observed in single knock-out studies.[24]

There are several key requirements of a caged compound to be successful in biological studies: (*i*) the caged compound should neither agonize nor antagonize the system, (*ii*) after irradiation, the compound should be released rapidly and in high yield, (*iii*) the photo-byproducts should be inert within the system, and (*iv*) the photolytic conversion must be accessible in an intracellular environment such that the downstream events can be immediately monitored.[10] Other factors to consider include the quantum yield of uncaging, the wavelength of excitation, and the extinction coefficient of excitation (see below). A caging group can mask a functional group through two different strategies: steric bulk and electronic induction. The steric bulk strategy involves using a caging group to spatially block an interaction prior to photoliberation. The electronic induction strategy employs a caging group to withdraw or distribute electron density such that a key interaction cannot take place before photolysis. A study in which caged cation chelators were synthesized to tightly bind divalent calcium upon irradiation illustrates these two different strategies.[12]

1-8. Caging Groups and Photophysical Properties

The most commonly used caging groups in biological studies are based on the *ortho*-nitrobenzyl moiety. The *o*-nitrobenzyl group is inert within living cells, has a good quantum yield of uncaging (Φ) on the microsecond-millisecond timescale, and can be excited with near-visible UV light (> 350 nm), which does not cause radiative damage to cells. Additionally, when attached to biological molecules, *o*-nitrobenzyl compounds and the corresponding photo-byproducts are water-soluble at physiological concentrations. Original studies demonstrated that intracellular thiols (e.g., glutathione) act as effective scavenging agents for the nitrososbenzene

photo-byproducts.[10, 33] The proposed mechanism of photolytic release for *o*-nitrobenzyl ethers is shown in Scheme 1.1 where **X** is the key functional group of the biological effector.[33]

Scheme 1.1. *Photochemical decomposition of* o*-nitrobenzyl caged molecules.*

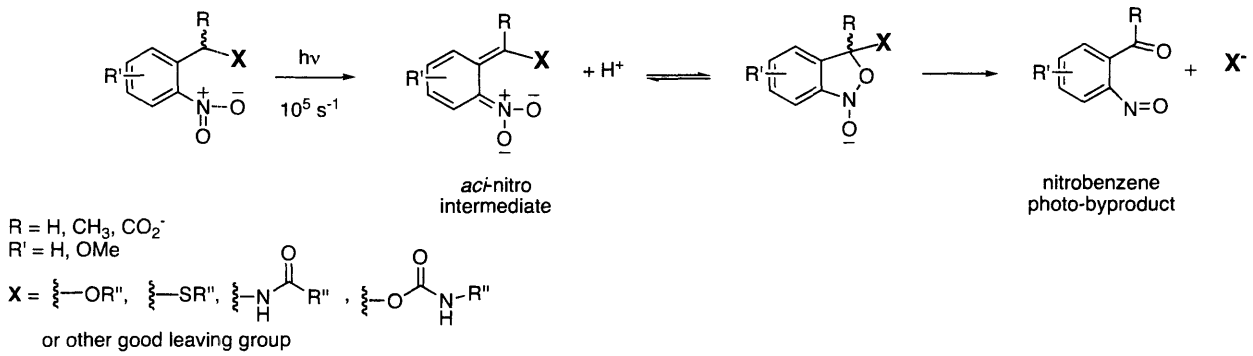

The cyclization and subsequent breakdown of the *aci*-nitro intermediate has been spectroscopically monitored to determine the rate of release of the product. More recent research suggests that hemiketal formation may be involved during the photolytic release of 1-(2-nitrophenyl)ethyl ethers.[34] The released nitroso-acetaldehyde (R = H) was found to be much more reactive in a biological context than released nitroso-acetophenone (R = CH_3),[10] likely due to the higher intrinsic reactivity of the aldehyde toward nucleophiles.

It is significant to note that the quantum yield of uncaging is a measure of photoliberation efficiency and not a measure of the rate of uncaging. The quantum yield describes how many caging groups are released for every photon absorbed by the group. The speed of the breakdown of the excited species to release the effector molecule determines the rate of uncaging. The *o*-nitrobenzyl groups have uncaging rates on the microsecond timescale.[18, 33]

Furthermore, the intensity of the light source can have a significant effect on the apparent rate of uncaging of a sample. For example, a light source sending a large number of photons focused on the sample, such as a laser, will appear to have a faster rate of uncaging than a more diffuse source, such as a UV lamp. The actual rate of the breakdown of the photo-excited state does not change between such circumstances; however, the large number of photons from the laser will proportionally uncage more molecules than the UV lamp, and thus analysis on the minute time scale will appear that the laser is uncaging the sample more quickly.

Another important physical characteristic for selecting a caging group is the product of the quantum yield and the extinction coefficient at the excitation wavelength ($\Phi \bullet \varepsilon$) or the photosensitivity of the caging group.[7] It is not uncommon for a caging group to have an excellent

ε and a poor Φ, and vice versa. Therefore, the product of these values is critical to selecting an efficient caging group.

1-9. Selection of the 1-(2-Nitrophenyl)ethyl-Cage for Phosphopeptides and Phosphoproteins

For the purpose of synthesizing caged phosphopeptides and phosphoproteins, the *o*-nitrobenzyl derivative 1-(2-nitrophenyl)ethyl moiety was chosen. There was abundant literature precedent for use of the *o*-nitrobenzyl derivatives at the time of the initial syntheses. The 1-(2-nitrophenyl)ethyl group was selected because it releases a ketone rather than an aldehyde as a photo-byproduct. Groups without any substitution at the benzylic position release an aldehyde, which is highly reactive in the cellular environment (as described in Section 1-8). The 1-(2-nitrophenyl)ethyl group has a maximum absorption at λ = 259 nm, with a strong extinction coefficient (ε_{max} = 5,700 $M^{-1}cm^{-1}$).[35] The absorption spectrum is broad, and thus the aromatic group still absorbs significantly at high-end UV (λ = 365 nm). Caging moieties can been modified on the aromatic ring to include electron donating substituents which help to red-shift the absorption band; for example, the 4,5-dimethoxy-2-nitrobenzyl group can be uncaged with light as far out as λ = 420 nm. However, the 4,5-dimethoxy-2-nitrobenzyl derivative suffers from a poorer quantum yield. For the studies described in this thesis, uncaging with λ = 365 nm was sufficient and thus the 1-(2-nitrophenyl)ethyl-caging group, which had strong literature precedent, was employed.

1-10. Embarkment

As the number of tools for studying signal transduction grows, the amount of information mined from the use of these tools is amplified. Currently available tools for studying signal transduction have already provided significant information about the behavior of signaling molecules in cell lysates and in living cells that would not be possible by other means. Chemical tools have the inherent ability to be modified by the researcher; the growing feasibility of the required manipulations to prepare probes is further increasing their availability. Therefore, the advancement of chemical tools to study signaling networks will lend heavily to the foundation of understanding how cells function.

Caged compounds afford a researcher spatial and temporal control over the release of an effector molecule in a biological system, and studies with these probes have just scratched the

surface of understanding cell signaling pathways. In particular, for the study of phosphorylation regulated signaling, caged phosphopeptides and phosphoproteins are tools that will yield a great amount of information about the function of phosphorylated species in real time. Within this thesis, two methods to synthesize caged phosphopeptides are described (Chapter 2). A seminal example in which these tools yielded information about cell cycle control is then described in detail (Chapter 3). The synthesis that allowed extension of the caged phosphopeptide methodolgy to caged phosphoproteins is also described (Chapter 4). Finally, the progress toward application of caged phosphoproteins in live cell assays is also discussed (Chapter 5).

References

(1) Shogren-Knaak, M. A.; Alaimo, P. J.; Shokat, K. M. "Recent Advances in Chemical Approaches to the Study of Biological Systems," *Annual Review of Cell and Developmental Biology* **2001**, *17* 405-433.

(2) Hunter, T. "Signaling—2000 and Beyond," *Cell* **2000**, *100 (1)*, 113-127.

(3) Manning, G.; Whyte, D. B.; Martinez, R.; Hunter, T.; Sudarsanam, S. "The Protein Kinase Complement of the Human Genome," *Science* **2002**, *298* 1912-1934.

(4) Hunter, T. "Protein Kinases and Protein Phosphatases: The Yin and Yang of Protein Phosphorylation and Signaling," *Cell* **1995**, *80 (2)*, 225-236.

(5) In *Dynamic Studies in Biology: Phototriggers, Photoswitches and Caged Biomolecules*; Goeldner, M. and Givens, R., Eds.; John Wiley & Sons, Inc.: Hoboken, New Jersey, **2005**, 584.

(6) Zou, K.; Cheley, S.; Givens, R. S.; Bayley, H. "Catalytic Subunit of Protein Kinase A Caged at the Activating Phosphothreonine," *Journal of the American Chemical Society* **2002**, *124 (28)*, 8220-8229.

(7) Zou, K.; Miller, W. T.; Givens, R. S.; Bayley, H. "Caged Thiophosphotyrosine Peptides," *Angewandte Chemie-International Edition* **2001**, *40 (16)*, 3049-3051.

(8) Furuta, T.; Iwamura, M. "New Caged Groups: 7-substituted Coumarinylmethyl Phosphate Esters," *Methods in Enzymology* **1998**, *291* 50-63.

(9) Turner, A. D.; Pizzo, S. V.; Rozakis, G.; Porter, N. A. "Photoreactivation of Irreversibly Inhibited Serine Proteinases," *Journal of the American Chemical Society* **1988**, *110 (1)*, 244-250.

(10) Kaplan, J. H.; Forbush, B., III; Hoffman, J. F. "Rapid Photolytic Release of Adenosine 5'-Triphosphate from a Protected Analogue: Utilization by Na:K Pump of Human Red Blood Cell Ghosts," *Biochemistry* **1978**, *17 (10)*, 1929-1935.

(11) Kaplan, J. H.; Ellis-Davies, G. C. R. "Photolabile Chelators for the Rapid Photorelease of Divalent Cations," *Proceedings of the National Academy of Sciences, U. S. A.* **1988**, *85 (17)*, 6571-6575.

(12) Adams, S. R.; Kao, J. P. Y.; Tsein, R. Y. "Biologically Useful Chelators that Take Up Ca^{2+} Upon Illumination," *Journal of the American Chemical Society* **1989**, *111 (20)*, 7957-7968.

(13) Shigeri, Y.; Tatsu, Y.; Yumoto, N. "Synthesis and Application of Caged Peptides and Proteins," *Pharmacology and Therapeutics* **2001**, *91 (2)*, 85-92.

(14) Curley, K.; Lawrence, D. S. "Light-Activated Proteins," *Current Opinion in Chemical Biology* **1999**, *3 (1)*, 84-88.

(15) Ellis-Davies, G. C. R. "Development and Application of Caged Calcium," *Methods in Enzymology* **2003**, *360* 226-238.

(16) Marriott, G.; Roy, P.; Jacobson, K. "Preparation and Light-Directed Activation of Caged Proteins," *Methods in Enzymology* **2003**, *360 (Biophotonics, Part A)*, 274-288.

(17) Petersson, E. J.; Brandt, G. S.; Zacharias, N. M.; Dougherty, D. A.; Lester, H. A. "Caging Proteins Through Unnatural Amino Acid Mutagenesis," *Methods in Enzymology* **2003**, *360 (Biophotonics, Part A)*, 258-273.

(18) Wieboldt, R.; Gee, K. R.; Niu, L.; Ramesh, D.; Carpenter, B. K.; Hess, G. P. "Photolabile Precursors of Glutamate: Synthesis, Photochemical Properties, and Activation of Glutamate Receptors on a Microsecond Time Scale," *Proceedings of the National Academy of Sciences, U. S. A.* **1994**, *91 (19)*, 8752-8756.

(19) Grewer, C.; Madani Mobarekeh, S. A.; Watzke, N.; Rauen, T.; Schaper, K. "Substrate Translocation Kinetics of Excitatory Amino Acid Carrier 1 Probed with Laser-Pulse Photolysis of a New Photolabile Precursor of D-Aspartic Acid," *Biochemistry* **2001**, *40 (1)*, 232-240.

(20) Walker, J. W.; Gilbert, S. H.; Drummond, R. M.; Yamada, M.; Sreekumar, R.; Carraway, R. E.; Ikebe, M.; Fay, F. S. "Signaling Pathways Underlying Eosinophil Cell Motility Revealed by Using Caged Peptides," *Proceedings of the National Academy of Sciences, U. S. A.* **1998**, *95 (4)*, 1568-1573.

(21) Roy, P.; Rajfur, Z.; Jones, D.; Marriott, G.; Loew, L.; Jacobsen, K. "Local Photorelease of Caged Thymosin Beta4 in Locomoting Keratocytes Causes Cell Turning," *Journal of Cell Biology* **2001**, *153 (5)*, 1035-1048.

(22) Rothman, D. M.; Vazquez, M. E.; Vogel, E. M.; Imperiali, B. "General Method for the Synthesis of Caged Phosphopeptides: Tools for the Exploration of Signal Transduction Pathways," *Organic Letters* **2002**, *4 (17)*, 2865-2868.

(23) Rothman, D. M.; Vazquez, M. E.; Vogel, E. M.; Imperiali, B. "Caged Phospho-Amino Acid Building Blocks for Solid-Phase Peptide Synthesis," *Journal of Organic Chemistry* **2003**, *68 (17)*, 6795-6798.

(24) Nguyen, A.; Rothman, D. M.; Stehn, J.; Imperiali, B.; Yaffe, M. B. "Caged Phosphopeptides Reveal a Temporal Role for 14-3-3 in G1 Arrest and S-Phase Checkpoint Function," *Nature Biotechnology* **2004**, *22 (8)*, 993-1000.

(25) Ghosh, M.; Ichetovkin, I.; Song, X.; Condeelis, J. S.; Lawrence, D. S. "A New Strategy for Caging Proteins Regulated by Kinases," *Journal of the American Chemical Society* **2002**, *124 (11)*, 2440-2441.

(26) Ghosh, M.; Song, X.; Mouneimne, G.; Sidani, M.; Lawrence, D. S.; Condeelis, J. S. "Cofilin Promotes Actin Polymerization and Defines the Direction of Cell Motility," *Science* **2004**, *304 (5671)*, 743-746.

(27) McMurray, J. S.; Coleman, D. R., IV; Wang, W.; Campbell, M. L. "The Synthesis of Phosphopeptides," *Biopolymers (Peptide Science)* **2001**, *60 (1)*, 3-31.

(28) Pan, P.; Bayley, H. "Caged Cysteine and Thiophosphoryl Peptides," *FEBS Letters* **1997**, *405 (1)*, 81-85.

(29) Hahn, M. E.; Muir, T. W. "Photocontrol of Smad2, a Multiphosphorylated Cell-Signaling Protein, Through Caging of Activating Phosphoserines," *Angewandte Chemie-International Edition* **2004**, *43* 5800-5803.

(30) Rothman, D. M.; Petersson, E. J.; Vazquez, M. E.; Brandt, G. S.; Dougherty, D. A.; Imperiali, B. "Caged Phosphoproteins," *Journal of the American Chemical Society* **2005**, *127 (3)*, 846-847.

(31) Barltrop, J. A.; Plant, P. J.; Schofield, P. "Photosensitive protective groups," *Chemical Communications* **1966**, 822-823.

(32) Engels, J.; Schlaeger, E. J. "Synthesis, Structure, and Reactivity of Adenosine Cyclic 3',5'-Phosphate Benzyl Triesters," *Journal of Medicinal Chemistry* **1977**, *20 (7)*, 907-911.

(33) Walker, J. W.; Reid, G. P.; McCray, J. A.; Trentham, D. R. "Photolabile 1-(2-Nitrophenyl)ethyl Phosphate Esters of Adenine Nucleotide Analogs. Synthesis and Mechanism of Photolysis," *Journal of the American Chemical Society* **1988**, *110 (21)*, 7170-7177.

(34) Corrie, J. E. T.; Barth, A.; Munasinghe, V. R. N.; Trentham, D. R.; Hutter, M. C. "Photolytic Cleavage of 1-(2-Nitrophenyl)ethyl Ethers Involves Two Parallel Pathways and Product Release is Rate-Limited by Decomposition of a Common Hemiacetal Intermediate," *Journal of the American Chemical Society* **2003**, *125 (28)*, 8546-8554.

(35) Haugland, R. P. In *Handbook of Fluorescent Probes and Research Products*; Gregory, J., Eds.; Molecular Probes: Eugene, OR, **2005**, 966.

Chapter 2
Two Synthetic Methods for Caged Phosphopeptides

Introduction

Two synthetic methods that give general access to peptides incorporating the caged phosphoserine moiety are described in this chapter. Both methods make use of a novel phosphitylation reagent incorporating the 1-(2-nitrophenyl)ethyl caging group. The first method is an interassembly approach that enables the synthesis of caged phosphopeptides without oxidation-sensitive residues C-terminal to the caged phosphoserine.[1] The second method is a building block approach to synthesize any caged phosphopeptide within the limits of Fmoc-SPPS (N^{α}-fluorenylmethoxycarbonyl solid phase peptide synthesis).[2] While the interassembly approach is limited to laboratories capable of performing organic chemistry manipulations on a solid support, the building block approach is accessible to any scientist with peptide synthesis capabilities. Using these methods, several peptides were synthesized and characterized as targets for biological studies. Furthermore, quantum yield measurements were performed and it was found that all the peptides had quantum yields comparable to literature values for other compounds including similar *ortho*-nitrobenzyl derived caging groups.

Results and Discussion

2-1. Interassembly Approach

Initially, a "consensus sequence" peptide, CS, was developed to test the chemistry of the interassembly methodology. A literature search was performed on the substrate sequences of the serine kinases. The information was used to develop a CS that incorporates the amino acid residues that most commonly flank the active phosphoserine in the protein. One study attempted to compile such a consensus for sequence recognition by the protein kinases which act upon the serine/threonine and tyrosine kinases.[3] The residues surrounding the amino acid that is phosphorylated during signal transduction vary considerably; however, it is known that proline and arginine residues are frequently found proximal to the recognition site. Most often, proline appears at the (n+1) site, and arginine appears at the (n-2) and/or the (n-3) site.[3] Therefore, the "consensus sequence" Arg-Arg-Gly-**Ser**-Pro-Gly was designed in order to test the chemistry of

synthesizing a peptide with caged phosphoserine (**Ser** is the kinase substrate residue). It is significant to note that several residues commonly employed in Fmoc-SPPS have side chains that require stringent deprotection steps, and it was important to test the stability of the photolabile caging group to these conditions. One of the more difficult residues with which to work in Fmoc-SPPS is arginine: the nucleophilic guanidinium group requires stable protection to prevent side reactions. Of the available arginine protecting groups, the benzyl-sulfonyl- derivatives, such as Pbf (2,2,4,6,7-pentamethyldihydrobenzofuran-5-sulfonyl-), are most commonly used for their relative ease of removal, but even these groups require several hours of agitation in greater than 90% trifluoroacetic acid (TFA) for deprotection. This initially presented the challenge of selecting a caging group stable to such harsh conditions. In addition to the favorable biological properties of the *ortho*-nitrophenylethyl group presented in Chapter 1, the caging group is stable to strong acid and base conditions, making it ideal for use in Fmoc-SPPS.

Scheme 2.1 *Synthesis of O-1-(2-nitrophenyl)ethyl-O'-β-cyanoethyl-N,N-diisopropylphosphoramidite,* **4**.

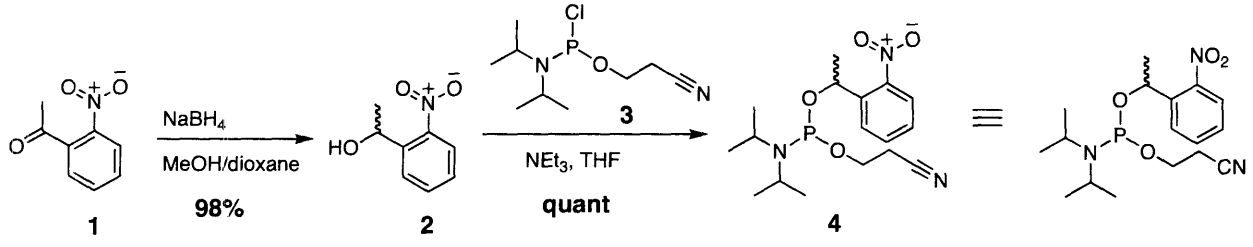

The initial method to synthesize caged phospho-peptides was termed an interassembly approach of Fmoc-SPPS. An interassembly approach is one in which a non-native moiety is introduced into a growing peptide chain while it is still attached to the resin. Literature precedent demonstrated that phosphopeptides can be synthesized in such a manner using a mixed phosphoramidite.[4] Additionally, it has been reported that mono-protected phosphates are ideal for Fmoc-SPPS.[5] Therefore, a new phosphitylation reagent was synthesized to incorporate a 1-(2-nitrophenyl)ethyl caging group, as seen in Scheme 2.1. Briefly, 2-nitroacetophenone (**1**) was reduced with sodium borohydride to the corresponding racemic alcohol, **2**. The chloro-substituent of the DNA synthesis reagent **3** was then substituted with the alcohol **2** to afford the mixed phosphoramidite **4**. The racemic benzylic methyl on the caging group should not affect

uncaging. Experiments performed using such a racemic mixture of the caging group form the foundation of uncaging studies with a *ortho*-nitrophenylethyl caged phosphoryl group.[6]

Scheme 2.2 *Synthesis of caged phosphopeptide via the interassembly approach.*

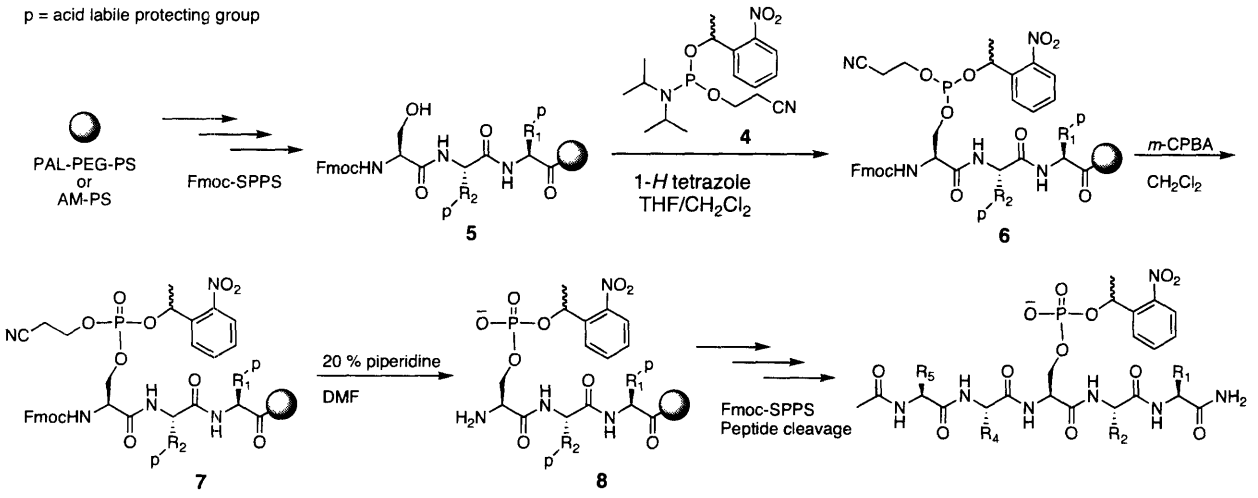

Phosphoramidite **4** was incorporated into a growing peptide chain as shown in Scheme 2.2. A peptide was synthesized on solid support using standard Fmoc-SPPS procedures, and the target serine residue was incorporated without side chain protection (**5**). The serine was then phosphitylated with **4** activated by 1-*H* tetrazole to afford the phosphite peptide **6**. The tervalent phosphorus* species was then oxidized to the pentavalent species **7** using *meta*-cholorperoxybenzoic acid (*m*-CPBA). When the Fmoc-group on the N-terminus of the peptide was removed with basic conditions for chain elongation, the temporary cyanoethyl protecting group on the phosphate was concurrently removed (**8**). The caged phosphate was stable to further Fmoc-SPPS and stringent peptide cleavage conditions: greater than 90 % trifluoroacetic acid (TFA). Peptides with caged phosphothreonine or caged phosphotyrosine were also accessible by using similar methodology.[1]

* Throughout the text, the term *tervalent phosphorus* refers to phosphorus with four pairs of electrons, even though it may be tricoordinate. The *pentavalent species* is that with five pairs of electrons, and it is often tetracoordinate. See reference 7.

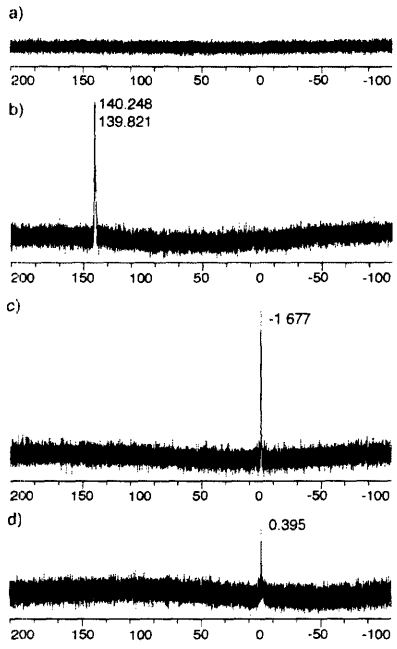

Figure 2.1. ^{31}P MAS NMR of peptide on AM-PS resin. Shifts are shown in δ (ppm) relative to H_3PO_4 (δ = 0 ppm). See reference 1.

a) Free serine, **5**.
b) Phosphite, **6**.
c) Phosphate, **7**.
d) Deprotected phosphate **8**.

While the peptide depicted in Scheme 2.2 has unspecified side chains flanking the caged phosphoserine residue, the different phosphorus states corresponding to the numbers under each peptide can be visualized using ^{31}P Magic Angle Spinning Nuclear Magnetic Resonance spectroscopy (MAS-NMR). The peptide cpSer-Pro-Gly was synthesized on high loading aminomethylated polystyrene resin (AM-PS) and the progression of the reactions was monitored by the phosphorus NMR shifts. As seen in Figure 2.1, the free serine peptide has no ^{31}P signal. Upon phosphitylation, there is a ^{31}P shift characteristic of a tricoordinate, tervalent phosphite species.[7] After oxidation, the ^{31}P signal shifts to the characteristic range of a tetracoordinate, pentavalent phosphate. Finally, upon removal of the cyanoethyl and Fmoc groups, a slight shift in the ^{31}P spectrum is observed, though it remains in the spectral region of a phosphate species. In addition to the MAS-NMR measurements, final peptide products were cleaved from the resin and their identities were confirmed by reversed phase High Performance Liquid Chromatography (HPLC) and Electrospray Ionization Mass Spectrometry (ESI-MS). It is significant to note that only those peptides with tetracoordinate, pentavalent phosphorus could be identified by HPLC and MS. The phosphite intermediate is unstable to the peptide cleavage and analysis conditions, and thus MAS-NMR was employed as a method of monitoring reaction progression.

2-2. Building Block Approach

While the interassembly approach affords access to a wide variety of caged phosphopeptides, it contains two potential limitations. First, sequences that contain oxidation-sensitive residues (such as methionine or tryptophan) C-terminal to the caged phosphoserine, would be oxidized upon transformation of the tervalent phosphorus to the pentavalent species (Scheme 2.3). Additionally, laboratories interested in peptide tools for studying phosphorylation that are not equipped to perform the organic chemistry manipulations on the resin cannot utilize the interassembly approach. In order to circumvent these limitations, a building block approach was developed such that any caged phosphopeptide can be synthesized within the limits of Fmoc-SPPS.

Scheme 2.3 *Oxidation of sensitive residues on bead.*

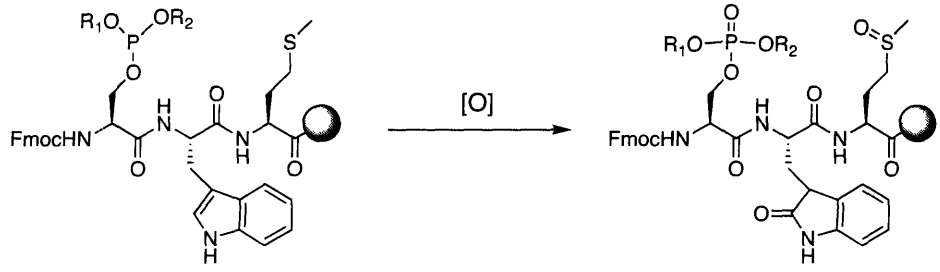

The synthesis of the caged phosphoserine building block incorporates the same phosphoramidite reagent as the interassembly approach. As seen in Scheme 2.4, the Fmoc-and trityl-protected serine derivative **9** was first transformed into the *tert*-butyl ester **10** using *tert*-butyl trichloroacetimidate. The hydroxyl side chain was then deprotected in mild acid to afford **11**. The serine was phosphitylated using the aforementioned reagent (**4**) and subsequently oxidized with *m*CPBA to give the fully protected derivative **12**. Finally, the free acid **13** was generated by treatment with acid at room temperature. It is important that the deprotection is run at 23 °C or warmer; lower room temperatures resulted in failed reactions. Caged phosphothreonine and caged phosphotyrosine building blocks were also accessible using this general synthetic route with minor alterations to the procedure.[2] These building blocks have been successfully incorporated into multiple polypeptide chains within the limits of standard Fmoc-SPPS.

Scheme 2.4 *Synthesis of* N^{α}*-Fmoc-phospho-(O-1-(2-nitrophenyl)ethyl-O'-β-cyanoethyl)-L-serine,* **13**.

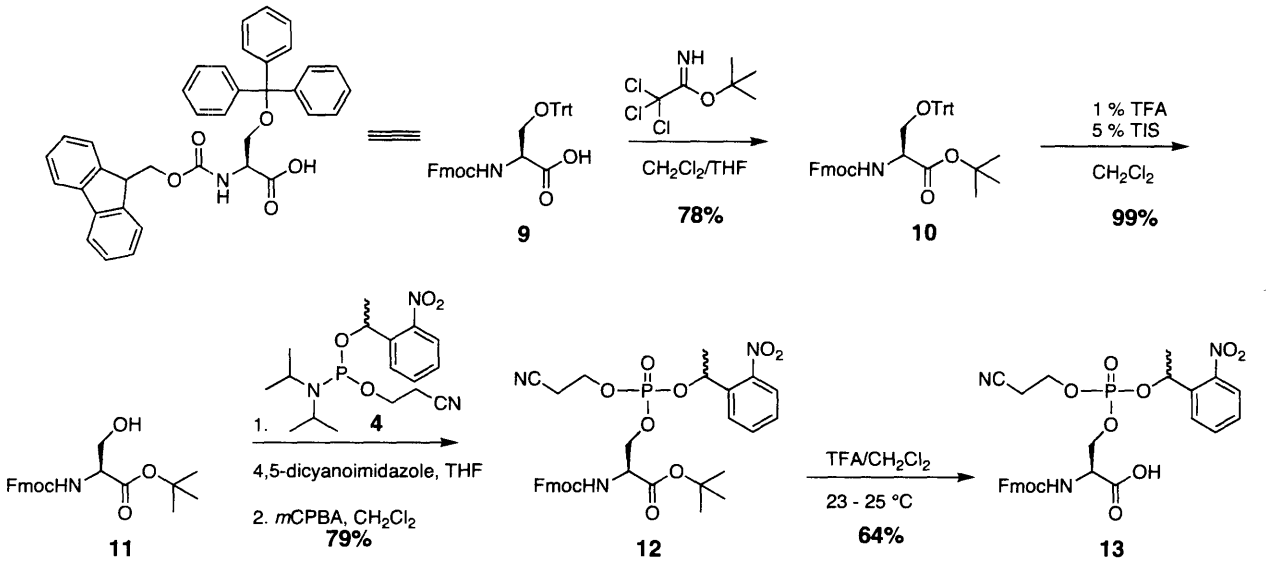

2-3. Peptides Synthesized for Biological Targets

Following successful incorporation of the caged phosphoserine moiety into the CS, creating cpCS, several other peptides were synthesized for potential biological experiments in collaboration with other research groups.

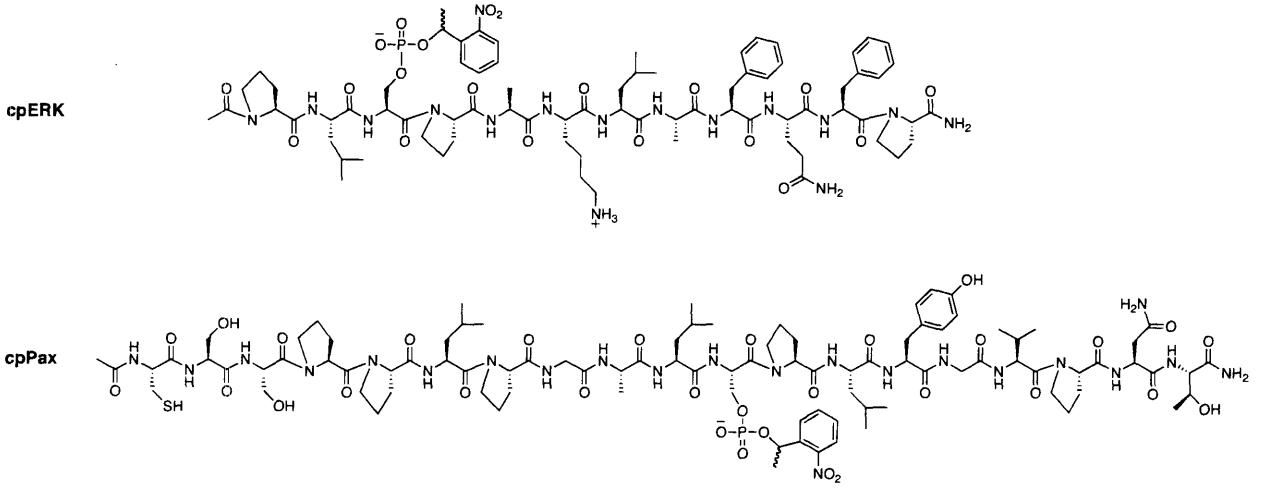

Figure 2.2. Caged phosphopeptides cpERK and cpPAX were synthesized and characterized for use in biological studies.

Two peptides, cpERK and cpPax (Figure 2.2), were synthesized and characterized, though ultimately were not used for biological studies. cpERK was designed to bind to the

family of extracellular signal-regulated kinases, ERKs. ERKs make up a group of mitogen activated protein kinases, MAPKs, and have been implicated in multiple signaling pathways, including those implicated in cell motility, differentiation, and proliferation. Concerning cell motility, ERKs are thought to be involved in the Integrin adhesion pathway, closely linked to calpain function. M-calpain (the isoform that requires near millimolar concentrations of Ca^{2+} for proteolytic activity *in vitro*) may be involved in growth-factor-mediated motility, or chemokinesis. It has been proposed that epidermal growth factor (EGF) activates homodimerization of the EGF receptor (EGFR), which in turn activates phosphorylation of ERK. The phosphorylated ERK can then phosphorylate serine 50 in M-calpain, placing M-calpain in the active form, which is necessary for tail de-adhesion in cell motility.[8] With a caged phospho-derivative of an ERK antagonist peptide, we aimed to "turn off" chemokinesis when the cage is removed by photolysis: the phosphopeptide would block ERK's ability to activate M-calpain and halt cell de-adhesion. The substrate peptide Pro-Leu-**cpSer**-Pro-Ala-Lys-Leu-Ala-Phe-Gln-Phe-Pro (cpERK) was recommended[9] because the dodecamer contains the core ERK recognition motif, Pro-Leu-**Ser**-Pro, and an ERK docking motif, Phe-Xaa-Phe-Pro.

The cpPax peptide was designed to mimic a portion of paxillin, a 68 kDa focal adhesion protein involved in multiple aspects of cell migration and Integrin binding. It is a multi-domain protein that binds to several structural and regulatory partners, functioning as a scaffold for recruiting other proteins involved in cell adhesion, cell motility and growth control.[10] The cpPax sequence was taken from Ser169-Thr186 of human paxillin, with Ser178 as the phosphorylation target. Phosphorylation of several tyrosine residues is important for downstream binding interactions, but the immediate function of the phosphoserine residues on Paxillin remains unknown to date. For the purpose of *in vitro* experiments, a caged phospho-, a phospho- and a free serine peptide analog of cpPax would have been conjugated to sepharose beads via an N-terminal cysteine residue and used in protein pull down assays to determine the ability to bind paxillin-binding partners.[11]

A third peptide, cpRSLP (Figure 2.3), was synthesized and characterized for studying the family of 14-3-3 proteins in a collaborative effort with the Yaffe Lab (M. I. T. Department of Biology). The biological design and implications of this peptide substrate are discussed in detail in Chapter 3.

cpRSLP

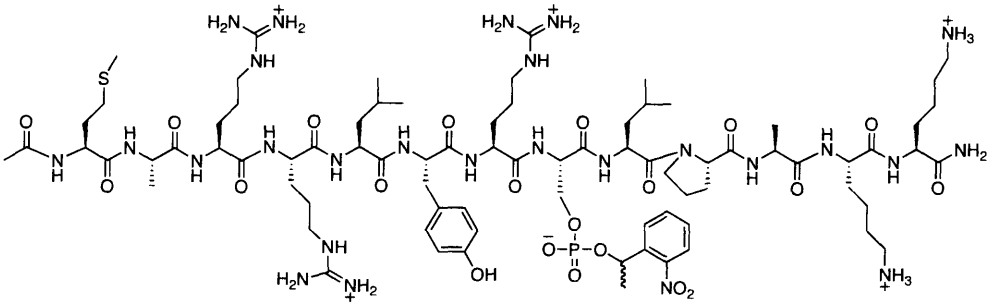

Figure 2.3. Peptide synthesized and characterized for studying the 14-3-3 protein family, cpRSLP.

2-4. Quantum Yield Measurements

The quantum yields of uncaging, Φ, for the peptides were found to be comparable to literature values, and apparently peptide dependent. It was possible to measure the quantum yield by comparing the loss of caged peptide to the loss of a standard with a known quantum yield that was subjected to the same conditions.[12] As explained in the literature, by taking into account the A_{350} values of the standard and the sample and then quantifying the amount of standard and sample lost by photolysis, the quantum yield of the sample may be calculated using the following equation:

$$\Phi_{sample} = \Phi_{standard} \times \frac{\%\Delta sample}{\%\Delta standard} \times \frac{A_{350}\ standard}{A_{350} sample}$$

The standard used for these measurements was 1-(2-nitrophenyl)ethyl-phosphate, which has a known quantum yield of 0.54.[12] In brief, the caged phosphate or caged phosphopeptide was irradiated for 15 seconds in order to uncage 10 to 20% of the peptide. All samples were photolyzed at λ = 365 nm and an intensity of 7330 $\mu W/cm^2$ in a glass vessel with a 1mm path length. The amount of caged compound lost after irradiation was quantified by reverse phase HPLC analysis. Using a photochemically inactive internal standard of 1 mM inosine in each sample, the area of caged compound on each HPLC trace was normalized to that of inosine at t = 0 and t = 15 s post irradiation. All solutions were made in dH_2O, pH 7.1, with 5mM dithiothreitol (DTT) to prevent side reactions of the photochemical by-product, nitrosoacetophenone, with the caged or uncaged samples (Chapter 1). Each experiment was performed in triplicate. The quantum yields of those peptides characterized are shown in Table 2.1.

Table 2.1. Quantum yield of uncaging for various peptides.

Peptide	Quantum Yield (Φ)
cpCS: Ac-RRG**cpS**PG-$CONH_2$	0.21
cpERK: Ac-PL**cpS**PAKLAFQFP-$CONH_2$	0.26
cpRSLP: Ac-MARRLYR**cpS**LPAKK-$CONH_2$	0.42

Key **cpS**: caged phosphoserine.

Although the Φ of all the peptides tested falls within the range of reported literature values for the 1-(2-nitrophenyl)ethyl moiety, it appears that Φ is dependent upon peptide sequence. It is possible that different residues flanking the caged phosphoserine create significantly different remote environments, such that the leaving group (the phospho-peptide) becomes better or worse depending on those flanking residues. However, these residues do not yield through-bond effects on the phosphopeptide. It is also possible that those same residues may stabilize or destabilize the *aci*-nitro-intermediate discussed in Chapter 1; a stabilized intermediate would likely result in a reduced quantum yield. However, these explanations are only speculation, and no further experiments were performed.

In addition to measuring the quantum yield of the peptides, several light sources with different power outputs were tested to investigate the effect of light intensity upon the rate of uncaging. Note that Φ only measures the relative efficiency of uncaging, and not the rate of uncaging. cpERK was subjected to different light sources with varying intensity as shown in Table 2.2. Time course experiments were performed to determine the amount of cpERK uncaged by the various sources, as illustrated in Figure 2.4.

Table 2.2. Light sources tested for uncaging.

Source	Wavelength	Power at the Sample
Transilluminator*	365 nm	7.3 mW
Fluorometer†	300 nm	3.0 mW (estimate)
N_2 Laser A	337 nm	3.0 mW
N_2 Laser B	337 nm	6.0 mW

* Ultra Violet Products (UVP) High Performance Ultraviolet Transilluminator

† Jobin Yvon Horiba FluoroMax-P Fluorometer

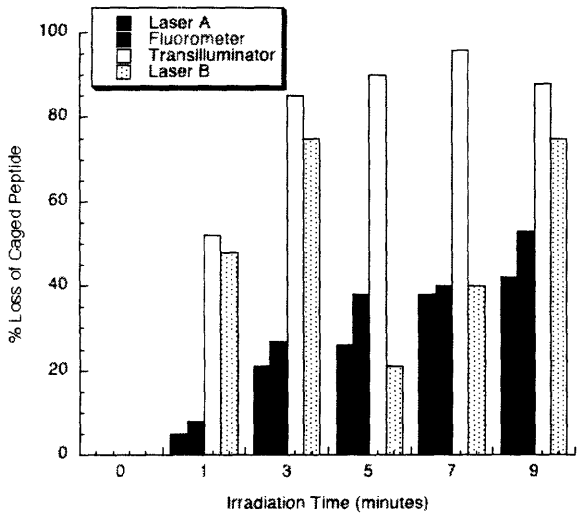

Figure 2.4. Amount of caged peptide lost by photolysis from various light sources. Samples of cpERK (274 μM with 500 μM inosine, 500 μM DTT) were irradiated with various sources and aliquots removed for analysis by reverse phase HPLC. The amount of cpERK removed by uncaging is plotted along the Y-axis.

The inconsistent data for the Laser B, which appears to demonstrate rapid uncaging followed by recaging of the peptide, likely appeared because the sample was not stirred during irradiation. Therefore, if the aliquot for analysis had been removed from the direct path of the laser (e.g., t = 1, 3 minutes), more uncaging was detected; if the sample was removed from an area in the cell not directly in the path of the laser (t = 5, 7 minutes), less uncaging was observed. In either case, the measurements are not truly reflective of what would be observed in a homogenous solution. Even so, it is possible to see from these experiments that higher intensity light sources cause a more rapid rate of uncaging. The best uncaging is seen with the transilluminator or Laser B, both over 6 mW at the sample. While the transilluminator appears to have the best rate of uncaging, it is significant to note that the samples become heated while sitting on the surface of the transilluminator for more than five minutes. The same heating was not observed with the lasers.

Conclusion

Two methods to synthesize peptides incorporating *ortho*-nitrophenylethyl caged phosphoserine have been described: the interassembly approach and the building block approach. Through these methods scientists can access any caged phosphoserine peptide within the limits of Fmoc-SPPS. Additionally, several caged phosphopeptides were synthesized for biological studies, and their quantum yields were measured. The quantum yields were found to be comparable to those of literature values of other *ortho*-nitrobenzyl caged compounds with similar substitutions.

Experimental

2-0. General Synthetic Procedures

All peptide synthesis reagents were purchased from PerSeptive Biosystems (Applied Biosystems, Foster City, CA) or Novabiochem (EMD Biosciences, San Diego, CA), and all other chemicals were purchased from Aldrich (St. Louis, MO). Anhydrous dichloromethane, CH_2Cl_2, was distilled from calcium hydride, and anhydrous tetrahydrofuran, THF, was distilled from sodium/benzophenone. ^1H NMR spectra were acquired on a Bruker Avance (DPX) 400 MHz spectrometer or a Varian Mercury 300 MHz spectrometer. ^{13}C NMR spectra were acquired on a Varian INOVA 500 MHz spectrometer. ^{31}P NMR spectra were acquired on a Varian Mercury 300 MHz spectrometer, and all MAS ^{31}P NMR spectra were acquired on a Varian INOVA 500 MHz spectrometer. Chemical shifts are reported in ppm from a standard (tetramethylsilane for ^1H, chloroform for ^{13}C, H_2PO_4 for ^{31}P), and *J* values are in hertz. Thin-layer chromatography (TLC) was carried out on Merck 60 F_{254} 250-μm silica gel plates. High-performance liquid chromatography was performed using a Waters 600E HPLC fitted with a Waters 600 automated control module and a Waters 2487 dual wavelength absorbance detector recording at 228 and 280 nm. For analytical HPLC a Beckman Ultrasphere C_{18}, 5 μm, 4.6 x 150 mm reverse-phase column was used. For preparative separations a YMC-pack, C_{18}, 250 x 20 mm reversed phase column was used. The standard gradient for analytical and preparatory HPLC was 93:7 to 0:100 over 35 minutes (water:acetonitrile, 0.1% TFA). Electrospray Ionization Mass Spectrometry (ESI-MS) was performed on a PerSeptive Biosystems *Mariner™ Biospectrometry Workstation* (Turbo Ion Source). "cp" denotes "caged phospho-."

General Peptide Synthesis Procedures. Peptides were prepared by standard N^{α}-fluorenylmethoxycarbonyl solid phase peptide synthesis (Fmoc-SPPS) on [5-(4-Fmoc-aminomethyl-3,5-dimethoxyphenoxy)valeric acid]-polyethyleneglycol-polystyrene (Fmoc-peptide amide linker-PEG-PS or Fmoc-PAL-PEG-PS) resin. For example, 1.00 g (200 μmol) Fmoc-PAL-PEG-PS (0.2 mmole/g loading; 1% DVB) was allowed to swell for five minutes with 5 mL CH_2Cl_2 followed by five minutes with 5 mL *N,N*-dimethylformamide (DMF) in a 100 mL peptide synthesis reaction vessel. The resin was deprotected with 3 x 5 mL of 20% piperidine in DMF (five minutes each), then rinsed 5 x 5 mL DMF (one minute each).

In each coupling step, 2 equivalents (400 μmol) Fmoc-protected amino acid and 2 equivalents (400 μmol) benzotriazole-1-yl-oxy-tris-pyrrolidino-phosphonium hexafluorophosphate (PyBOP) dissolved in 5.0 mL DMF were added to the resin, and the coupling was initiated by addition of 4 equivalents (800 μmol) *N,N*-diisopropylethylamine (DIPEA). Each coupling was allowed to run at room temperature for at least one hour. The resin was then rinsed 2 x 5 mL DMF (one minute each) followed by 2 x 5 mL CH_2Cl_2 (one minute each). After each coupling reaction, a few beads of resin were tested with trinitrobenzene sulfonic acid (TNBS) to check for free amines. Upon a negative test, the amino acid was deprotected as above for chain elongation.

Peptides were cleaved with 90% trifluoroacetic acid (TFA), 5% CH_2Cl_2, 2.5% water, and 2.5% triisopropylsilane (TIS), then triturated in ice-cold diethyl ether, unless otherwise noted, and purified by HPLC. Concentrations of the purified stock solutions were determined by quantitative amino acid analysis of hydrolyzed peptides (2 hours at 145°C with 6 N HCl and phenol), or by UV absorption of the nitrophenyl group (ε_{max} at A_{259} = 5700 $M^{-1}cm^{-1}$ in MeOH).

2-1. Interassembly Approach

1-(2-nitrophenyl)ethanol (NPE-OH), **2.** To 2'-nitroacetophenone (1.0 g, 6.1 mmol) in 14.4 mL of methanol:dioxane (3:2 by volume) sodium borohydride (690 mg, 18.2 mmol) was added and stirred in a cool water bath, 0 °C, for 20 minutes. The mixture was allowed to stir for 2.5 hours longer at room temperature (progress monitored by TLC in chloroform, $CHCl_3$, and detected by UV). The reaction was quenched with 50 mL of water, and then stirred at room temperature for 30 minutes. The mixture was extracted into $CHCl_3$ (3 x 30 mL), dried over sodium sulfate (Na_2SO_4) and concentrated under reduced pressure. The alcohol was dried *in vacuo* overnight to give a yellow oil, 990.9 mg (97.9%): ^{1}H NMR (400 MHz, $CDCl_3$) δ ppm: 7.9 (d, J= 8.0 Hz, 1 H), 7.9 (d, J= 8.0 Hz, 1 H), 7.7 (t, J= 7.2 Hz, 1 H), 7.4 (t, J= 7.6 Hz, 1 H), 5.4 (q, J= 6.4 Hz, 12.4 Hz, 1 H), 2.4 (s, 1H), 1.6 (d, J= 6.4 Hz, 3H). ^{13}C NMR (125.8 MHz, $CDCl_3$) δ ppm: 148.1, 141.5, 134.1, 128.5, 128.0, 124.7, 65.9, 24.7. See spectra 2.1 and 2.2.

O-*1-(2-nitrophenyl)ethyl*-O'-*β-cyanoethyl*-N,N-*diisopropylphosphoramidite,* **4.** A solution of 2-cyanoethyl diisopropylchlorophosphoramidite (471 μL, 2.11 mmol) in 1.7 mL of anhydrous CH_2Cl_2 was added to a stirring solution of *ortho*-nitrophenylethyl alcohol (294 mg, 1.76 mmol)

and freshly distilled triethylamine (589 μL, 4.23 mmol) in 8.8 mL of anhydrous CH_2Cl_2 at room temperature in the dark. The reaction was monitored by the disappearance of the *ortho*-nitrophenylethyl alcohol by TLC in 65:25:4 methanol:chloroform:water. The reaction mixture was washed with 10% sodium bicarbonate solution ($NaHCO_3$) (2 x 30 mL). The organic layer was then dried over Na_2SO_4 and concentrated under reduced pressure. The product was dried *in vacuo* overnight to give a dark yellow oil, 646 mg (quantitative). ^1H NMR (400 MHz, $CDCl_3$) δ: 7.9 (m, 2 H), 7.7 (m, 1 H), 7.4 (m, 1 H), 5.6 (m, 1 H), 3.9 (m, 2 H), 3.7 (m, 2 H), 2.5 (m, 2 H), 1.6 (dd, J= 2.4 Hz, 6.8 Hz, 3H), 1.2 (m, 12 H). ^{31}P NMR (121 MHz, $CDCl_3$) δ: 148.2 (d, J= 45.6 Hz). See spectra 2.3 and 2.4.

In general, peptides were synthesized up to the serine to be phosphitylated, which was coupled with an unprotected hydroxyl side chain. The resin was dried *in vacuo* overnight and swollen in 50:50 anhydrous CH_2Cl_2:anhydrous THF. The peptide on resin was then coupled with the phosphoramidite reagent (5 equivalents) and 1*H*-tetrazole (5 equivalents) overnight, and all further steps were kept in the dark. The reaction was quenched with 10 % $NaHCO_3$ and the resin was rinsed with 50:50 CH_2Cl_2:THF, then CH_2Cl_2. The phosphitylated resin was then oxidized with *meta*-chloroperoxybenzoic acid (*m*CPBA, 2 equivalents) in CH_2Cl_2 for one hour. The reaction was quenched with 10% $NaHCO_3$, and the resin was rinsed well with CH_2Cl_2. The subsequent deprotection of the Fmoc-amine concurrently removed the cyanoethyl protection on the phosphate, and standard Fmoc-SPPS procedures were employed to complete peptide synthesis. A sample peptide is described below:

cpERK:

Ac-PL-phospho-1-(2-nitrophenyl)ethyl-seryl-PAKLAFQFP-$CONH_2$

Fmoc-SPAKLAFQFP-(PAL-PEG-PS). Fmoc-SPAKLAFQFP-(PAL-PEG-PS) was synthesized using standard Fmoc-SPPS as described above. Data for a portion of cleaved resin: Analytical reversed phase HPLC, t_R= 26.2 min. MS (ESI), *m/z* calculated for $C_{69}H_{91}N_{13}O_{14}$: 1327.5 $(M+H)^+$ and 664.3 $(M+2H)^{2+}$. Found *m/z* 1326.8 $(M+H)^+$ and 663.9 $(M+2H)^{2+}$.

*Fmoc-phosphi-(*O*-1-(2-nitrophenyl)ethyl-*O*'-β-cyanoethyl)seryl-PAKLAFQFP-(PAL-PEG-PS).* The resin-bound decapeptide Fmoc-SPAKLAFQFP-(PAL-PEG-PS) (200 mg resin, 40 μmol) was dried overnight *in vacuo*. A portion of *O*-1-(2-nitrophenyl)ethyl-*O'*-β-cyanoethyl-*N,N*-diisopropylphosphoramidite (73.5 mg, 200 μmol) was added the resin, and the vessel was flushed with nitrogen. The resin was swollen in 3.0 mL of 50:50 anhydrous CH_2Cl_2:anhydrous THF for 10 minutes. The system was charged with 1*H*-tetrazole (14 mg, 200 μmol) and flushed again with nitrogen. The reaction was agitated overnight in the dark, upon which 3.0 mL of 10% $NaHCO_3$ solution was added to the reaction mixture and allowed to mix for several minutes. The resin was rinsed with 50:50 CH_2Cl_2:THF (2 x 5 mL), and then further with CH_2Cl_2 (2 x 5 mL).

*Fmoc-phospho-(*O*-1-(2-nitrophenyl)ethyl-*O*'-β-cyanoethyl)seryl-PAKLAFQFP-(PAL-PEG-PS).* In a peptide synthesis vessel, Fmoc-phosphi-(*O*-1-(2-nitrophenyl)ethyl-*O'*-β-cyanoethyl)seryl-PAKLAFQFP-(PAL-PEG-PS) (200mg resin, 40 μmol) was swollen in CH_2Cl_2. The resin was placed in 3.0 mL of CH_2Cl_2, and *m*CPBA (13.8 mg, 80 μmol) was added to the solution and allowed to agitate for one hour at room temperature in the dark. The reaction mixture was then treated with 3.0 mL of 10% $NaHCO_3$ solution for 5 minutes, and the resin was rinsed with CH_2Cl_2 (3 x 5 mL). Reversed phase HPLC revealed one major and one minor peak. The minor peak (t_R = 26.76 min, 26.5%) corresponded to the starting material. The major peak (t_R = 28.76 minutes, 73.5%) was the desired C-terminal product. MS (ESI), *m/z* calculated for $C_{80}H_{102}N_{15}O_{19}P$: 1609.7 $(M+H)^+$ and 805.4 $(M+2H)^{2+}$. Found *m/z* 805.0 $(M+2H)^{2+}$ and 816.0 $(M+H+Na)^{2+}$.

Ac-PL-phospho-1-(2-nitrophenyl)ethyl-seryl-PAKLAFQFP-CONH$_2$. Chain elongation was carried out by standard Fmoc SPPS in the dark. After the last residue was added, the *N*-terminus was acetyl capped with acetic anhydride (37.8 μL, 400 μmol) and pyridine (32.3 μL, 400 μmol). Reverse phase HPLC (t_R = 24.6 min). MS (ESI) *m/z* calculated for $C_{75}H_{109}N_{16}O_{20}P$: 1586.7 $(M+H)^+$ and 793.9 $(M+2H)^{2+}$. Found *m/z* 793.5 $(M+2H)^{2+}$, 804.5 $(M+H + Na)^{2+}$, and 815.5 $(M+2Na)^{2+}$.

Magic Angle Spinning NMR

The progression of the phosphitylation/oxidation reactions were monitored by Magic Angle Spinning ^{31}P NMR on Aminomethylated Polystyrene HL resin (Novabiochem, 0.85 mmole/g loading). The sequence H_2N-cpSer-Pro-Gly-$CONH_2$ was synthesized on a 200 mg scale as above, and a 10 mg portion of resin was removed at each step for analysis (^{31}P δ in ppm, 200 MHz):

- Fmoc-Ser-Pro-Gly-(AM-PS): no ^{31}P signal. See spectrum 2.5.
- Fmoc-phosphi-(*O*-1-(2-nitrophenyl)ethyl-*O'*-β-cyanoethyl)seryl-Pro-Gly-(AM-PS): 140.25 (d, J = 85.4 Hz). See spectrum 2.6.
- Fmoc-phospho-(*O*-1-(2-nitrophenyl)ethyl-*O'*-β-cyanoethyl)seryl-Pro-Gly-(AM-PS): -1.68 (s). See spectrum 2.7.
- Phospho-1-(2-nitrophenylethyl)seryl-Pro-Gly-(AM-PS): 0.40 (s). See spectrum 2.8.

2-2. Building Block Approach

N^{α}-*Fmoc-hydroxytrityl-L-serine tert-butyl ester,* **10**. N^{α}-Fmoc-hydroxytrityl-L-serine (2.17 g, 3.80 mmole) was dissolved in 12.6 mL anhydrous CH_2Cl_2:THF 4:1 by volume. To the stirring solution was added t-butyl 2,2,2-tricholoracetimidate (2.72 mL, 15.20 mmole). The reaction was allowed to stir at room temperature overnight under argon. The reaction was then concentrated under reduced pressure and redissolved in ethyl acetate (EtOAc) (50 mL). The solution was washed with 10% $NaHCO_3$ (2 x 100 mL), and then saturated sodium chloride (brine) (1 x 100 mL). The organic layer was dried over magnesium sulfate ($MgSO_4$), filtered, and concentrated. The crude product was purified by chromatography on a short plug of basic alumina (1:1 hexanes/EtOAc, R_f = 0.68) to give the product (1.85 g) in 78% yield. ^1H NMR (300 MHz, $CDCl_3$) δ ppm: 7.75 (d, J_{HH} = 7.5 Hz, 2H), 7.62 (q, J_{HH} = 4.8 Hz, 2H), 7.41-7.19 (m, 19H), 5.83 (J_{HH} = 8.1 Hz, 1H), 4.39 (m, 3H), 4.25 (t, J_{HH} = 6.9 Hz, 1H), 3.47 (s, 2H), 1.44 (s, 9H).. ^{13}C NMR (125.8 MHz, $CDCl_3$) δ ppm: 170.3, 156.6, 144.7, 144.6, 144.3, 142.1, 142.0, 129.4, 128.7, 128.5, 128.0, 127.9, 126.0, 127.0, 120.8, 87.1, 83.1, 68.0, 64.8, 55.7, 47.9, 28.8. ESI-MS: $[MNa]^+$ 648.2708 (obsd) , 648.2720 (calcd). See spectra 2.9 and 2.10.

N^{α}-*Fmoc-L-serine tert-butyl ester,* **11**. N^{α}-Fmoc-hydroxytrityl-L-serine tert-butyl ester (1.85 g, 2.96 mmole) was dissolved in 70 mL CH_2Cl_2 with 1% trifluoroacetic acid (TFA) and 5% triisopropylsilane. The solution was allowed to stir at room temperature for one hour. The mixture was diluted with CH_2Cl_2 (100 mL), and washed with 10% $NaHCO_3$ (2 x 100 mL) and

then brine (1 x 100 mL). The crude mixture was dried over $MgSO_4$, filtered, and concentrated under reduced pressure. The crude product was purified by silica gel flash chromatography (1:1 hexanes/EtOAc, R_f = 0.28) to give the product (1.12 g) in 99% yield. ^1H NMR (300 MHz, $CDCl_3$) δ ppm: 7.74 (d, J_{HH} = 7.2 Hz, 2H), 7.59 (d, J_{HH} = 7.2 Hz, 2H), 7.40 (t, J_{HH} = 7.5 Hz, 2H), 7.31 (t, J_{HH} = 8.4 Hz, 2H), 5.75 (d, J_{HH} = 6.3 Hz, 1 H), 4.40 (d, J_{HH} = 7.2 Hz, 2H), 4.33 (t, J_{HH} = 3.6 Hz, 1H), 4.22 (t, J_{HH} = 6.9 Hz, 1H), 3.92 (d, J_{HH} = 2.1 Hz, 2H), 2.22 (bs, 1H), 1.48 (s, 9H). ^{13}C NMR (125.8 MHz, $CDCl_3$) δ ppm: 170.5, 157.2, 144.6, 144.5, 142.01, 141.99, 128.4, 127.8, 125.9, 120.72, 120.71, 83.5, 67.9, 64.2, 57.4, 47.8, 28.7. ESI-MS $[MH]^+$ 384.1816 (obsd), 384.1805 (calcd). See spectra 2.11 and 2.12.

N^{α}-*Fmoc-phosphi-(*O-*1-(2-nitrophenyl)ethyl-*O'-*β-cyanoethyl)-*L-*serine tert-butyl ester,* **12**. In a round bottom flask under argon, N^{α}-Fmoc-L-serine tert-butyl ester (930 mg, 2.43 mmole) was dissolved in 12 mL anhydrous THF, and left stirring. In a pear-shaped flask under argon, *O*-1-(2-nitrophenyl)-ethyl-*O'*-β-cyanoethyl-*N,N*-diisopropylphosphoramidite (1.51 g, 4.12 mmole) and 4,5-dicyanoimidazole (487 mg, 4.12 mmole) were dissolved in 12.3 mL anhydrous THF, and allowed to stir for several minutes in the dark. The phosphoramidite solution was added into the stirring serine solution *via* cannula under positive argon pressure, and allowed to stir at room temperature in the dark overnight, under inert conditions. The reaction was judged complete by disappearance of the starting material and appearance of the product by TLC (EtOAc/hexanes, R_f = 0.43). The crude mixture was concentrated under reduced pressure and redissolved in EtOAc (100 mL). The solution was washed with 10% $NaHCO_3$ (2 x 100 mL), and then brine (1 x 100 mL). The crude material was dried over Na_2SO_4, filtered, concentrated under reduced pressure, and used immediately in the following reaction.

N^{α}-*Fmoc-phospho-(*O-*1-(2-nitrophenyl)ethyl-*O'-*β-cyanoethyl)-*L-*serine tert-butyl ester,* **12**. N^{α}-Fmoc-phosphi-(1-nitrophenylethyl-2-cyanoethyl)-L-serine tert-butyl ester (1.58 g, 2.43 mmole) was dissolved in 97.2 mL CH_2Cl_2. *meta*-Chloroperoxybenzoic acid (837 mg, 4.86 mmole) was added to the solution and allowed to stir in the dark at room temperature for one hour. The solution was then washed with 10% $NaHCO_3$ (2 x 100 mL), and then brine (1 x 100 mL). The organic layer was dried over $MgSO_4$, filtered, and concentrated under reduced pressure. The product was purified by silica gel flash chromatography (1:2 hexanes/EtOAc, R_f = 0.23) to give

the product (1.27 g) in 79% yield over two steps. ^{1}H NMR (300 MHz, $CDCl_3$) δ ppm: 7.94 (m, 1H), 7.73 (d, J_{HH} = 7.5 Hz, 3H), 7.60 (d, J_{HH} = 5.7 Hz, 3H), 7.38 (m, 5H), 6.14 (m, 1H), 5.79 (m, 1H), 4.42 (m, 4H), 4.23 (m, 4H), 2.65 (m, 2H), 1.72 (m, 3H), 1.47 (m, 9H). ^{13}C NMR (125.8 MHz, $CDCl_3$) δ ppm: 168.3, 156.6 (d, J_{PC} = 4.0 Hz), 147.5, 144.5 (d, J_{PC} = 4.0 Hz), 141.9 (d, J_{PC} = 2.4 Hz), 137.7, 134.7 (m), 129.8, 128.5 (d, J_{PC} = 2.4 Hz), 128.3, 128.2 (d, J_{PC} = 5.7 Hz), 127.8, 125.9, 125.4 (m), 120.7, 117.1, 84.1 (m), 74.2 (m), 68.7 (m), 68.0 (d, J_{PC} = 12.8 Hz), 63.1 (m), 55.4 (m), 47.7, 28.6 (t, J_{PC} = 2.3 Hz), 24.9 (dd, J_{PC} = 5.2 Hz, J_{PC} = 2.89 Hz), 20.3 (d, J_{PC} = 7.4 Hz). ^{31}P NMR (121.5 MHz, $CDCl_3$) δ ppm: -2.20, –2.31, -2.41. ESI-MS $[MNa]^+$ 688.2011 (obsd), 688.2031 (calcd). See spectra 2.13, 2.14, and 2.15.

N^{α}-*Fmoc-phospho-(*O-*1-(2-nitrophenyl)ethyl-*O'-*β-cyanoethyl)-*L-*serine,* **13**. *N^{α}*-Fmoc-phospho-(*O*-1-(2-nitrophenyl)ethyl-*O'*-β-cyanoethyl)-L-serine tert-butyl ester (500 mg, 751 μmole) was dissolved in 35.6 mL CH_2Cl_2 at 25 °C in the dark. A 3.75 mL aliquot of triisopropylsilane was added to the solution, followed by 35.6 mL of TFA. The solution was allowed to stir in the dark at 25 °C for 2 hours. CH_2Cl_2/TFA was removed by evaporation. The mixture was then redissolved in EtOAc (80 mL), washed with 10% $NaHCO_3$ to pH 5, and then washed with brine (1 x 50 mL). The product was purified by silica gel flash chromatography (65:25:4 $CHCl_3$/MeOH/H_2O, R_f = 0.44) to give the final product (293 mg) in 64% yield. ^{1}H NMR (300 MHz, $CDCl_3$) δ ppm: 7.92 (d, J_{HH} = 8.1 Hz, 1H), 7.73 (d, J_{HH} = 7.5 Hz, 3H), 7.64 (m, 3H), 7.38 (m, 5H), 6.15 (m, 1H), 6.00 (m, 1H), 4.58 (m, 8H), 2.67 (m, 2H), 1.73 (m, 3H). ^{13}C NMR (125.8 MHz, $CDCl_3$) δ ppm: 171.1, 156.7, 147.5 (d, J_{PC} = 4.0 Hz), 144.5 (d, J_{PC} = 21.7 Hz), 142.0, 137.4 (m), 134.8 (m), 129.9 (m), 128.5, 128.3, 127.9 (d, J_{PC} = 4.0 Hz), 126.0 (m), 125.4 (m), 120.7, 117.3 (dd, J_{PC} = 9.7 Hz, J_{PC} = 16.1 Hz), 74.7 (m), 68.6 (m), 68.2 (m), 63.5 (m), 54.8 (d, J_{PC} = 7.4 Hz), 47.7 (m), 20.2, 14.9 (dd, J_{PC} = 15.0 Hz, J_{PC} = 7.4 Hz). ^{31}P NMR (121.5 MHz, $CDCl_3$) δ ppm: -3.09. ESI-MS $[MNa]^+$ 632.1412 (obsd), 632.1405 (calcd). See spectra 2.16, 2.17, and 2.18.

2-3. Peptides for Biological Studies

Characterization of peptides by either the interassembly or the building block approach:

cpCS: Ac-RRGcpSPG-CONH$_2$

Reverse phase HPLC (t_R = 20.0 min). MS (ESI) *m/z* calculated for $C_{34}H_{55}N_{14}O_{13}P$: 899.9 $(M+H)^+$. Found *m/z* 899.6 $(M+H)^+$. See spectrum 2.19.

cpERK: Ac-PLcpSPAKLAFQFP-CONH$_2$

Reverse phase HPLC (t_R = 26.6 min). MS (ESI) *m/z* calculated for $C_{75}H_{109}N_{16}O_{20}P$: 1585.8 $(M+H)^+$ and 793.4 $(M+2H)^{2+}$. Found *m/z* 1586.5 $(M+H)^+$, 793.7 $(M+2H)^{2+}$. See spectrum 2.20.

cpRSLP: Ac-MARRLYRcpSLPAKK-CONH$_2$

Reverse phase HPLC (t_R = 21.2 min). MS (ESI) *m/z* calculated for $C_{80}H_{135}N_{26}O_{21}PS$: 1861.1 $(M+H)^+$, 621.0 $(M+3H)^{3+}$, and 466.0 $(M+4H)^{4+}$. Found *m/z* 621.8 $(M+3H)^{3+}$, 466.8 $(M+4H)^{4+}$. See spectrum 2.21.

cpPAX: Ac-CSSPPLPGALcpSPLYGVPET-CONH$_2$

Reverse phase HPLC (t_R = 23.3 min). MS (ESI) *m/z* calculated for $C_{95}H_{144}N_{21}O_{32}PS$: 2156.3 $(M+H)^+$ and 1101.7 $(M+2H+2Na)^{2+}$. Found *m/z* 1102.5 $(M+2H+2Na)^{2+}$. See spectrum 2.22.

2-4. Quantum Yield Calculations

Samples were irradiated with a UVP UV Transilluminator, 365 nm, 7330 μW/cm^2 at the surface, in vessels with a 1mm path length. The quantum yield, Φ, of each peptide was determined by comparison to the known Φ of caged phosphate as previously reported.[12] An A_{350} value was measured for each sample at a 1mm path length in water, pH 7.1. Below is a sample calculation for cpERK.

$$\Phi_{cpERK} = \Phi_{cp} \times \frac{\%\Delta cpERK}{\%\Delta cp} \times \frac{A_{350}\ cp}{A_{350} cpERK}$$

$$\Phi_{cpERK} = 0.54 \times \frac{16.38\%}{18.50\ \%} \times \frac{0.01911}{0.03506}$$

$$\Phi_{cpERK} = 0.2606$$

$$\Phi_{cpERK} = 0.26$$

Data Table for caged phosphate (500 μM):

Peak Name	Retention Time (minutes)	Average Area	Average Normalized Area	Average A_{350} in water, pH 7.1
Inosine (t = 0)	3.36	0.559	1.000	-----
Caged P (t = 0)	14.91	16.737	29.941	0.01911
Inosine (t = 15 s)	3.21	0.686	1.000	-----
Caged P (t = 15 s)	14.69	16.739	24.401	-----

Data Table for cpERK (547 μM):

Peak Name	Retention Time (minutes)	Average Area	Average Normalized Area	Average A_{350} in water, pH 7.1
Inosine (t = 0)	3.30	0.641	1.000	----
cpERK (t = 0)	30.47	24.664	38.477	0.03506
Inosine (t = 15 s)	3.37	0.713	1.000	----
cpERK (t = 15 s)	30.58	22.939	32.173	----

ΦcpERK = 0.26

Data Table for cpRSLP (266 μM):

Peak Name	Retention Time (minutes)	Average Area	Average Normalized Area	Average A_{350} in water, pH 7.1
Inosine (t = 0)	2.90	0.5916	1.000	----
cpRSLP (t = 0)	23.99	5.0259	8.495	0.01477
Inosine (t = 15 s)	2.98	0.6540	1.000	----
cpRSLP (t = 15 s)	23.96	4.9348	7.546	----

ΦcpRSLP = 0.42

Data Table for cpCS (757 μM):

Peak Name	Retention Time (minutes)	Average Area	Average Normalized Area	Average A_{350} in water, pH 7.1
Inosine (t = 0)	3.26	0.6310	1.000	----
cpCS (t = 0)	17.92	47.3558	75.049	0.04952
Inosine (t = 15 s)	3.28	0.6251	1.000	----
cpCS (t = 15 s)	17.93	38.3391	61.333	----

ΦcpCS = 0.21

cpPAX: quantum yield not measured; peptide was never used in biological studies.

Testing photolysis sources

The sources used in this study were as listed in Table 2.2. In all cases, the sample consisted of 274 μM cpERK, 500 μM inosine, and 500 μM DTT. A sample was irradiated for 9 minutes total, and aliquots were removed from each sample at 2 minute increments for HPLC analysis. The percent loss of caged phosphopeptide was determined as for quantum yield measurements.

References

(1) Rothman, D. M.; Vazquez, M. E.; Vogel, E. M.; Imperiali, B. "General Method for the Synthesis of Caged Phosphopeptides: Tools for the Exploration of Signal Transduction Pathways," *Organic Letters* **2002**, *4 (17)*, 2865-2868.

(2) Rothman, D. M.; Vazquez, M. E.; Vogel, E. M.; Imperiali, B. "Caged Phospho-Amino Acid Building Blocks for Solid-Phase Peptide Synthesis," *Journal of Organic Chemistry* **2003**, *68 (17)*, 6795-6798.

(3) Pinna, L. A.; Ruzzene, M. "How Do Protein Kinases Recognize Their Substrates?" *Biochimica et Biophysica Acta - Molecular Cell Research* **1996**, *1314 (3)*, 191-225.

(4) Kupihar, Z.; Varadi, G.; Monostori, E.; Toth, G. "Preparation of an Asymmetrically Protected Phosphoramidite and Its Application in Solid-Phase Synthesis of Phosphopeptides," *Tetrahedron Letters* **2000**, *41 (22)*, 4457-4461.

(5) Wakamiya, T.; Saruta, K.; Yasuoka, J.; Kusmoto.S. "An Efficient Procedure of Solid-Phase Synthesis of Phosphopeptides by the Fmoc Strategy," *Chemistry Letters* **1994**, 1099-1102.

(6) Kaplan, J. H.; Forbush, B., III; Hoffman, J. F. "Rapid Photolytic Release of Adenosine 5'-Triphosphate from a Protected Analogue: Utilization by Na:K Pump of Human Red Blood Cell Ghosts," *Biochemistry* **1978**, *17 (10)*, 1929-1935.

(7) Emsley, J.; Hall, D. In *The Chemistry of Phosphorus: Environmental, Organic, Inorganic, Biochemical and Spectroscopic Aspects*; Eds.; Harper and Row: London, **1976**, 563.

(8) Glading, A.; Lauffenburger, D. A.; Wells, A. "Cutting to the Chase: Calpain Proteases in Cell Motility," *Trends in Cell Biology* **2002**, *12 (1)*, 46-54.

(9) Yaffe, M. B. "Cell Migration/Signaling Glue Grant," *personal communication*, **2001**.

(10) Turner, C. E. "Molecules in Focus: Paxillin," *International Journal of Biochemistry and Cell Biology* **1998**, *30 (9)*, 955-959.

(11) Huang, C. "Paxillin Peptides," *personal communication*, **2002**.

(12) Ellis-Davies, G. C. R.; Kaplan, J. H. "Nitrophenyl-EGTA, a Photolabile Chelator that Selectively Binds Ca^{2+} with High Affinity and Releases it Rapidly Upon Photolysis," *Proceedings of the National Academy of Sciences, U. S. A.* **1994**, *91 (1)*, 187-191.

Chapter 3
Revealing a Global Temporal Role for 14-3-3 in Cell Cycle Regulation

Portions of this chapter have been published in *Nature Biotechnology* as noted in the text.[1] Dr. Justine Stehn (Yaffe Lab, M. I. T.) performed cell lysate assays; Dr. Ahnco Nguyen (Yaffe Lab, M. I. T.) performed Isothermal Calorimetery (ITC) and cell cycle analysis assays.

Introduction

There is considerable interest in studying phosphoserine/threonine-binding domains, which constitute an expanding collection of modular signaling domains with significant roles in regulating pathways such as mitosis, cell response to DNA damage, and apoptosis.[2] These domains contain a subset termed 14-3-3 proteins, which have been extensively studied. The name of the protein family comes from the fraction number of DEAE-cellulose chromatography and its migration position in starch-gel electrophoresis. Studies have revealed that more than 50 signaling molecules can be regulated by 14-3-3 proteins, and they are thought to play a pivotal role in the regulation of protein kinase activation, cell cycle control, neural development and bacterial or viral pathogenesis.[3] The 14-3-3 family comprises dimeric, α-helical, cup-shaped molecules present in high abundance in eukaryotic cells. In humans there are seven distinct isoforms that bind to each other to form homodimers or heterodimers which are biologically active.[1] The dimers form a cleft which preferentially binds phosphopeptides or phosphoproteins containing an **RS**x[*p***S**/*p***T**]x**P** or **R**xθx[*p***S**/*p***T**]x**P** motif[4, 5] (uppercase bold denotes the most conserved residues, the prefix *p* denotes phosphoryl-, θ denotes aromatic or aliphatic residues, and x represents any amino acid). While the structural basis of 14-3-3 protein interactions with a target peptide have been elucidated, the physiological effect of the 14-3-3 family in mammalian cells remained elusive.[3]

Most 14-3-3 family members display functional redundancy since the residues that line the binding cleft are highly conserved among all 14-3-3 isoforms.[6] The multiplicity of isoforms present in cells creates functional redundancy in the case that one isoform is knocked out or down-regulated within the cell. A single isoform knockout would be compensated for with the other six isoforms, and simultaneously knocking out all seven isoforms is technically daunting, if not impossible. Therefore, classical genetics approaches to elucidate the global and temporal roles for 14-3-3 proteins are not suitable for studying this protein family. We aimed to determine the global and temporal role of 14-3-3 protiens in live cells by effectively knocking out the entire protein family upon uncaging of a phosphopeptide designed to bind within the 14-3-3 dimer

cleft. In this case study, the caged phosphopeptide acts as a masked inhibitor of 14-3-3. The peptide sequence MARRLYRSLPAKK was designed by structural analysis of the 14-3-3 binding cleft;[4] the highlighted serine residue is that which is phosphorylated when bound to 14-3-3.

At the time of the studies discussed below, 14-3-3 had been implicated in the regulation of mitosis by association with several proteins known to regulate mitotic entry, including Cdc25C, Chk1, Wee1 and Cdk2.[1, 7, 8] However, its precise role was unknown. Additionally, it was thought that S-phase checkpoint arrest after DNA damage did not involve 14-3-3; rather, Chk1/2-regulated ubiquitin-mediated degradation of Cdc25A was thought to cause the arrest.[9, 10] With the caged phosphopeptides, we were able to determine a temporal functional role for the 14-3-3 family at M-phase entry in cells cycling normally and at S-phase checkpoint for cells with DNA damage.

Results and Discussion

3-1. Design and Synthesis of Peptides for In Vitro Studies

In order to effectively bind all isoforms of 14-3-3 in cell systems, either *in vitro* or *in vivo*, several series of peptides containing the sequence MARRLYRSLPAKK were synthesized. The first series of N-acetyl capped peptides were synthesized for *in vitro* binding assays. The complete sequences are shown in Figure 3.1. Three of the peptides are in different phosphorylation states: unphosphorylated (Ac-RSLP), phosphorylated (Ac-cpRSLP), or caged phosphorylated (Ac-cpRSLP). The last peptide, Ac-cpMAQQ, represents a scrambled sequence that includes a centrally located caged phosphoserine residue but is missing the key binding residues flanking the phosphoserine such that the uncaged peptide cannot bind 14-3-3. This peptide was synthesized to serve as an ultimate negative control: the uncaging event and sudden appearance of phosphopeptide should have no effect on the system under study.

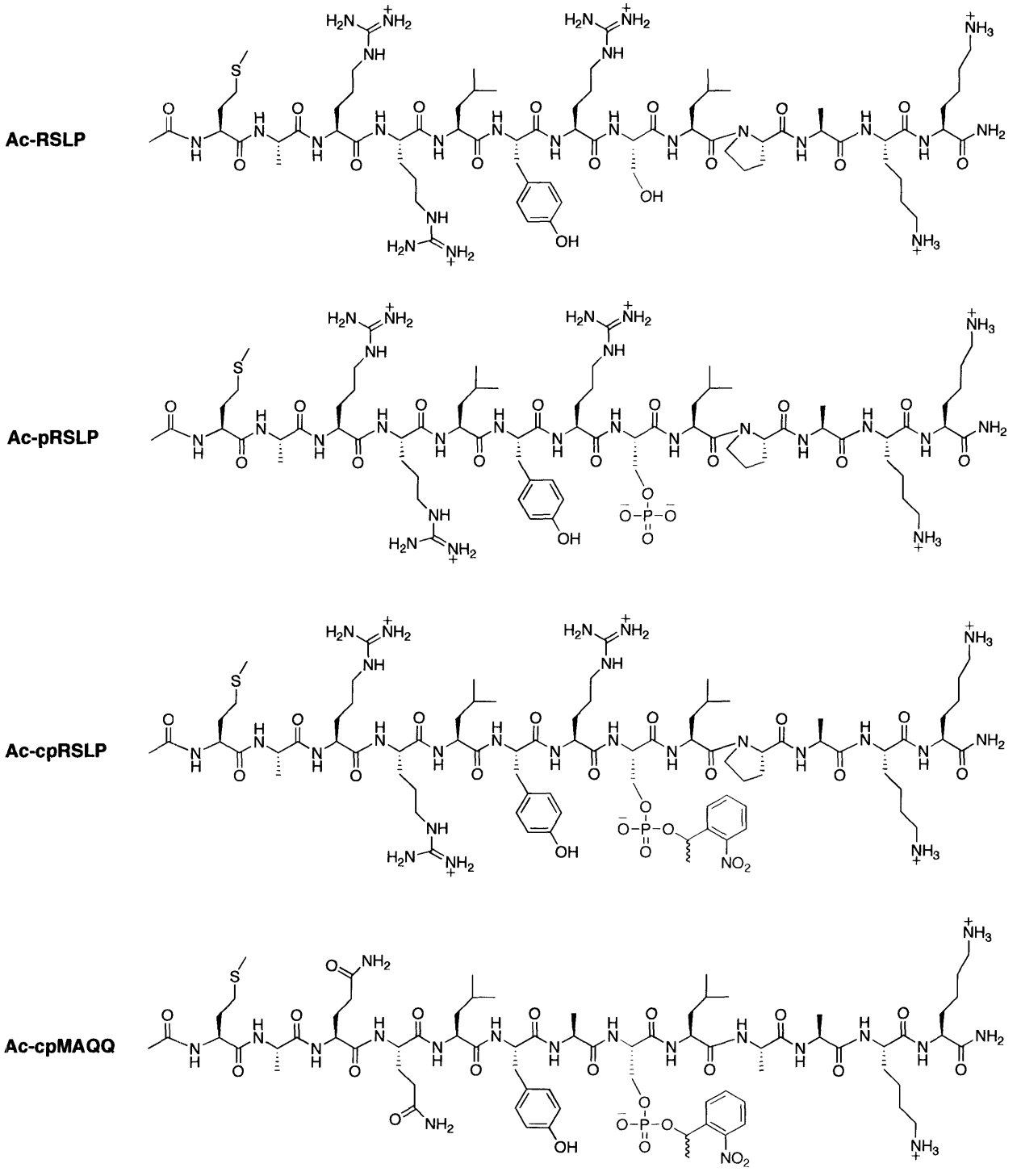

Figure 3.1. Peptides synthesized for *in vitro* binding studies of 14-3-3 proteins. Three peptides represent three phosphorylation states of the target peptide, Ac-RSLP, Ac-pRSLP, and Ac-cpRSLP. The last peptide represents a mutant sequence for a negative control, Ac-cpMAQQ. The serine of interest is highlighted in red.

3-2. In Vitro Binding of Peptides to 14-3-3

The quantum yield of Ac-cpRSLP was successfully determined (Φ = 0.43, Chapter 2). Also, the amount of phospho-peptide released under the conditions used for live cell assays was measured. After 90 seconds of irradiation at λ = 365nm, approximately 80% of the phosphopeptide was photoliberated as determined by HPLC analysis (Figure 3.2). Next, isothermal calorimetry (ITC) and *in vitro* assays were performed in collaboration with the Yaffe lab (Department of Biology, M. I. T.) to determine the peptides binding to 14-3-3 proteins. Isothermal Calorimetery measurements revealed a 35,000-fold increase in the binding affinity of the phosphopeptide for 14-3-3-β after uncaging. The binding constant of the caged phosphopeptide was 900 μM, and after UV-irradiation, the binding constant was 25 nM (Figure 3.3).

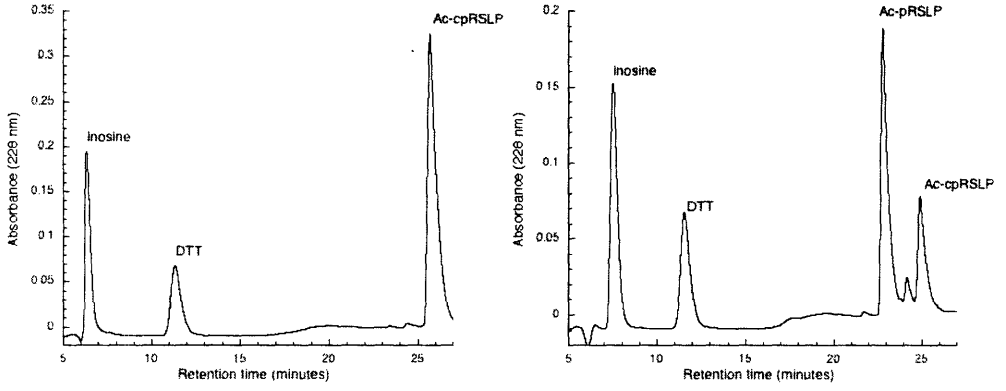

Figure 3.2. Photochemical cleavage of Ac-cpRSLP peptide.[1] Ac-cpRSLP was analyzed by HPLC before or after UV-A irradiation (left or right panel, respectively). Ac-cpRSLP and Ac-pRSLP were confirmed by mass spectrometry (ESI-MS). Internal marker inosine and dithiothreitol (DTT) are labeled.

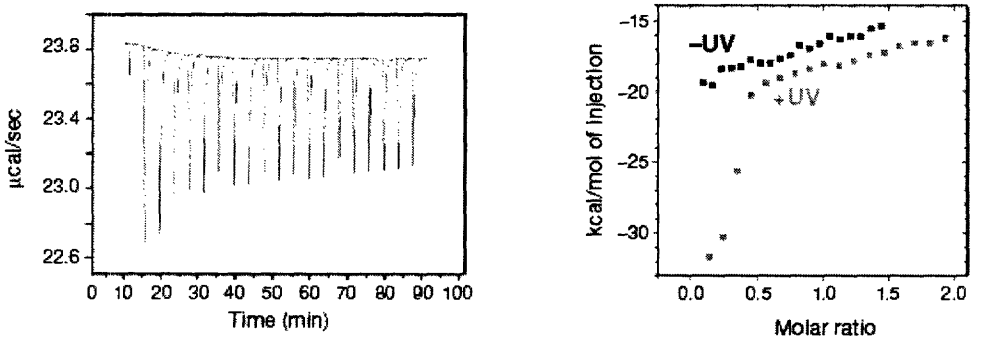

Figure 3.3. ITC demonstrates UV-A induced release of high-affinity 14-3-3 peptide.[1] Left panel: UV-A irradiated peptide was serially pulse-injected into a solution of 14-3-3-β. Right panel: Analysis of the heat trace shows low- and high-affinity 14-3-3 binding peptides with binding constants of ~900 μM and 25 nM, respectively (gray squares). Without UV-A-irradiation, only the low-affinity species is present (black squares).

Next the peptides were tested to determine the potential to displace endogenous ligands for 14-3-3 in whole cell lysates. In the first assay, bead immobilized glutathione S-transferase (GST)-14-3-3-β and ζ were incubated together with the peptide to be tested, and then subjected to endogenous ligands from U2OS cell lysates (U2OS, osteosarcoma cells). Each peptide, RSLP, pRSLP, cpRSLP (no UV), cpRSLP (with UV), and a control without peptide was incubated with the 14-3-3 beads followed by cell lysate. Binding was detected by SDS-PAGE and Western analysis blot with a mode 2 antibody to probe for phospho-specific binding events (Figure 3.4a). It appeared that cpRSLP has the activity of pRSLP after UV treatment, and could compete off the endogenous ligands. Additionally, neither RSLP nor cpRSLP without UV treatment affected ligand binding to 14-3-3. The second *in vitro* assay involved the same competition experiment, but the peptides were first incubated in cell lysate, then added to the immobilized 14-3-3 and probed for binding (Figure 3.4b). The results were identical to those of the first assay. These experiments also demonstrated that the proteases present within a cell would not degrade the caged or uncaged peptide. Western analysis revealed that the peptides were indeed stable to the components of a cell system.

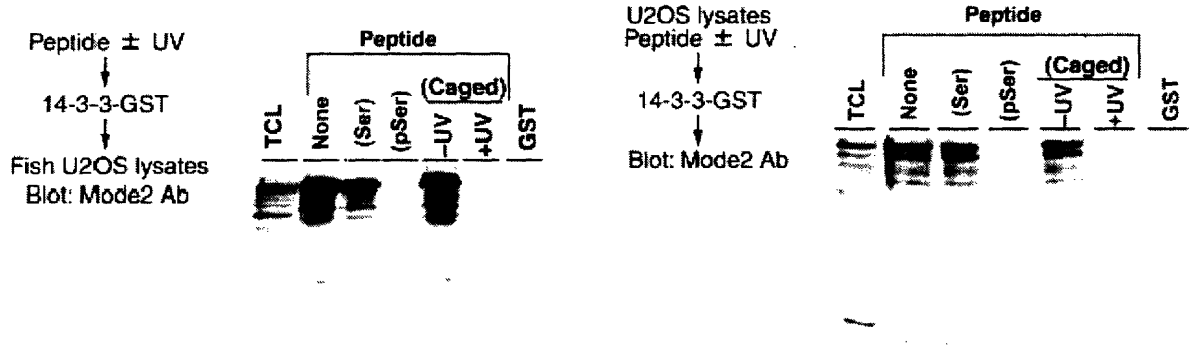

Figure 3.4. Uncaged but not caged phosphopeptide competes with endogenous cellular proteins for binding to 14-3-3.[1] Left panel: Ac-cpRSLP (Caged) before or after UV-A-irradiation was incubated with bead-immobilized GST-14-3-3-β and ζ, then added to U2OS cell lysates. 14-3-3 bound proteins detected by immunoprecipitation with a polyclonal antibody against the 14-3-3 binding motif. Controls show proteins bound by GST-14-3-3 beads pre-incubated with Ac-pRSLP (pSer), Ac-RSLP (Ser), with no peptide, or by beads containing GST alone. TCL denotes total cell lysate. Right panel: Ac-cpRSLP (Caged) before or after UV-A-irradiation were incubated with U2OS cell lysates for 30 minutes, then GST-14-3-3-β and ζ beads were added and bound proteins detected as in the left panel. Controls are as described in the left panel.

3-3. Design and Synthesis of Peptides for Live Cell Assays

In order to introduce the caged phospho-peptides into large living cell populations, a mild and efficient method of incorporation was desired. Protein Transduction Domains (PTDs) are cell internalization sequences derived from natural proteins known to translocate biomolecules across cell membranes via a passive transport mechanism. Therefore, these cell membrane permeable sequences are able to carry cargo by what has been dubbed a "Trojan horse" approach.[11] Both an analog of the HIV-TAT protein transduction domain, PTD4, and the single substitution mutant of the third helix of the Antennapedia homeodomain, 3Ah, are well characterized in the literature, displaying the ability to carry in various types of cargo.[12, 13] Three PTDs were analyzed for introducing caged phosphopeptides into cell populations. One, 3Ah, was most efficient in its relative ease of synthesis and efficient cellular uptake.

The three PTDs tested were: PTD4[12] (GGGYARAAAYQARA-$CONH_2$), and arginine tryptophan analog of 3Ah[11] (RRWRRWWRRWWRRWRR), and 3Ah[13] (RQIKIWFQNRR-Nle-KWKK-$CONH_2$). A FITC (fluorescein-5-isothiocyanate) tag was coupled to the N-terminus of each internalization sequence. The spectroscopic properties of FITC allowed peptide visualization without interfering with the caging group (FITC λ_{abs} = 494 nm, λ_{em} = 519 nm; nitrophenylethyl $\lambda_{abs} \leq$ 365 nm). Due to the difficulty of cleavage and purification of the "all" arginine and tryptophan analog of 3Ah, persuit of this sequence was discontinued. PTD4 was successfully synthesized with an N-terminal fluorescein tag. The single substitution mutant 3Ah (the native Antennapedia homeodomain contains a methionine instead of norleucine) was synthesized with an N-terminal fluorescein tag in place of the arginine-tryptophan analog. This sequence was slightly more difficult to purify than PTD4 because the arginine protecting groups used in Fmoc SPPS required longer cleavage times (see Chapter 2), while the tryptophan residues favored shorter cleavage times to prevent alkylation on C3 of the indole ring. Ultimately, carefully timed conditions with high scavenger concentrations afforded the desired peptide.

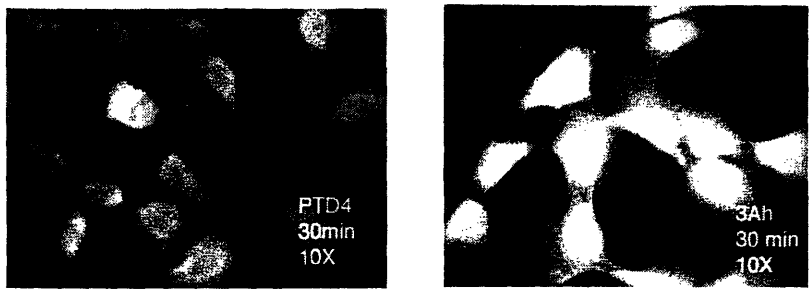

Figure 3.5. FITC-PTD4 and FITC-3Ah peptides in Rat1 fibroblasts. Cells at 70% confluence were incubated with 12.5 μM peptide for 30 minutes, rinsed with phosphate buffered saline, fixed with methanol, and imaged. Images are unaltered.

The fluorescein labeled peptides, FITC-PTD4 and FITC-3Ah, were tested for their ability to enter Rat1 fibroblast cells. Cells were approximately 70 % confluent when they were incubated with either peptide at 12.5 μM in culture media. Cells were rinsed several times before fixing and imaging. After 30 minutes, FITC-3Ah was internalized by the cells, which was evidenced by their bright fluorescence, while cells with FITC-PTD4 were rather dim (Figure 3.5). The 3Ah peptide was selected as the internalization sequence for future experiments because of its ability to permeate cells and its relative synthetic ease.

Initially the PTD was included at the C-terminal end of the target peptide sequence, cpRSLP, with a Gly-Gly linker. This construct was prepared by standard Fmoc-SPPS; the caged phosphoserine was installed *via* the interassembly approach as previously described (Chapter 2) and the peptide was stored in the dark. During the synthesis of the linear construct, test cleavages revealed that the cyanoethyl-group on the caged phosphate was still intact, even after successive rounds of coupling and with 20% piperidine Fmoc-deprotection treatments. Several deprotection conditions were tested to remove the cyanoethyl-group without causing β-elimination of the phosphate group. A limit to the base concentration was essential because too much base caused phosphate elimination (Figure 3.6b) before the desired cyanoethyl-group removal (Figure 3.6a). Conditions tested include: higher concentrations of piperidine in *N*,*N*-dimethylformamide (DMF) (25%, 30%, or 50% piperidine), 20% piperidine in *N*-methylpyrrolidinone (NMP, to break up any potential secondary structure resulting from the internalization sequence), and increasing concentrations of the strong base 1,8-diazabicyclo[5.4.0]undec-7-ene (DBU) in dichloromethane (20%, 25%, or 30% DBU). Unfortunately, all treatments resulted in either β-elimination of the

phosphate or no reaction. Therefore, a new approach was selected in which the cargo peptide was tethered to 3Ah via a disulfide bond.

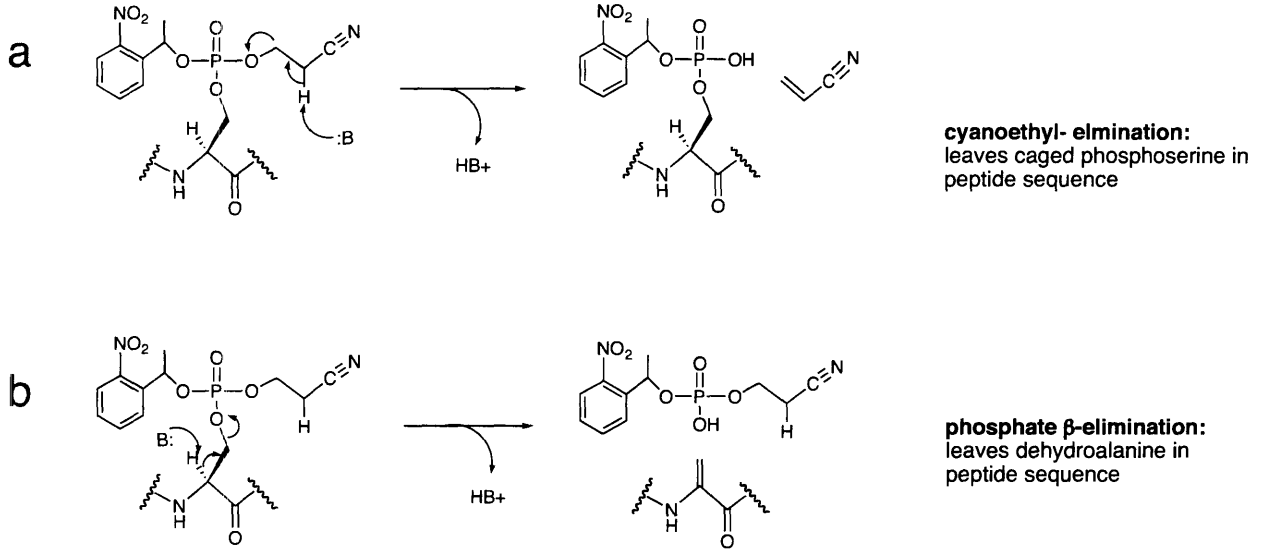

Figure 3.6. Possible β-elimination reactions during longer caged phosphopeptide synthesis. **a**) The desired elimination of the temporary cyanoethyl- protecting group. **b**) The undesired elimination of the entire phosphate group.

With the disulfide construct, it was possible to internalize the target peptides via the PTD; once in the reducing environment of the cell, the disulfide was reduced, and each peptide would then act independently within the cell. Towards this end, heterodimerization of cysteine containing peptides was previously reported.[14] A more recent study compared a releasable disulfide linked internalization-target sequence conjugate to a non-releasable construct.[15] While the non-releasable construct efficiently internalized the target sequence, the *in vivo* activity suffered significantly. In contrast, the disulfide-linked peptide had the ability to be internalized and was able to affect the target system with high success.[15] The loss of function in the non-releasable construct may have stemmed from secondary structure interactions of the extended peptide. An alternative structural state caused by interactions with the PTD may prevent a given peptide from reaching the intended target.

Fluorescein tagged RSLP target sequences were linked to the 3Ah sequence by a disulfide bond as in Scheme 3.1. Fluorescein labeled-peptides were synthesized using standard Fmoc-SPPS; caged phosphopeptides were synthesized using the building block approach described in Chapter 2. The 3Ah peptide **15** was synthesized by standard Fmoc-SPPS, and activated with 2,2'-dithiobis(5-nitropyridine) to afford **16**. Next, **16** was coupled with the

Scheme 3.1 *Synthesis of FRSLP-SS-3Ah peptide series: peptides for cellular uptake.*

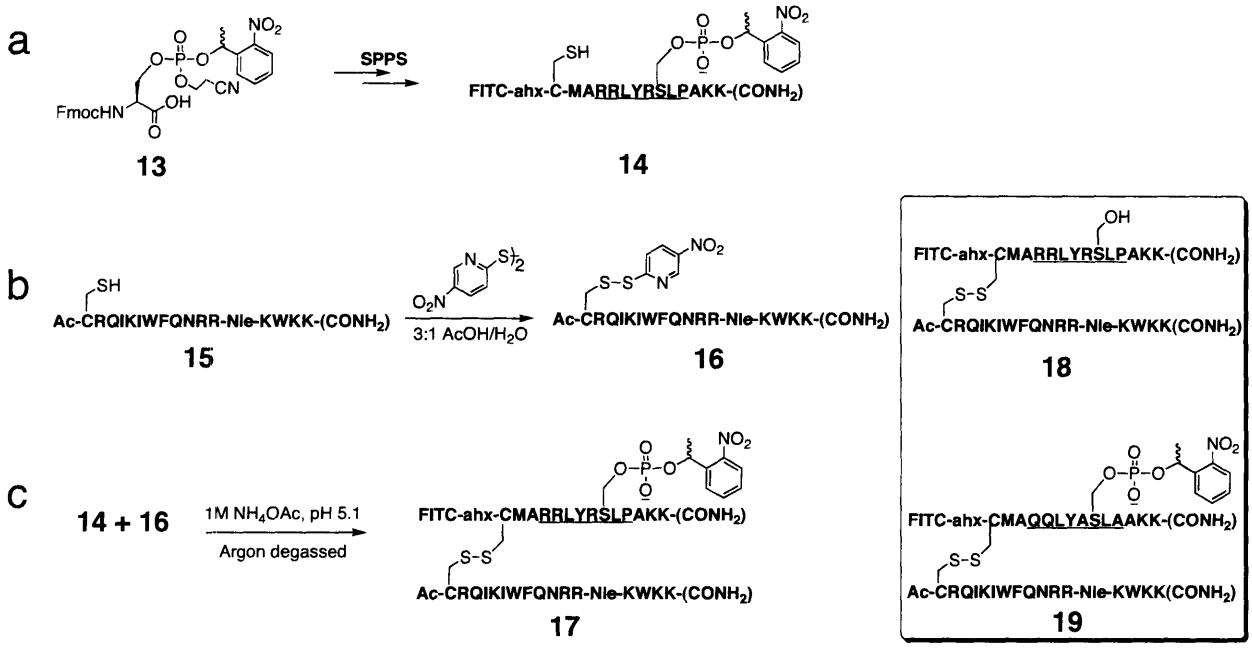

fluorescein-tagged peptide **14** in relatively low pH buffer (pH 5.1) under inert atmosphere to generate the disulfide linked construct **17**. The control constructs with a free serine (**18**) or the mutant sequence (**19**) were also synthesized in this manner. Several coupling conditions were tested in order to synthesize the desired mixed disulfide and avoid oxidation to symmetric disulfides. Low pH (3 to 4) did not allow for proper coupling, most likely due to the large number of basic residues on both peptides. The positively charged species at low pH would repel each other and would not be able to come into close enough contact to react and form the heterodimer. Alternatively, if the pH was raised (6 to 8) to encourage the peptide association, base catalyzed oxidation and homodimerization became a significant problem. Unfortunately, the mutant peptide was particularly difficult to couple to the antennapedia (3Ah) portion. Figure 3.7 demonstrates the rapid decomposition of the desired compound (**19**) to deactivated 3Ah (**15**) and homodimerized scrambled peptide. This phenomenon was not found to be pH dependent, but rather time dependent; as the reaction progressed at various pH values (4 to 6) homodimer formed at similar rates. Ultimately, sufficient peptide was synthesized for biological experiments.

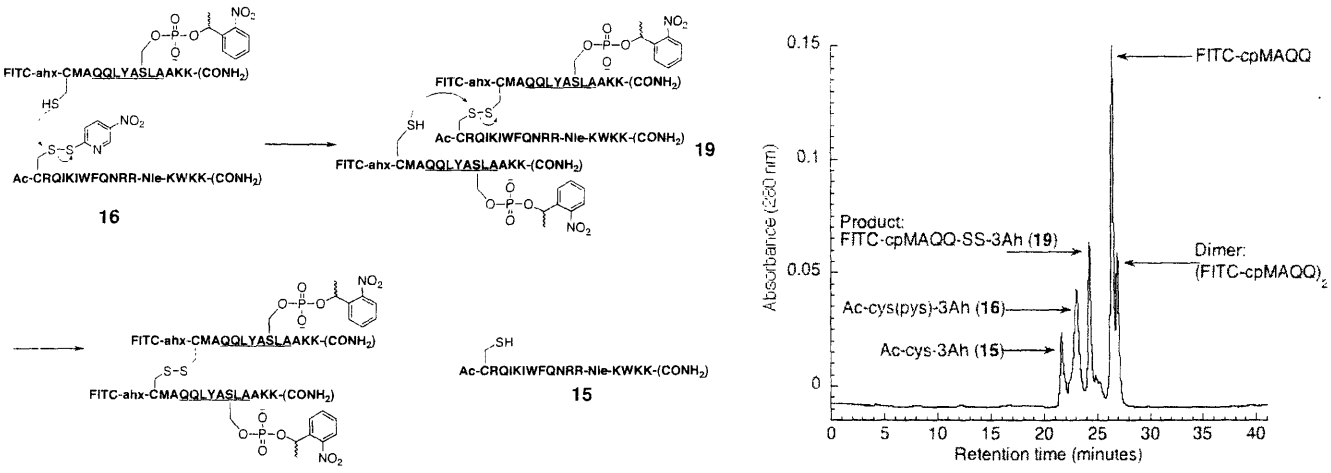

Figure 3.7. Decomposition of FMAQQ-SS-3Ah, **19**. Left panel: Schematic of decomposition process. Right panel: Analytical HPLC trace of reaction mixture at initial reaction time (t = 0). Products were assigned by ESI-MS and labeled appropriately.

The constructs were tested for their ability to be internalized into Rat 1 fibroblast cells, and compared to positive and negative controls as shown in Figure 3.8. All constructs tethered to 3Ah were taken up by cells significantly better than the corresponding non-3Ah analogs. It is interesting to note the background fluorescence observed in the FITC tagged RSLP peptides not conjugated to the 3Ah sequence. This low level of background may be due to the positively charged nature of the RSLP sequence (5 of the 13 residues are basic). A common feature of the natural protein transduction sequences is the prevalence of arginine and lysine residues. For further discussion of this phenomenon, please see reference 16.

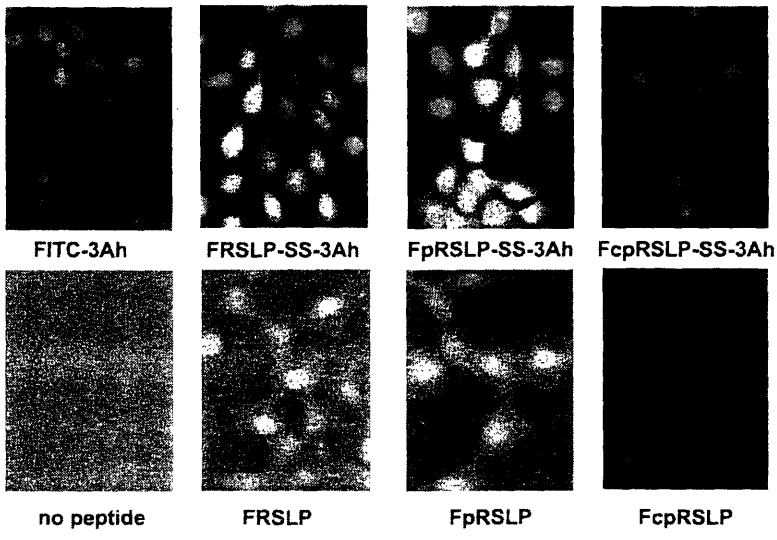

Figure 3.8. FRSLP and FRSLP-SS-3Ah peptide series in Rat1 fibroblasts Cells were grown to 70 % confluence and then incubated with 12.5 μM peptide for 30 minutes at 37°C. Cells were rinsed with phosphate buffered saline, fixed with methanol, and imaged. Images are unaltered.

With successful uptake into Rat 1 fibroblasts, peptides were introduced into U2OS cells (which are the preferred cells for the analysis of 14-3-3 function) and a series of control experiments were performed to ensure neither the free serine analog nor UV-A irradiation of the cells would cause any aberrant effects in the cells. U2OS cells were synchronized with mimosine (a plant nonprotein amino acid known to cause G1/S phase arrest)[17] and released from the block. One set of cells was left untreated (No UV), one set of cells was UV-A irradiated (+UV), and a third set of cells was treated with the free serine construct **18** and UV-A irradiated. All cells were monitored for their cell cycle progression by Fluorescence-Activated Cell Sorting (FACS) analysis (Figure 3.9). No difference was observed in the progression through the cell cycle with the various conditions tested.

*3-4. Defining a Global Temporal Role for 14-3-3**

At the time of the experiments, the 14-3-3 family of proteins had been implicated in regulation of mitotic-phase entry by association with various proteins known to regulate this portion of the cell cycle. However, 14-3-3 interacted with proteins that either had positive or negative effects on G2/M phase progression.[1, 7, 8] Therefore, in order to elucidate the role of 14-3-3, caged phosphopeptides were used to effectively knock out the 14-3-3 family in synchronized cells so that downstream cell cycle effects could be monitored. U2OS cells were synchronized with mimosine in G1/S, released, and treated with either peptide **17** or **18** at a time point corresponding to late S phase or very early G2 (t = 9 h after mimosine release). After 30 minutes, cells were exposed to UV-A irradiation (λ = 365 nm) for 90 seconds and analyzed at subsequent time points by both FACS analysis and immunohistochemistry with an antibody to the known mitotic marker phospho-histone H3 (Figure 3.10).

* A significant portion of this section is taken from reference 1, which was originally written by Professor Michael Yaffe (M. I. T. Department of Biology).

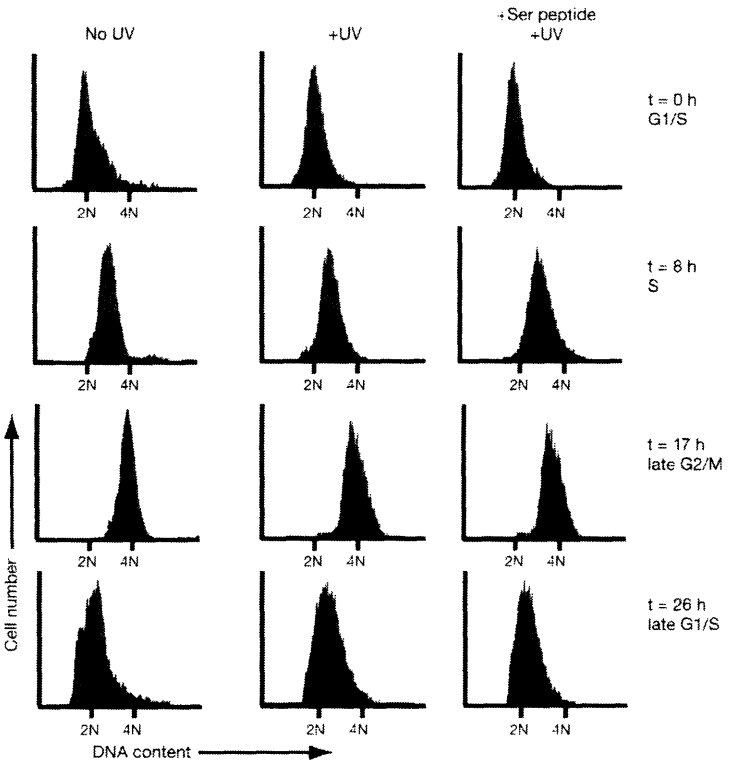

Figure 3.9. UV-A irradiation of cells in the absence or presence of serine-containing control peptides does not affect cell cycle progression.[1] U2OS cells were synchronized with mimosine. The cells were released, and either left untreated, UV-A-irradiated or UV-A irradiated 30 minutes after addition of the serine control peptide **18**. At various time points cells were analyzed by FACS. No difference was observed under any of the three conditions for progression through the cell cycle.

Control experiments demonstrated that UV-A irradiation 9 h after mimosine release does not disturb subsequent cell cycle progression (Figure 3.10a). Next, synchronized cells in the absence or presence of the caged phosphopeptide **17** were UV-A irradiated and their cell cycle progression monitored. As seen in Figure 3.10b and c, the population treated with **17** demonstrated three key features due to the loss of 14-3-3 function. First, there was a significant amount of cell death associated with peptide treated cells 5 h after 14-3-3 disruption (59 % live cells versus 80 % live cells in the control population). Second, at this same time point, many of the live cells displayed an accelerated and intense phospho-histone H3 staining relative to the control (Figure 3.10d). This suggests that disruption of 14-3-3 at the S/G2 boundary leads to uncontrolled premature entry into M phase accompanied by mitotic catastrophe. Finally, there was a significant reduction in the stable G1 cell population and an associated increase in the G2/M population by 17 hours post-mimosine release in the peptide treated cells versus the

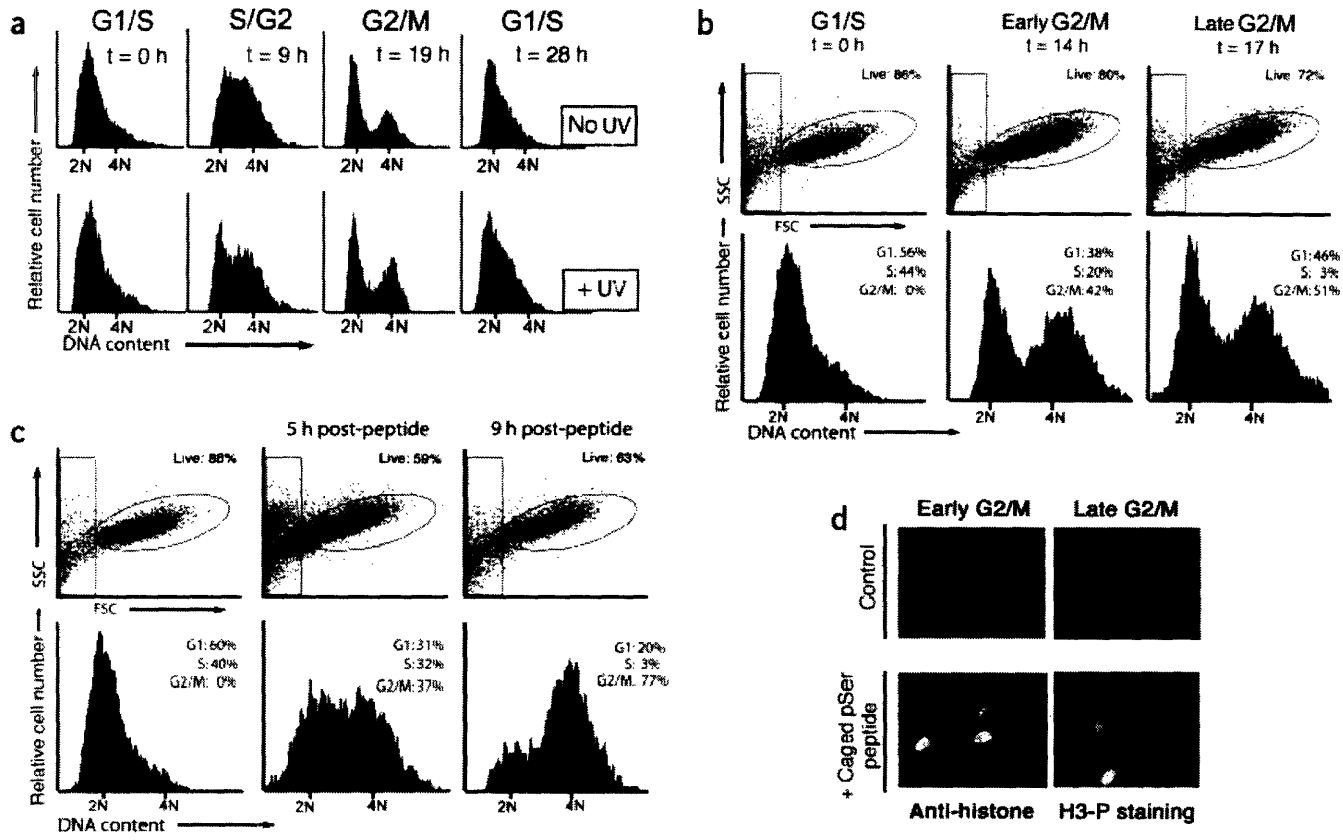

Figure 3.10. Coordinated, synchronous loss of 14-3-3 function results in aberrant cell cycle progression and G1 release.[1] **a**) U2OS cells were synchronized with mimosine and released; 9 h after release one population of cells was UV-A irradiated and the control population left untreated. Cells were collected for FACS analysis of DNA content as a measure of cell cycle progression. **b**, **c**) The same passage of cells from **a** were synchronized with mimosine and released. At 9 h post-release, cells in **c** were treated with caged phosphopeptide **17**; at 9.5 h both populations of cells were UV-A irradiated. Cells were analyzed by FACS for cell cycle progression. **d**) Cells from **b** and **c** were fixed and stained with an antibody that recognizes phospho-histone H3.

control sample. These results serve as evidence that 14-3-3 proteins normally regulate the onset and timing of mitosis in cycling cells as well as play a critical role in maintaining stable interphase arrest in non-cycling cells. Most notably, synchronization of the cells followed by controlled uncaging of the inhibitor peptide allowed the elucidation of the 14-3-3 protein family role in real time.

Next, the caged phosphopeptide was used to examine the function of 14-3-3 in S phase checkpoint function in response to DNA damage. S phase arrest after DNA damage results from Chk1/2-regulated ubiquitin-mediated degradation of CdC25A, a process that was not thought to involve 14-3-3 binding.[9, 10] In order to test if 14-3-3 proteins are necessary for S phase checkpoint function, U2OS cells were synchronized, released, and a subset was incubated with the peptide **17** during mid-S phase (6.5 hours post release). Cells were then exposed to UV-A and UV-B

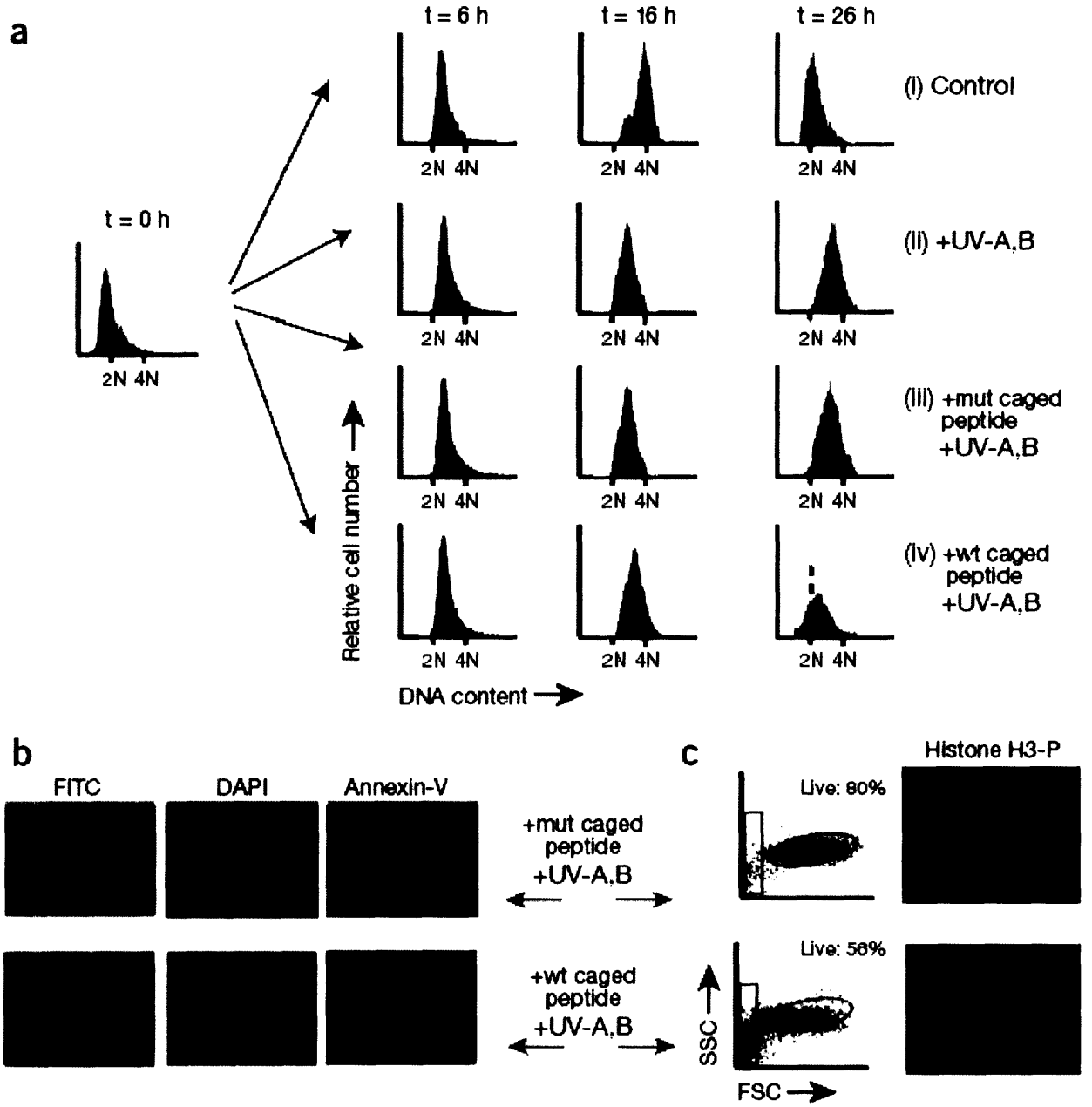

Figure 3.11. Coordinated, synchronous loss of 14-3-3 function results in dysfunctional, DNA-damage induced S phase cell cycle checkpoint.[1] **a**) U2OS cells were synchronized with mimosine and split into four separate conditions: **i**) control untreated, nonirradiated cells, **ii**) cells exposed to UV-A/B irradiation 7 h after release, **iii**) cells pre-incubated with **19** before UV-A/B irradiation, and **iv**) cells treated with **17** before UV-A/B irradiation. Cell cycle progression was analyzed by FACS. The sub-G1 population lies to the left of the dashed red line in the lower right panel in **iv**. **b**) Cells treated with mutant (**19**) or wild-type (**17**) peptide from panels **iii** or **iv** in **a** were analyzed for programmed cell death 9 h post irradiation. 40 to 50 % of the **17** treated cells stained positively with PE-conjugated annexin-V. **c**) Cells from **iii** and **iv** that survived 19 h post irradiation were examined for cell size by FACS and for histone H3-phosphorylation.

irradiation (λ = 365 nm and 302 nm, respectively) for 90 seconds to simultaneously uncage **17** and induce DNA damage.[18] The control peptide **19** was tested for any effect on S phase

checkpoint function under identical conditions. Peptide **19** corresponds to Ac-cpMAQQ (Figure 3.1) in which the critical residues necessary for 14-3-3 binding had been mutated. All cell populations were analyzed by FACS at different time points after mimosine release (Figure 3.11a). Non-irradiated control cells progressed through the normal cell cycle while irradiated control cells initiated and maintained S phase arrest throughout the ensuing 19 hours (Figure 3.11a, panels i and ii). Cells that were pretreated with the mutant control peptide **19** displayed the same S phase arrest as irradiated control cells (Figure 3.11a, panel iii). However, cells that were pretreated with peptide **17** (wild type or wt) were unable to sustain S phase arrest (Figure 3.11a, panel iv), resulting in 40 to 50 % early apoptotic death by 16 h post release as revealed by annexin-V staining (Figure 3.11b). Additionally, a sub-G1 population was visualized by propidium iodine staining after 26 hours post release (Figure 3.11a, panel iv). A sub-G1 population by FACS analysis denotes cells undergoing apoptosis; they will have lost some of their DNA due to DNA fragmentation in later apoptosis. By 26 hours, the remaining surviving cells were smaller (note the shift in the moment of forward and side-scattering ellipse in Figure 3.11c), and displayed prominent phospho-histone H3 staining (Figure 3.11c), suggesting that these cells were undergoing mitotic catastrophe. The global disruption of 14-3-3 resulted in a loss of S phase checkpoint function after UV-B irradiation, and this observation was unexpected since S phase checkpoint function had been thought to be mediated by Chk-1/2 regulated degradation of Cdc25A. However, with the global temporal role for 14-3-3 observed in these experiments, it may be that 14-3-3 negatively regulates Cdc25A. Further supporting these observations, it was recently found that Cdc25A binds 14-3-3 after Chk1 activation.[19] Once again, it is noteworthy that the technology and availability of caged phosphopeptides allowed the real time information that merits future investigation in 14-3-3 function.

Conclusion

Caged phosphopeptides were applied to 14-3-3 family protein binding experiments. A phosphopeptide sequence was designed to bind to active 14-3-3 dimers, and the corresponding caged phosphopeptide was synthesized. *In vitro*, the caged phosphopeptide could not bind 14-3-3; however, upon uncaging by UV-A irradiation the released peptide bound the target protein as well as the native phosphopeptide. Further, a series of peptide constructs was synthesized for studying the function of the 14-3-3 family of proteins in large cell populations. The disulfide

linkage between the target peptide and the PTD 3Ah was reduced within the cellular environment allowing each peptide to act independently of each other. Experiments that incorporated these peptides into synchronized cells determined two global temporal roles for the 14-3-3 protein family in cell cycle progression: 14-3-3 is necessary for G2/M phase progression and DNA-damage induced S phase checkpoint function. The technology integrated within the caged phosphopeptides afforded the observations that led to these conclusions. Cells could be synchronized and then the phosphopeptide released with temporal control; the phosphopeptide binds extremely tightly in the 14-3-3 binding cleft, essentially knocking out all isoforms of 14-3-3. It was only with this temporal control that the effects of simultaneously binding all isoforms of 14-3-3 within a cycling cell population could be observed.

Experimental

3-0. General Synthetic Procedures

All peptides were synthesized using standard Fmoc-SPPS as described in Chapter 2, unless otherwise noted. All caged phosphopeptides were synthesized *via* one of the methods described in Chapter 2. Additional chemical reagents were purchased from Aldrich; Fluorescein-5-isothiocyanate, isomer I (FITC) was purchased from Molecular Probes, Inc. (Eugene, OR).

3-1. Design and Synthesis of Peptides for In Vitro Studies

Ac-RSLP: Ac-MARRLYRSLPAKK-CONH$_2$

Reverse phase HPLC (t_R = 20.9 min). MS (ESI) *m/z* calculated for $C_{72}H_{127}N_{25}O_{16}S$: 1632.0 $(M+H)^+$ and 408.8 $(M+4H)^{4+}$. Found *m/z* 408.6 $(M+4H)^{4+}$.

Ac-pRSLP: Ac-MARRLYRpSLPAKK-CONH$_2$

Reverse phase HPLC (t_R = 20.3 min). MS (ESI) *m/z* calculated for $C_{72}H_{128}N_{25}O_{19}PS$: 1711.0 $(M+H)^+$, 571.0 $(M+3H)^{3+}$, and 428.5 $(M+4H)^{4+}$. Found *m/z* 572.3 $(M+3H)^{3+}$, 429.2 $(M+4H)^{4+}$.

Ac-cpRSLP: Ac-MARRLYRcpSLPAKK-CONH$_2$

Reverse phase HPLC (t_R = 21.2 min). MS (ESI) *m/z* calculated for $C_{80}H_{135}N_{26}O_{21}PS$: 1862.1 $(M+H)^+$, 621.0 $(M+3H)^{3+}$, and 466.0 $(M+4H)^{4+}$. Found *m/z* 621.8 $(M+3H)^{3+}$, 466.8 $(M+4H)^{4+}$.

Ac-cpMAQQ: Ac-MAQQLYAcpSLAAKK-CONH$_2$

Reverse phase HPLC (t_R = 25.6 min). MS (ESI) *m/z* calculated for $C_{73}H_{118}N_{19}O_{23}PS$: 1693.9 $(M+H)^+$. Found 1693.6 $(M+H)^+$, 846.8 $(M+2H)^{2+}$.

3-2. In Vitro Binding of Peptides to 14-3-3

Biological assays were performed as developed, optimized, and described in Reference 1. All peptides were dissolved in dH_2O, pH 7.1, with 5 mM DTT final concentration. Stock concentrations of Ac-RSLP and Ac-pRSLP were determined by quantitative amino acid analysis. Stock concentrations of Ac-cpRSLP and Ac-cpMAQQ were determined by UV absorbance (ε_{max} at A_{259} = 5700 $M^{-1}cm^{-1}$ in MeOH).

For binding competition assays in buffer, Ac-cpRSLP was irradiated in a 1 mm path length vessel with a UVP Transilluminator (365 nm, 7330 $\mu W/cm^2$) for five minutes, and aliquots were removed and analyzed by reverse phase HPLC to confirm release of the caging group.

For binding competition assays in total cell lysate, the caged peptide was first mixed with the cell lysate, and then irradiated in a glass vial for five minutes as above. The mixtures were then incubated with 14-3-3 β/ζ GST beads and prepared for the immuno-precipitation assay.

Western blot analysis used a Mode-2 primary antibody specific for the phospho-binding site of 14-3-3.[1]

3-3. Design and Synthesis of Peptides for Live Cell Assays

FITC-PTD4. Fmoc-PTD4 (Fmoc-GGYARAAARQARA-$CONH_2$) was synthesized by standard Fmoc-SPPS as described in Chapter 2. Fmoc-ε-aminohexanoic acid (ahx) (28.3 mg, 80 μmole) was coupled to the peptide (200 mg resin, 40 μmole) using standard coupling conditions. Following standard deprotection protocol, fluorescein-5-isothiocyanate (FITC) (31.2 mg, 80

μmole) in 2.0 mL DMF was added to the resin, and coupling was initiated with DIPEA (27.4 μL, 160 μmole). The coupling was allowed to run overnight in the dark. The resin was rinsed with DMF (2 x 5 mL x 1 min) and then with CH_2Cl_2 (2 x 5 mL x 1 min). The peptide was cleaved with 90% TFA, 5% CH_2Cl_2, 2.5% TIS, and 2.5% dH_2O for three hours in the dark. The peptide was triturated with diethyl ether, allowed to air dry, and purified by reverse phase HPLC (t_R = 23.36 min). MS (ESI) *m/z* calculated for $C_{81}H_{114}N_{26}O_{21}S$: 1820.7 $(M+H)^+$, 910.9 $(M+2H)^{2+}$, 607.6 $(M+3H)^{3+}$, and 455.9 $(M+4H)^{4+}$. Found *m/z*: 910.5 $(M+2H)^{2+}$, 607.3 $(M+3H)^{3+}$, and 455.7 $(M+4H)^{4+}$.

A stock solution was made in phosphate buffered saline (PBS+: 900 μM calcium chloride, 2.67 mM potassium chloride, 1.47 mM potassium phosphate, 500 μM magnesium chloride, 138 mM sodium chloride, 8.1 mM sodium phosphate, pH 7.1). The concentration was determined by UV absorbance (ε_{max} at A_{495} = 74,500 $M^{-1}cm^{-1}$ at pH 9.0) in 50 mM KPO_4H_2 buffer, pH 9.0.

FITC-3Ah. Fmoc-3Ah (Fmoc-RQIKIWFQNRR-Nle-KWKK-$CONH_2$) was synthesized by standard Fmoc-SPPS as described in Chapter 2. Fmoc-ε-ahx (28.3 mg, 80 μmole) was coupled to the peptide (200 mg resin, 40 μmole) using standard coupling conditions. Following standard deprotection protocol, FITC (31.2 mg, 80 μmole) in 2.0 mL DMF was added to the resin, and the coupling was initiated with DIPEA (27.4 μL, 160 μmole). The coupling was allowed to run overnight in the dark. The resin was rinsed with DMF (2 x 5 mL x 1 min) and then with CH_2Cl_2 (2 x 5 mL x 1 min). The peptide was cleaved with 82% TFA, 8.5% ethanedithiol (EDT), 8.0% TIS, and 1.5% dH_2O, shaking for 90 minutes in the dark, and then with fresh solution for an additional 30 minutes. The peptide was triturated with diethyl ether, allowed to air dry, and purified by reverse phase HPLC (t_R = 24.3 min). MS (ESI) *m/z* calculated for $C_{132}H_{193}N_{37}O_{25}S$: 2731.3 $(M+H)^+$. Found *m/z*: 456.1 $(M+6H)^{6+}$, 547.1 $(M+5H)^{5+}$, and 683.6 $(M+4H)^{4+}$.

A stock solution was made in PBS+ and the concentration was determined by UV absorbance as for FITC-PTD4.

Internalization data. Rat 1 fibroblasts were cultured in Dubelco's Modified Eagle Medium (DMEM) supplemented with 10% Fetal Bovine Serum (FBS) at 37°C and 5% CO_2.

Cells were seeded onto 18 mm square cover slips and grown until 70% confluent. Cells were incubated with 12.5 μM final concentration of fluorescein labeled peptide at 37°C, 5% CO_2 for 15 minutes, 30 minutes, 1 hour, or 4 hours. Cells were rinsed with PBS+ (3 x 1 min) and fixed with ice-cold methanol for five minutes. The cover slips were mounted onto glass microscope slides with 50:50 (v/v) glycerol/water and allowed to dry overnight, dark, room temperature. Once dry, the cover slips were sealed. Slides were viewed under a fluorescence microscope through a fluorescein filter with a 100 W Mercury lamp. Images were captured with a CCD camera using SPOT software and Adobe Photoshop 5.5. No modifications were made to the images.

General synthesis of disulfide linked peptides. Ac-cys(pys)-3Ah, **16**, was synthesized as described below. FITC-cys-Peptides were synthesized using standard Fmoc-SPPS as described in Chapter 2; those containing a caged phosphoserine were synthesized using the building block method described in Chapter 2. Coupling was performed using either **Method A** or **Method B**:

Method A: Individual peptides were dissolved in a minimal amount of 1M ammonium acetate (NH_4OAc) buffer, pH 5.1, degassed by bubbling with argon. Peptide stocks were quantified by UV absorbance (10 to 15 mM), and stored at –80 °C. One equivalent of each peptide was added in a reaction vessel flushed with argon, and allowed to agitate for three hours.

Method B: Each lyophilized peptide was added to a reaction vessel in an approximately 1:1 ratio, and the vessel flushed with argon. Degassed 1M NH_4OAc buffer, pH 5.1 was added to the dry peptides to approximately 10 mM, and the mixture was allowed to agitate for three hours.

For either method, the reaction mixture was quenched with 0.1% TFA in dH_2O (to double the reaction volume), and then extracted several times with EtOAc. The aqueous layer containing the desired peptide construct was purified by reverse phase HPLC. Peptides were characterized by reverse phase HPLC and MS (ESI).

Ac-cys(pys)3Ah, **16**. Ac-cys-3Ah (**15**, Ac-CRQIKIWFQNRR-Nle-KWKK-$CONH_2$) was synthesized using standard Fmoc-SPPS conditions as described in Chapter 2. 2,2'-dithiobis(5-

nitropyridine) (39 mg, 125 μmole) was dissolved in 3:1 AcOH/H_2O (5 mL) to make a 25 mM solution. 4 mL of solution (100 μmole) was added to lyophilized Ac-cys-3Ah (20 μmole), and allowed to mix vigorously for 5 hours. The solvent was removed *in vacuo*, and the residue dissolved in 10 mL of 1:1 EtOAc/dH_2O. The aqueous layer was extracted with EtOAc (3 x 5 mL), and then purified by reverse phase HPLC (t_R = 21.6 min). MS (ESI) *m/z* calculated for $C_{115}H_{180}N_{38}O_{23}S_2$: 2527.1 $(M+H)^+$, 506.2 $(M+5H)^{5+}$, 632.5 $(M+4H)^{4+}$. Found: 506.4 $(M+5H)^{5+}$ and 632.7 $(M+4H)^{4+}$.

F-cys-RSLP. FITC-CMARRLYRSLPAKK-$CONH_2$. Analytical reversed phase HPLC (t_R = 22.0 min). MS (ESI) *m/z* calculated for $C_{100}H_{152}N_{28}O_{22}S_3$: 2194.6 $(M+H)^+$, 439.7 $(M+5H)^{5+}$, 549.4 $(M+4H)^{4+}$, 732.2 $(M+3H)^{3+}$. Found 439.9 $(M+5H)^{5+}$, 549.6 $(M+4H)^{4+}$, 732.4 $(M+3H)^{3+}$.

F-cys-pRSLP. FITC-CMARRLYRpSLPAKK-$CONH_2$. Analytical reversed phase HPLC (t_R = 17.9 min). MS (ESI) *m/z* calculated for $C_{100}H_{153}N_{28}O_{25}S_3P$: 2274.7 $(M+H)^+$, 455.7 $(M+5H)^{5+}$, 569.4 $(M+4H)^{4+}$, 758.9 $(M+3H)^{3+}$. Found 455.8 $(M+5H)^{5+}$, 569.6 $(M+4H)^{4+}$, 759.1 $(M+3H)^{3+}$.

F-cys-cpRSLP, **14**. FITC-CMARRLYRcpSLPAKK-$CONH_2$. Analytical reversed phase HPLC (t_R = 20.6 min). MS (ESI) *m/z* calculated for $C_{108}H_{160}N_{29}O_{27}S_3P$: 2423.7 $(M+H)^+$, 485.5 $(M+5H)^{5+}$, 606.7 $(M+4H)^{4+}$. Found 485.6 $(M+5H)^{5+}$, 606.7 $(M+4H)^{4+}$.

F-cys-cpMAQQ. FITC-CMAQQLYcpSLAAKK-$CONH_2$. Analytical reversed phase HPLC (t_R = 27.7, 28.0 min, diastereomers). MS (ESI) *m/z* calculated for $C_{101}H_{144}N_{22}O_{29}PS_3$: 2256.6 $(M+H)^+$, 752.9 $(M+3H)^{2+}$, 1128.8 $(M+2H)^{2+}$. Found 753.0 $(M+3H)^{2+}$, 1129.0 $(M+2H)^{2+}$.

FRSLP-SS-3Ah, **18**. (FITC-CMARRLYRSLPAKK-$CONH_2$)-S-S-(Ac-CRQIKIWFQNRR-Nle-KWKK-$CONH_2$). Analytical reversed phase HPLC (t_R = 23.6 min). MS (ESI) *m/z* calculated for $C_{210}H_{328}N_{64}O_{43}S_4$: 4565.5 $(M+H)^+$, 653.1 $(M+7H)^{7+}$, 761.8 $(M+6H)^{6+}$, 913.9 $(M+5H)^{5+}$. Found 653.2 $(M+7H)^{7+}$, 761.9 $(M+6H)^{6+}$, 913.9 $(M+5H)^{5+}$.

FpRSLP-SS-3Ah. (FITC-CMARRLYRpSLPAKK-$CONH_2$)-S-S-(Ac-CRQIKIWFQNRR-Nle-KWKK-$CONH_2$). Analytical reversed phase HPLC (t_R = 23.6 min). MS (ESI) *m/z* calculated for

$C_{210}H_{329}N_{64}O_{46}PS_4$: 4645.5 $(M+H)^+$, 664.5 $(M+7H)^{7+}$, 775.1 $(M+6H)^{6+}$, 929.9 $(M+5H)^{5+}$. Found 664.7 $(M+7H)^{7+}$, 775.4 $(M+6H)^{6+}$, 930.1 $(M+5H)^{5+}$.

FcpRSLP-SS-3Ah, **17**. (FITC-CMARRLYRcpSLPAKK-$CONH_2$)-S-S-(Ac-CRQIKIWFQNRR-Nle-KWKK-$CONH_2$). Analytical reversed phase HPLC (t_R = 24.1 min). MS (ESI) *m/z* calculated for $C_{218}H_{336}N_{65}O_{48}PS_4$: 4794.7 $(M+H)^+$, 685.8 $(M+7H)^{7+}$, 800.0 $(M+6H)^{6+}$, 959.7 $(M+5H)^{5+}$, 1199.4 $(M+4H)^{4+}$. Found 693.2 $(M+ 2Na +7H)^{7+}$, 808.6 $(M+ 2Na +6H)^{6+}$, 969.9 $(M+ Na+ 5H)^{5+}$, and 1212.4 $(M +2Na +4H)^{4+}$.

FcpMAQQ-SS-3Ah, **19**. (FITC-CMAQQLYAcpSLAAKK-$CONH_2$)-S-S-(Ac-CRQIKIWFQNRR-Nle-KWKK-$CONH_2$). Analytical reversed phase HPLC (t_R = 24.3 min). MS (ESI) *m/z* calculated for $C_{211}H_{320}N_{58}O_{50}PS$: 4628.4 $(M+H)^+$, 926.5 $(M+5H)^{5+}$, 772.2 $(M+6H)^{6+}$. Found 926.3 $(M+5H)^{5+}$, 771.9 $(M+6H)^{6+}$.

3-4. Defining a Global Temporal role for 14-3-3

Experiments were performed as described in Reference 1.

Acknowledgements

I would like to acknowledge Professor Michael Yaffe as well as post-doctoral researchers Justine Stehn and Ahnco Nguyen (Cancer Research Center, Department of Biology, M. I. T.) for their significant contributions to this chapter. I thank M. Yaffe for designing the target peptide, RSLP, the scrambled peptide, MAQQ, and developing the biological experiments to study 14-3-3. I thank J. Stehn for performing the *in vitro* binding experiments, and A. Nguyen for performing the ITC, FACS, and staining experiments with such precious peptide samples.

References

(1) Nguyen, A.; Rothman, D. M.; Stehn, J.; Imperiali, B.; Yaffe, M. B. "Caged Phosphopeptides Reveal a Temporal Role for 14-3-3 in G1 Arrest and S-Phase Checkpoint Function," *Nature Biotechnology* **2004**, *22 (8)*, 993-1000.

(2) Yaffe, M. B.; Elia, A. E. "PhsophoSerine/Threonine-Binding Domains," *Current Opinion in Cell Biology* **2001**, *13 (2)*, 131-138.

(3) Ishii, M.; Kurachi, Y. "The 14-3-3 Protein as a Novel Regulator of Ion Channel Localization," *Journal of Physiology* **2002**, *545 (1)*, 2.

(4) Yaffe, M. B.; Rittinger, K.; Volinia, S.; Caron, P. R.; Aitken, A.; Leffers, H.; Gamblin, S. J.; Smerdon, S. J.; Cantley, L. C. "The Structural Basis for 14-3-3: Phosphopeptide Binding Specificity," *Cell* **1997**, *91 (7)*, 961-971.

(5) Muslin, A. J.; Tanner, J. W.; Allen, P. M.; Shaw, A. S. "Interaction of 14-3-3 with Signaling Proteins is Mediated by the Recognition of Phosphoserine," *Cell* **1996**, *84 (6)*, 889-897.

(6) Rittinger, K.; Budman, J.; Xu, J.; Volinia, S.; Cantley, L. C.; Smerdon, S. J.; Gamblin, S. J.; Yaffe, M. B. "Structural Analysis of 14-3-3 Phosphopeptide Complexes Identifies a Dual Role for the Nuclear Export Signal of 14-3-3 in Ligand Binding," *Molecular Cell* **1999**, *4 (2)*, 153-166.

(7) Rothblum-Oviatt, C. J.; Ryan, C. E.; Piwnica-Worms, H. "14-3-3 Binding Regulates Catalytic Activity of Human Wee1 Kinase," *Cell Growth and Differentiation* **2001**, *12 (12)*, 581-589.

(8) Laronga, C.; Yang, H. Y.; Neal, C.; Lee, M. H. "Association of the Cyclin-Dependent Kinases and 14-3-3 Sigma Negatively Regulates Cell Cycle Progression," *Journal of Biological Chemistry* **2000**, *275 (30)*, 23106-23112.

(9) Bartek, J.; Lukas, J. "Pathways Governing G1/S Transition and Their Response to DNA Damage," *FEBS Letters* **2001**, *490 (3)*, 117-122.

(10) Busino, L.; Donzelli, M.; Chiesa, M.; Guardavaccaro, D.; Ganoth, D.; Dorrello, N. V.; Hershko, A.; Pagano, M.; Draetta, G. F. "Degradation of Cdc25A by Beta-TrCP During S Phase and in Response to DNA Damage," *Nature* **2003**, *426 (6962)*, 87-91.

(11) Dunnican, D. J.; Doherty, P. "Designing Cell-Permeant Phosphopeptides to Modulate Intracellular Signaling Pathways," *Biopolymers (Peptide Science)* **2001**, *60 (1)*, 45-60.

(12) Ho, A.; Schwarze, S. R.; Mermelstein, S. J.; Waksman, G.; Dowdy, S. F. "Synthetic Protein Transduction Domains: Enhanced Transduction Potential *in Vitro* and *in Vivo*," *Cancer Research* **2001**, *61 (2)*, 474-477.

(13) Ruzza, P.; Donella-Deana, A.; Calderan, A.; Brunati, A.; Massimino, M. L.; Elardo, S.; Mattiazzo, A.; Pinna, L. A.; Borin, G. "Antennapedia/HS1 Chimeric Phosphotyrosyl Peptide: Conformational Properties, Binding Capability to c-Fgr SH2 Domain and Cell Permeability," *Biopolymers (Peptide Science)* **2001**, *60 (4)*, 290-306.

(14) Rabanal, R.; DeGrado, W. F.; Dutton, P. L. "Use of 2,2'-dithiobis(5-nitropyridine) for the Heterodimerization of Cysteine Containing Peptides. Introduction of the 5-nitro-2-pyridinesulfenyl Group," *Tetrahedron Letters* **1996**, *37 (9)*, 1347-1350.

(15) Chen, L.; Wright, L. R.; Chen, C. H.; Oliver, S. F.; Wender, P. A.; Mochly-Rosen, D. "Molecular Transporters for Peptides: Delivery of a Cardioprotective Epsilon-PKC Agonist Peptide into Cells and Intact Ischemic Heart Using a Transport System, R_7," *Chemistry and Biology* **2001**, *8 (12)*, 1123-1129.

(16) Carrigan, C. N.; Imperiali, B. "The Engineering of Membrane-Permeable Peptides," *Analytical Biochemistry* **2005**, *in press*

(17) Lalande, M. "A Reversible Arrest Point in the Late G1 Phase of the Mammalian Cell Cycle," *Experimental Cell Research* **1990**, *186 (2)*, 332-339.

(18) Ravanat, J. L.; Douki, T.; Cadet, J. "Direct and Indirect Effects of UV Radiation on DNA and Its Components," *Journal of Photochemistry and Photobiology B* **2001**, *63 (1-3)*, 88-102.

(19) Chen, M. S.; Ryan, C. E.; Piwnica-Worms, H. "Chk1 Kinase Negatively Regulates Mitotic Function of Cdc25A Phosphatase Through 14-3-3 Binding," *Molecular and Cellular Biology* **2003**, *23 (21)*, 7488-7497.

Chapter 4
Synthesis of Full-length Caged Phosphoproteins

Portions of this chapter have been published in the *Journal of the American Chemical Society* as noted in the text[1] (Copyright © 2005 American Chemical Society). M. E. Vazquéz (Imperiali Lab, M. I. T.) synthesized 4PO-cpTyr-OCH_2CN; E. James Petersson (Dougherty Lab, CalTech) performed *in vitro* suppression reactions with nAChR.

Introduction

The majority of kinase substrates are functional as full-length proteins; therefore, a generally applicable method for the synthesis of site-directed caged phosphoproteins is desirable. The technology to incorporate caged phospho-amino acids into full-length protein is described in this chapter.[1] This method takes advantage of the nonsense codon suppression methodology, an overview of which is depicted in Figure 4.1.[2] Briefly, the gene of interest is mutated at the site of unnatural amino acid incorporation to one of the "blank" stop (or nonsense) codons in the genetic code, often the amber codon TAG. An orthogonal suppressor tRNA with the corresponding anti-codon to the amber codon is ligated to a dinucleotide that has been chemically acylated with the desired non-natural amino acid. When the mRNA of the mutated gene is placed in a translation system with the designed tRNA, the ribosomal machinery incorporates the unnatural amino acid at the amber codon position, thus suppressing the nonsense codon.

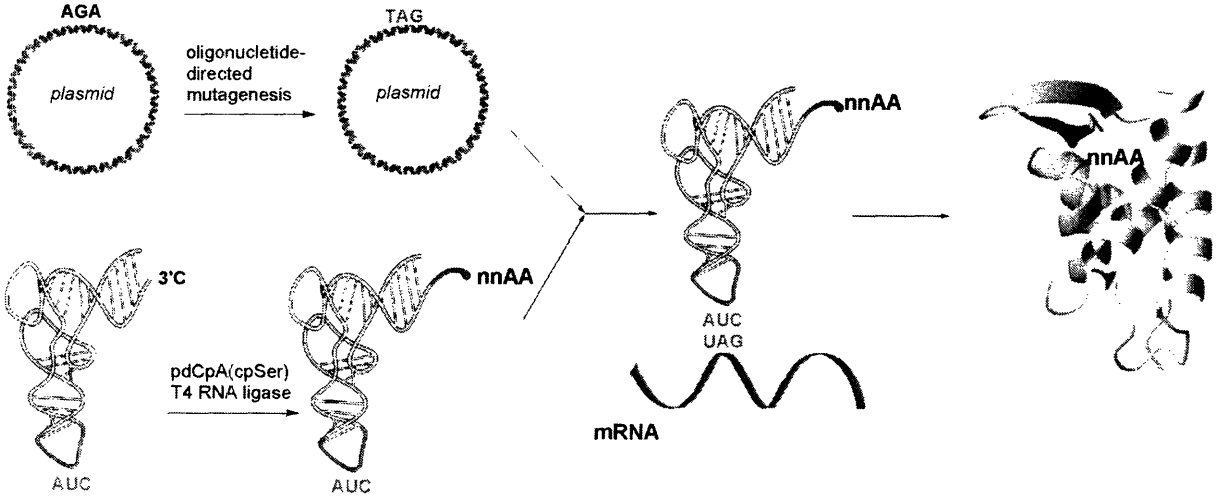

Figure 4.1. Overview of the nonsense codon suppression method. Oligonucleotide-directed mutagenesis of the gene converts the target amino acid codon to the amber stop codon. A corresponding tRNA with the matching anti-codon is ligated to a chemically acylated dinucleotide containing the non-natural amino acid. When the mRNA of the mutated gene and the tRNA are combined in a translation system, the non-natural amino acid is incorporated at the amber stop codon position, thus suppressing the nonsense codon. (nnAA= non-natural amino acid)

A novel phosphitylation reagent was developed in order to synthesize the appropriately protected amino acid derivatives for the chemical acylation of the designated suppressor tRNA. Suppression experiments were performed in two proteins: at position 122 of nicotine acetylcholine receptor α-subunit (nAChR-α) and at position 153 of murine vasodilator stimulated phosphoprotein (mVASP). All three commonly phosphorylated residues (serine, threonine, and tyrosine) were successfully incorporated as their caged analogues in the test protein nAChR-α. The incorporation of caged phosphoserine was successful in the phospho-regulated protein mVASP (for further discussion, see Chapter 5). The generally applicable method for synthesizing full-length caged phosphoproteins will broaden the field of study opened by the successful caged phosphopeptide methodology.

Results and Discussion

4-1. Chemical Synthesis

In general, the chemical acylation of the tRNA is accomplished by coupling the unnatural amino acid to a dinucleotide that corresponds the 3'-end of the suppressor tRNA. This acylated dinucleotide is then biochemically ligated to the suppressor tRNA in which the two 3'-nucleotides are absent (see below, section 4-2). There are several key features of the protecting groups on a non-natural amino acid for coupling to the 3'-dinucleotide of the suppressor tRNA. The amine-protecting group must be one that is removed under mild conditions such that the deprotection can be performed on the intact tRNA immediately prior to suppression translation reactions.[3] The most common protecting group is the caging group 6-nitroveratryloxy carbamate (NVOC)[2, 4] which is removed with UV-A irradiation (Figure 4.2a). Because the side-chain for the target amino acid is light-sensitive, the 4-pentenoyl amide was used. This group is removed with iodine in water at room temperature (Figure 4.2b).[5, 6] The amino acid activation implements a cyanomethyl ester, which has been shown in the literature to selectively mono-acylate the dinucleotide at the 2'- or 3'-hydroxyl groups, and to not acylate the aniline amines of the nucleotide bases.[4]

Figure 4.2. Amino acids activated by cyanomethyl ester for coupling to the dinucleotide. **a**) NVOC-protected amine. **b**) 4-pentenoyl protected amine.

Scheme 4.1 *β-elimination of caged phosphate with transient cyanoethyl protection.*

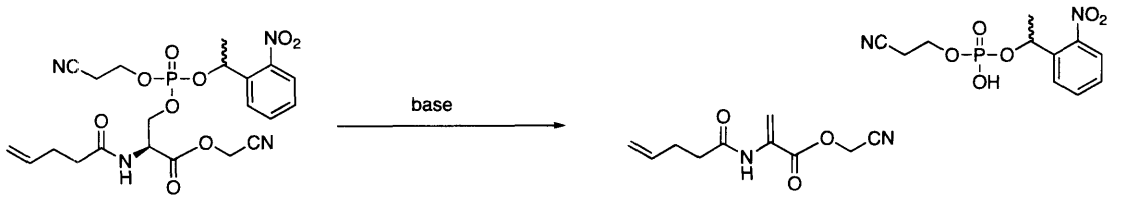

Several attempts were made to synthesize the appropriate caged phosphoserine and threonine analogs via the phosphoramidite **4** (Chapter 2). Unfortunately, the 4-pentenoyl amide and cyanomethyl ester of a caged phosphoserine with the transient β-cyanoethyl protecting group undergoes β-elimination of the phosphate during basic deprotection (Scheme 4.1). Therefore, a non-base labile transient phosphate protecting group was required in the phosphitylating reagent. It was known from peptide synthesis experiments that the *ortho*-nitrophenylethyl caging group is stable to strong acid (Chapter 2). Thus, a phosphoramidite was synthesized with the transient acid-labile *tert*-butyl protecting group. In an initial attempt to synthesize the phosphoramidite **20**, a dichlorophosphoramidite was treated with *tert*-butyl alcohol and *ortho*-nitrophenylethyl alcohol in sequences with various solvents, concentrations, equivalents, and temperatures (Scheme 4.2). However, in every experiment a homo-di-substituted phosphoramidite resulted rather than the desired mixed phosphoramidite.

Scheme 4.2 *Attempted synthesis of* O*-1-(2-nitrophenyl)ethyl-*O'*-tertbutyl-*N,N*-diisopropyl phosphoramidite,* **20**.

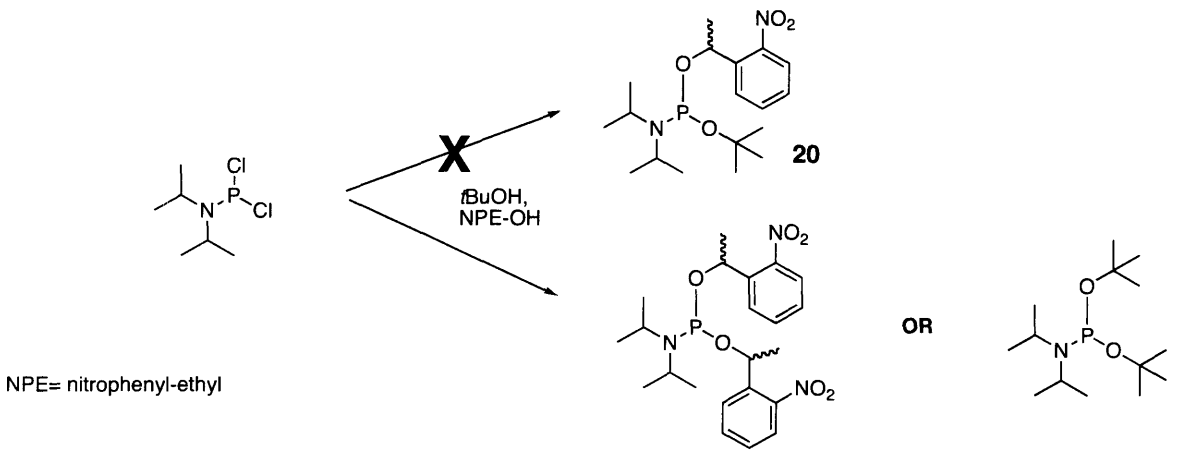

NPE= nitrophenyl-ethyl

In a further attempt, hexaethyl phosphorus triamide **21** was used in place of the dichlorophosphoramidite to decrease the reactivity of the trivalent phosphorus starting material (Scheme 4.3). The less reactive starting material allowed each diethylamine substituent on phosphorus to be replaced under controlled activation by 4,5-dicyanoimidazole[7] as seen in Scheme 4.3. The progress of the reaction was monitored by ^{31}P NMR, and the shifts relative to

phosphoric acid (δ = 0.00 ppm) are shown below each chemical species. First, **21** was activated to **22** with just under one equivalent of 4,5-dicyanoimidazole, which was subsequently replaced with the bulky *tert*-butoxy group to generate **23**. Note that after incorporation of the *t*-butyl alcohol, only one chemical species was detectable by ^{31}P NMR. As incorporation of 4,5-dicyanoimidazole into **21** was very rapid, it is likely that **23** was the later structure shown with both the *t*-butoxy and imidazole substituents; however, this intermediate could not be isolated for further experiments. Addition of the secondary *ortho*-nitrophenylethyl alcohol to **23** gave the desired mixed phosphoramidite **24** in 74 % isolated yield. It is of significance that reducing the reactivity of the starting material does not completely eliminate the formation of the homo-di-substituted phosphoramidites **25** and **26**. Though these species persisted under all reaction conditions, the desired mixed phosphoramidite **24** was the major product and was easily isolated by silica gel column chromatography.

Scheme 4.3 *Synthesis of O-1-(2-nitrophenyl)ethyl-O'-tertbutyl-N,N-diethyl phosphoramidite,* **24**.

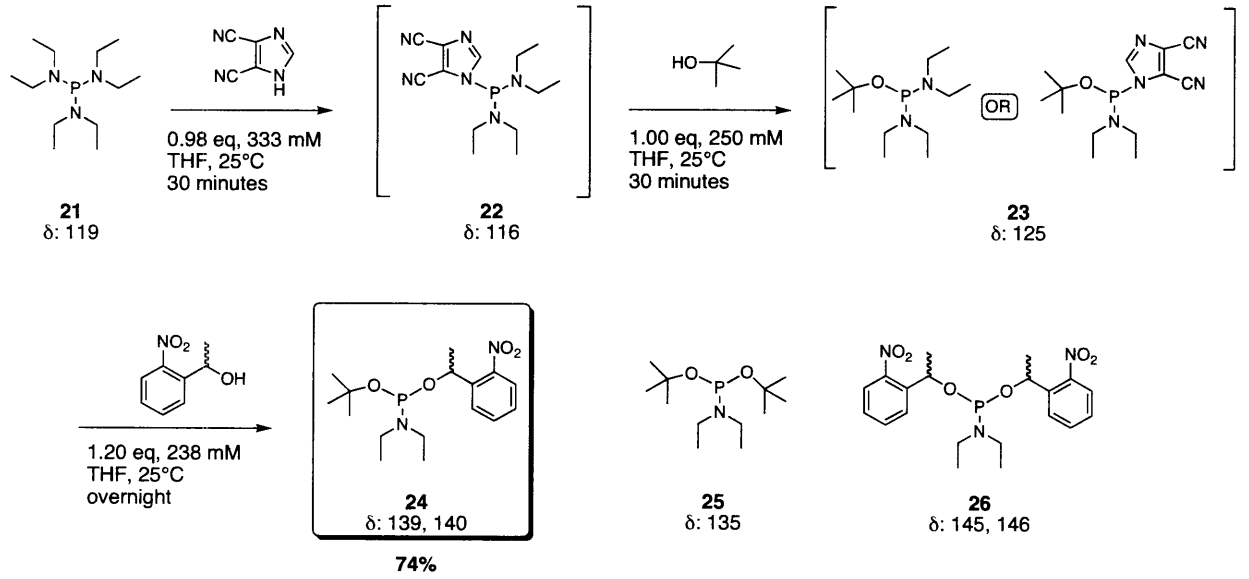

Phosphoramidite **24** was employed in the synthesis of the appropriately activated serine and threonine derivatives for coupling to the 3'-dinucleotide of the tRNA. Initially, the serine and threonine derivatives were synthesized as in Scheme 4.4 (optimum yield for each reaction shown). The commercially available amino acids, **27a** or **27b**, were converted to the 4-pentenoyl amide derivatives with 4-pentenoic anhydride in the presence of *N,N*-diisopropylethylamine (DIPEA). Next, the free acids were activated as the cyanomethyl esters **29a** and **29b** by slow addition of 1,8-diazabicyclo[5.4.0]undec-7-ene (DBU) in neat chloroacetonitrile. The hydroxyl

groups were revealed by deprotection of the *tert*-butyl ethers in trifluoroacetic acid (TFA) with a small amount of the cation scavenger triisopropylsilane (TIS). The free hydroxyl serine and threonine intermediates **30a** and **30b** were phosphitylated with phosphoramidite **24** activated by 4,5-dicyanoimidazole. The phosphite intermediates were immediately oxidized to the more stable phosphate species **31a** and **31b** with *tert*-butyl hydroperoxide. The fully protected phosphate intermediates were carried directly to the final deprotection before purification and characterization. The transient *t*-butyl ester on the phosphate was removed under mildly acidic conditions to generate the amino acid derivatives **32a** and **32b** in high yield. These caged phospho-amino acids were coupled to the 3'-dinucleotide of the suppressor tRNA. The analogous tyrosine derivative was synthesized using the phosphoramidite **4** (Chapter 2) via a modified procedure;[1] since there is no labile proton β to the caged phosphate on the tyrosine, there was no risk of β-elimination of the phosphate.

Scheme 4.4 *Synthesis of* N$^{\alpha}$*-4-pentenoyl-phospho(nitrophenylethyl)-L-serine cyanomethyl ester,* **32a**, *and* N$^{\alpha}$*-4-pentenoyl-phospho(nitrophenylethyl)-L-threonine cyanomethyl ester,* **32b**.

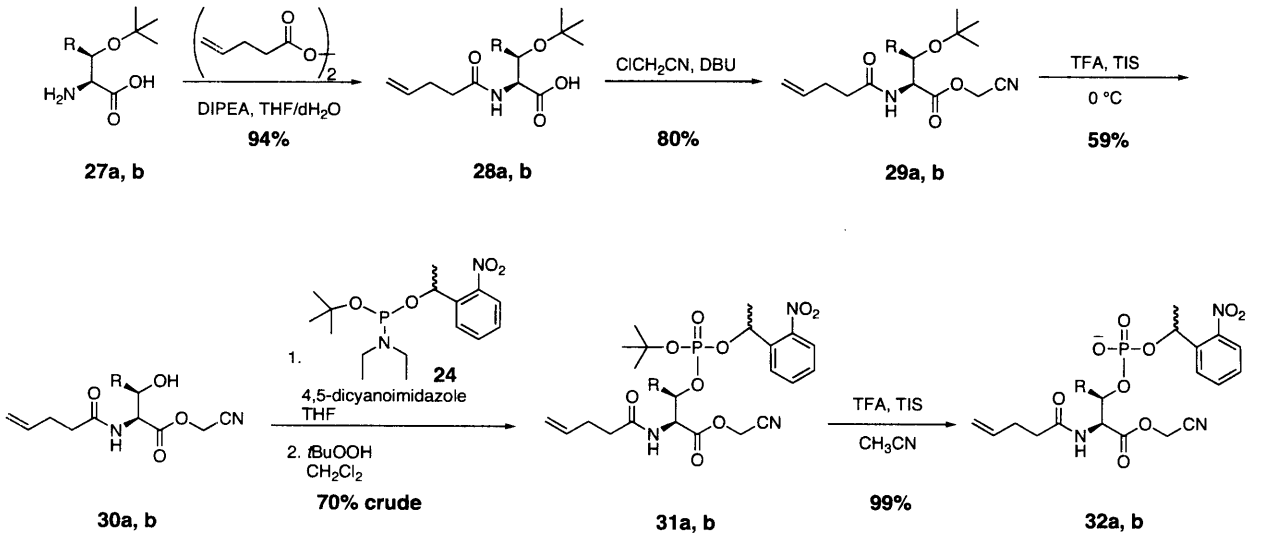

a, R = H, Serine
b, R = CH_3, Threonine

The overall yield for the three-step synthesis of the threonine intermediate **30b** was an acceptable 59%; however, in the case of **30a**, the yield was only 19%. Once all the serine derivative had been consumed, an alternate route to **30a** was undertaken (Scheme 4.5). Serine, **33**, was selectively acylated on the free amine with 4-pentenoic anhydride in a basic solution of sodium bicarbonate. The free acid **34** was then converted to the cyanomethyl ester **30a** with

chloroacetonitrile in a solution of anhydrous DMF and triethylamine. The synthesis was modified from previously reported work[8] and gives a (non-optimized) two-step yield of 32%, which is an improvement over the original three-step route that yields only 19%.

Scheme 4.5 *Alternate synthesis of* N^{α}*-4-pentenoyl-L-serine cyanomethyl ester,* **30a**.

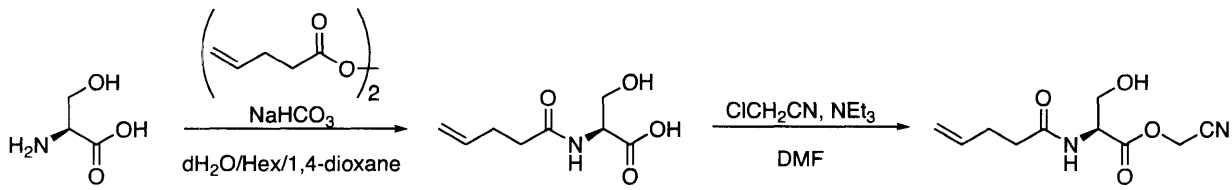

33 **34** **30a**

The caged phospho-amino acid derivatives were coupled to the 3'-dinucleotide of the suppressor tRNA: 5'-phospho-2'-deoxycytidylyl-(3', 5')-phosphoadenosine, or pdCpA (**35**, Scheme 4.6). The tetrabutylammonium salt of pdCpA (or activated pdCpA) was synthesized as previously reported[2] with minor modifications as noted in the Experimental section. As seen in Scheme 4.6, a cyanomethyl ester activated amino acid was coupled to the 2' or 3' hydroxyl groups of the adenosine ribose ring of pdCpA in the presence of 250 mM tetrabutylammonium salt. The ester linkage at the ribose ring can rapidly migrate between the 2' and 3' hydroxyl groups, therefore it is sufficient to acylate either hydroxyl group; interconversion in aqueous buffer at pH 7.3, 37 °C is rapid with $t_{1/2}$ = 1-11 s^{-1}.[4]

The coupling conditions described in the original literature is activated pdCpA with the cyanomethyl ester in anhydrous DMF without any additives.[4] These conditions produced no product with the caged phospho-amino acids. Due to the negatively charged phosphate groups in the pdCpA and the caged phospho-amino acids, bringing the two reactants together was a challenge. A range of temperatures and concentrations of starting materials were tested (25 °C to 55 °C, and 40 mM to 200 mM), however suitable conditions could not be identified. Adding an excess of dry NBu_4OAc salt to a 100 mM solution of the reactants in DMF at room temperature finally permitted some reaction to take place. The NBu_4OAc additive afforded the desired product, but also yielded a significant amount of β-elimination side-product with the serine and threonine derivatives. Therefore, a range of NBu_4OAc concentrations (10 mM to 500 mM) was tested to determine the concentration yielding the highest desired product to β-elimination product ratio. Lower concentrations afforded no product, while 500 mM gave mostly β-elimination product. Starting materials in a solution of 250 mM NBu_4OAc yielded the acylated

Scheme 4.6 *Synthesis of amino acyl-pdCpAs,* **36a**, **36b**, *and* **37**.

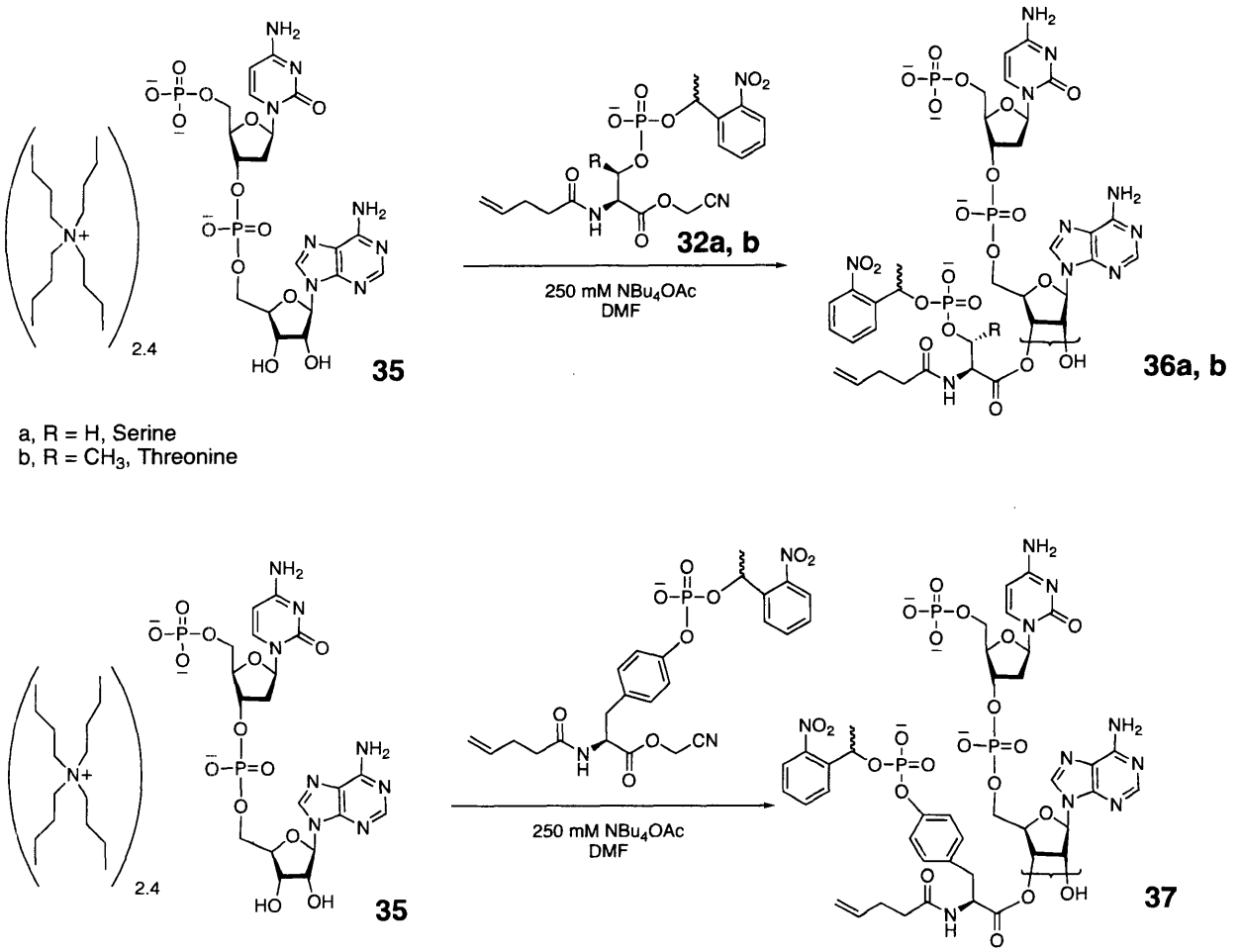

dinucleotide as the major product, and thus this condition was used for all further coupling reactions. It is likely that the tetrabutylammonium cation of the additional salt acts to neutralize and solubilize the phosphate charges of the starting materials. Additionally, the extra base produced by the salt at high concentrations is probably the culprit behind the β-elimination side products. The corresponding caged phospho-serine, threonine, and tyrosine N^{α}-4-pentenoyl protected acylated dinucleotides (4PO-cpAA-pdCpAs) were characterized by HPLC and electrospray ionization mass spectrometry (ESI-MS) (**36a**, **36b**, and **37**, respectively).

4-2. Semi-synthesis and Molecular Biology

To generate the full-length suppressor tRNA acylated with the caged phospho-amino acids ($tRNA_{CUA}^{cpAA}$s) an appropriate truncated tRNA for ligation is necessary. The glutaminyl *Tetrahymenya thermophila* derived amber codon suppressor tRNA TH73G behaves orthogonally

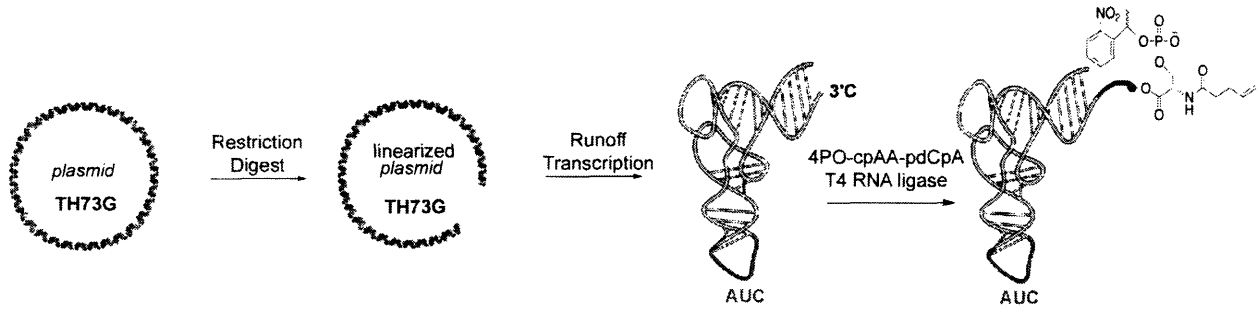

Figure 4.3. Semisynthesis of acylated suppressor tRNA. A plasmid containing the gene for the TH73G tRNA is linearized by restriction digest; the linear template allows *in vitro* runoff transcription to biochemically synthesize the tRNA with the last two 3'-bases absent. The promiscuous T4 RNA ligase ligates the chemically acylated dinucleotide to the 3'-end of the tRNA, yielding full length acylated suppressor tRNA.

in eukaryotic translation systems[9] which is important for mammalian protein translation (see 4-3 below). The general semi-synthesis procedure to generate $tRNA_{CUA}^{cpAA}$s is depicted in Figure 4.3. The TH73G plasmid was amplified in DH5α cells, purified by standard techniques, and digested with FokI just after the TH73G gene; this allowed the RNA polymerase to synthesize uniform tRNAs by falling off the template just after the gene was transcribed. Run off transcription from the linear DNA template produced the 74-mer $tRNA_{CUA}^{-CA}$ which contained the corresponding amber anti-codon loop ($_{CUA}$) and was missing the two 3'-terminal nucleotides ($^{-CA}$). Upon ligation of the 4PO-cpAA-pdCpAs to the $tRNA_{CUA}^{-CA}$ with the promiscuous T4 RNA ligase, the full-length 76-mer $tRNA_{CUA}^{cpAA}$s were formed. The product $tRNA_{CUA}^{cpAA}$s were confirmed by matrix assisted laser desorption ionization time of flight mass spectrometry (MALDI-TOF MS), electrospray ionization time of flight mass spectrometry (ESI-TOF MS), or denaturing polyacrylamide gel electrophoresis (D-PAGE). MALDI-TOF spectra were clear and no deconvolution of data was necessary to visualize the ligated tRNA from the starting material or any hydrolysis products.[1] Unfortunately, acquiring these spectra was difficult, and therefore ESI-TOF and D-PAGE analyses were used in combination to confirm the complete formation of the product $tRNA_{CUA}^{cpAA}$s.

Along with the full-length $tRNA_{CUA}^{cpAA}$s, the other unique component of the suppression reaction is mRNA with an amber codon at an appropriate site. The general molecular biological scheme to generate this mRNA is shown in Figure 4.4. First, the amber codon is introduced into a plasmid containing the target gene via oligonucleotide directed mutagenesis. Next, the DNA template is linearized at the 3'-terminus of the gene using a restriction digest; again this allows

the RNA polymerase to synthesize uniform mRNA strands by dropping off the template just after the gene is transcribed. The mRNA containing the amber codon is biochemically synthesized *in vitro* by run off transcription.

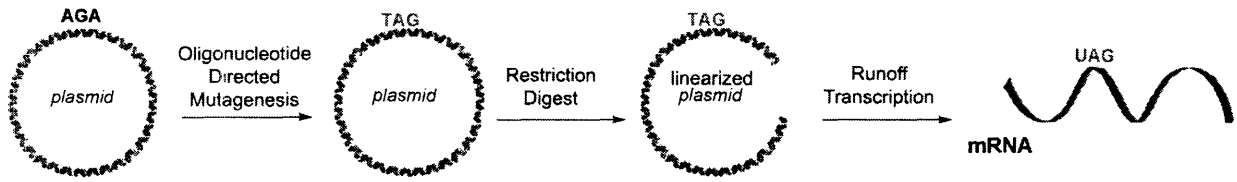

Figure 4.4. Biochemical synthesis of mutant mRNA. The plasmid with the target gene is mutated using site-directed mutagenesis techniques to introduce the amber stop codon at the desired position. The plasmid is linearized by restriction enzymes just after the original stop codon of the gene. *In vitro* runoff transcription produces the full-length mutant mRNA containing the amber stop codon.

A mutant nAChR-α A122Z plasmid was prepared as previously reported.[10] A mutant mVASP S153Z plasmid was prepared by converting serine 153 to the amber codon TAG via oligonucleotide-directed mutagenesis. The gene was cloned into a vector with a 6XHis tag at the N-terminus of the protein. For a discussion of the purification tag and its placement, see Chapter 5. Each mRNA was produced by run-off transcription and confirmed by glyoxal-agarose gel electrophoresis.

4-3. Protein synthesis

In the nonsense suppression methodology, protein synthesis is often accomplished separately from transcription and frequently in an *in vitro* translation system. There are several *in vitro* systems available, and selection depends on the nucleic acid sequence encoding the protein and the scale of synthesis desired. In general, the translation systems are extracts from *E. coli*, rabbit reticulocytes, or wheat germ. The extracts contain the ribosomal elements, energy system (creatine phosphate and creatine phosphokinase), tRNAs and tRNA synthetases from that species, and elongation and release factors from that species necessary for protein translation. Amino acids are added separately to the system; therefore, radiolabeled amino acids may be selectively added for analysis of proteins synthesized exclusively from added mRNA. There are examples of nonsense suppression in which the protein was translated in *Xenopus* oocytes and the protein studied within the context of the living cell.[11] Additionally, coupled or linked transcription/translation systems from the aforementioned organisms are commercially available in which plasmid or linear DNA is the nucleic acid template for protein synthesis, obviating the

purification of intermediate mRNA. However, experience has shown that these systems are less efficient in nonsense suppression reactions.[12]

The original methodology describes the use of an *E. coli* extract system.[2] This system is ideal for prokaryotic proteins and those eukaryotic proteins that do not contain a significant number of *E. coli* rare codons in the nucleic acid sequence. Rare codons are those that may appear infrequently in an organism's genome.[13] For example, a common mammalian codon for proline is CCC. This is a rare codon in *E. coli*, and *E. coli* do not produce many prolyl-tRNAs with the cognate GGG anticodon. If a mammalian protein with few prolines encoded by CCC is translated in an *E. coli* derived system, the protein could potentially be synthesized without a problem. However, if a mammalian protein with multiple proline residues encoded by CCC is translated in an *E. coli* derived system, there will not be sufficient $tRNA_{GGG}^{Pro}$s available, and truncation products are likely to be a significant problem. In such a case, a eukaryotic derived system, such as wheat germ or rabbit reticulocyte, should be used. Additionally, the scale of protein synthesis required will affect the system used. Typical analysis reactions (50 μL scale) produce low nanogram quantities of protein and are accessible through any system. However, *E. coli* and wheat germ extracts can be prepared on larger scales, such that milliliter scale reactions may be performed to produce micro- to milligram quantities of protein.[14] Further, translations may be run in dialysis systems such that nutrients can be continually fed into the system as a concentrated protein sample is synthesized.[15]

The mVASP protein is of mammalian origin and contains several sections of proline rich domains encoded by the CCC codon. Therefore, analytical translation experiments were performed in a rabbit reticulocyte translation system. While useful for preliminary analysis, this system is not amenable to large-scale protein preparations due to the cost and difficulty of obtaining cell preparations. Therefore, future work will focus on the preparation of large-scale protein synthesis using a wheat germ system (Chapter 6).

Both mVASP and nAChR wild-type (WT) proteins were synthesized as controls in an *in vitro* rabbit reticulocyte lysate translation system. The primary antibody used to detect mVASP by western blot analysis was rabbit derived; therefore, it was necessary to purify the protein from the rabbit system in order to probe with an anti-rabbit secondary antibody. The protein was purified using the N-terminal 6XHis-tag and nickel-nitrilotriacetic acid (Ni-NTA) as described in the Experimental section. Detection using the less sensitive anti-His6 antibody was not possible

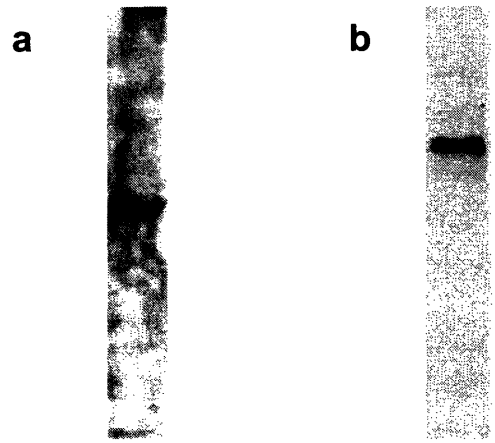

Figure 4.5. Western blot analysis of nAChR-WT and mVASP-WT proteins. a) nAChR was detected by an HA-epitope tag and loaded onto SDS-PAGE within the translation mixture. b) mVASP was detected with a rabbit-derived polyclonal anti-body after purification from the translation mixture.

because the amounts of protein produced using this system were so small. Detection of nAChR was not complicated by the use of the rabbit derived system; protein purification was unnecessary and the protein was detected within the translation mixture. As seen in Figure 4.5, both nAChR-WT and mVASP-WT appeared as well defined bands by their respective western blot analysis.

Nonsense suppression reactions were performed as depicted in Figure 4.6. The 4-pentenoyl amine protecting group on the charged tRNA was removed in iodine and water at room temperature for ten minutes, then immediately combined with the mRNA and other translation components. The reactions were allowed to incubate at 30 °C for up to three hours in the dark before being stored at –80 °C to prevent degradation. Test suppressions, in which a free serine, phosphoserine, free threonine, phosphothreonine, free tyrosine, or phosphotyrosine was introduced at the amber codon, used an amino acyl tRNA charged with an NVOC-protected amine. The NVOC group was removed by irradiation (λ = 365 nm) for five minutes at room temperature, and then immediately added to the remaining translation components as with the caged phospho-amino acid suppression experiments.

Initial suppression experiments with the caged phospho-amino acids were performed with nAChR-α A122Z mRNA.[10] The nAChR-α is known to accept non-natural amino acids in several positions using the suppression method. The nAChR-α A122Z transcript was introduced to the translation system with either uncharged full-length $tRNA_{CUA}$, $tRNA_{CUA}^{Ser, Thr, Tyr}$, $tRNA_{CUA}^{pSer, pThr, pTyr}$, or $tRNA_{CUA}^{cpSer, cpThr, or\ cpTyr}$. As seen in Figure 4.7, the suppression reactions were successful in all cases. The incorporation of the caged phospho-amino acids was particularly satisfying as previous experiments have demonstrated poor incorporation efficiency with phospho-amino acids.[16, 17] While the suppression with the $tRNA_{CUA}^{cpAA}$s is less efficient than with the free

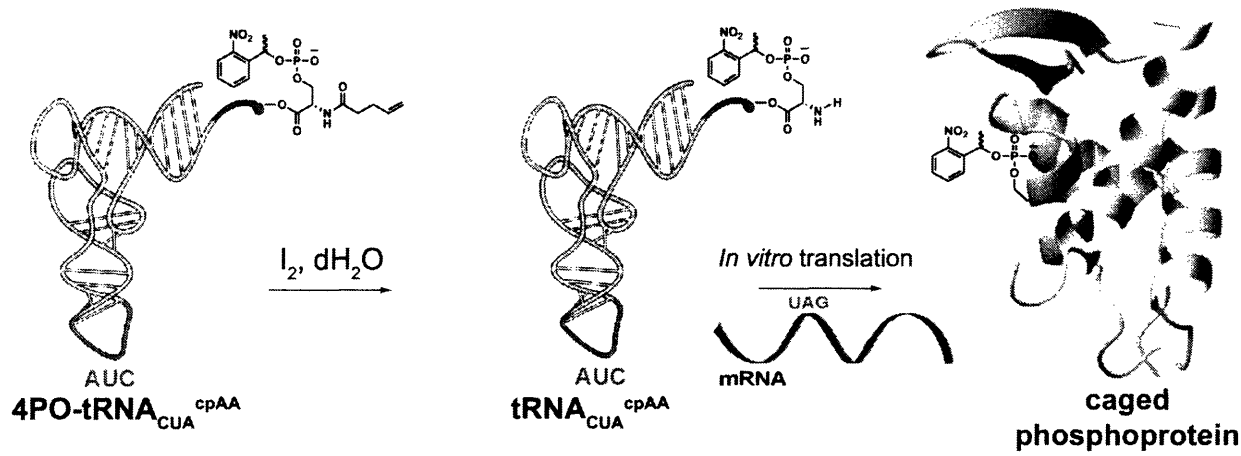

Figure 4.6. Nonsense suppression reaction with 4PO-protected tRNA. The suppressor tRNA is deprotected with iodine in water immediately prior to addition to the *in vitro* translation system. In the presence of the mutant mRNA, the tRNA suppresses the amber codon to incorporate the unnatural amino acid at the desired site.

hydroxyl-amino acids, there is still significant translation of full-length protein. The lower suppression efficiency of the $tRNA_{CUA}^{cpAA}$s may be due to a lowered affinity of the elongation factors to tRNA with negatively charged amino acids. Ulhenbeck and coworkers have demonstrated that there is a thermodynamic compensation among the backbone of the acceptor and T helices of the tRNA, the amino acid with which it has been charged, and the elongation factors (i.e., EF-Tu) involved in polypeptide elongation.[18, 19] It highly likely that this balance is offset with a TH73G $tRNA_{CUA}$ that has been acylated with a negatively charged amino acid. Also, glutaminyl tRNAs (from which TH73G was derived) have a low inherent EF-Tu affinity.[18, 20] Therefore, a possible future endeavor may be to evolve $tRNA_{CUA}$ species that reestablish the thermodynamic balance when acylated with negatively charged amino acids.

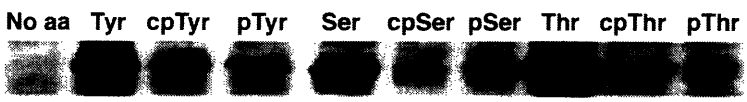

Figure 4.7. Suppression of nAChR-α A122Z.[1] nAChR-α A122Z mRNA was translated with $tRNA_{CUA}$ acylated with the amino acid above each lane. "No aa" refers to full-length $tRNA_{CUA}$ that has not been acylated with an amino acid.

Next, suppression reactions were performed using mVASP S153Z mRNA. The transcript was introduced to the translation system with either uncharged full-length $tRNA_{CUA}$, $tRNA_{CUA}^{Ser}$, or $tRNA_{CUA}^{cpSer}$. As seen in Figure 4.8, the suppression reactions were successful. The

incorporation of caged phosphoserine at position 153 was especially encouraging because this protein was not known to accept non-natural amino acids in general, let alone at a critical position for protein function (see Chapter 5).

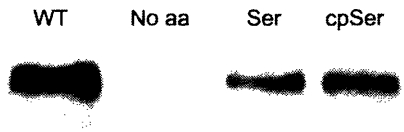

Figure 4.8. Suppression of mVASP S153Z. mVASP S153Z mRNA was translated with $tRNA_{CUA}$ acylated with the amino acid above each lane. "No aa" refers to full-length $tRNA_{CUA}$ that has not been acylated with an amino acid. A mVASP-WT lane was run for a control.

Conclusion

The successful development of a method to incorporate caged phospho-amino acids into full-length proteins has been described. A new phosphoramidite reagent was employed in the synthesis of the caged phospho-amino acid analogs with the obligatory protecting groups for coupling to the 3'-dinucleotide of a truncated suppressor tRNA. Full-length suppressor tRNAs charged with caged phospho-amino acids were effectively incorporated into a test protein, nAChR-α. Additionally, caged phosphoserine was successfully incorporated into the phospho-regulated protein mVASP in place of the critical residue, S153. The availability of this methodology allows the incorporation of caged phospho-amino acids via nonsense codon suppression into any position of a full-length protein without requiring other modifications or mutations to the protein.

Experimental

4-0. General Synthetic Procedures

All chemicals were purchased from Aldrich unless otherwise noted in the text; all anhydrous reagents were prepared as described in Chapter 2. All NMR spectroscopy and HPLC analysis and purification were performed as described in Chapter 2. DEPC dH_2O for use with RNA is dH_2O mixed with 0.1 % (v/v) diethyl pyrocarbonate overnight at room temperature, then autoclaved for one hour. In order to prevent aberrant RNase degradation of samples, all RNA samples (and other reagents to be used with RNA) were handled with aerosol barrier micropipette tips and DEPC-treated water in a separate space where fresh gloves were worn at

all times. Additionally, all RNA samples were stored dry at –80 °C when possible to further prevent RNase or chemical degradation.

4-1. Chemical Synthesis

*O-1-(2-nitrophenyl)ethyl-O'-tertbutyl-N,N-diethyl phosphoramidite (**24**).* To an oven dried flask with stir bar, hexaethyl phosphorus triamide (1.37 mL, 5.00 mmole) and 4,5-dicyanoimidazole (0.58 g, 4.90 mmole) were dissolved in anhydrous tetrahydrofuran (THF, 15 mL) under inert atmosphere. In an oven dried pear-shaped flask, *tert*-butyl alcohol (0.48 mL, 5.00 mmole) was dissolved in anhydrous THF (5.0 mL). In a separate oven dried pear-shaped flask, 1-2-(nitrophenyl)ethyl alcohol (1.00 g, 6.00 mmole) was dissolved in anhydrous THF (1 mL). The *t*BuOH solution was delivered to the phosphoramidite mixture *via* cannula, and the reaction was allowed to stir at room temperature for 15 minutes, at which point the nitrophenylethyl alcohol mixture was delivered to the reaction flask *via* cannula. The mixture was allowed to stir overnight in the dark at room temperature. The mixture was then concentrated under reduced pressure, and re-dissolved in ethyl acetate (EtOAc, 150 mL). The organic solution was washed with 20% sodium bicarbonate ($NaHCO_3$, 2 x 150 mL) and brine (1 x 150 mL), then dried over magnesium sulfate ($MgSO_4$), filtered, and concentrated. The final product was purified by silica gel flash chromatography (98:2 hexanes/triethylamine (NEt_3), R_f: 0.73,) to give **24** (1.27 g) in 74.0 % yield. ^{1}H NMR (300 MHz, $CDCl_3$) δ ppm: 7.92 (td, J_{HH} = 1.8 Hz, J_{HH} = 8.4 Hz, 2H), 7.65 (tt, J_{HH} = 1.5 Hz, J_{HH} = 7.5, 1H), 7.40, (tt, J_{HH} = 1.5 Hz, J_{HH} = 8.4 Hz, 1 H), 5.55 (m, 1 H), 3.06 (m, 4H), 1.57 (dd, J_{HH} = 4.5 Hz, J_{HH} = 6.3 Hz, 3H), 1.30 (d, J_{HH} = 19.5 Hz, 9H), 1.08 (dt, J_{HH} = 6.0 Hz, J_{HH} =43.5 Hz, 6 H). ^{13}C NMR (125.8 MHz, $CDCl_3$) 147.9, 142.3 (d, J_{PC} = 1.7 Hz), 142.0 (d, J_{PC} = 2.3 Hz), 133.8 (d, J_{PC} = 6.3 Hz), 129.6 (d, J_{PC} = 6.9 Hz), 128.2, 124.5 (d, J_{PC} = 12.1 Hz), 75.5 (dd, J_{PC} = 12.2 Hz, J_{PC} = 10.9 Hz), 67.0 (dd, J_{PC} = 15.5 Hz, J_{PC} = 8.6 Hz), 38.3 (d, J_{PC} = 21.2 Hz), 31.3 (dd, J_{PC} = 8.6 Hz, J_{PC} = 4.5 Hz), 25.9 (dd, J_{PC} = 10.3 Hz, J_{PC} = 3.4 Hz), 15.6 (dd, J_{PC} = 20.8 Hz, J_{PC} = 3.4 Hz). ^{31}P NMR (121.5 MHz, $CDCl_3$) δ ppm: 139.93, 139.16 (diastereomeric mixture). Product is not stable to MS measurements. See spectra 4,1, 4.2, and 4.3.

N^{α}*-4-pentenoyl-L-serine cyanomethyl ester (**30a**)* was synthesized by **Method A** or **B**:

Method A:

N^{α}-*4-pentenoyl-O-tert-butyl-L-serine* (**28a**): H-*O-tert*-butyl-L-serine (**27a**, 500 mg, 3.10 mmole) and *N,N*-diisopropylethylamine (DIPEA, 633 μL, 3.70 mmole) were dissolved in THF (30 mL) and water (30 mL). 4-pentenoic anhydride (676 μL, 3.70 mmole) was dissolved in THF (2 mL), and added to the serine solution. The reaction was monitored by TLC (1:1:0.01 hexanes/EtOAc/acetic acid (AcOH), R_f = 0.30), stained with iodine and ninhydrin. After the disappearance of starting material, the THF was removed under reduced pressure, and the water layer extracted with EtOAc (3 x 100 mL). The organic portions were dried over $MgSO_4$, filtered and concentrated under reduced pressure. The product was purified by silica gel flash chromatography (827 mg) in 93.7% yield. ^{1}H NMR (300 MHz, $CDCl_3$) δ ppm: 6.99 (d, J_{HH} = 8.1 Hz, 1 H), 5.70 (m, 1 H), 4.94 (q, J_{HH} = 17.1, 10.2, 10.2 Hz, 2 H), 4.64 (m, 1 H), 3.71 (dd, J_{HH} = 9 Hz, J_{HH} = 3 Hz, 1 H), 3.46 (dd, J_{HH} = 9.3 Hz, J_{HH} =3 Hz, 1 H), 2.25 (s, 4 H), 0.99 (s, 9 H). ^{13}C NMR (125.8 MHz, $CDCl_3$) δ ppm: 176.0, 173.9, 136.7, 115.8, 73.7, 61.9, 53.0, 35.3, 29.7, 27.3. ESI-MS: $[M-H]^-$ 242.1401 (obsd), 242.1398 (calcd). See spectra 4.4 and 4.5.

N^{α}-*4-pentenoyl-O-tert-butyl-L-serine cyanomethyl ester* (**29a**): N^{α}-4-pentenoyl-*O-tert*-butyl-L-serine (825 mg, 3.39 mmole) was dissolved in chloroacetonitrile (644 μL, 10.20 mmole), and cooled to 0°C, stirring, under argon. Diazabicyclo[5.4.0]undec-7-ene (DBU, 507 μL, 3.39 mmole) was slowly added to the stirring mixture. The reaction was allowed to warm to room temperature, and stir overnight under argon. The reaction mixture was diluted with EtOAc (150 mL), washed with water (2 x 150 mL), then brine (1 x 150 mL), dried over $MgSO_4$, filtered and concentrated (1:1 hexanes/EtOAc, R_f = 0.41) (765 mg, 79.9%). ^{1}H NMR (300 MHz, $CDCl_3$) δ ppm: 6.81 (d, J_{HH} = 8.7 Hz, 1 H), 5.83 (m, 1 H), 5.11 (q, J_{HH} = 18.3, 6.6, 9.9 Hz, 2 H), 4.84 (m, 3 H), 3.86 (dd, J_{HH} = 9.3 Hz, J_{HH} = 3.3 Hz, 1 H), 3.58 (dd, J_{HH} = 9.3 Hz, J_{HH} = 3.3, 1 H), 2.38 (s, 4 H), 1.16 (s, 9 H). ^{13}C NMR (125.8 MHz, $CDCl_3$) δ ppm: 172.7, 169.6, 137.1, 115.7, 114.5, 73.8, 61.9, 52.7, 49.2, 35.2, 29.5, 27.3. ESI-MS: $[MNa]^+$ 305.1478 (obsd), 305.1472 (calcd). See spectra 4.6 and 4.7.

N^{α}-*4-pentenoyl-L-serine cyanomethyl ester* (**30a**): N^{α}-4-pentenoyl-*O-tert*-butyl-L-serine cyanomethyl ester (750 mg, 2.69 mmole) was dissolved in an ice-cold solution of triflouroacetic acid (TFA) with 1 % (v/v) triisopropylsilane (TIS). The reaction was stirred at 0°C for 4 hours, and determined complete by TLC (EtOAc, R_f = 0.43). The reaction mixture was poured into ice-

cold saturated $NaHCO_3$ (250 mL) and EtOAc (120 mL). The organic layer was washed with saturated $NaHCO_3$ (3 x 100 mL), then brine (1 x 100 mL), dried over $MgSO_4$, filtered, and concentrated under reduced pressure. The mixture was purified by silica gel flash chromatography to give the product (156 mg) in 25.6% yield. ^{1}H NMR (300 MHz, $CDCl_3$) δ ppm: 6.90 (d, J_{HH} = 7.8 Hz, 1 H), 5.87 (m, 1 H), 5.10 (t, J_{HH} = 19.5, 10.8 Hz, 2 H), 4.80 (d, J_{HH} = 1.5 Hz, 3 H), 4.70 (m, 1 H), 4.06 (dd, J_{HH} = 11.7 Hz, J_{HH} = 3.6, 3.3 Hz, 1 H), 3.87 (dd, J_{HH} = 11.4 Hz, J_{HH} = 3.6, 3.6 Hz, 1 H), 2.38 (d, J_{HH} = 3.0 Hz, 4 H). ^{13}C NMR (125.8 MHz, $CDCl_3$) δ ppm: 173.5, 169.8, 137.0, 116.4, 114.5, 63.0, 54.6, 49.7, 35.8, 29.8. ESI-MS: $[MNa]^+$ 249.0847 (obsd), 249.0846 (calcd). See spectra 4.8 and 4.9.

Method B:

Modified from reference 8.

*N^{α}-4-pentenoyl-L-serine-OH (**34**):* H-*O*-L-serine (**33**, 500 mg, 4.75 mmole) and sodium bicarbonate (560 mg, 6.66 mmole) were dissolved in water (60 mL) and hexanes (30 mL), rapidly stirring at room temperature. The anhydride (1.22 mL, 6.66 mmole) was dissolved in 1,4-dioxane (15 mL) and added in one portion to the serine/base mixture. The reaction was monitored by TLC in 65:25:4 $CHCl_3$/MeOH/dH_2O (R_f = 0.19)(stained with ninhydrin or iodine), and determined complete after two hours. The reaction was quenched with dH_2O (pH=1 with HCl, 250 mL), and extracted with CH_2Cl_2 (250 mL). The aqueous layer was then extracted with 2 x 100 mL CH_2Cl_2. Saturated NaCl was then added to the aqueous layer (350 mL), which was extracted with THF (3 x 150 mL). The THF portions were combined, dried over $MgSO_4$, filtered, and concentrated under reduced pressure to give the product in 63.4% yield (564 mg). ^{1}H NMR (300 MHz, D_2O) δ ppm: 5.81 (m, 1H), 5.00 (m, 2H), 4.41 (m, 1H), 3.87 (m 2H), 2.31 (m, 4H). See spectrum 4.10.

*N^{α}-4-pentenoyl-L-serine cyanomethyl ester (**30a**): N^{α}*-4-pentenoyl-L-serine-OH (564 mg, 3.01 mmole) was dissolved in anhydrous DMF (16.7 mL) under argon at room temperature and left stirring. Triethylamine (1.26 mL, 9.03 mmole) was added to the stirring solution. Chloroacetonitrile (8.4 mL, 133 mmole) was slowly added to the stirring serine solution, and allowed to mix overnight at room temperature under argon. The reaction was determined complete by TLC in 65:25:4 $CHCl_3$/MeOH/dH_2O (R_f = 0.84) (stained with iodine). The reaction

mixture was concentrated under reduced pressure, then re-dissolved in EtOAc (200 mL) and water (100 mL). The organic layer was washed with water (2 x 100 mL) then brine (1 x 100 mL), dried over $MgSO_4$, filtered, and concentrated under reduced pressure. The product was purified by silica gel flash chromatography (EtOAc, $R_f = 0.33$) to give the pure product in 51% yield (345 mg). ^1H NMR (300 MHz, $CDCl_3$) δ ppm: 6.67 (d, J_{HH} = 7.5 Hz, 1 H), 5.89 (m, 1H), 5.13 (tdd, J_{HH} = 18.6 Hz, J_{HH} = 1.5 Hz, J_{HH} = 1.2 Hz, 2H), 4.82 (d, J_{HH} = 3.0 Hz, 2H), 4.76 (m, 1H), 4.09 (m, 2H), 3.09 (bs, 1H), 2.42 (m, 4H). See spectrum 4.11.

N$^{\alpha}$-*4-pentenoyl-phospho*(O-*nitrophenylethyl*-O'-*tert-butyl*)-L-*serine cyanomethyl ester* (**31a**): *N*$^{\alpha}$-4-pentenoyl-L-serine cyanomethyl ester (**30a**, 150 mg, 663 μmole) was dissolved in anhydrous THF (2.0 mL), in a round bottom flask fitted with an oven dried stir bar under argon. In a separate pear flask, *O*-1-(2-nitrophenyl)ethyl-*O'-tert*butyl-*N,N*-diethyl phosphoramidite (**24**, 340 mg, 995 μmole) and 4,5-dicyanoimidazole (157 mg, 1.33 mmole) were dissolved in anhydrous THF (1.3 mL), and kept dark. The phosphoramidite solution was delivered to the serine solution via syringe, and the reaction was allowed to stir overnight, under argon, in the dark. The reaction was judged complete by loss of starting material by TLC. The mixture was concentrated under reduced pressure, and redissolved in EtOAc (50 mL). The organic layer was washed with 10% $NaHCO_3$ (2 x 80 mL), brine (1 x 80 mL), then dried over sodium sulfate (Na_2SO_4), decanted and concentrated. The phosphite mixture was then oxidized with *tert*-butyl hydroperoxide (*t*BuOOH, 266 μL of 5 M solution in decane, 1.33 mmole) in dichloromethane (CH_2Cl_2, 10 mL) for one hour, in the dark. The mixture was diluted with CH_2Cl_2 (50 mL), and washed with 10% $NaHCO_3$ (2 x 80 mL) and brine (1 x 80 mL), then dried over $MgSO_4$, filtered and concentrated. The product was partially purified by silica gel flash chromatography (1:2 hex/EtOAc, $R_f = 0.26$), and carried on to the next step before final purification (68.2%).

N$^{\alpha}$-*4-pentenoyl-phospho(nitrophenylethyl)-L-serine cyanomethyl ester* (**32a**): *N*$^{\alpha}$-4-pentenoyl-phospho(1-nitrophenylethyl-2-*tert*-butyl)-L-serine cyanomethyl ester (69 mg, 135 μmole) was dissolved in acetonitrile (MeCN, 4.0 mL) at room temperature, stirring, and kept dark. A solution of TFA (1.0 mL) with TIS (50 μL) was added to the solution, and stirred for 10 minutes at room temperature. The mixture was then poured into ice-cold saturated $NaHCO_3$ (4.0 mL). The product mixture was purified by reverse phase HPLC. (93:7 to 0:100 water/MeCN/0.1% TFA,

over 35 minutes, R_t = 22.68 min) in 99% yield (61.0 mg). ^{1}H NMR (300 MHz, $CDCl_3$) δ ppm: 8.00 (ddd, J_{HH} = 8.1 Hz, J_{HH} = 3.6, 3.6 Hz, J_{HH} = 1.5, 1.2, 1.2, 1.5 Hz, 1 H), 7.79 (m, 2 H), 7.53 (m, 1 H), 6.04 (m, 1 H), 5.86 (m, 1 H), 5.11 (m, 2 H), 4.88 (m, 3 H), 4.40 (m, 3 H), 2.40 (d, J_{HH} = 7.5 Hz, 4 H), 1.71 (dd, J_{HH} = 6.3 Hz, J_{HH} = 1.2, 1.2 Hz, 3 H). ^{13}C NMR (125.8 MHz, $CDCl_3$) δ ppm: 173.7 (d, J_{PC} = 4.5 Hz), 168.3, 147.3, 137.5, 137.0, 134.6 (d, J_{PC} = 8.7 Hz), 129.5 (d, J_{PC} = 1.8 Hz), 128.2 (d, J_{PC} = 2.4 Hz), 125.0 (d, J_{PC} = 2.9 Hz), 116.3 (d, J_{PC} = 3.4 Hz), 114.2, 73.3, 67.2, 52.8 (d, J_{PC} = 6.3 Hz), 50.1 (d, J_{PC} = 7.4 Hz), 35.5 (d, J_{PC} = 3.5 Hz), 29.7 (d, J_{PC} = 2.3 Hz), 24.7 (m). ^{31}P (121.5 MHz, $CDCl_3$): -1.382. ESI-MS: $[M-H]^-$ 454.1017 (obsd), 454.1021 (calcd). See spectra 4.12, 4.13, and 4.14.

N^{α}-*4-pentenoyl-O-tert-butyl-L-threonine (***28b***):* H-*O-tert*-butyl-L-threonine (**27b**, 500 mg, 2.85 mmole) and DIPEA (683 μL, 3.99 mmole) were dissolved in THF (40 mL) and water (10 mL). 4-pentenoic anhydride (730 μL, 3.99 mmole) was dissolved in THF (5 mL), and added to the threonine solution. The reaction was monitored by TLC (1:1:0.01 hexanes/EtOAc/AcOH, R_f = 0.31), stained with iodine and ninhydrin. After the disappearance of starting material, the mixture was concentrated under reduced pressure, and the product was purified by silica gel flash chromatography (625 mg, 85.3%). ^{1}H NMR (300 MHz, $CDCl_3$) δ ppm: 6.74 (d, J_{HH} = 8.4 Hz, 1 H), 5.88 (m, 1 H), 5.12 (q, J_{HH} = 17.4, 8.1, 10.2 Hz, 2 H), 4.60 (dd, J_{HH} = 8.7 Hz, J_{HH} = 2.7, 2.4 Hz, 1 H), 4.32 (m, 1 H), 2.43 (m, 4 H), 1.20 (s, 9 H), 1.71 (d, J_{HH} = 6.6 Hz, 3 H). ^{13}C NMR (125.8 MHz, $CDCl_3$) δ ppm: 174.3, 174.0, 136.9, 116.0, 75.2, 67.2, 57.7, 35.6, 29.7, 28.4, 20.1. ESI-MS: $[M-H]^-$ 256.1551 (obsd), 256.1554 (calcd). See spectra 4.15 and 4.16.

N^{α}-*4-pentenoyl-O-tert-butyl-L-threonine cyanomethyl ester (***29b***):* N^{α}-4-pentenoyl-*O-tert*-butyl-L-threonine (390 mg, 1.51 mmole) was dissolved in chloroacetonitrile (478 μL, 7.55 mmole) and cooled to 0°C, stirring, under argon. DBU (226 μL, 1.51 mmole) was slowly added to the stirring mixture. The reaction was allowed to warm to room temperature, and stir overnight under argon. The reaction mixture was diluted with EtOAc (100 mL), washed with water (2 x 100 mL) and brine (1 x 100 mL), then dried over $MgSO_4$, filtered and concentrated (1:1 hexanes/EtOAc, R_f = 0.43) (321 mg, 71.7%). ^{1}H NMR (300 MHz, $CDCl_3$) δ ppm: 6.39 (d, J_{HH} = 9.0 Hz, 1 H), 5.91 (m, 1 H), 5.14 (q, J_{HH} = 17.1, 7.5, 10.2 Hz, 2 H), 4.78 (d, J_{HH} = 3.0 Hz, 2 H), 4.61 (dd, J_{HH} = 9.3 Hz, J_{HH} = 2.1, 1.8 Hz, 1 H), 4.27 (m, 1 H), 2.42 (d, J_{HH} = 2.7 Hz, 4 H), 1.21 (d, J_{HH} = 6.3 Hz, 3 H),

1.14 (s, 9H). ^{13}C NMR (125.8 MHz, $CDCl_3$) δ ppm: 173.1, 169.9, 137.1, 115.9, 114.3, 74.5, 67.2, 57.7, 49.1, 35.5, 29.5, 28.6, 21.0. ESI-MS: $[MNa]^+$ 319.1617 (obsd), 319.1628 (calcd). See spectra 4.17 and 4.18.

N^{α}-*4-pentenoyl-L-threonine cyanomethyl ester (***30b***):* N^{α}-4-pentenoyl-*O-tert*-butyl-L-threonine cyanomethyl ester (315 mg, 1.06 mmole) was dissolved in an ice-cold solution of TFA with 1% (v/v) TIS. The reaction was stirred at 0°C for two hours, and determined to be complete by TLC (1:1 hex/EtOAc, R_f = 0.15). The reaction mixture was poured into ice-cold saturated $NaHCO_3$ (80 mL) and EtOAc (80 mL). The organic layer was washed with saturated $NaHCO_3$ (2 x 80 mL) and brine (1 x 80 mL), then dried over $MgSO_4$, filtered, and concentrated under reduced pressure. The mixture was purified by silica gel flash chromatography to give the product (150 mg) in 59.0% yield. ^1H NMR (300 MHz, $CDCl_3$) δ ppm: 6.39 (d, J_{HH} = 8.4 Hz, 1 H), 5.90 (m, 1 H), 5.14 (t, J_{HH} = 17.4, 13.8 Hz, 2 H), 4.87 (q, J_{HH} = 15.6, 7.5, 15.6 Hz, 2 H), 4.69 (dd, J_{HH} = 9.0 Hz, J_{HH} = 2.7, 2.4 Hz, 1 H), 4.46 (qd, J_{HH} = 6.3, 6.3, 6.3 Hz, J_{HH} = 2.4, 2.4, 2.4, 2.4 Hz, 1 H), 2.43 (d, J_{HH} = 2.7 Hz, 4 H), 1.27 (t, J_{HH} = 4.2, 2.1 Hz, 3 H). ^{13}C NMR (125.8 MHz, $CDCl_3$) δ ppm: 173.7, 170.2, 137.1, 116.4, 114.5, 68.0, 57.5, 49.6, 36.0, 29.8, 20.6. ESI-MS: $[MNa]^+$ 263.1005 (obsd), 263.1002 (calcd). See spectra 4.19 and 4.20.

N^{α}-*4-pentenoyl-phospho(*O-*nitrophenylethyl*-O'-*tert-butyl)-L-threonine cyanomethyl ester (***31b***):* N^{α}-4-pentenoyl-L-threonine cyanomethyl ester (140 mg, 582 μmole) was dissolved in anhydrous THF (2 mL), in a round bottom flask fitted with an oven dried stir bar under argon. In a separate pear flask, *O*-1-(2-nitrophenyl)ethyl-*O'-tert*butyl-*N,N*-diethyl phosphoramidite (**24**, 299 mg, 874 μmole) and 4,5-dicyanoimidazole (137 mg, 1.16 mmole) were dissolved in anhydrous THF (1 mL), and kept dark. The phosphoramidite solution was delivered to the threonine solution via syringe, and the reaction was allowed to stir overnight, under argon, in the dark. The reaction was judged complete by loss of starting material by TLC. The mixture was concentrated under reduced pressure, and re-dissolved in EtOAc (80 mL). The organic layer was washed with 10 % $NaHCO_3$ (2 x 80 mL), brine (1 x 80 mL), then dried over Na_2SO_4, decanted and concentrated. The phosphite mixture was then oxidized with *t*BuOOH (232 μL of 5 M solution in decane, 1.16 mmole) in dichloromethane (CH_2Cl_2, 10 mL) for one hour, in the dark. The mixture was diluted with CH_2Cl_2 (70 mL), and washed with 10% $NaHCO_3$ (2 x 80 mL), brine (1 x 80 mL), then dried

over $MgSO_4$, filtered and concentrated The product was partially purified by silica gel flash chromatography (R_f = 0.19, 1:1 hex/EtOAc) and carried on to the next step before final purification (70.1%).

N^{α}-*4-pentenoyl-phospho(1-nitrophenylethyl)-L-threonine cyanomethyl ester (***32b***):* N^{α}-4-pentenoyl-phospho(1-nitrophenylethyl-2-*tert*-butyl)-L-threonine cyanomethyl ester (250 mg, 476 μmole) was dissolved in MeCN (3.5 mL) at room temperature, stirring, and kept dark. A solution of TFA (3.5 mL) with TIS (70 μL) was added to the solution, and stirred for 15 minutes at room temperature. The mixture was then poured into ice-cold saturated $NaHCO_3$ (10 mL). The mixture was purified by reverse phase HPLC (93:7 to 0:100 water/acetonitrile/0.1% TFA over 35 minutes, R_t = 23.86 min) in 41.0% yield (92.0 mg). ^{1}H NMR (300 MHz, $CDCl_3$) δ ppm: 8.00 (d, J_{HH} = 7,=.8 Hz, 1 H), 7.79 (m, 2 H), 7.55 (m, 1 H), 6.89 (t, J_{HH} = 7.2, 9.0 Hz, 1 H), 6.53 (bs, 1 H), 6.05 (m, 1 H), 5.87 (m, 1 H), 5.13 (m, 2 H), 4.92 (m, 6 H), 2.42 (d, J_{HH} = 2.1 Hz, 4 H), 1.74 (d, J_{HH} = 6.3 Hz, 3 H), 1.35 (dd, J_{HH} = 24.0 Hz, J_{HH} = 6.3, 6.6 Hz, 3 H). ^{13}C NMR (125.8 MHz, $CDCl_3$) δ ppm: 174.8, 169.1 (d, J_{PC} = 6.3 Hz), 147.8 (d, J_{PC} = 12.1 Hz), 137.6 (t, J_{PC} = 4.7 Hz), 137.0, 134.7 (d, J_{PC} = 2.3 Hz), 129.8, 128.5 (d, J_{PC} = 15.5 Hz), 125.2 (d, J_{PC} = 2.3 Hz), 116.8 (d, J_{PC} = 3.4 Hz), 114.5 (d, J_{PC} = 4.7 Hz), 75.8 (t, J_{PC} = 5.8 Hz), 73.7 (t, J_{PC} = 5.2 Hz), 56.6 (dd, J_{PC} = 5.8 Hz, J_{PC} = 2.4 Hz), 50.5 (d, J_{PC} = 10.3 Hz), 35.9 (d, J_{PC} = 1.1 Hz), 30.1, 24.9 (dd, J_{PC} = 8.7 Hz, J_{PC} = 5.3 Hz), 19.2 (dd, J_{PC} = 9.2 Hz, J_{PC} = 2.3 Hz). ^{31}P (121.5 MHz, $CDCl_3$): -1.13, -1.17. ESI-MS: $[M-H]^-$ 468.1168 (obsd), 468.1177 (calcd). See spectra 4.21, 4.22, and 4.23.

5'-Phospho-2'-deoxycytidylyl(3',5')phosphoadenosine (pdCpA, ***35****).* pdCpA was synthesized as previously reported with the following minor modifications.[2] In phosphitylation steps, tetrazole was replaced with 4,5-dicyanoimidazole. In oxidation steps, two equivalents of *t*BuOOH was added to the reactant stirring in CH_2Cl_2 rather than using iodine in THF/water. The final deprotection of pdCpA was performed with 10% (v/v) aqueous ammonium hydroxide instead of concentrated ammonium hydroxide (30% (v/v)). After final deprotection, the pdCpA was purified by reverse phase preparatory HPLC in a 93:7 to 0:100 water:acetonitrile (0.1% TFA) gradient over 35 minutes (t_R = 5.8 min), and no desalting step was necessary. The tetrabutylammonium salt of pdCpA was prepared by ion exchange chromatography, as described,[2] and it was important to dissolve the dinucleotide in slightly acidic water before

application to the column to ensure exchange of protons to tetrabutylammonium. The number of equivalents of the counter ion was determined by ^{1}H NMR (with an increased delay time to correct for aromatic vs. aliphatic integrations). The phosphoramidite reagent *O*-Cytidylyl(*N*-benzyl)-*O*-β-cyanoethyl-*N,N*-diisopropyl-phosphoramidite was purchased from SynGen, Inc. (San Carlos, CA); the phosphoramidite reagent bis-*O,O'*-β-cyanoethyl-*N,N*-diisopropyl-phosphoramidite was purchased from Toronto Research Chemicals (Toronto, Canada).

*4PO-cpSer/cpThr/cpTyr-pdCpA (***36a**, **36b**, **37***):* In general, pdCpA(NBu_4)$_{2.4}$ (10 mg, 8.2 μmol), 4PO-cpAA-OCH_2CN (21 μmole), and tetrabutylammonium acetate (NBu_4OAc) were placed under vacuum overnight. The NBu_4OAc was made up to a 250 mM solution in anhydrous DMF. This solution (100 μL) was used to dissolve the dinucleotide, and then the mixture was added to the amino acid ester under nitrogen. The reaction was allowed to mix at room temperature under nitrogen, and monitored by reverse phase HPLC. Upon complete loss of starting material, the reaction was quenched with 2:1 water/acetonitrile (0.1% TFA) (1.5 mL). The reaction was purified by preparative reverse phase HPLC, and confirmed by ESI-MS. The 4PO-cpSer/cpThr/cpTyr-pdCpA was dissolved in DMSO and quantitated by UV (ε_{max} A_{260}: 30,700 $M^{-1}cm^{-1}$), and stored at –80 °C. 4PO-cpSer-pdCpA: R_t = 23.23 min; ESI-MS: $[MNa]^+$ 1059.0, $[MNaH]^{2+}$ 530.0 (obsd), 1057.7, 529.3 (calcd). 4PO-cpThr-pdCpA: R_t = 23.40 min; ESI-MS: $[MNa]^+$ 1072.9, $[MH]^+$ 1049.0 (obsd), 1072.7, 1049.7 (calcd). 4PO-cpTyr-pdCpA: R_t = 25.80 min; ESI-MS: $[MH]^+$ 1111.2, $[M+2H]^{2+}$ 556.1 (obsd), 1111.0, 556.0 (calcd).

4-2. Semisynthesis and Molecular Biology

TH73G ($tRNA_{CUA}^{-CA}$*).* The gene for the $tRNA_{CUA}^{-CA}$ was received from the Dougherty Lab (California Institute of Technology),[9] amplified in chemically competent DH5α cells and purified according to standard procedure. The plasmid DNA (343 μg) was linearized with FokI restriction enzyme (New England Biolabs) according to manufacturer's recommendations. Upon confirmation of digestion by analytical agarose gel electrophoresis, the DNA was purified by phenol/chloroform/isoamyl (PCI) extraction. The tRNA was transcribed from the DNA template using the T7-MEGAshortscript High Yield Transcription Kit (Ambion) according to the manufacturer's protocol. The tRNA was purified by PCI extraction and precipitated with a 1:1 mixture of ethanol:isopropanol at –20°C for at least one hour. After centrifugation, aspiration,

and drying, the pellet was dissolved in 0.1% DEPC-treated water and quantified by UV (RNA: Concentration (μg/mL) = A_{260}/0.025). Aliquots of 20 μg were made in DEPC-treated dH_2O and stored at –80 °C. Additionally, 2% agarose analytical gel electrophoresis (stained with ethidium bromide) revealed a single strong band at approximately 75 bp.

Ligation to the $tRNA_{CUA}^{-CA}$ was performed as follows:

1. 30 μL of 10 mM 4-(2-hydroxyethyl)-1-piperazine-ethanesulfonic acid (HEPES), pH 7.5 was added to 30 μg $tRNA_{CUA}^{-CA}$ in 15 μL DEPC dH_2O.
2. This microfuge tube was placed in a beaker of boiling water, which was set in a bucket of ice water. The sample was allowed to cool to ~ 37 °C (water temperature measured at the top of the beaker where the sample was floating).
3. While the sample was cooling, the rest of the reaction was assembled:
   - 12 μL pdCpA-aa, ~ 3mM in DMSO
   - 12 μL 10 X T4 RNA ligase buffer (New England Biolabs)
   - 45 μL DEPC dH_2O
   - 6 μL T4 RNA ligase (New England Biolabs, 20 U/μL)
4. When the tRNA/HEPES was cooled to ~ 37 °C, it was added to the reaction mixture, and the contents briefly vortexed and centrifuged. The reaction was incubated at 37 °C for 2 hours.
5. The reaction was quenched by adding 17.5 μL DEPC dH_2O and 12.5 μL 3.0 M NaOAc, pH 5.0 (150 μL total).
6. The amino-acyl tRNA was purified by PCI extractions as follows:
   a. 150 μL 25:24:1 phenol/chloroform/isoamyl alcohol
   b. 68.7 μL DEPC dH_2O + 6.3 μL 3.0 M NaOAc, pH 5.0
   c. 225 μL 24:1 chloroform/isoamyl alcohol
7. The combined aqueous layers were combined with 700 μL 1:1 *Et*OH/*iPr*OH, briefly vortexed, and precipitated overnight by standing at – 20 °C.
8. Samples were recovered by microcentrifuging at maximum speed for 15 minutes at 4 °C.
9. The supernatant was removed by pipetting, and samples were dried under vacuum for 30 minutes.
10. Samples were stored dry at – 80 °C until ready to de-salt, at which point they were dissolved in 30 μL 1mM NaOAc, pH 4.5, and desalted using BD Biosciences CHROMA SPIN-30 DEPC dH_2O columns (following manufacturer's instructions). The desalted samples were quantified by measuring the UV A_{260} of a diluted sample, confirmed by ESI-TOF MS, and stored at – 80 °C. (UV A_{260}/0.025 = Concentration in μg/mL)

MALDI-TOF MS measurements were preformed as reported.[1] For ESI-TOF MS measurements, a PerSeptive Biosystems™ Mariner Workstation was used. DNA samples were stocked in dH_2O (~100 μM), $tRNA_{CUA}^{-CA}$ samples were stocked in DEPC dH_2O (~ 350 μM), and $tRNA_{CUA}^{cpAA}$ samples were stocked as above (~20 μM). Samples were diluted to 5- 25 μM using 60:20:20

MeCN/*iPr*OH/10 mM NH_4OAc with 20 mM piperidine and 10 mM imidazole. The samples were infused toward the detector using a syringe pump injector without heat, and detected in negative ion mode. The data peaks were de-convoluted by hand as piperidinium salts of the parent ion. The most accurate measurements were made with data corresponding to lower charge states, and thus higher *m/z* ratios (above 1200.0 Da).

Exemplary data series are as follows:

$tRNA_{CUA}^{-CA}$: 1199.9 = $[M+6pip-20]^{20-}$
1332.9 = $[M+6pip-18]^{18-}$
1410.2 = $[M+6pip-17]^{17-}$
1505.8 = $[M+7pip-16]^{16-}$
1599.9 = $[M+5pipi-15]^{15-}$

$tRNA_{CUA}^{cpSer}$: 1466.2 = $[M+5pip-17]^{17-}$
1567.3 = $[M+7pip-16]^{16-}$
1671.6 = $[M+7pip-15]^{15-}$
1661.1 = $[M+5pip-15]^{15-}$
1793.0 = $[M+7pip-14]^{14-}$

Additionally, the acylated tRNA was analyzed by Denaturing Polyacrylamide Gel Electrophoresis (D-PAGE): The general protocol and buffers can be found in "Current Protocols in Molecular Biology; 2.12.1-2.12.7: Purification of Oligonucleotides Using Denaturing Polyacrylamide Gel Electrophoresis" (http://www.interscience.wiley.com/c_p/index.htm). **Note:** even though the procedure states that a 6% gel will resolve a 70 bp oligonucleotide, the 74 or 76 bp tRNA samples ran near the bottom of the gel with no resolution.

More optimum gel conditions were as follows: 12% polyacrylamide, 1.5 mm thick, 10 well. A 0.5 μg sample of tRNA in ~10 μL urea loading buffer was loaded per well. A 1:5 mixture of nucleic acid loading buffer (containing xylene blue, 5X)/urea loading buffer was loaded on the outside lanes. The gel was run at 140V for ~ 2 hours (until the xylene blue was about 1 cm from the bottom of the plate; the bromophenol blue had dropped off a long time before then). The gel was soaked in dilute ethidium bromide, which was sufficient to visualize the tRNA on a transilluminator and capture an image for documentation.

nAChR cloning: The nAChR-a gene was prepared as previously reported.[10]

mVASP cloning: The mVASP gene was received from the Gertler Lab (Massachusetts Institute of Technology) in a pBS-KSII vector with an upstream T5 promoter. The site specific mutagenesis of Ser153TAG (S153Z, where Z represents the amber stop codon TAG) was performed following the Stratagene QuikChange protocol and the following primers: sense 5'-GAG CGC CGG GTC TAG AAT GCA GGA GGC CC; antisense 5'-GGG CCT CCT GCA TTC TAG ACC CGG CGC TC. Underlined bases comprise the amber stop codon. Several

colonies were picked for sequencing; one sample with the correct sequence was kept for further use.

Both the WT and S153Z mVASP genes were amplified from the pBS-KSII vectors using PCR with *Pfu* Turbo Polymerase (Stratagene, La Jolla, CA) and the following primers to include an N-terminal 6XHis-tag: Forward 5'- CACC ATG CAT CAT CAT CAT CAT CAT GGA TCC ATG AGC GAG ACG GTC ATC-3' Reverse 5'- TCA AGG AGA ACC CCG CTT CCT CAG-3'. The products were purified by agarose gel electrophoresis and stored at -20 °C. The products were then used in the TOPO directional cloning reaction as described by the manufacturer (TOPO Directional Cloning: pcDNA3.1/V5-His; Invitrogen, Carlsbad, CA). Colonies were picked and plasmid DNA purified by standard procedure. The DNA was screened by a single restriction enzyme digest: Sal I will cut the empty vector into two pieces, 2.3 and 3.2 kb in length, while it will cut the pcDNA/mVASP vectors into two pieces, 2.1 and 4.4 kb in length. Several samples with the insert were submitted for sequencing, and one of each plasmid sample with the correct sequence was stored at –20 °C for future work. Plasmid names: pcDNA-His-mVASP-WT and pcDNA-His-mVASP-S153Z.

mRNA: Plasmid DNA of WT and S153Z mVASP was amplified in DH5α cells using standard protocol. Approximately 100 μg of each plasmid were linearized with PmeI (which cuts directly after the non-amber stop codon), purified by agarose gel electrophoresis, and redissolved in DEPC treated water. The mRNA was then transcribed from the templates using the Ambion T7 mMessage mMachine® High Yield Capped RNA Transcription Kit (catalog # 1344). The transcription reactions were set up according to manufacturer's protocol without the radiolabel tracer. After incubation for two hours at 37 °C, and subsequent incubation with DNase I, the reaction was quenched using water and ammonium acetate solution (0.1 final volume of 5 M NH_4OAc with 100 mM EDTA). The mRNA was purified and recovered using phenol/chloroform/isoamyl alcohol extraction, quantified using UV: $A_{260}/0.025$ = concentration (μg/mL), and stored in DEPC treated water at – 80 °C.

The mRNA was analyzed using glyoxal-agarose gels. Bis-Pipes-Tris-EDTA (BPTE) buffer was prepared and stocked as a 10X solution at room temperature (note: no DEPC water was necessary, as the mRNA was not recovered from the gels). The glyoxal reaction mixture was

prepared according to literature procedure, and stored in small aliquots at – 80 °C.[21] Briefly, the procedure follows:

De-ionizing the Glyoxal:

Immediately before use, the glyoxal was passed through a small column of mixed-bed ion-exchange resin (Bio-Rad AG-510-X8) and the pH of the eluent was monitored. Once the pH was > 5.5, the glyoxal was used immediately, or stored in aliquots under N_2 at – 20 °C.

Glyoxal Reaction Mixture: ***USE EXTRA CAUTION WHEN HANDLING***

DMSO	6 mL
e-ionized glyoxal	2 mL
10 X BPTE buffer	1.2 mL
80 % glycerol in water	0.6 mL
ethidium bromide (10 mg/mL in dH_2O)	0.2 mL
Total	10 mL

Divide into small aliquots (100 to 200 μL), and store at – 80 °C.

To analyze the mRNA, the sample (at least 1 μg in 1 – 2 μL) was mixed with 10 μL glyoxal reaction mixture and incubated at 55 °C for one hour. Meanwhile, the agarose gel with 1 X BPTE buffer (1.5 % for 0.5 – 8.0 kb mRNA) was prepared. After incubation, the samples were chilled in an ice bath for 10 minutes, and then centrifuged for 5 seconds to bring everything to the bottom of the tube. Next, 5 X nucleic acid gel loading buffer (2 μL) was added to each sample, and immediately loaded into the gel. New England Biolab's Tri-Dye DNA marker was loaded with ethidium bromide (0.5 μL per lane) in the outermost lanes. The gel was electrophoresed at 50 V for 2 hours (running at higher voltage caused the RNA to smear).

4-3. Protein Synthesis

Translation or Suppression Reactions (mVASP or nAChR). Translation reactions were performed using the rabbit reticulocyte lysate translation kit (Promega, Madison, WI) following manufacturer's instructions. The RNase inhibitor SUPERase•In™ was purchased from Ambion (Austin, TX).

In general, translation reactions were set up as follows:

Component	WT	Mutant
DEPC dH_2O	15 μL	15 – **xx** μL
Complete amino acids mix	2.5 μL	2.5 μL
RNase Inhibitor	1.0 μL	1.0 μL

deprotected tRNA	--------	10 μg in **xx** μL
mRNA (2 μg/μL)	1.5 μL	1.5 μL
Rabbit Reticulocyte Lysate	30.0 μL	30.0 μL
TOTAL	50.0 μL	50.0 μL

Each reaction mixture was incubated at 30 °C for 2 to 3 hours. If samples were not immediately purified, they were stored at – 80 °C.

*4PO-tRNA was deprotected by adding equal volume of tRNA to saturated I_2 solution in dH_2O, and incubating for 10 minutes at 27 °C. NVOC-tRNA was deprotected by irradiation with λ = 365 nm for 5 minutes (7 mW/cm^2). The deprotected tRNA was at a *final* concentration of 2 μg/μL.*

Purification of proteins and analysis

nAChR proteins were not purified; analysis was performed as by E. J. P. (CalTech): PAGE samples were prepared by mixing 10 μL of unpurified rabbit reticulocyte translation mix with 4 μL 6X SDS gel loading buffer and diluting to a total volume of 24 μL. Samples were run at 150 V on a 10% polyacrylamide Readygel (BioRad, Hercules, CA) in 1X Tris/Glycine/SDS buffer (10X stock from BioRad). Protein was transferred to nitrocellulose membrane, which was blocked with 5% milk in 1 X PBS (Irvine Scientific, Santa Ana, CA) with 0.1% (v/v) Tween 20 (Sigma-Aldrich) for 1 hour. The blot was labeled with mouse anti-HA epitope primary antibody (Covance Research Products, Grand Rapids, MI) for 1 hour at a 1:3000 dilution in the 5% milk solution. After washing with 3 times 1 X PBS + 0.1% (v/v) Tween 20, the membrane was labeled for 1 hour with horse radish peroxidase-conjugated goat anti-mouse secondary antibody (Jackson Immunoresearch Laboratories, West Grove, PA). The blot was washed with 3 times 1 X PBS + 0.1% (v/v) Tween 20 and developed with Supersignal West Pico chemiluminescence reagents from Pierce (Rockford, IL) on Amersham (Buckinghamshire, England) Hyperfilm.

His-tagged mVASP proteins were purified by **Method C** or **D** below:

Method C: pH based elution from Ni-NTA resin (buffers stored at 4 °C)

Buffer A: 100 mM NaH_2PO_4, 2% SDS, 2 mM β-mercaptoethanol, pH 8.0
Buffer B: 50 mM mM NaH_2PO_4, 150 mM NaCl, 2 mM β-mercaptoethanol, pH 8.0
Buffer C: Buffer B, pH 7.0
Buffer D: Buffer B, pH 4.5
Buffer E: Buffer B, pH 7.0 with 1XBSA

In all bead steps, liquid was carefully removed with flat gel loading tip:

1. 100 µL Qiagen Ni-NTA agarose beads (~50% slurry) was placed in an eppendorf tube and the liquid removed.
2. Beads were washed 3 x 200 µL Buffer B.
3. 100 µL Buffer A was added to 50 µL reaction mixture, which was then added to the beads.
4. Beads were rocked at 4°C for two hours.
5. Spin columns were prepared as follows: 2 columns per reaction
    a. Columns: Millipore Ultrafree-MC 30,000 NMWL Filter unit (cat. # UFC3BTK00); or appropriate MW cutoff concentration columns.
    b. Columns were blocked with 300 µL Buffer E, rocking for 2 hr. at RT.
    c. Buffer E was removed by pipette; the columns were washed 3 x 400 µL Buffer B, using a pipette.
6. Liquid was removed from beads and saved as "A."
7. Beads were washed with 4 x 100 µL Buffer C (washes saved as "C").
8. 100 µL Buffer D was added to beads and rocked at 4 °C or RT for two hours.
9. Buffer D was removed from beads, added to 100 µL Buffer B, and saved as "D." An additional 100 µL Buffer D was added to the beads and rocked at room temperature for 30 minutes.
10. The second Buffer D elution was removed and added to "D."
11. "C" and "D" samples were concentrated as follows: each sample was loaded into a prepared column, and concentrated for 15 minutes at 4,000 g. Then 1 to 5 minute increments at 4,000 g were added until ~ 40 µL remained.
12. 6 µL concentrate was sufficient to load per well of SDS-PAGE to visualize by western analysis.

Method D: imidazole based elution from Ni-NTA resin (buffers stored at room temperature):

Buffer A: 100 mM NaH_2PO_4, 300 mM NaCl, 0.2% SDS, pH 7.8
Buffer B: Buffer A with 5 mM imidazole
Buffer C: Buffer A with 300 mM imidazole
Buffer D: Buffer E with 1X BSA (make as needed)
Buffer E: 100 mM NaH_2PO_4, 300 mM NaCl, pH 7.4

In all bead steps, liquid was carefully removed with flat gel loading tip.

1. 100 µL Qiagen Ni-NTA agarose beads (~50 % slurry) were placed in an eppendorf tube and the liquid removed.
2. The beads were washed 3 x 100 µL Buffer A.
3. 100 µL Buffer A and 50 µL reaction mixture were added to the beads.
4. The beads were rocked at 4°C for two hours.
5. Spin columns were prepared as follows: 2 columns per reaction
    a. Columns: Millipore Ultrafree-MC 30,000 NMWL Filter unit (cat. # UFC3BTK00); or appropriate MW cutoff concentration columns.
    b. Columns were blocked with 350 µL Buffer D, rocking for 2 hr. at RT.

c. Buffer D was removed by pipette; columns were washed 4 x 350 μL Buffer E, using a pipette.

6. Liquid was removed from beads and saved as "A."
7. Beads were washed 4 x 200 μL Buffer B (saved washes as "B").
8. 200 μL Buffer C was added to the beads and rocked at 4 °C or RT for two hours.
9. Buffer C was removed from beads and saved as "C." An additional 200 μL Buffer C was added to beads and rocked at room temperature for 30 minutes.
10. The second Buffer C elution was removed and added to "C."
11. "B" and "C" samples were concentrated as follows: each sample was loaded into a prepared column, and concentrated for 7 minutes at 4,000 *g*. Then 1 to 5 minute increments at 4,000 *g* were added until ~ 40 μL remained.
12. 6 μL concentrate was sufficient per well of an SDS gel to visualize by western analysis.

The translation efficiency of mVASP was analyzed using hand cast 10% SDS-PAGE, and transferred to nitrocellulose for western blotting. The membrane was blocked with 5% BSA in Tris Buffered Saline with 0.05% Tween-20 (TBST) overnight. The membrane was probed with a polyclonal rabbit anti-mVASP primary antibody (Gertler Lab, M. I. T.) for 2 hours at a 1:1000 dilution in TBST. After washing the membrane 4 times with TBST, it was labeled with an alkaline phosphatase conjugated goat anti-rabbit secondary antibody (Pierce Biotechnology, Rockford, IL) for 2 hours. The membrane was washed 4 times TBST and visualized using 1-Step NBT/BCIP: Nitro-Blue Tetrazolium Chloride/5-Bromo-4-Chloro-3'-Indoylphosphate p-Toluidine Salt (Pierce Biotechnology, Rockford, IL). Alternatively, the membrane was labeled for 1 hour with horse radish peroxidase-conjugated goat anti-rabbit secondary antibody (Upstate). The blot was washed 3 times 1 X PBS + 0.1% (v/v) Tween 20 and developed as for nAChR.

Acknowledgements

I would like to acknowledge the Cell Migration Consortium and D. A. Dougherty (CalTech) for the opportunity to learn the techniques of the nonsense codon suppression methodology and to establish the appropriate protocol in our labs at M. I. T. A special thank you to D. A. Dougherty, E. J. Petersson, H. A. Lester, and the entire Dougherty group for being so welcoming and creating a great learning environment for two months.

References

(1) Rothman, D. M.; Petersson, E. J.; Vazquez, M. E.; Brandt, G. S.; Dougherty, D. A.; Imperiali, B. "Caged Phosphoproteins," *Journal of the American Chemical Society* **2005**, *127 (3)*, 846-847.

(2) Ellman, J.; Mendel, D.; Anthony-Cahill, S.; Noren, C. J.; Schultz, P. G. "Biosynthetic Method for Introducing Unnatural Amino Acid Site-specifically into Proteins," *Methods in Enzymology* **1991**, *202* 301-336.

(3) Schuber, F.; Pinck, M. "On the Chemical Reactivity of Aminoacyl-tRNA Ester Bond. 1. Influence of pH and Nature of the Acyl Group on the Rate of Hydrolysis," *Biochimie* **1974**, *56 (3)*, 383-390.

(4) Robertson, S. A.; Ellman, J. A.; Schultz, P. G. "A General and Efficient Route for Chemical Aminoacylation of Transfer RNAs," *Journal of the American Chemical Society* **1991**, *113 (7)*, 2722-2729.

(5) Debenham, J. S.; Madsen, R.; Roberts, C.; Fraser-Reid, B. "Two New Orthogonal Amine-Protecting Groups that Can Be Cleaved Under Mild or Neutral Conditions," *Journal of the American Chemical Society* **1995**, *117 (11)*, 3302-3303.

(6) Lodder, M.; Golovine, S.; Laikhter, A. L.; Karginov, V. A.; Hecht, S. M. "Misacylated Transfer RNAs Having a Chemically Removable Protecting Group," *Journal of Organic Chemistry* **1998**, *63 (3)*, 794-803.

(7) Wilk, A.; Chimielewski, M. K.; Grajkowski, A.; Phillips, L. R.; Beaucage, S. L. "The 3-(*N-tert*-Butylcarboxamido)-1-propyl Group as an Attractive Phosphate/Thiophosphate Protecting Group for Solid-Phase Oligodeoxyribonucleotide Synthesis," *Journal of Organic Chemistry* **2002**, *67 (18)*, 6430-6438.

(8) Brandt, G. S. Site-Specific Incorporation of Synthetic Amino Acids into Functioning Ion Channels; *Ph.D.*, California Institute of Technology, **2003**.

(9) Saks, M. E.; Sampson, J. R.; Nowak, M. W.; Kearney, P. C.; Du, F.; Abelson, J. N.; Lester, H. A.; Dougherty, D. A. "An Engineered Tetrahymena $tRNA^{Gln}$ for in Vivo Incorporation of Unnatural Amino Acids into Proteins by Nonsense Suppression," *Journal of Biological Chemistry* **1996**, *271 (38)*, 23169-23175.

(10) England, P. M.; Lester, H. A.; Dougherty, D. A. "Mapping Disulfide Connectivity Using Backbone Ester Hydrolysis," *Biochemistry* **1999**, *38 (43)*, 14409-14415.

(11) Petersson, E. J.; Brandt, G. S.; Zacharias, N. M.; Dougherty, D. A.; Lester, H. A. "Caging Proteins Through Unnatural Amino Acid Mutagenesis," *Methods in Enzymology* **2003**, *360 (Biophotonics, Part A)*, 258-273.

(12) Petersson, E. J. *Unpublished Data*, **2003**.

(13) Kane, J. F. "Effects of Rare Codon Clusters on High-level Expression of Heterologous Proteins in *Escherichia coli*," *Current Opinion in Biotechnology* **1995**, *6 (5)*, 494-500.

(14) Cornish, V. W. A New Tool for Studying Protein Structure and Function (Ribonucleotide Reductase); *Ph.D.*, University of California, Berkeley, **1996**.

(15) Madin, K.; Sawasaki, T.; Ogasawara, T.; Endo, Y. "A Highly Efficient and Robust Cell-free Protein Synthesis System Prepared from Wheat Embryos: Plants Apparently Contain a Suicide System Directed at Ribosomes," *Proceedings of the National Academy of Sciences, U. S. A.* **2000**, *97 (2)*, 559-564.

(16) Short, G. F., III; Laikhter, A. L.; Lodder, M.; Shayo, Y.; Arslan, T.; Hecht, S. M. "Probing the S1/S1' Substrate Binding Pocket Geometry of HIV-1 Protease with Modified Aspartic Acid Analogues," *Biochemistry* **2000**, *39 (30)*, 8768-8781.

(17) Arslan, T.; Mamaev, S. V.; Mamaeva, N. V.; Hecht, S. M. "Structurally Modified Firefly Luciferase. Effects of Amino Acid Substitution at Position 286," *Journal of the American Chemical Society* **1997**, *119 (45)*, 10877-10887.

(18) LaRiviere, F. J.; Wolfson, A. D.; Uhlenbeck, O. C. "Uniform Binding of Aminoacyl-tRNAs to Elongation Factor Tu by Thermodynamic Compensation," *Science* **2001**, *294 (5540)*, 165-168.

(19) Dale, T.; Sanderson, L. E.; Uhlenbeck, O. C. "The Affinity of Elongation Factor Tu for an Aminoacyl-tRNA Is Modulated by the Esterified Amino Acid," *Biochemistry* **2004**, *43 (20)*, 6159-6166.

(20) Asahara, H.; Uhlenbeck, O. C. "The tRNA Specificity of Thermus Thermophilus EF-Tu," *Proceedings of the National Academy of Sciences, U. S. A.* **2002**, *99 (6)*, 3499-3504.

(21) Sambrook, J.; Russell, D. W. In *Molecular Cloning: A Laboratory Manual "Separation of RNA According to Size: Electrophoresis of Glyoxylated RNA through Agarose Gels"*; Argentine, J., Eds.; Cold Spring Harbor Laboratory Press: Cold Spring Harbor, NY, **2001**, 7.27-7.30.

Chapter 5
Toward Reconstituting Directional Motility in VASP-null Cells

Portions of this chapter have been published in the *Journal of the American Chemical Society* as noted in the text.[1] Copyright © 2005 American Chemical Society. E. James Petersson (Dougherty Lab, CalTech) produced the data for the caged-mVASP and caged phospho-mVASP gel shift assay (Figure 5.8).

Introduction

Vasodilator stimulated phosphoprotein (VASP) is a protein of significant interest in cell migration. It is part of the Ena/VASP family which comprises actin binding proteins that localize to the actin stress fibers, the tips of filopodia and the lamellipodial leading edge of migrating fibroblasts.[2] Additionally, the Ena/VASP family has been implicated in other actin-based processes including axon guidance and T cell polarization.[3]

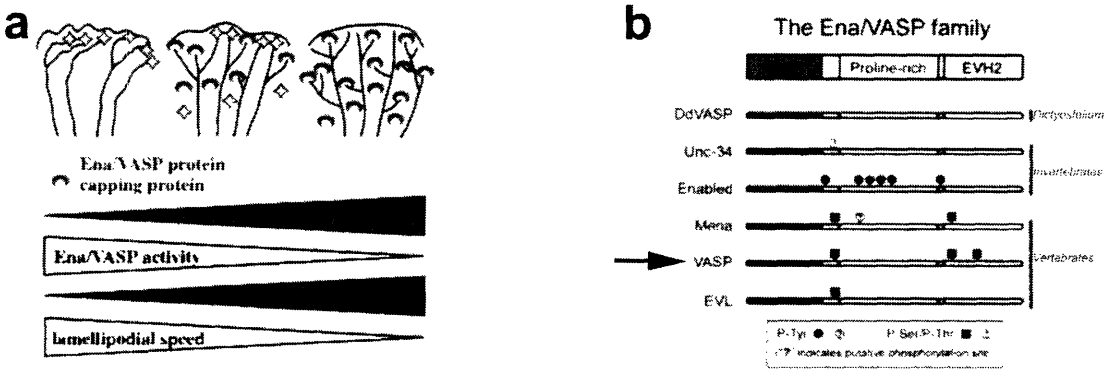

Figure 5.1. Ena/VASP activity and protein organization. **a**) Schematic of the relationship between Ena/VASP proteins and capping proteins regulating lamellipodial protrusion and whole cell motility.[2] **b**) Domains of the Ena/VASP family of proteins.[3] Phosphorylation sites are highlighted as in the key.

The relationship between Ena/VASP proteins and capping proteins is depicted in Figure 5.1a. The Ena/VASP activity at the leading edge of a migrating cell antagonizes actin capping protein activity, which results in longer, less branched filaments that cause more protrusion but less persistence. In contrast, reduced Ena/VASP activity at the leading edge of a migrating cell results in shorter, more branched actin filament networks that cause lower lamellipodial protrusion and higher lamellipodial persistence, and thus faster whole cell migration speeds.[2] Studies have been performed both *in vivo* and *in vitro* and suggest three possible mechanisms for VASP molecular function: anti-capping, anti-branching, and profilin recruitment.[3]

Serine 153 of murine VASP, mVASP, corresponds to Ser157 in human VASP. VASP contains three phosphorylation sites (Ser-157, Ser-239, and Thr-278) that are substrates for

cAMP- and cGMP-dependent serine and threonine kinases (PKA and PKG, respectively) (Figure 5.1b). Serine 157 is preferentially phosphorylated by PKA. The phosphorylation causes an apparent molecular weight shift on SDS-PAGE from 46 to 50 kDa, suggesting a change in the secondary structure of the protein.[3-5]

In cellular studies, Ser157 is phosphorylated by PKA upon detachment of fibroblasts and is dephosphorylated transiently during reattachment to fibronectin. Subsequent cell spreading is observed with synchronous heavy phosphorylation of VASP.[3, 6] Furthermore, VASP-analogs lacking a complementary Ser157 can localize properly in Ena/VASP-null cells but the hypermotility phenotype cannot be observed, likely because the analog cannot be phosphorylated by PKA.[7] The evidence supports the hypothesis that phosphorylation of Ser157 is crucial to VASP function and cell motility. What remains unknown is whether phosphorylation at Ser157 during cell movement represents the overall phosphorylation state of VASP within the cell or if VASP at the leading edge and at focal adhesions is differentially phosphorylated.[3]

To complicate matters further, VASP is a protein for which the *in vivo* phosphorylation state may not necessarily correspond with that observed in experiments performed *in vitro*. As just described, data collected from living cells suggests that VASP function is activated by phosphorylation. However, actin polymerization assays demonstrate that nonphosphorylated VASP can antagonize the capping activity of CapZ,[8] one of the suggested functions of VASP *in vivo*. Therefore, the challenge continues to understand how VASP is spatially and temporally phosphorylated within the cell during migration and adhesion.

The evolved nonsense suppression method was used to synthesize mVASP-S153cpS (Chapter 4). With this protein tool, it will be possible to determine if phosphoserine 153 is sufficient and/or necessary for migrating fibroblast directionality by restoring phospho-mVASP after spatially controlled uncaging in null cells. Ideally, randomly migrating mVASP-null fibroblasts on a surface will have no leading edge. After microinjection of caged phospho-mVASP, high-end UV can be administered to one edge of a cell to uncage phospho-mVASP, thus encouraging lamellipodial speed and giving the cell a direction.

Thus far, mVASP-WT (WT = wild type) has been translated in rabbit reticulocyte and wheat germ extracts. Proteins from both sources have been purified and subjected to gel shift assays. mVASP-S153cpS has been synthesized in the rabbit reticulocyte extract and subjected to

gel shift assays. Current efforts involve synthesis of mVASP-S153cpS in wheat germ extract for the scaled-up production of protein (Chapter 6).

Results and Discussion

5-1. Cloning and Molecular Biology

Initial translation experiments were performed in rabbit reticulocyte extracts. As explained in Chapter 4, a significant amount of background was observed in western blot analysis of samples taken directly from reticulocyte *in vitro* translation reactions because the secondary antibody was anti-rabbit. Therefore, in order to purify the protein and reduce background during analysis, a 6XHis-tag (six contiguous histidine residues) was introduced to the protein.

Initially, the mVASP-WT and mVASP-S153Z genes were cloned into vectors such that each gene was flanked by a T7 promoter and a C-terminal 6XHis-tag for purification (Figure 5.2). A C-terminal V5 epitope was already installed in the vector and left intact. The His-tag was chosen for straightforward purification *via* Ni-NTA resin. The tag was placed on the C-terminus such that only full-length protein would be purified away from the translation mixture. For example, proteins that were aberrantly truncated during the translation or that did not efficiently suppress the stop codon would not contain the His-tag, and would thus be washed away from efficiently translated protein during purification.

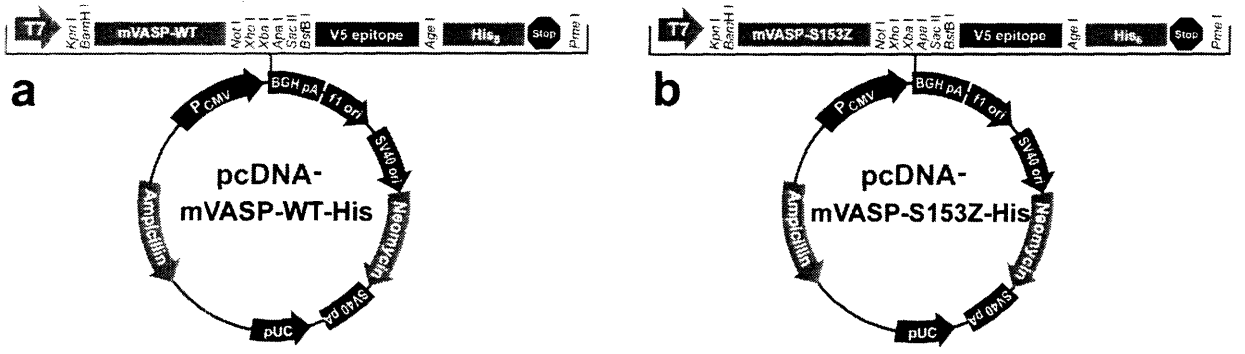

Figure 5.2. Plasmid maps of original vectors. **a**) pcDNA-mVASP-WT-His. **b**) pcDNA-mVASP-S153Z-His.

Briefly, the parent pBS-KSII-mVASP-WT vector was mutated to change serine 153 to the amber stop codon, TAG, *via* site-directed oligonucleotide mutagenesis. Both the WT and S153Z genes were cloned out of their respective parent vector by polymerase chain reaction (PCR) and purified by agarose gel electrophoresis and extraction. The genes were then ligated into the pDNA3.1/TOPO vector (Invitrogen) which contained the T7 promoter, V5 epitope, and

6XHis-tag as seen in Figure 5.2. Additionally, the vector has an upstream PCMV promoter that can be used if the technology is engineered into mammalian cell culture systems (see Chapter 6). Plasmids containing the insert in the proper direction were identified by restriction digest screening and confirmed by DNA sequencing. *In vitro* runoff transcription was performed as in Chapter 4 to yield the mRNA transcript of each gene.

In the first experiments, the mVASP-WT translation efficiency was tested in rabbit reticuloctye extracts, and very little protein was detectable by western blot analysis. After the protein was purified from the reaction mixture, there were no noticeably strong bands of mVASP-WT. Intriguingly, there was considerably strong translation of the mutant mVASP-S153Z (Figure 5.3). Several conditions were tested to evaluate better translation conditions for the wild type protein: switching brands of translation systems, attempting several lengths of incubation time, and eluting protein from Ni-NTA beads *via* pH rather than imidazole. None of the conditions improved the translation efficiency: the mVASP-WT still provided little if any translation, while the mVASP-S153Z appeared as strong bands in the western blot analysis.

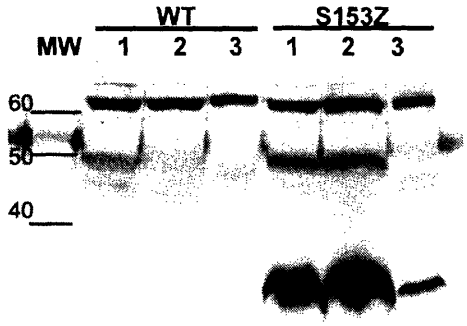

Figure 5.3. Poor translation efficiency of mVASP-WT-His but not mVASP-S153Z-His. Proteins were translated in rabbit reticulocyte extracts, run through Ni-NTA resin, and subjected to Western blot analysis with a polyclonal anti-mVASP antibody. Lanes: 1 = diluted flow through, 2 = washes, 3 = elution.

In order to determine if full-length mVASP-WT-His was being translated at all, several experiments were performed. First, unpurified translation reaction mixture was probed directly by Western analysis with the primary polyclonal anti-mVASP antibody, or one of two primary monoclonal antibodies: anti-His6 or anti-V5. The blots contained the positive control His-mVASP-WT (provided by M. Barzik, Gertler Lab, M. I. T.). As seen in Figure 5.4a, it appeared that the full mVASP-WT-His was not being translated. Furthermore, the pcDNA-mVASP-WT-His plasmid was introduced to a transcription/translation system to ensure that the problem did not stem from the mRNA. Even in this directly coupled transcription/translation system, the mVASP-WT-His construct did not fully translate (Figure 5.4b).

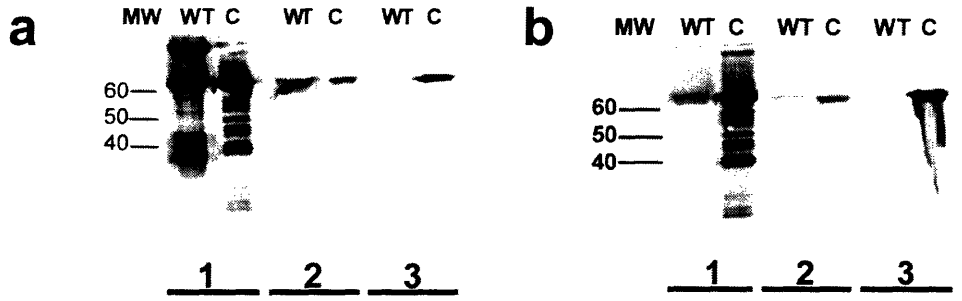

Figure 5.4. mVASP-WT-His is not fully translated. **a**) Translation mixture probed without purification. **b**) Transcription/translation mixture probed without purification. Lanes: WT = mVASP-WT-His from mRNA or plasmid DNA, C = control His-mVASP-WT protein. Nitrocellulose probed with the following primary antibodies: 1 = polyclonal anti-mVASP antibody, 2 = monoclonal anti-His6 antibody, 3 = monoclonal anti-V5 antibody.

At this time in the project, it became known that the native C-terminus of mVASP-WT is vital to its activity and it is rather sensitive to any additional residues.[9] It is likely that the combination of the V5 epitope and 6XHis tag at the C-terminus was too much bulk for mVASP. Therefore, two new constructs with N-terminal His-tags were subcloned into the pcDNA/TOPO vector (Figure 5.5). Briefly, the mVASP genes for the wild type and the truncated mutant were cloned out of the parent pBS-KSII vectors by PCR with a forward primer extending the N-terminus with a 6XHis tag and a reverse primer that incorporated a stop codon such that the C-terminal V5 epitope of the vector would not be translated. The PCR products were purified by agarose gel electrophoresis and extraction, and then ligated into the pcDNA3.1/TOPO vector. Plasmids including the insert in the proper direction were identified by restriction digest screening and confirmed by DNA sequencing. *In vitro* runoff transcription was performed as in Chapter 4 to yield the mRNA transcript of each gene.

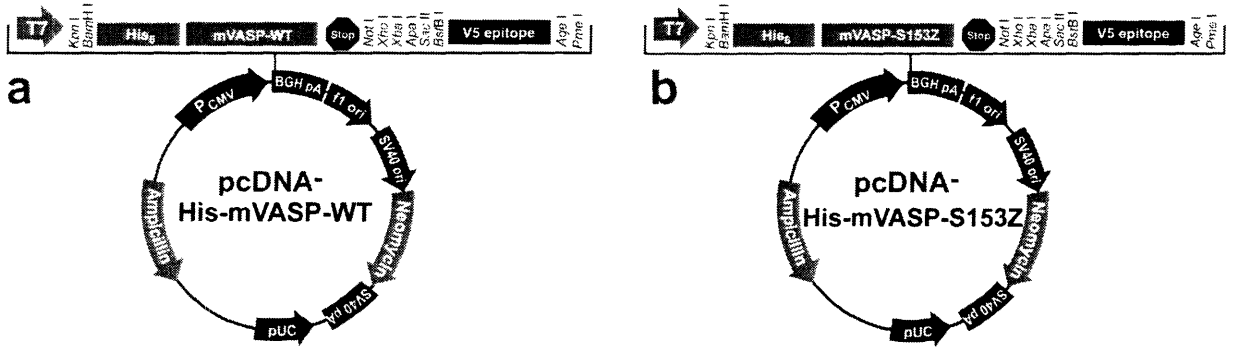

Figure 5.5. Plasmid maps of modified vectors with N-terminal His-tags. **a**) pcDNA-His-mVASP-WT and **b**) pcDNA-His-mVASP-S153Z.

The His-mVASP-WT and His-mVASP-S153Z transcripts were translated in rabbit reticulocyte extracts and purified *via* Ni-NTA resin by pH-based elutions. As seen in Figure 5.6, both transcripts with N-terminal His-tags translate well in rabbit reticulocyte extract. While the N-terminal purification tag is not ideal (any aberrant truncated protein or non-suppressed S153Z protein will be purified along with the full-length protein), there is no other purification option that would allow such resolution.

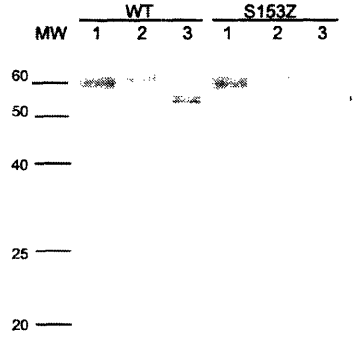

Figure 5.6. His-mVASP-WT and His-mVASP-S153Z translated and purified. Proteins were translated in rabbit reticulocyte lysate extract and purified *via* Ni-NTA beads by pH elutions. Lanes: 1 = flow through, 2 = washes, 3 = elution.

5-2. Protein Produced in Rabbit Reticulocyte Extract

With the new mVASP constructs, *in vitro* translation of the WT and S153Z proteins was first performed in rabbit reticulocyte lysate extract. As seen in Figure 5.6, the wild-type protein appears as two tight bands in western analysis due to the two phosphorylation states of the protein.[5] The wild-type protein produced by *in vitro* translation was assessed for native biochemical behavior. Phosphorylation by cAMP-dependent protein kinase A (PKA) and de-phosphorylation by λ-protein phosphatase (λ-Ppase) was tested on the purified protein (Figure 5.7). As expected, the protein demonstrated a positive gel-shift upon treatment with PKA, and a negative gel-shift upon treatment with λ-Ppase. Several conditions were tested to ensure complete phosphorylation by PKA, including extended incubation time and excess ATP; it was found that incubation for 30 minutes with 1 mM ATP was sufficient for complete phosphorylation (Figure 5.7, lane 2).

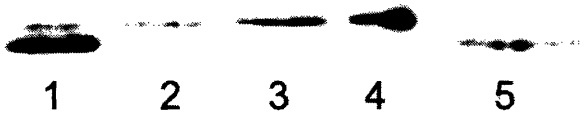

Figure 5.7. His-mVASP-WT produced in rabbit reticulocyte lysate extract treated with PKA or λ-Ppase. Lanes: 1 = His-mVASP-WT, 2 = His-mVASP-WT treated with PKA, 1mM ATP for 30 minutes, 3 = His-mVASP-WT treated with PKA, 1 mM ATP for one hour, 4 = His-mVASP-WT treated with PKA, 3 mM ATP for 30 minutes, 5 = His-mVASP-WT treated with λ-Ppase for 30 minutes.

Further gel shift experiments were performed on two more variants of mVASP synthesized by *in vitro* translation. The His-mVASP-S153Z transcript was suppressed with caged-serine (protected with the 6-nitroveratryloxycarbonyl group, NVOC)[10] and caged phosphoserine to synthesize His-mVASP-S153cS and His-mVASP-S153cpS, respectively (cS = caged serine, cpS = caged phosphoserine). Both of these proteins were examined in parallel with His-mVASP-WT protein produced by *in vitro* translation. As seen in Figure 5.8, His-mVASP-WT migrated as two bands, unless dephosphorylated by λ-Ppase, which caused the characteristic shift down or phosphorylated by PKA, which caused the characteristic shift up (lanes A1, A2, and A3, respectively). As an additional control, His-mVASP-WT was irradiated with UV-A (λ = 365 nm), treated with λ-Ppase and then analyzed to be sure that the light did not cause a change in band migration. Likewise, with the caging group on the serine hydroxyl group, His-mVASP-S153cS migrated as the unphosphorylated species in the absence or presence of PKA (lanes B2 and B1, respectively). Upon uncaging with high-end UV light, the serine hydroxyl group was liberated, and the subsequent phosphorylation by PKA caused the protein to migrate as the phosphorylated species (lane B3). Finally, the His-mVASP-S153cpS was evaluated by this gel shift assay. The full-length protein with the caged-phosphoserine migrated as the unphosphorylated species (lane C1). Upon uncaging with high-end UV light, the protein migrated with the shift characteristic of the phosphorylated species (lane C2). Upon uncaging and subsequent reaction with λ-phosphatase, the protein migrated as the unphosphorylated species (lane C3). Successful production of the caged phosphoserine protein in a rabbit reticulocyte lysate system was satisfying, and the full-length protein's expected gel shift mobility was particularly encouraging.

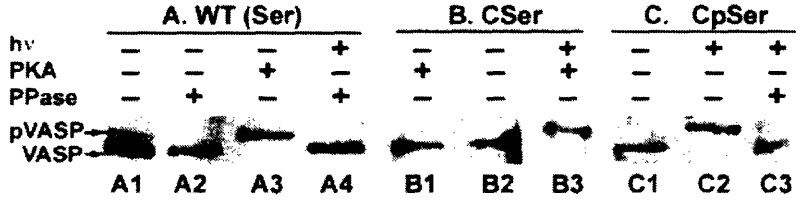

Figure 5.8. Gel shift assay of His-mVASP proteins produced by *in vitro* translation.[1] Lanes: A1 = His-mVASP-WT, A2 = His-mVASP-WT treated with λ-Ppase, A3 = His-mVASP-WT treated with PKA, A4 = His-mVASP-WT, irradiated then treated with λ-Ppase; B1 = His-mVASP-S153cS treated with PKA, B2 = His-mVASP-S153cS, B3 = His-mVASP-S153cS, irradiated then treated with PKA; C1 = His-mVASP-S153cpS, C2 = His-mVASP-S153cpS, irradiated, C3 = His-mVASP-S153cpS, irradiated then treated with λ-Ppase.

5-3. Protein Produced in Wheat Germ Extract

To further the caged phospho-mVASP experiments, a significant amount of protein was needed for biological assays. As described in Chapter 4, rabbit reticulocyte lysate systems are not amenable to large scale production; however, wheat germ systems are eukaryotic and have the potential to be prepared and used on large scales. Therefore, the N-terminal His-tagged proteins were translated in wheat germ extract.

First, the His-mVASP-WT and His-mVASP-S153Z transcripts were translated on analytical scales (50 μL) and subsequently purified from the reaction mixtures *via* Ni-NTA resin. The pH-based elutions from the resin used to purify protein from the rabbit system did not work well with the wheat germ system. Therefore, two imidazole elution procedures were tested: one with, and one without, SDS as a blocking agent. As seen in Figure 5.9, both systems were used successfully to purify the proteins from the wheat germ extract. Furthermore, the strong translation of the mammalian protein in the wheat germ extract demonstrates that there were no rare codon complications for this protein (see Chapter 4). This observation is extremely encouraging for the prospect of future scale-up production.

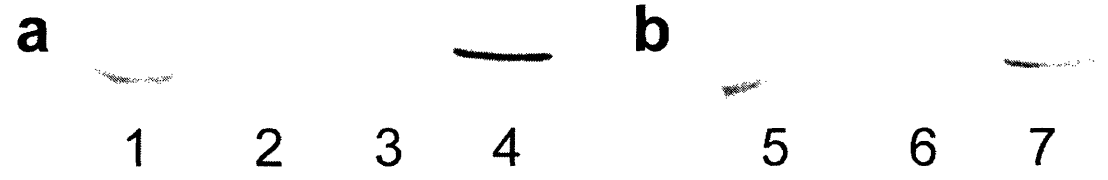

Figure 5.9. Purification *via* Ni-NTA resin of His-mVASP-WT translated in wheat germ extract. **a**) purified with imidazole/SDS and **b**) purified with imidazole, no SDS. Lanes: 1 = crude, 2 = flow through, 3 = wash, 4 = elution, 5 = crude, 6 = wash, 7 = elution.

To ensure that the protein produced in wheat germ extract behaves as the protein produced in the rabbit reticulocyte lysate extract, the same set of gel shift experiments were performed with purified WT protein. As seen in Figure 5.10, His-mVASP-WT does migrate as expected. Treatment with PKA causes the protein to migrate as the phosphorylated species, while treatment with λ-Ppase causes the protein to migrate as the unphosphorylated species (Lanes 2 and 3, respectively).

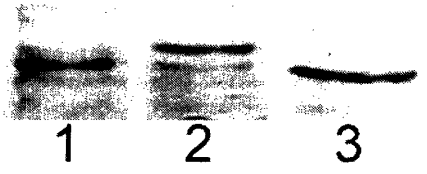

Figure 5.10. His-mVASP-WT translated in wheat germ extract treated with PKA or λ-Ppase. Lanes: 1 = His-mVASP-WT, 2 = His-mVASP-WT treated with PKA, 1 mM ATP for 30 minutes, 3 = His-mVASP-WT treated with λ-Ppase for 30 minutes.

5-4. Future Direction

The mVASP portion of the caged phosphoprotein project is very much a work in progress. Several experiments are desired with the caged phosphoprotein, including actin polymerization and binding partner assays *in vitro* and the ultimate microinjection studies in mVASP-null cells *in vivo*. In order to generate a significant amount of protein for these biochemical assays and microinjection experiments, a significant production scale increase is requisite. Toward this end, following establishing consistent suppression reactions in wheat germ on the analytical scale, a new commercially available system for large-scale protein translation in wheat germ extract will be utilized to produce His-mVASP-WT and His-mVASP-S153cpS. Further discussion can be found in Chapter 6.

Conclusion

The mVASP-WT protein was successfully produced by *in vitro* translation in rabbit or wheat germ derived systems. Proteins from both sources were subjected to gel shift assays to ensure that the proteins can be phosphorylated and de-phosphorylated as described in the literature.[5] Furthermore, the mVASP-S153cpS protein was successfully synthesized in the rabbit reticulocyte lysate system. Gel shift assays confirm that uncaging yields the phosphorylated protein, and further treatment with λ-Ppase dephosphorylates the uncaged phosphoprotein.

Experimental

5-0. General Procedures

All handling of RNA was performed as described in Chapter 4.

5-1. Cloning and Molecular Biology

The vectors pcDNA-His-mVASP-WT and pcDNA-His-mVASP-S153Z were cloned as described in Chapter 4. All mRNA was transcribed, purified, and analyzed as in Chapter 4. Translation reactions in rabbit reticulocyte lysate extract were performed and proteins purified as described in Chapter 4.

5-2. Protein Produced in Rabbit Reticulocyte Extract

Translation and suppression experiments were performed as described in Chapter 4. Proteins were purified from translation mixtures as in Chapter 4, Method C (pH-based elution).

PKA/λ-Ppase experiments. Biochemical experiments with *in vitro* translated His-mVASP-WT, -S153cS, or -S153cpS were performed as follows:

Phosphorylation:

5 μL purified/concentrated sample protein
10 μL dH_2O
2 μL 10 mM ATP
2 μL 10 X PKA buffer
1 μL PKA (protein kinase A, New England Biolabs; 2500 U/ μL)
20 μL total

The reaction was incubated for 30 minutes at 30 °C. The reaction was quenched with 5 μL 5X gel loading buffer, and the entire sample was loaded onto SDS-PAGE.

De-phosphorylation:

5 μL purified/concentrated sample protein
11 μL dH_2O
2 μL 20 mM $MnCl_2$
2 μL 10X λ -Ppase buffer
0.5 μL λ-Ppase (lambda phosphatase, New England Biolabs; 400 U/ μL)
20.5 μL total

The reaction was incubated for 30 minutes at 30 °C. The reaction was quenched with 5 μL 5X gel loading buffer, and the entire sample was loaded onto SDS-PAGE.

Uncaging: Uncaging of protein was performed in purification elution buffer containing at least 2mM dithiothreitol (DTT). The protein in buffer was placed in a clear walled microfuge tube, and exposed to λ = 365 nm (7 mW/cm^2) for 5 to 10 minutes. The uncaged protein was used immediately in experiments.

5-3. Protein Produced in Wheat Germ Extract

Translation with Wheat Germ Extract

For analytical scale translations, the Promega Wheat Germ Extract, Nuclease Treated (catalog #L4380), was used. **The mRNA must be denatured before running the reaction:** the mRNA was added to the DEPC dH_2O, and heated to 67 °C for 10 minutes. Meanwhile, the

remaining components were assembled. After the mRNA was cooled on ice for 2 minutes, it was added the remaining components to begin the reaction:

Component	Wild Type mRNA
DEPC dH_2O	17.0 – **xx** μL
Complete amino acids mixture	6.0 μL
RNAse Inhibitor	1.0 μL
Potassium Acetate (1M)	1.0 μL
mRNA (5.0 μg)	**xx** μL
Rabbit Reticulocyte Lysate	25 μL
Total	50 μL

The mixture was incubated at 25 °C for 2 hours (reactions were placed in a warm room to ensure that they were held at 25 °C). Reactions were cooled on ice to stop reaction. Proteins were purified as described in Chapter 4, Method D (imidazole-based elutions). Note that the imidazole should be removed before photochemical experiments.

Acknowledgements
I would like to acknowledge Professor Frank Gertler and post-doctoral associate Melanie Barzik for their contributions to this chapter: for the generous gifts of the mVASP plasmid, the polyclonal antibody, the control protein samples, and for their wealth of knowledge about mVASP and the opportunity to collaborate on discovering its role in cell motility.

(1) Rothman, D. M.; Petersson, E. J.; Vazquez, M. E.; Brandt, G. S.; Dougherty, D. A.; Imperiali, B. "Caged Phosphoproteins," *Journal of the American Chemical Society* **2005**, *127 (3)*, 846-847.

(2) Krause, M.; Bear, J. E.; Loureiro, J. J.; Gertler, F. B. "The Ena/VASP Enigma," *Journal of Cell Science* **2002**, *115 (Pt 24)*, 4721-4726.

(3) Krause, M.; Dent, E. W.; Bear, J. E.; Loureiro, J. J.; Gertler, F. B. "Ena/VASP Proteins: Regulators of the Actin Cytoskeleton and Cell Migration," *Annual Review of Cell and Developmental Biology* **2003**, *19* 541-564.

(4) Halbrugge, M.; Walter, U. "Purification of a Vasodilator-Regulated Phosphoprotein from Human Platelets," *European Journal of Biochemistry* **1989**, *185 (1)*, 41-50.

(5) Butt, E.; Abel, K.; Krieger, M.; Palm, D.; Hoppe, V.; Hoppe, J.; Walter, U. "cAMP- and cGMP-dependent Protein Kinase Phosphorylation Sites of the Focal Adhesion Vasodilator-stimulated Phosphoprotein (VASP) *in Vitro* and in Intact Human Platelets," *Journal of Biological Chemistry* **1994**, *269 (20)*, 14509-14517.

(6) Howe, A. K.; Hogan, B. P.; Juliano, R. L. "Regulation of Vasodilator-stimulated Phosphoprotein Phosphorylation and Interaction with Abl by Protein Kinase A and Cell Adhesion," *Journal of Biological Chemistry* **2002**, *277 (41)*, 38121-38126.

(7) Loureiro, J. J.; Rubinson, D. A.; Bear, J. E.; Baltus, G. A.; Kwiatkowski, A. V.; Gertler, F. B. "Critical Roles of Phosphorylation and Actin Binding Motifs, but Not the Central Proline-Rich Region, for Ena/Vasodilator-stimulated Phosphoprotein (VASP) Function During Cell Migration," *Molecular and Cellular Biology* **2002**, *13 (7)*, 2533-2546.

(8) Bear, J. E.; Svitkina, T. M.; Krause, M.; Schafer, D. A.; Loureiro, J. J.; Strasser, G. A.; Maly, I. V.; Chaga, O. Y.; Cooper, J. A.; Borisy, G. G.; Gertler, F. B. "Antagonism Between Ena/VASP Proteins and Actin Filament Capping Regulates Fibroblast Motility," *Cell* **2002**, *109 (4)*, 509-521.

(9) Gertler, F. B. "Sensitivity of C-terminus of VASP," *personal communication*, **2004**.

(10) Rajasekharan Pillai, V. N. "Photoremovable Protecting Groups in Organic Synthesis," *Synthesis* **1980**, *1980 (1)*, 1-27.

Chapter 6
Conclusions and Future Directions

Conclusions

Caged phosphopeptides and phosphoproteins afford a researcher spatial and temporal control over the release of the corresponding biologically active species within a living system. The synthesis and application of these chemical probes have been developed and detailed within this thesis. Two methods to synthesize 1-(2-nitrophenyl)ethyl caged phosphopeptides have been described (Chapter 2). These peptides demonstrated good quantum yields of uncaging as compared to literature values of other *ortho*-nitrobenzyl derived caged compounds. A seminal study in which these caged phosphopeptide tools yielded information about the 14-3-3 family's involvement in cell cycle control was discussed in detail (Chapter 3). The development of the synthesis that allowed the extension of the nonsense codon suppression methodology to include caged phosphoproteins was described (Chapter 4). The three most commonly phosphorylated amino acids (serine, threonine, and tyrosine) were each incorporated into the test protein nAChR in their caged phosphorylated form, and caged phosphoserine was incorporated into position 153 of mVASP for future biological studies. Finally, the progress toward application of caged phospho-mVASP in live cell assays was also discussed (Chapter 5).

The ability to study the phenotypic effect of a phosphorylation event in real time gives scientists some of the essential pieces of information necessary to solve the magnificent puzzle that is cell signaling networks. The continued evolution of the versatility and accessibility of these probes will provide the opportunity for a larger impact on studying phosphorylation in cellular signaling networks.

Future Directions

The caged phosphopeptide and phosphoprotein project has ample room to grow: from continued work with mVASP to further development of the site-directed incorporation of nonnatural amino acids. In particular, because the mVASP portion of the project is in early stages with promising results, it will be at the forefront of continuing research. After assuring that caged phosphoserine can be incorporated into mVASP consistently on an analytical scale in the wheat germ system, scale-up production will be established. Once larger amounts of caged phosphoprotein are available, several experiments can be performed to test the hypothesis that the phosphoserine 153 is the residue in mVASP critical for lamellipodial formation in cells.

These experiments will include actin polymerization assays and binding partner experiments *in vitro*, and microinjection into mVASP-null cells for uncaging *in vivo*.

Other aspects of the caged phosphoprotein project can extend in various directions. To further develop these types of probes at the chemical end, new phosphate analogs may be synthesized as their caged derivatives and incorporated into peptides or full-length protein *via* the adapted suppression methodology (i.e., caged phosphono- or caged thiophospho-amino acids). With the chemistry and molecular biology techniques unique to the nonsense codon suppression methodology established within the lab, other non-natural amino acids may also be incorporated into full-length protein (i.e., 6-*N,N*-Dimethylamino-2,3-naphthalimide, 6-DMN, G. Loving). Furthermore, the incorporation of non-natural amino acids may be accomplished in live mammalian cell culture systems. Recent literature reports demonstrate the ability to use the import of amino-acylated suppressor tRNA for the site-specific insertion of amino acid analogues into proteins in mammalian cell culture.[1] As this time, protein produced in this manner has been analyzed within cell lysates. Future experiments may involve studying the protein within the cells themselves. The availability of this type of system will enable structure-function studies *in vivo* such as protein-protein interactions, protein localization, etc., through the use of amino acid analogues that carry photo-activatable groups, fluorescent groups, or other chemically reactive probes.[1]

Another potential endeavor in the realm of the nonsense codon suppression methodology would be the development of a suppressor tRNA that is more compatible with negatively charged amino acids. As mentioned in Chapter 4, it is likely that the thermodynamic balance among the backbone of the acceptor and T helices of the tRNA, the amino acid, and the elongation factors involved in polypeptide elongation is offset with a TH73G $tRNA_{CUA}$ acylated with a negatively charged amino acid.[2, 3] Therefore, the evolution of a suppressor tRNA that can accommodate negatively charged artificial amino acids would benefit many researchers working to employ this methodology with unique chemical probes.

References

(1) Kohrer, C.; Xie, L.; Kellerer, S.; Varshney, U.; RajBhandary, U. L. "Import of Amber and Ochre Suppressor tRNAs into Mammalian Cells: A General Approach to Site-specific Insertion of Amino Acid Analogues into Proteins," *Proceedings of the National Academy of Sciences, U. S. A.* **2001**, *98 (25)*, 14310-14315.

(2) LaRiviere, F. J.; Wolfson, A. D.; Uhlenbeck, O. C. "Uniform Binding of Aminoacyl-tRNAs to Elongation Factor Tu by Thermodynamic Compensation," *Science* **2001**, *294 (5540)*, 165-168.

(3) Dale, T.; Sanderson, L. E.; Uhlenbeck, O. C. "The Affinity of Elongation Factor Tu for an Aminoacyl-tRNA Is Modulated by the Esterified Amino Acid," *Biochemistry* **2004**, *43 (20)*, 6159-6166.

2.1 ^{1}H Spectrum of 1-(2-nitrophenyl)ethanol, **2**.

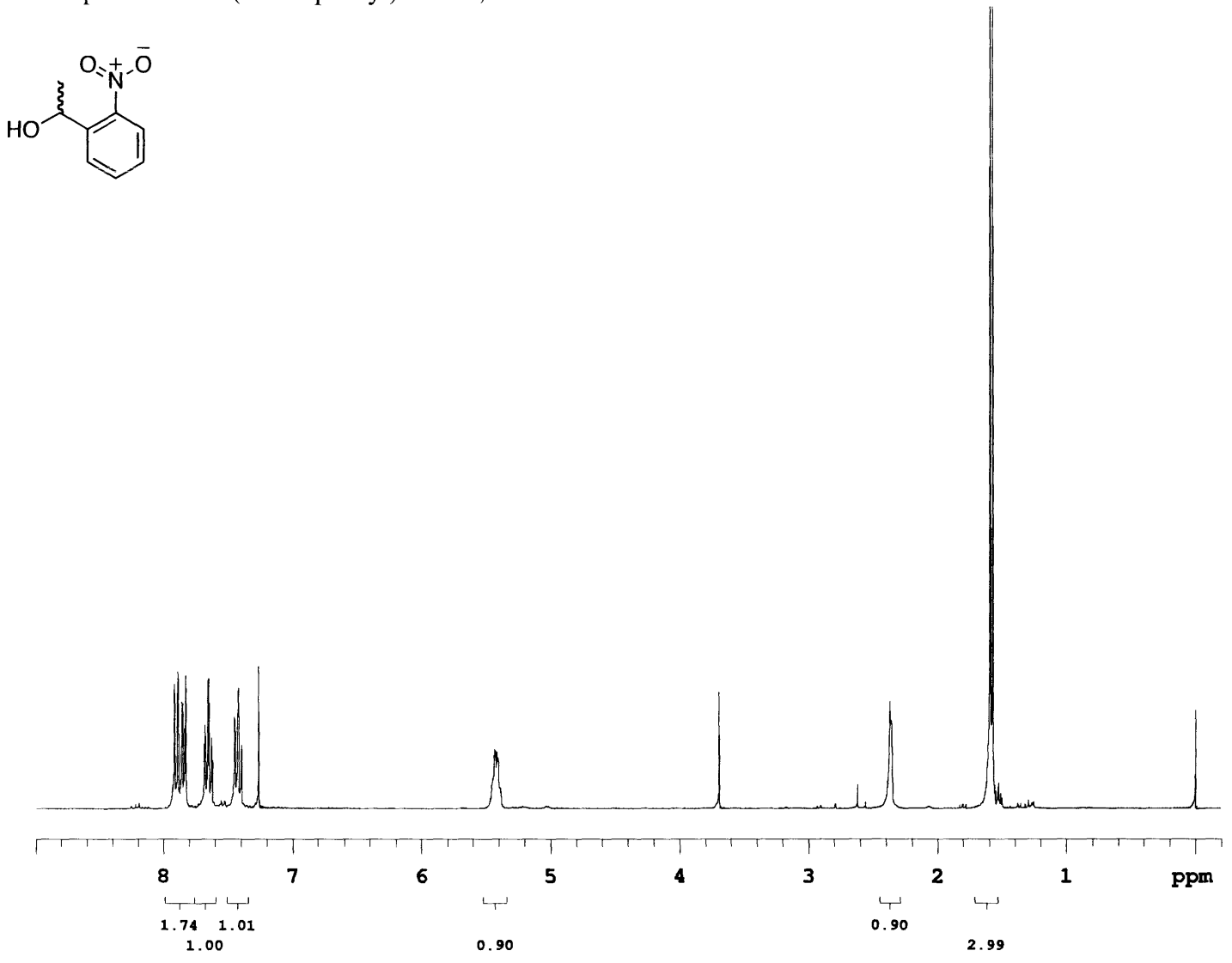

2.2 ^{13}C Spectrum of 1-(2-nitrophenyl)ethanol, **2**.

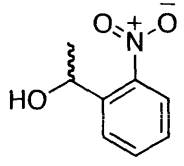

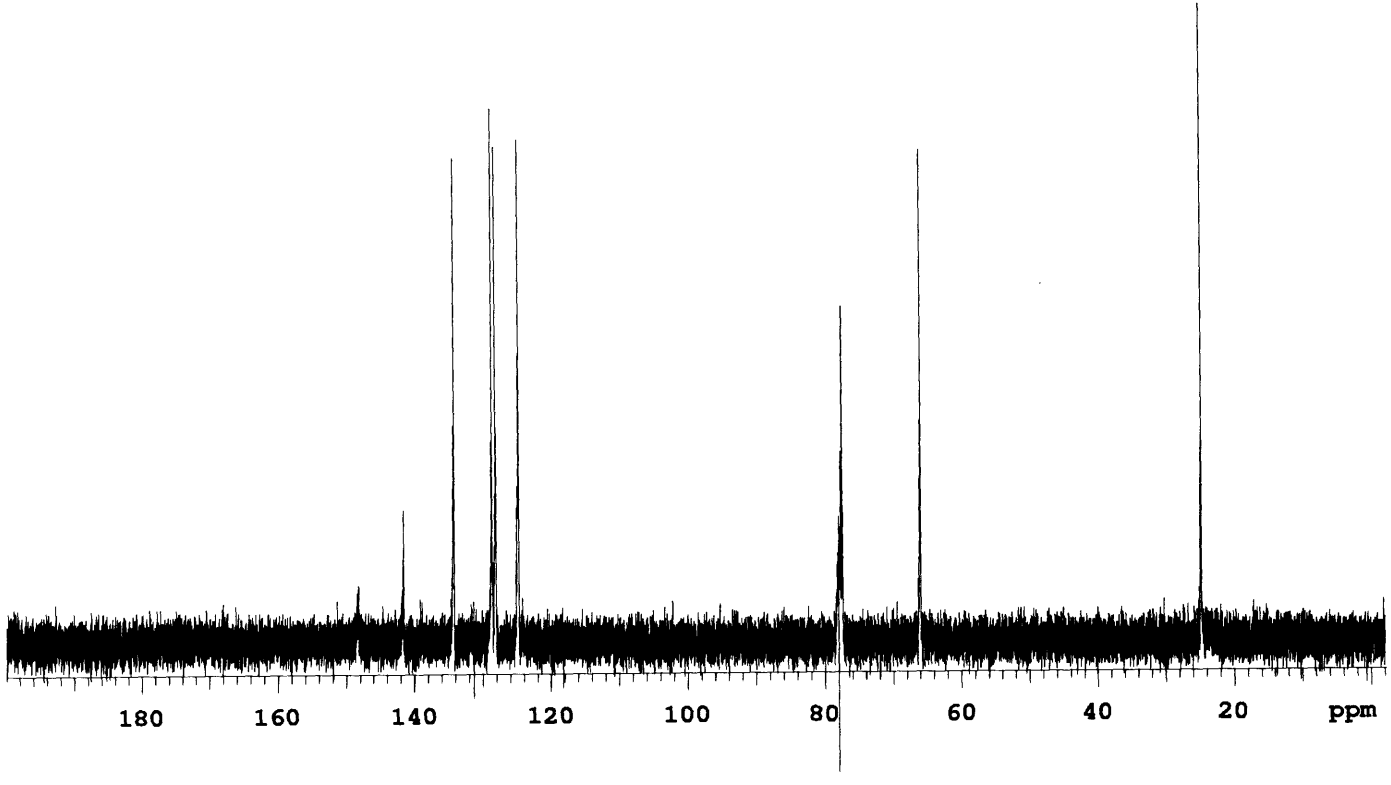

2.3 ^{1}H spectrum of *O*-1-(2-nitrophenyl)ethyl-*O'*-β-cyanoethyl-*N,N*-diisopropylphosphoramidite, **4**.

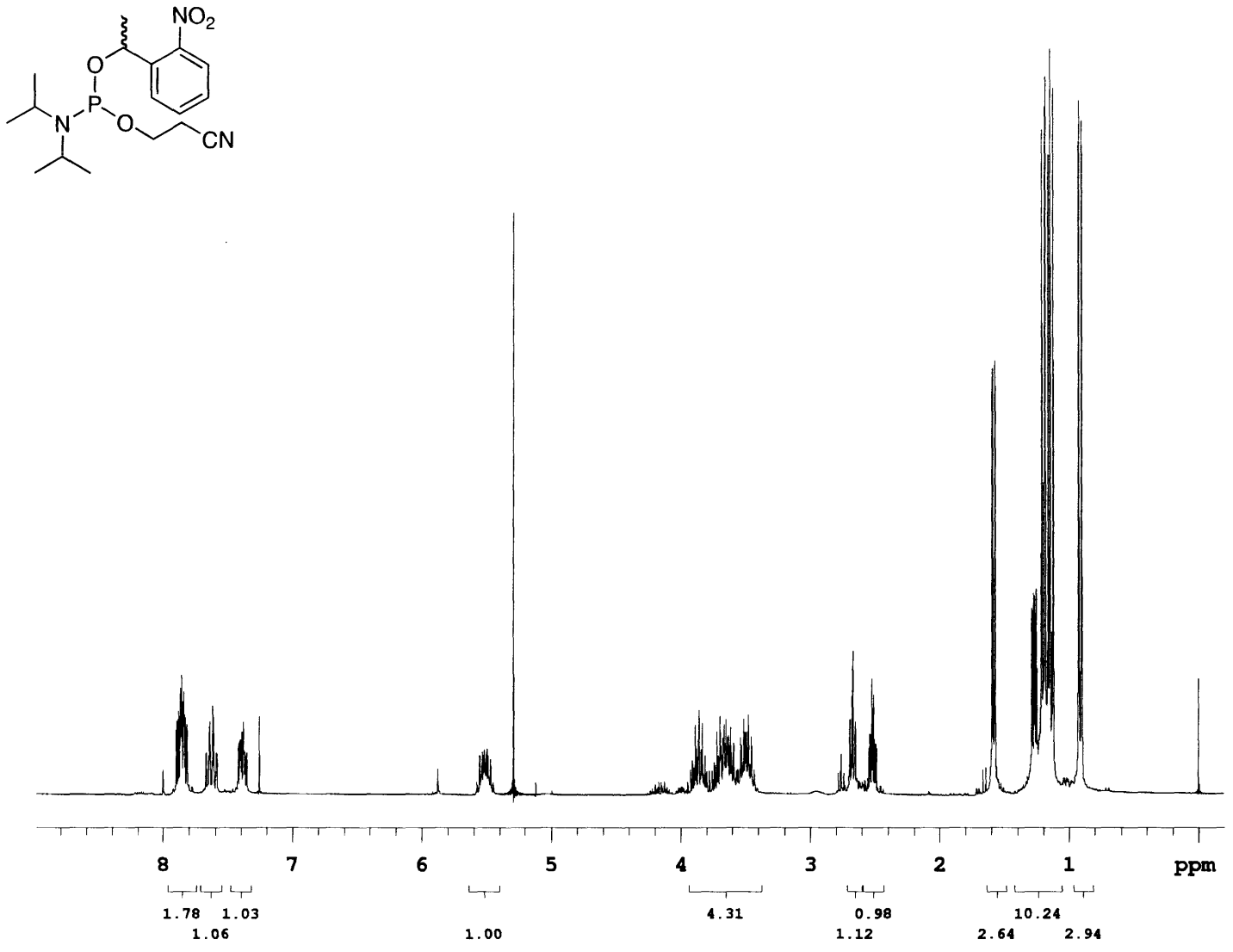

2.4 ^{31}P spectrum of *O*-1-(2-nitrophenyl)ethyl-*O*'-β-cyanoethyl-*N*,*N*-diisopropylphosphoramidite, **4**.

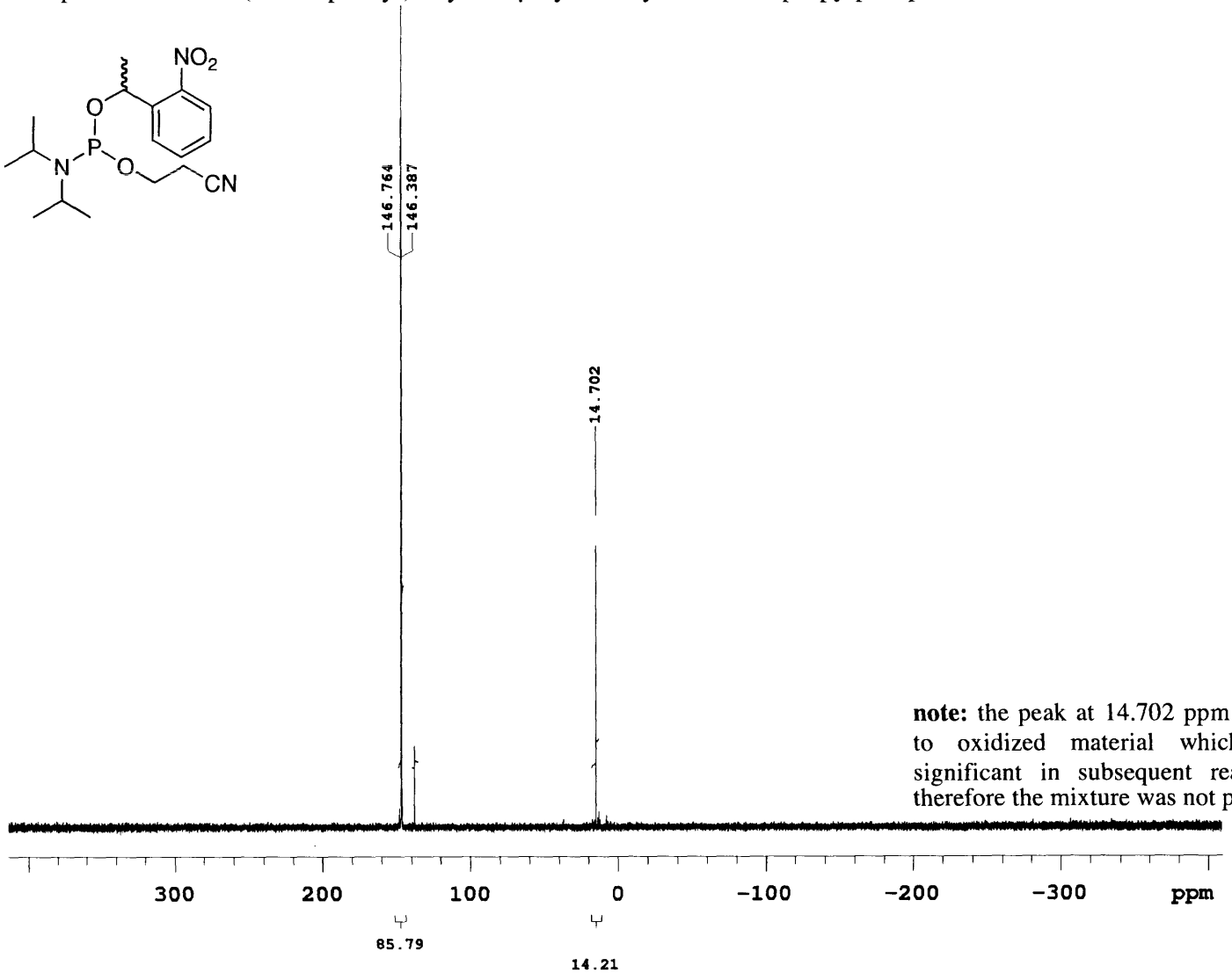

note: the peak at 14.702 ppm corresponds to oxidized material which was not significant in subsequent reactions, and therefore the mixture was not purified.

2.5 Magic Angle Spinning-^{31}P NMR spectrum of Fmoc-Ser-Pro-Gly-(AM-PS).

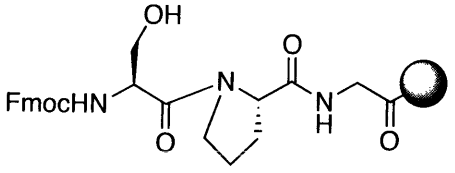

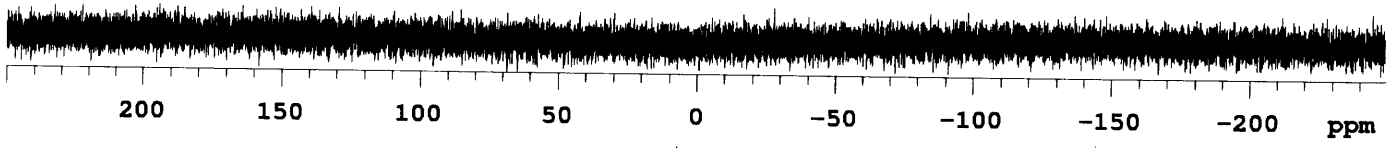

2.6 Magic Angle Spinning-^{31}P NMR spectrum of Fmoc-phosphi-(*O*-nitrophenylethyl-*O'*-cyanoethyl)seryl-Pro-Gly-(AM-PS).

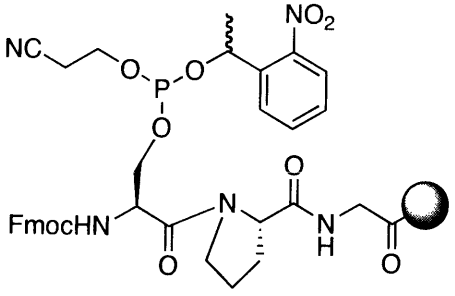

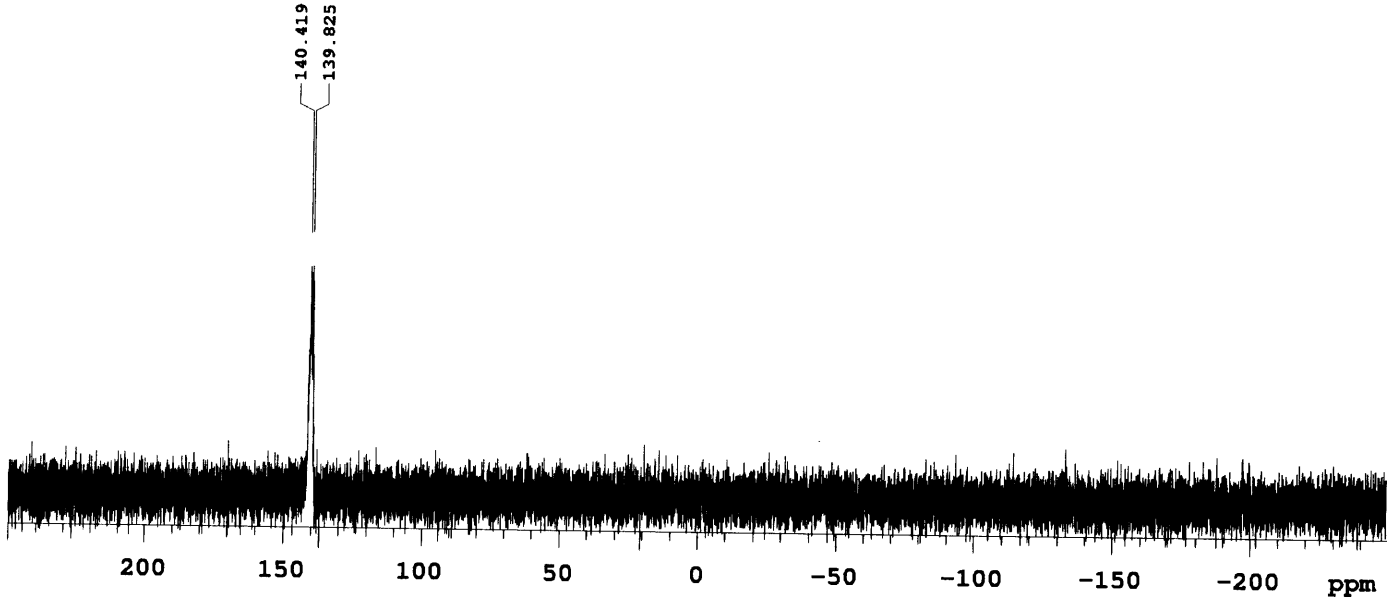

2.7 Magic Angle Spinning-^{31}P NMR spectrum of Fmoc-phospho-(*O*-nitrophenylethyl-*O'*-cyanoethyl)seryl-Pro-Gly-(AM-PS).

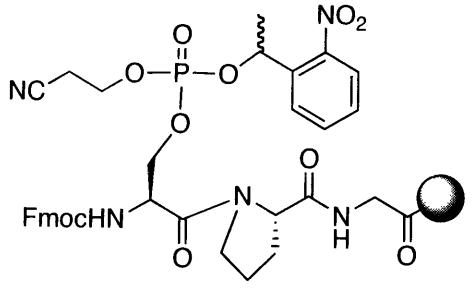

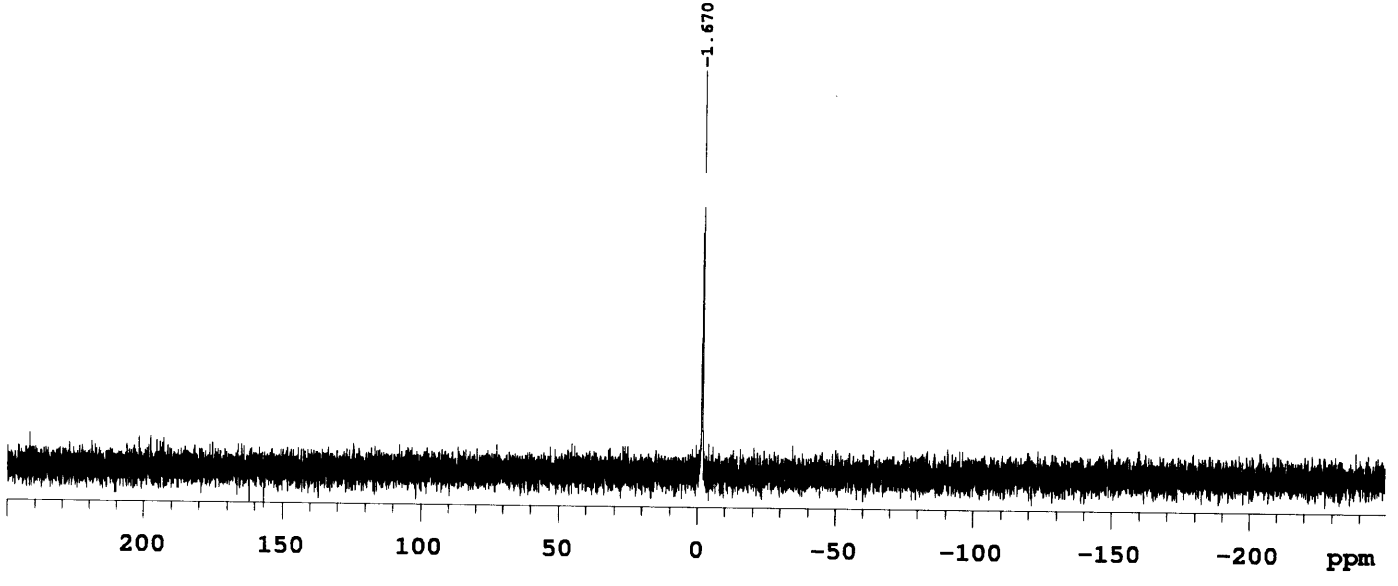

2.8 Magic Angle Spinning-^{31}P NMR spectrum of Phospho-(nitrophenylethyl)seryl-Pro-Gly-(AM-PS).

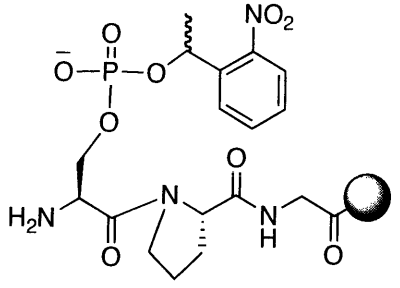

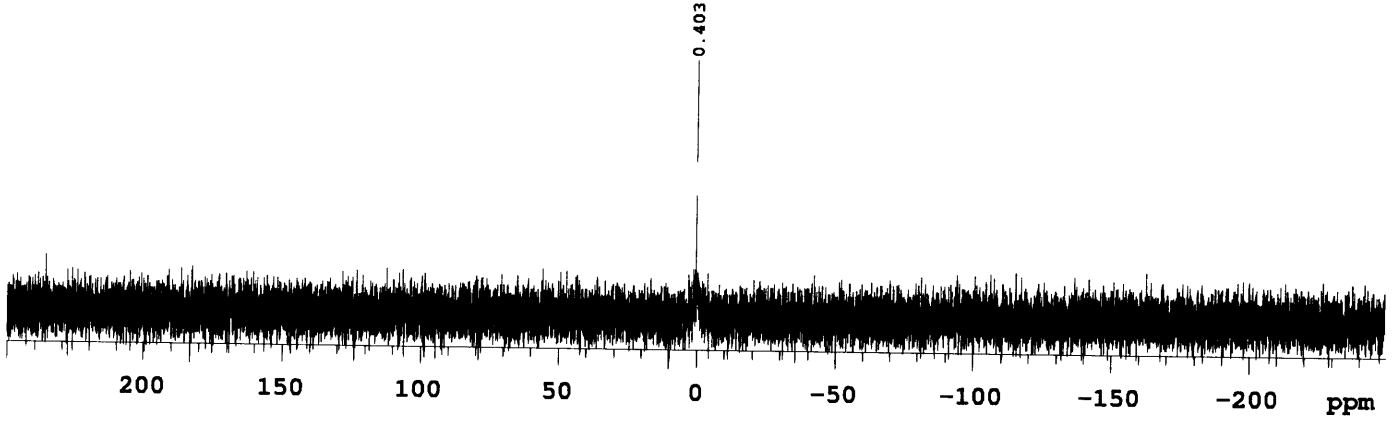

2.9 ^{1}H spectrum of N^{α}-Fmoc-hydroxytrityl-L-serine tert-butyl ester, **10**.

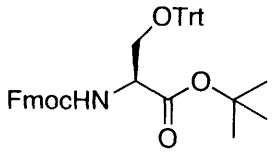

2.10 ^{13}C spectrum of N^{α}-Fmoc-hydroxytrityl-L-serine tert-butyl ester, **10**.

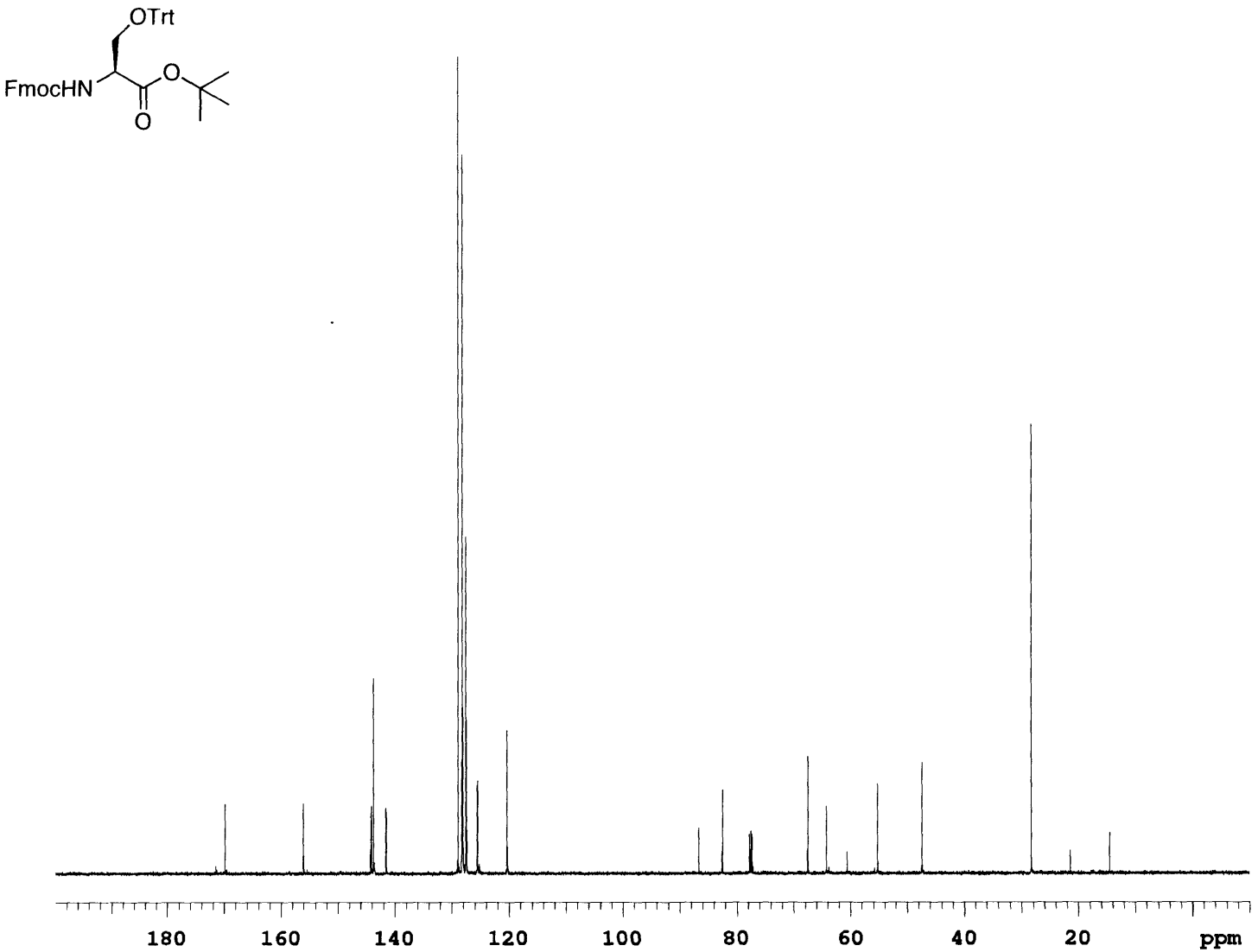

2.11 ^{1}H spectrum of N^{α}-Fmoc-L-serine tert-butyl ester, **11**.

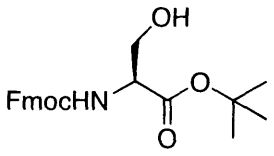

2.12 ^{13}C spectrum of N^{α}-Fmoc-L-serine tert-butyl ester, **11**.

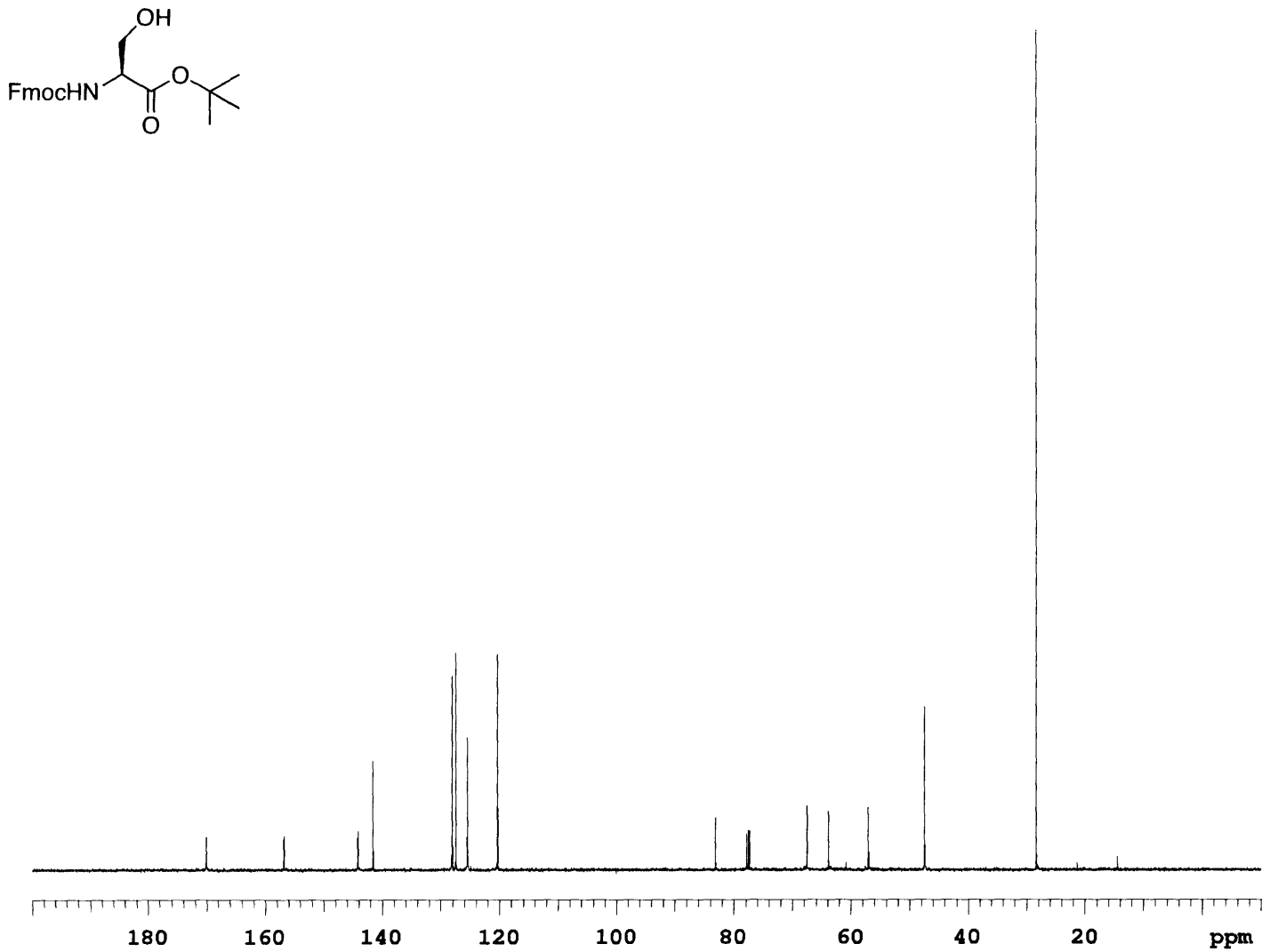

2.13 ^{1}H spectrum of N^{α}-Fmoc-phospho-(*O*-nitrophenylethyl-*O'*-β-cyanoethyl)-L-serine tert-butyl ester, **12**.

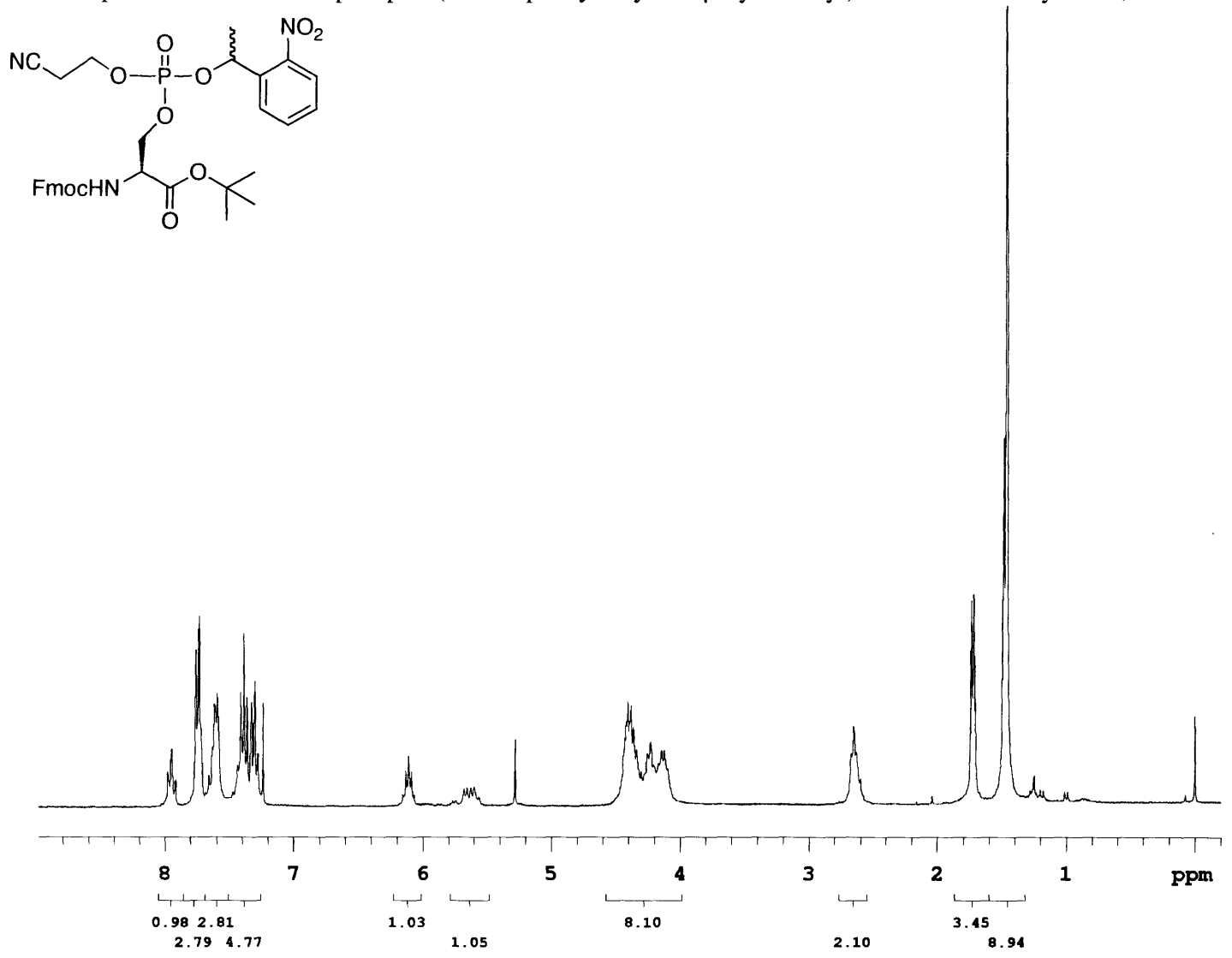

2.14 ^{13}C spectrum of N^{α}-Fmoc-phospho-(*O*-nitrophenylethyl-*O*'-β-cyanoethyl)-L-serine tert-butyl ester, **12**.

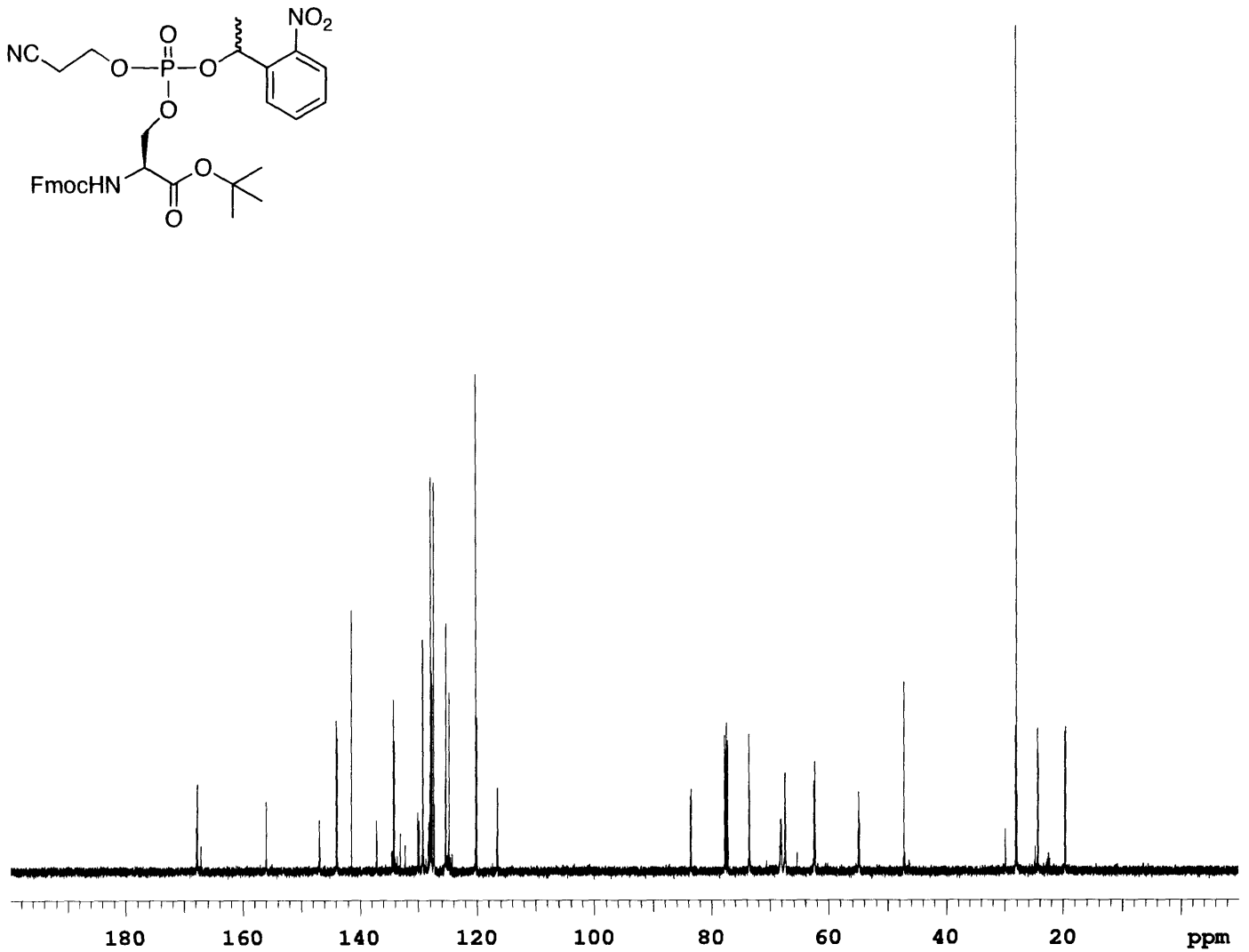

2.15 ^{31}P spectrum of N^{α}-Fmoc-phospho-(*O*-nitrophenylethyl-*O'*-β-cyanoethyl)-L-serine tert-butyl ester, **12**.

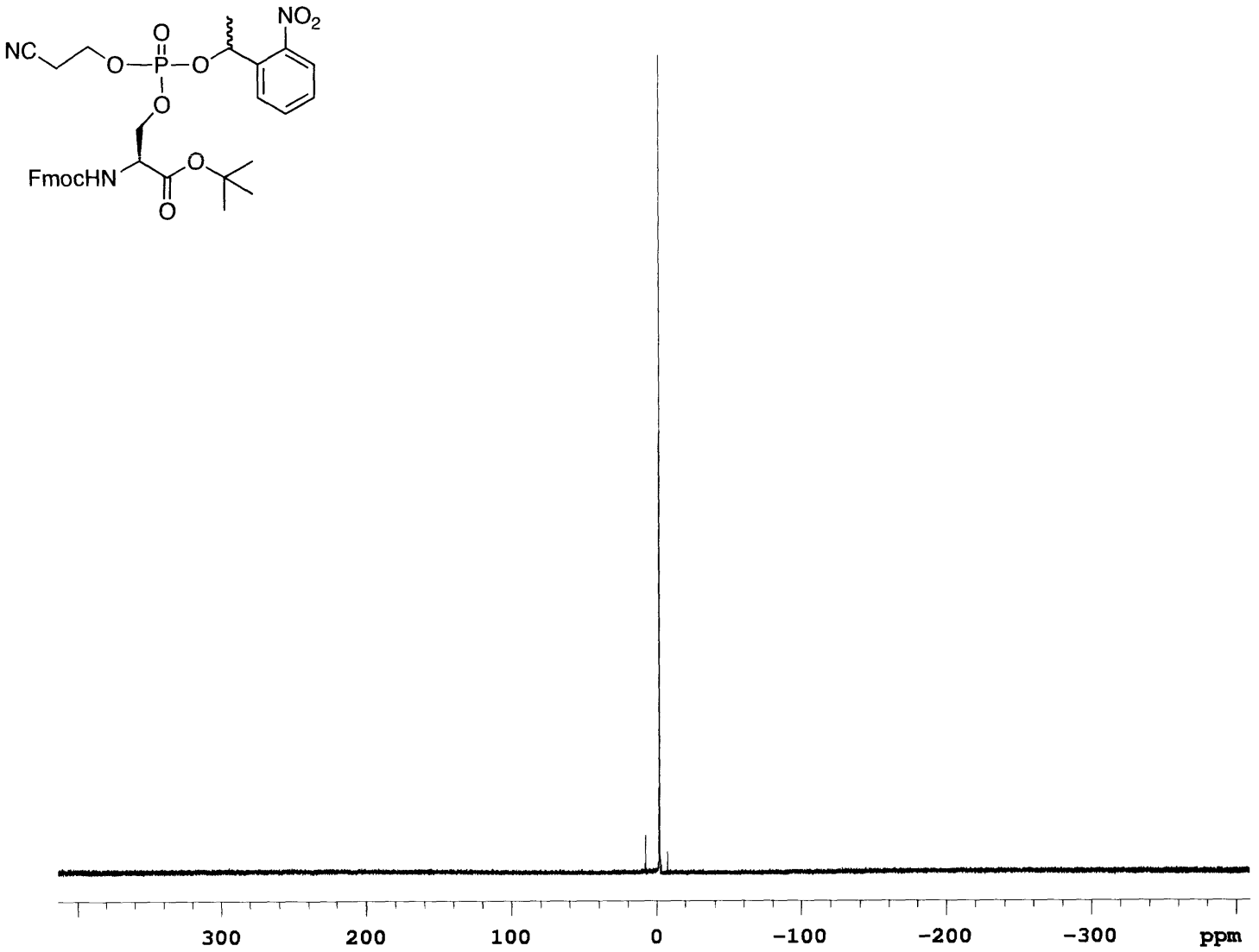

2.16 ^{1}H spectrum of N^{α}-Fmoc-phospho-(*O*-nitrophenylethyl-*O'*-β-cyanoethyl)-L-serine, **13**.

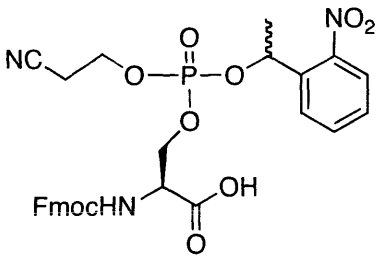

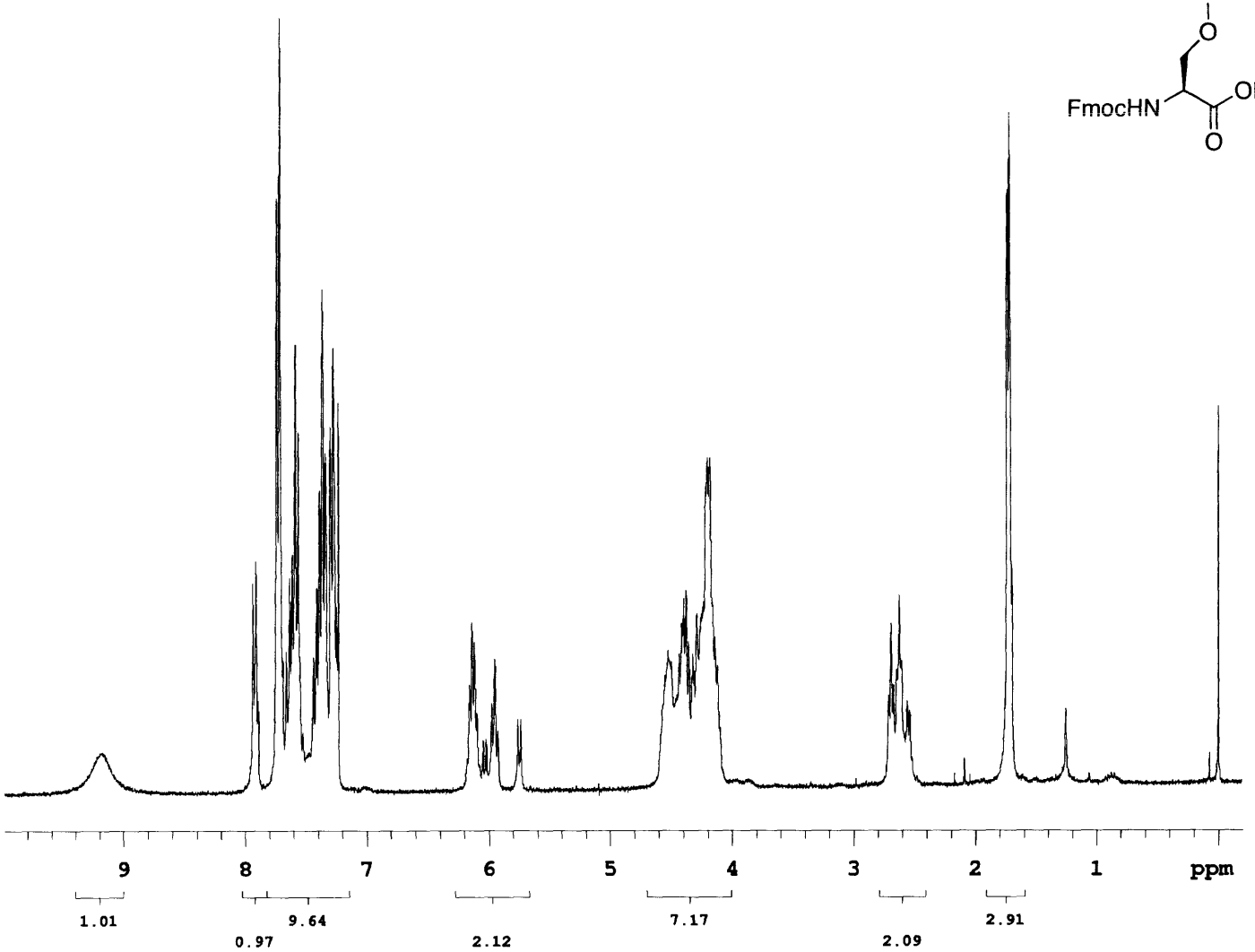

2.17 ^{13}C spectrum of N^{α}-Fmoc-phospho-(*O*-nitrophenylethyl-*O'*-β-cyanoethyl)-L-serine, **13**.

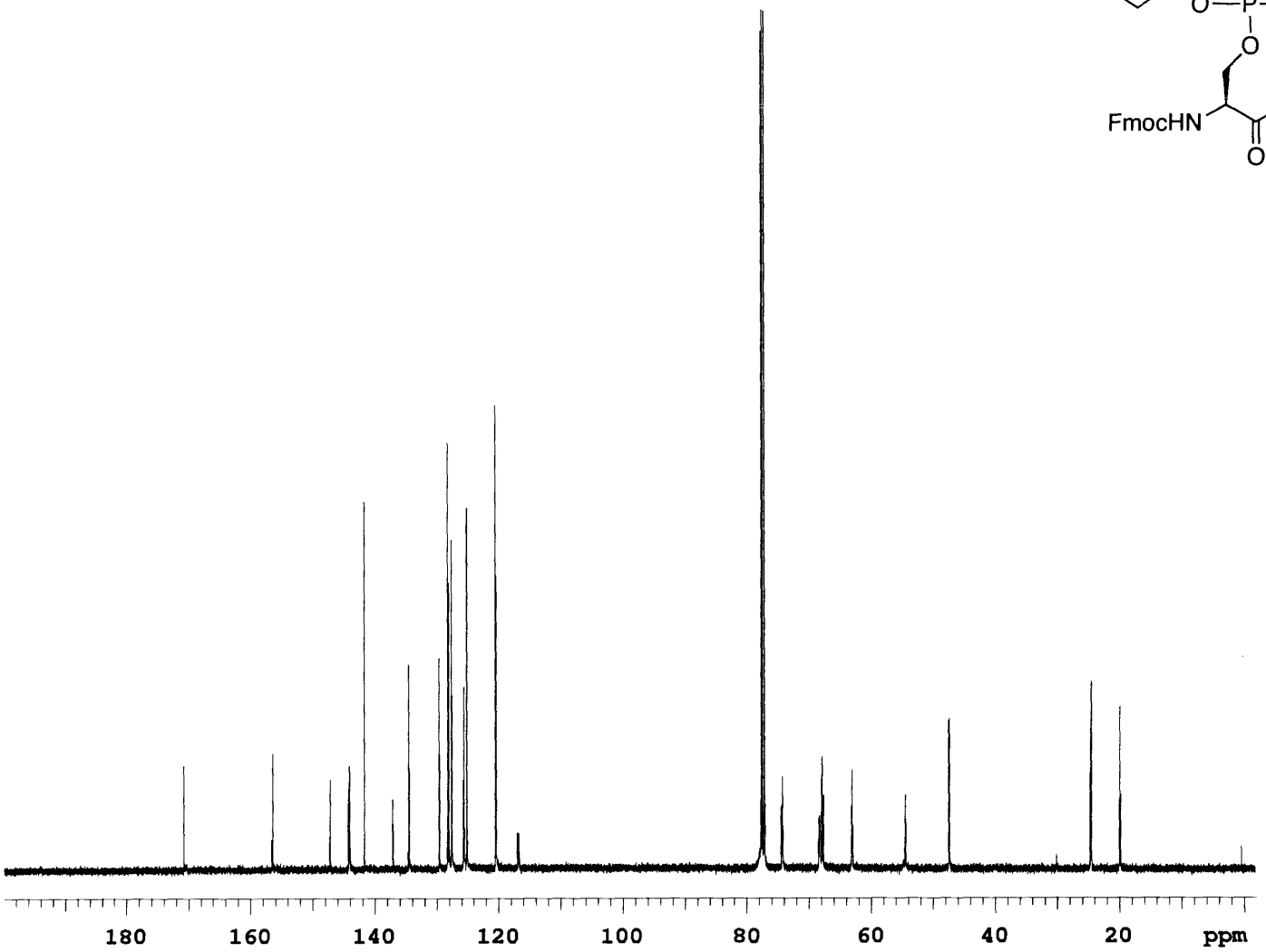

2.18 ^{31}P spectrum of N^{α}-Fmoc-phospho-(*O*-nitrophenylethyl-*O'*-β-cyanoethyl)-L-serine, **13**.

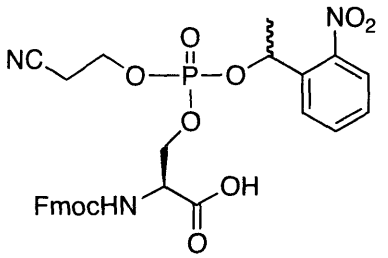

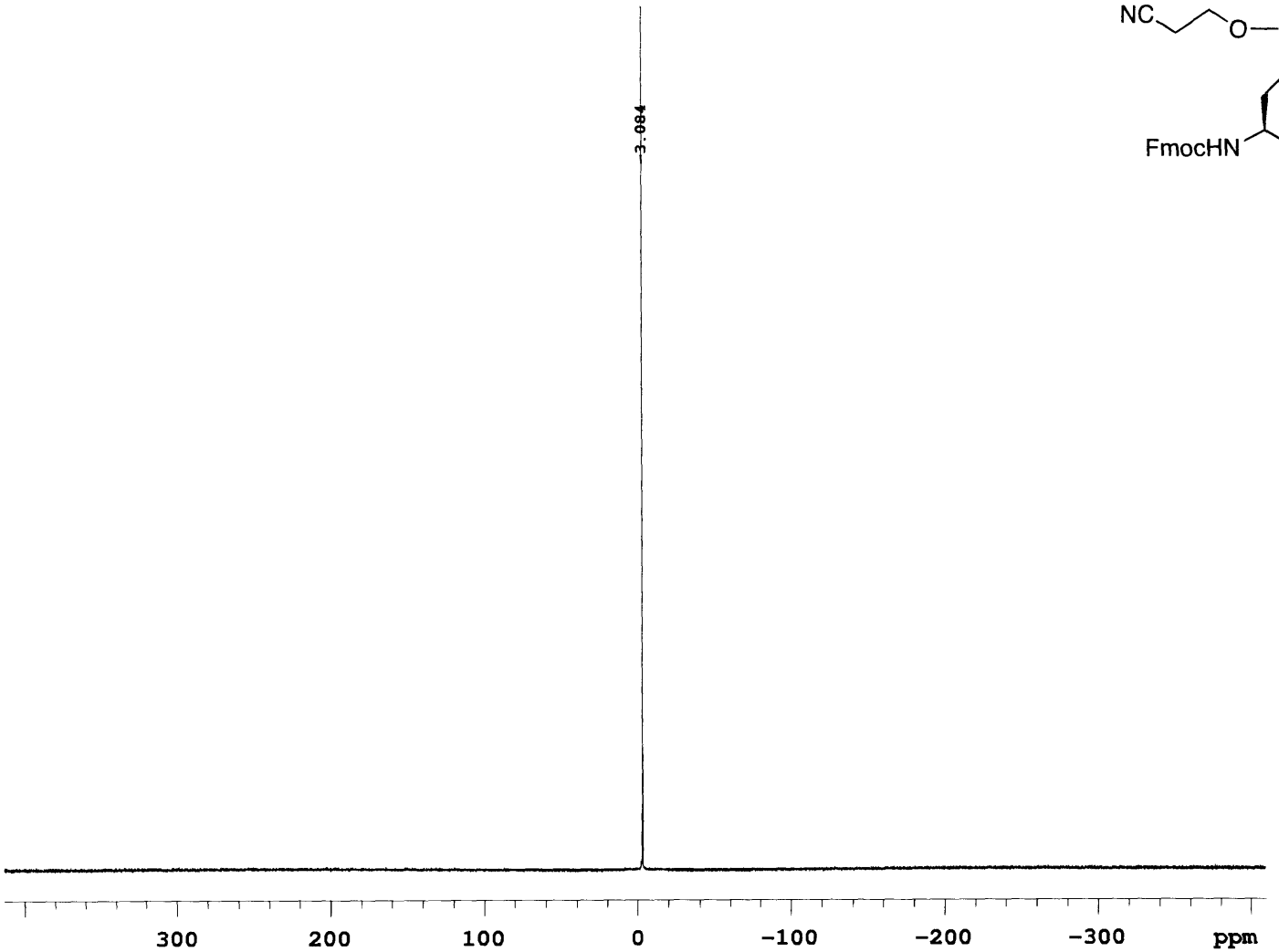

2.19 HPLC trace of cpCS: Ac-RRGcpSPG-$CONH_2$.

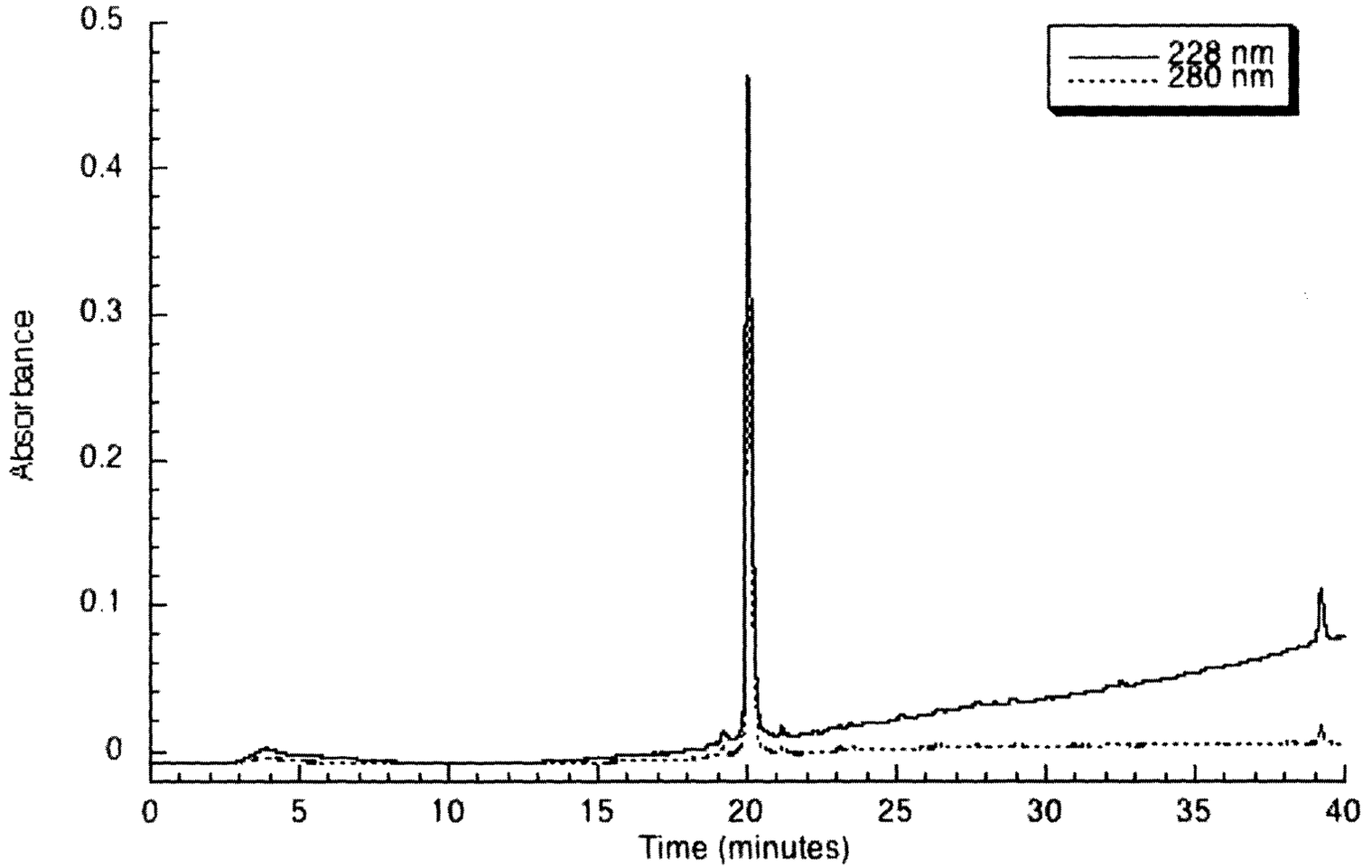

2.20 HPLC trace of cpERK: Ac-PLcpSPAKLAFQFP-$CONH_2$.

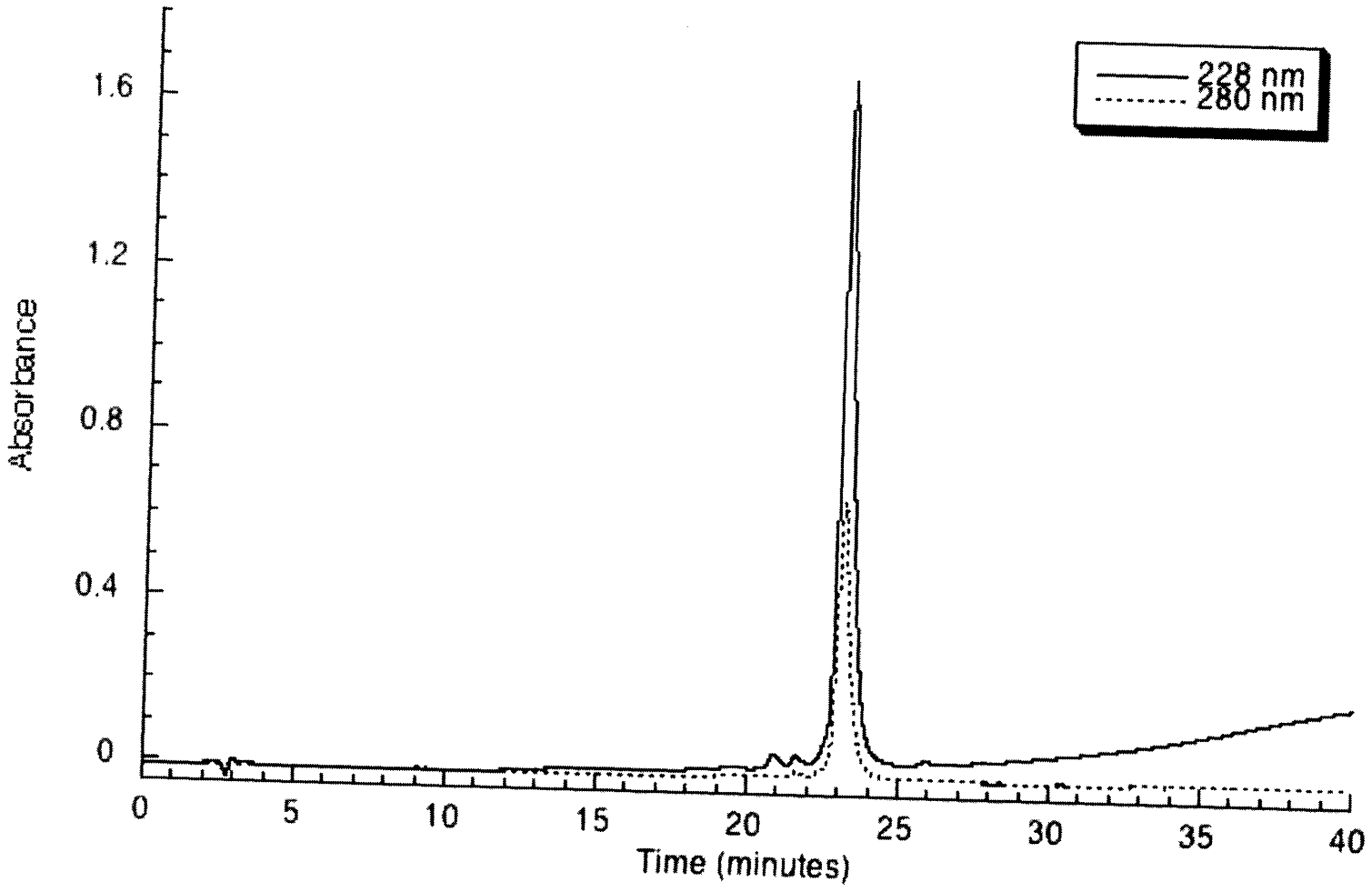

2.21 HPLC trace of cpRSLP: Ac-MARRLYRcpSLPAKK-$CONH_2$.

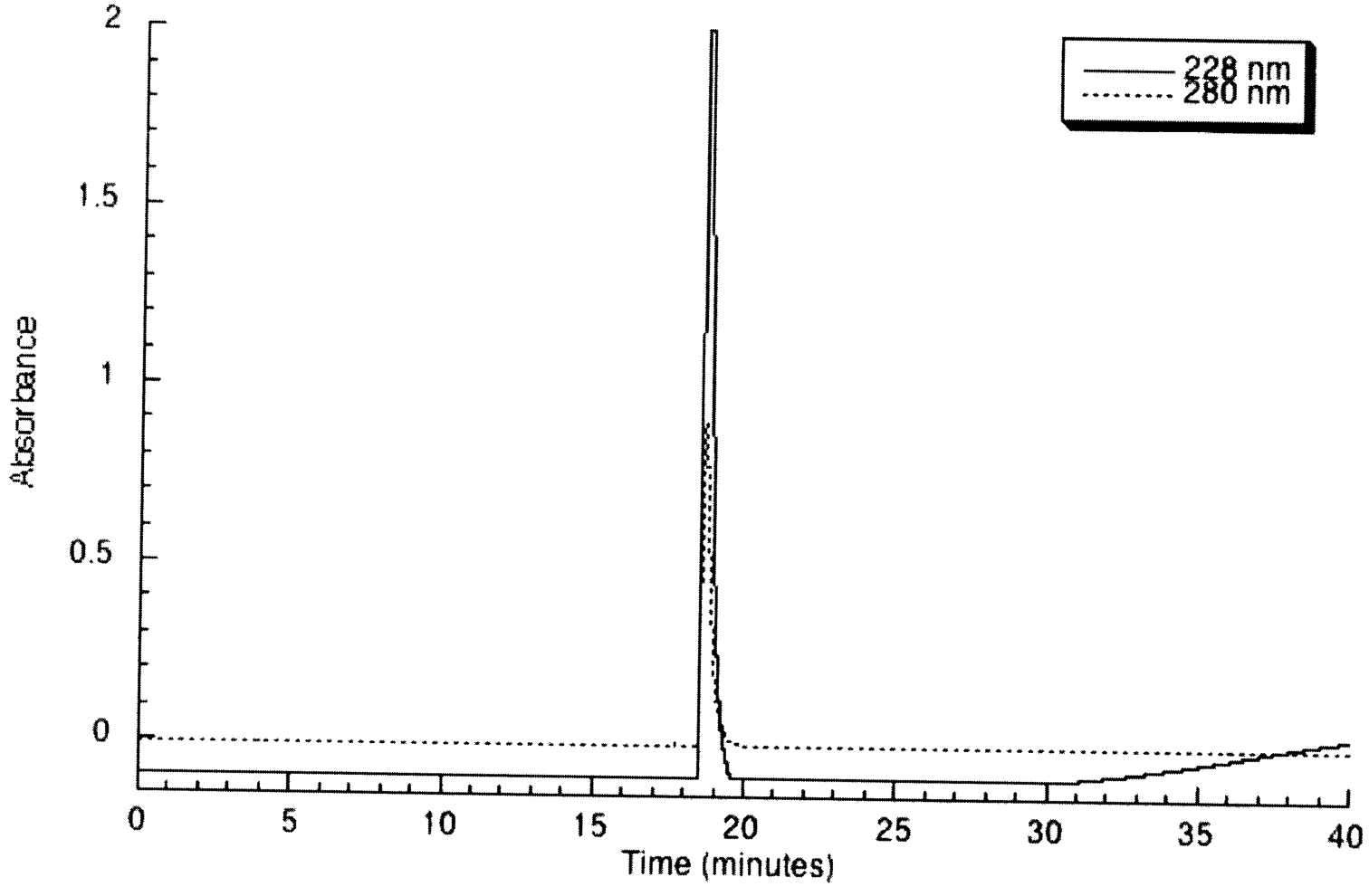

2.22 HPLC trace of cpPax: Ac-CSSPPLPGALcpSPLYGVPET-$CONH_2$.

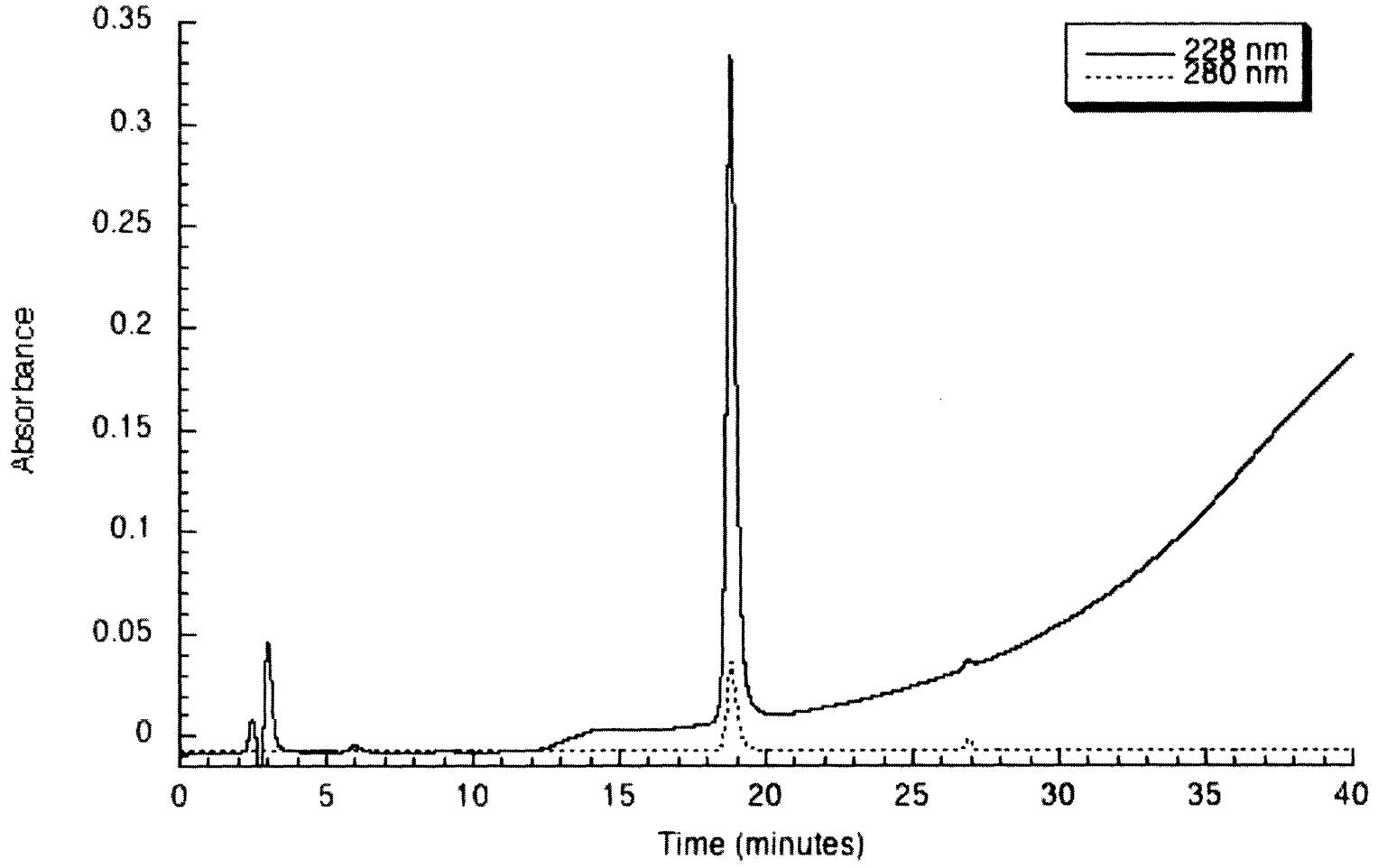

4.1 ^{1}H spectrum of *O*-1-(2-nitrophenyl)ethyl-*O'*-tertbutyl-*N,N*-diethyl phosphoramidite, **24**.

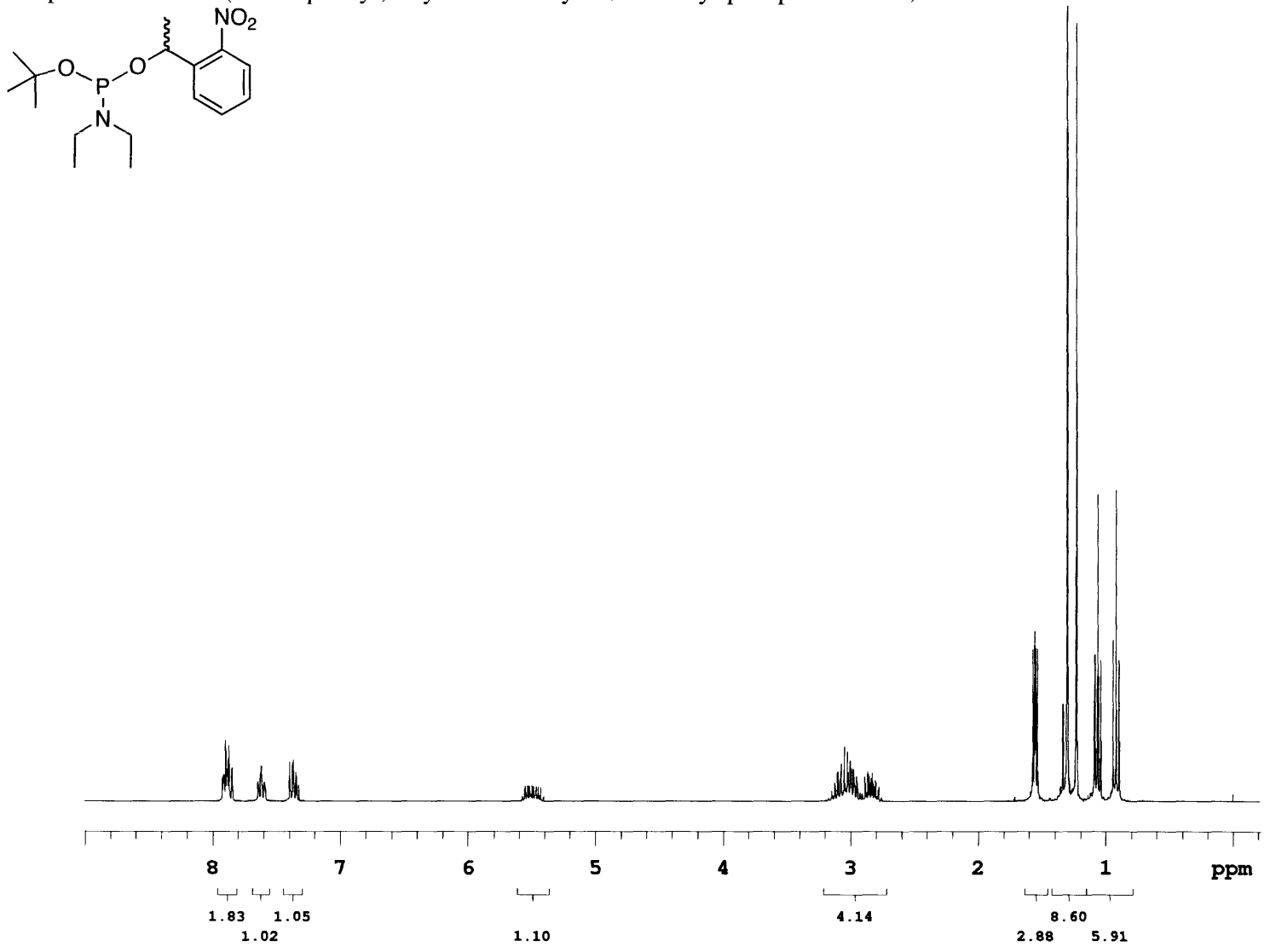

4.2 ^{13}C spectrum of of *O*-1-(2-nitrophenyl)ethyl-*O'*-tertbutyl-*N,N*-diethyl phosphoramidite, **24**.

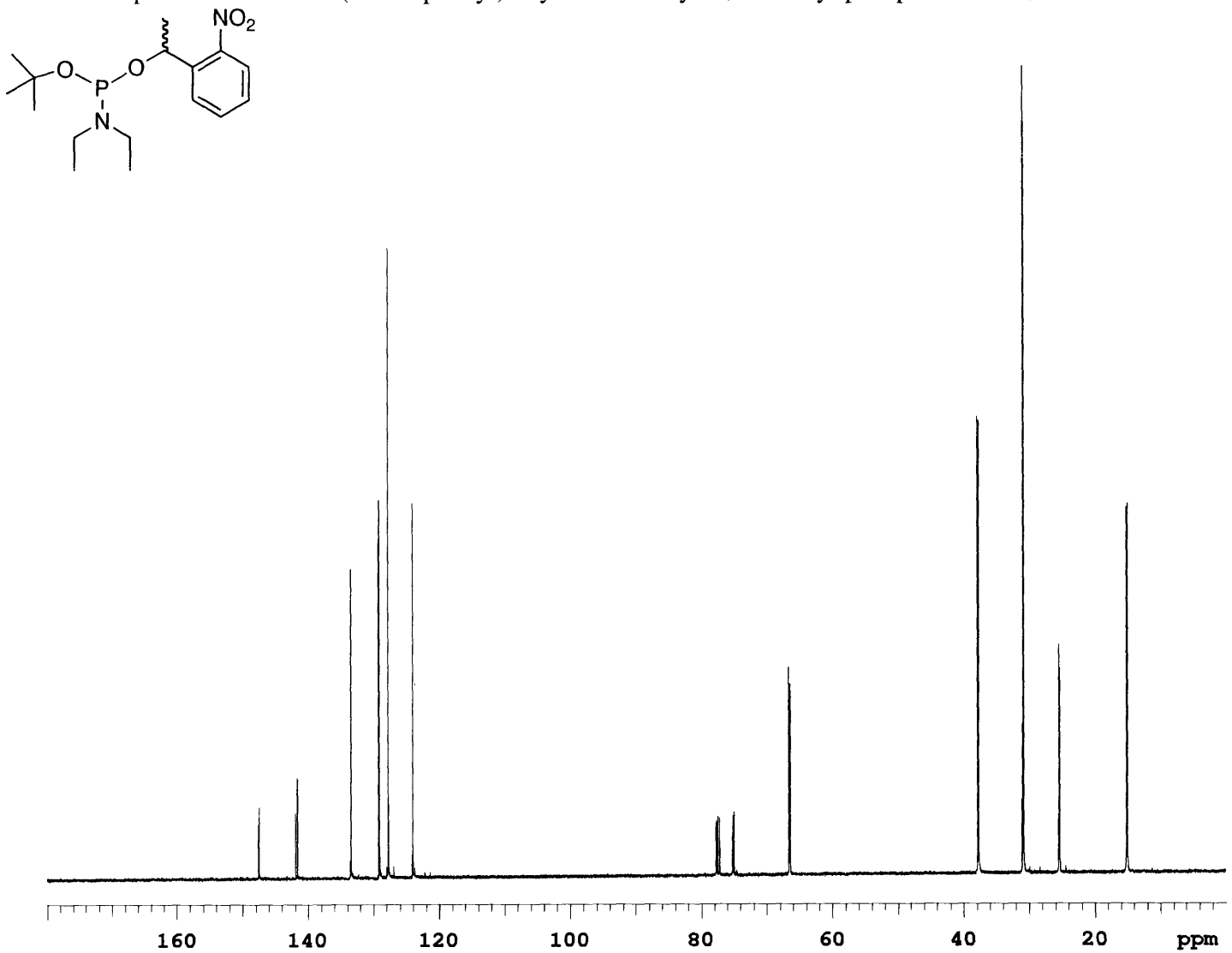

4.3 ^{31}P spectrum of of *O*-1-(2-nitrophenyl)ethyl-*O'*-tertbutyl-*N,N*-diethyl phosphoramidite, **24**.

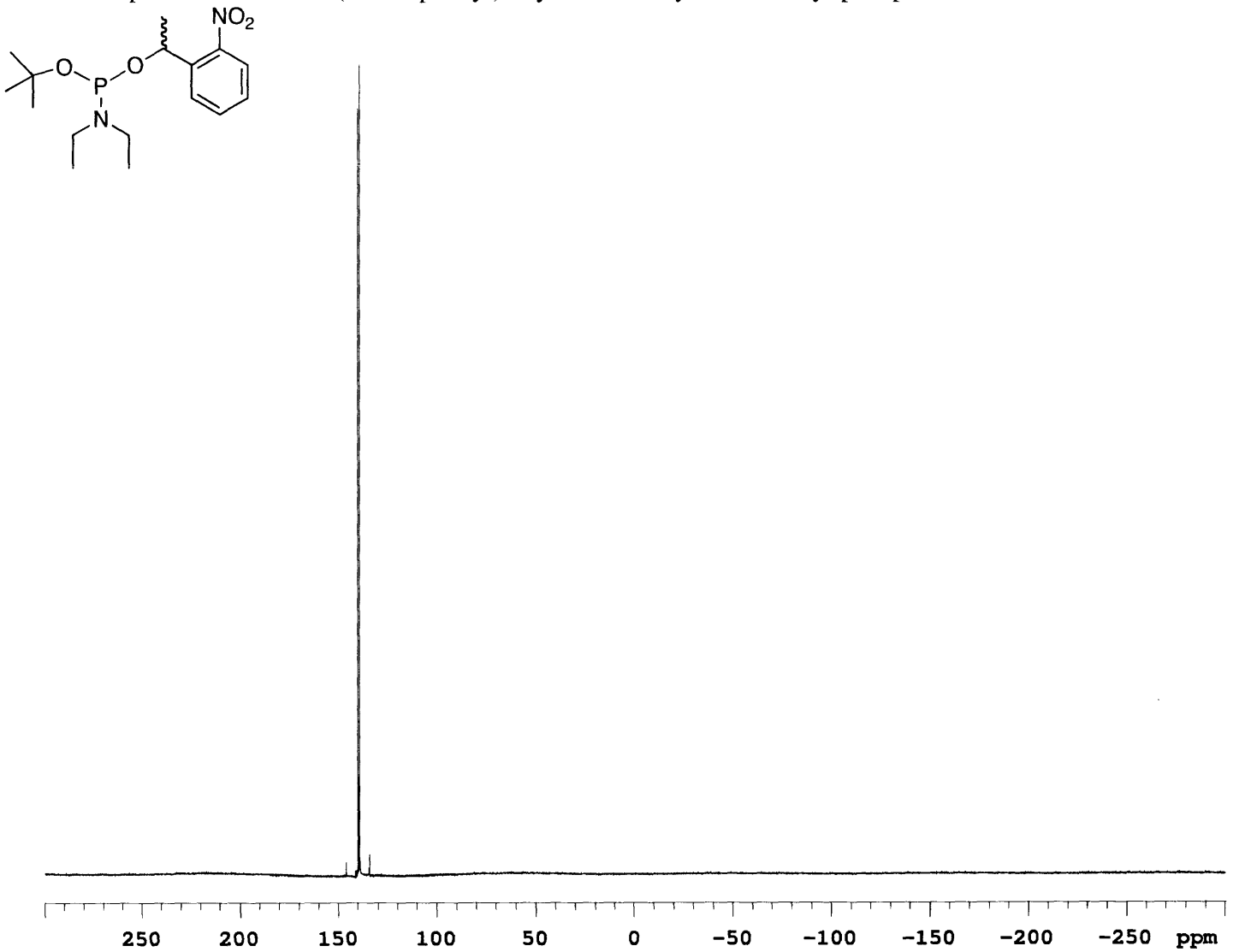

4.4 ^{1}H spectrum of N^{α}-4-pentenoyl-*O*-tert-butyl-L-serine, **28a**.

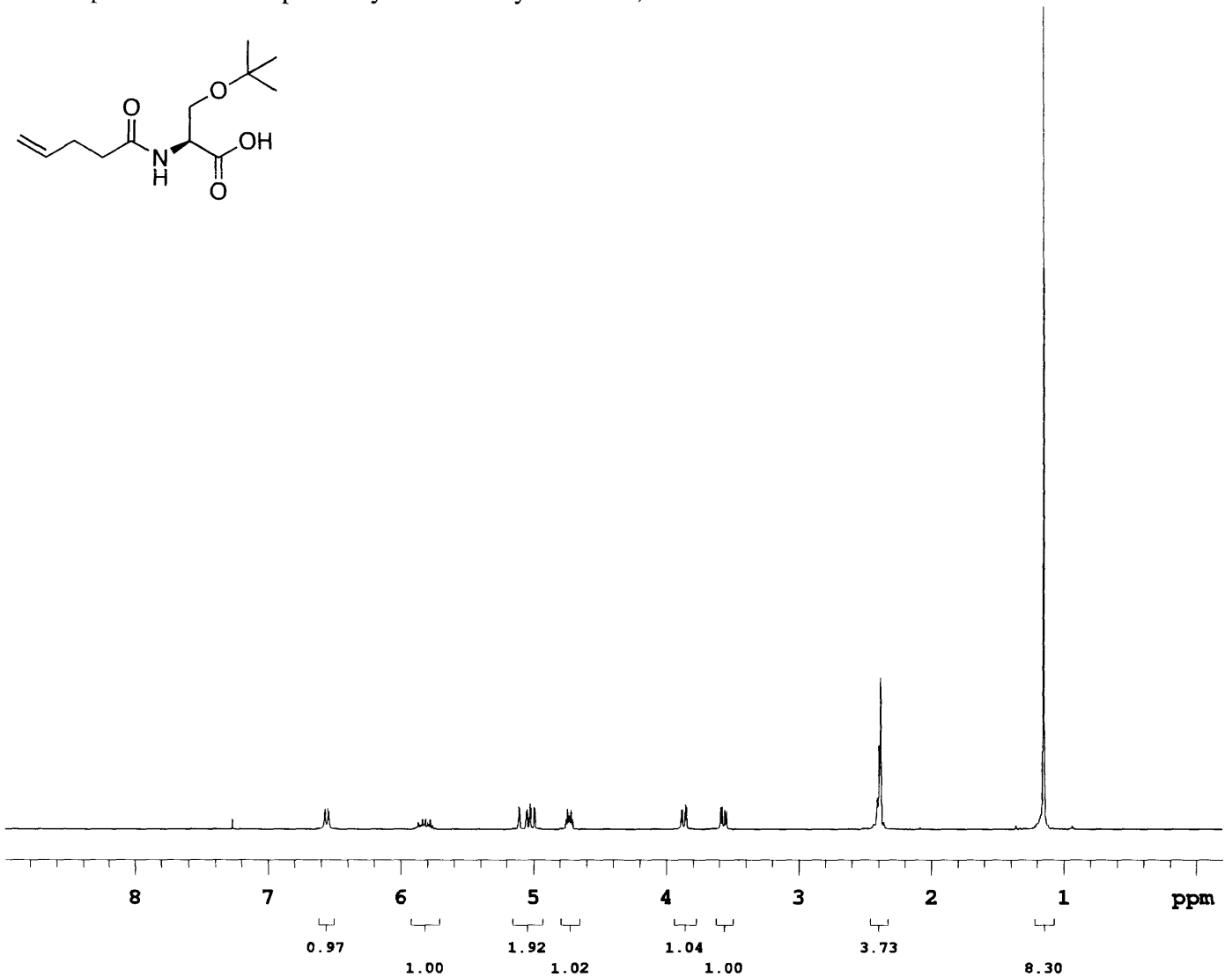

4.5 ^{13}C spectrum of N^{α}-4-pentenoyl-*O*-tert-butyl-L-serine, **28a**.

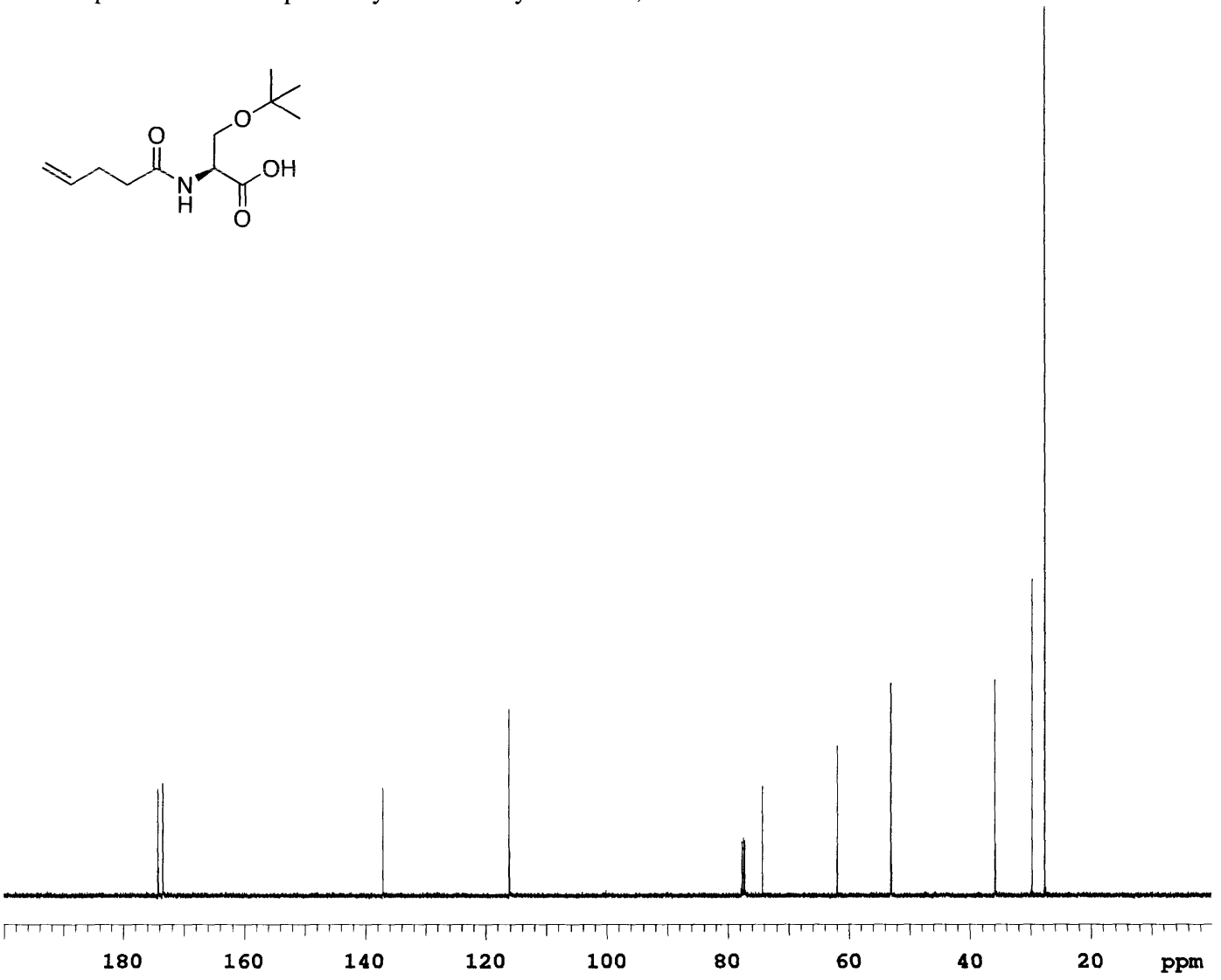

4.6 ^{1}H spectrum of N^{α}-4-pentenoyl-*O*-tert-butyl-L-serine cyanomethyl ester, **29a**.

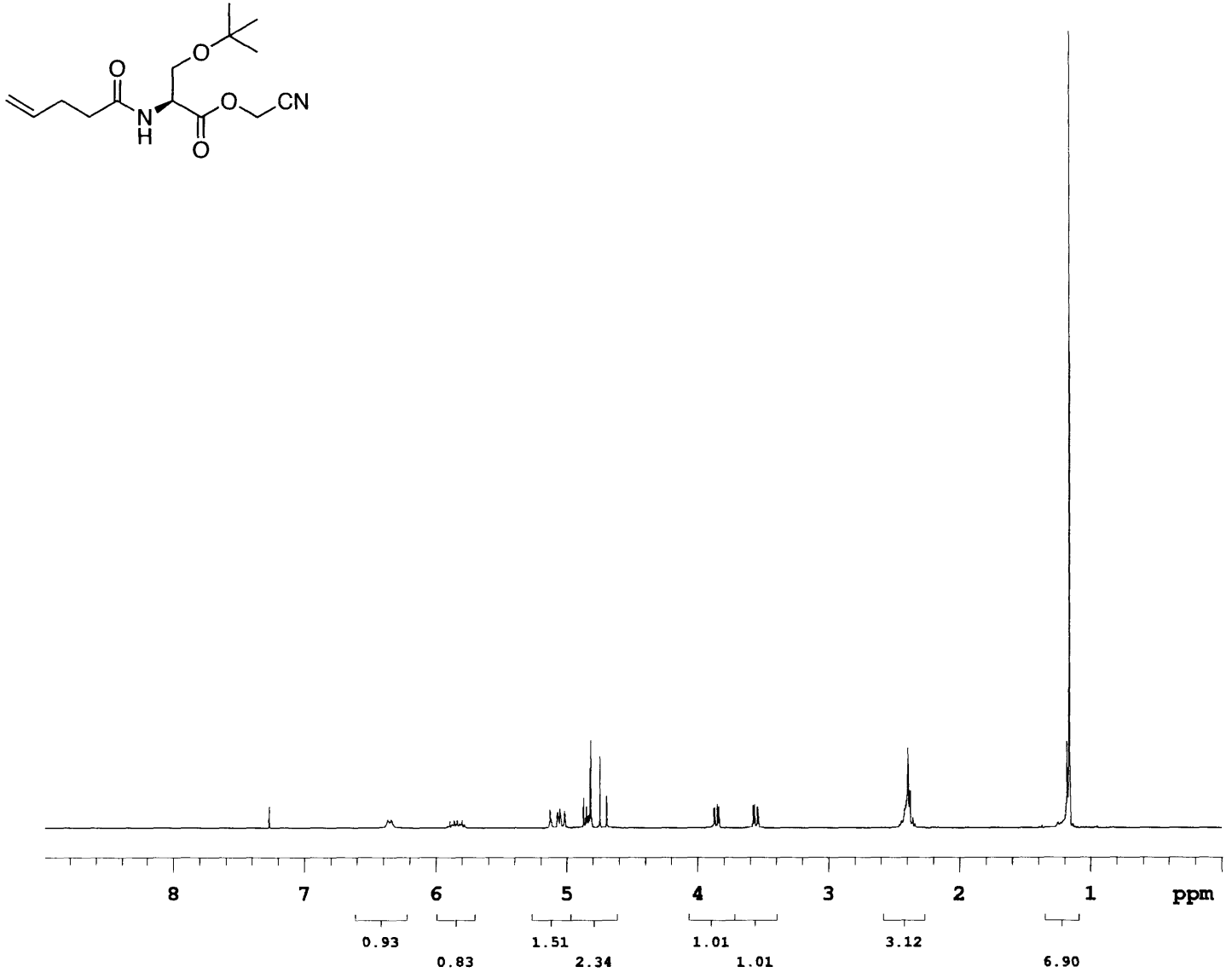

4.7 ^{13}C spectrum of N^{α}-4-pentenoyl-*O*-tert-butyl-L-serine cyanomethyl ester, **29a**.

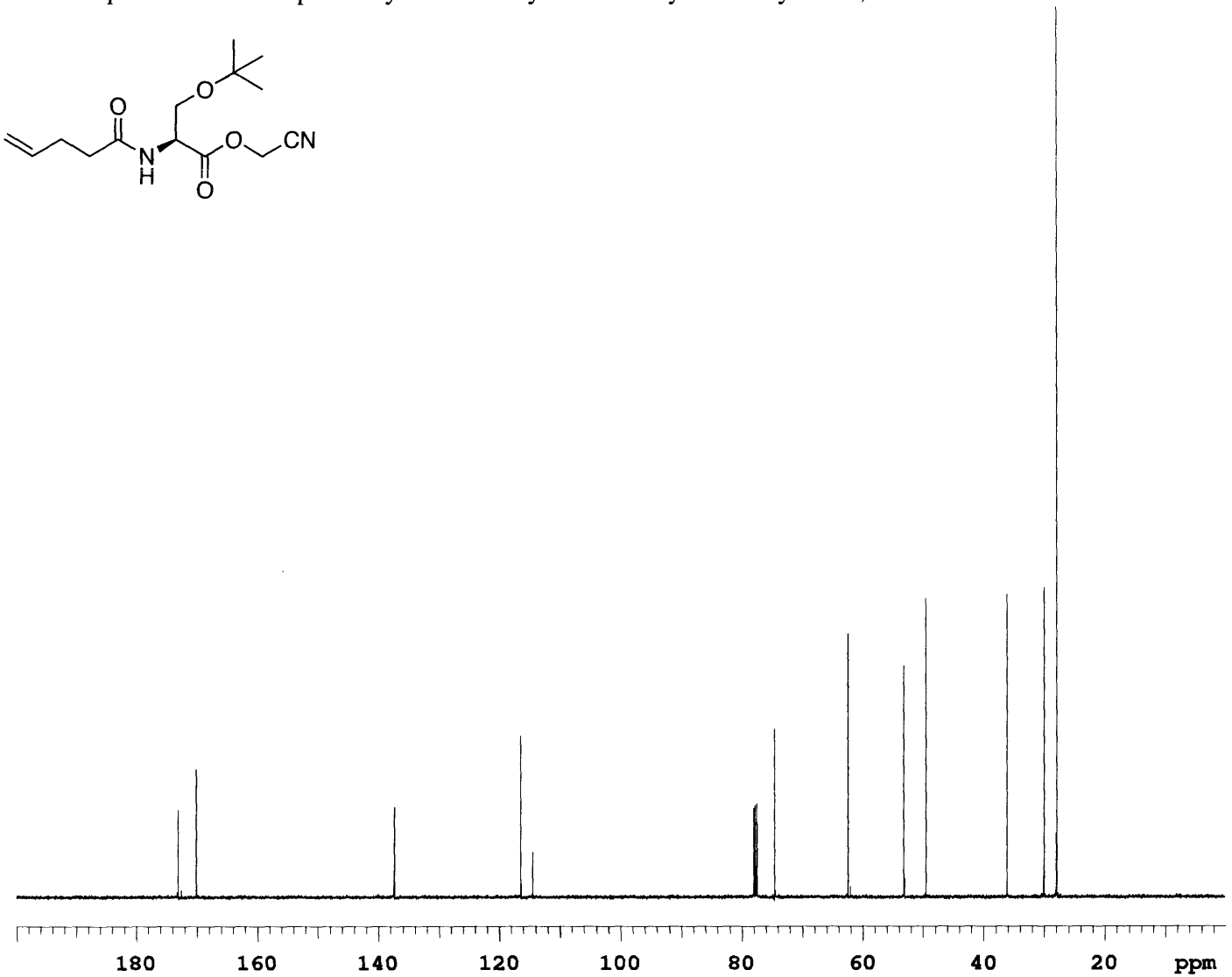

4.8 ^{1}H spectrum of N^{α}-4-pentenoyl-L-serine cyanomethyl ester, **30a**.

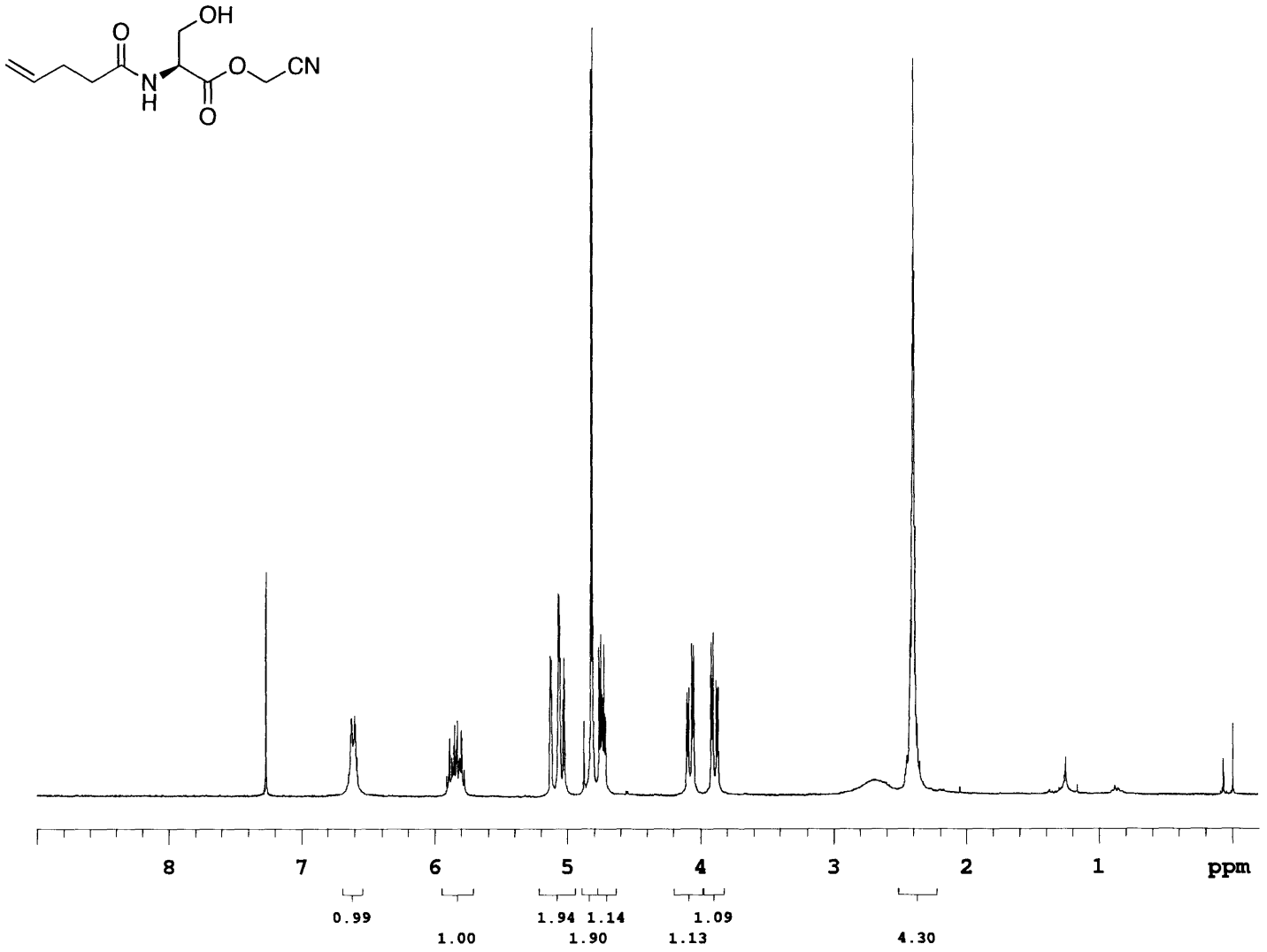

4.9 ^{13}C spectrum of N^{α}-4-pentenoyl-L-serine cyanomethyl ester, **30a**.

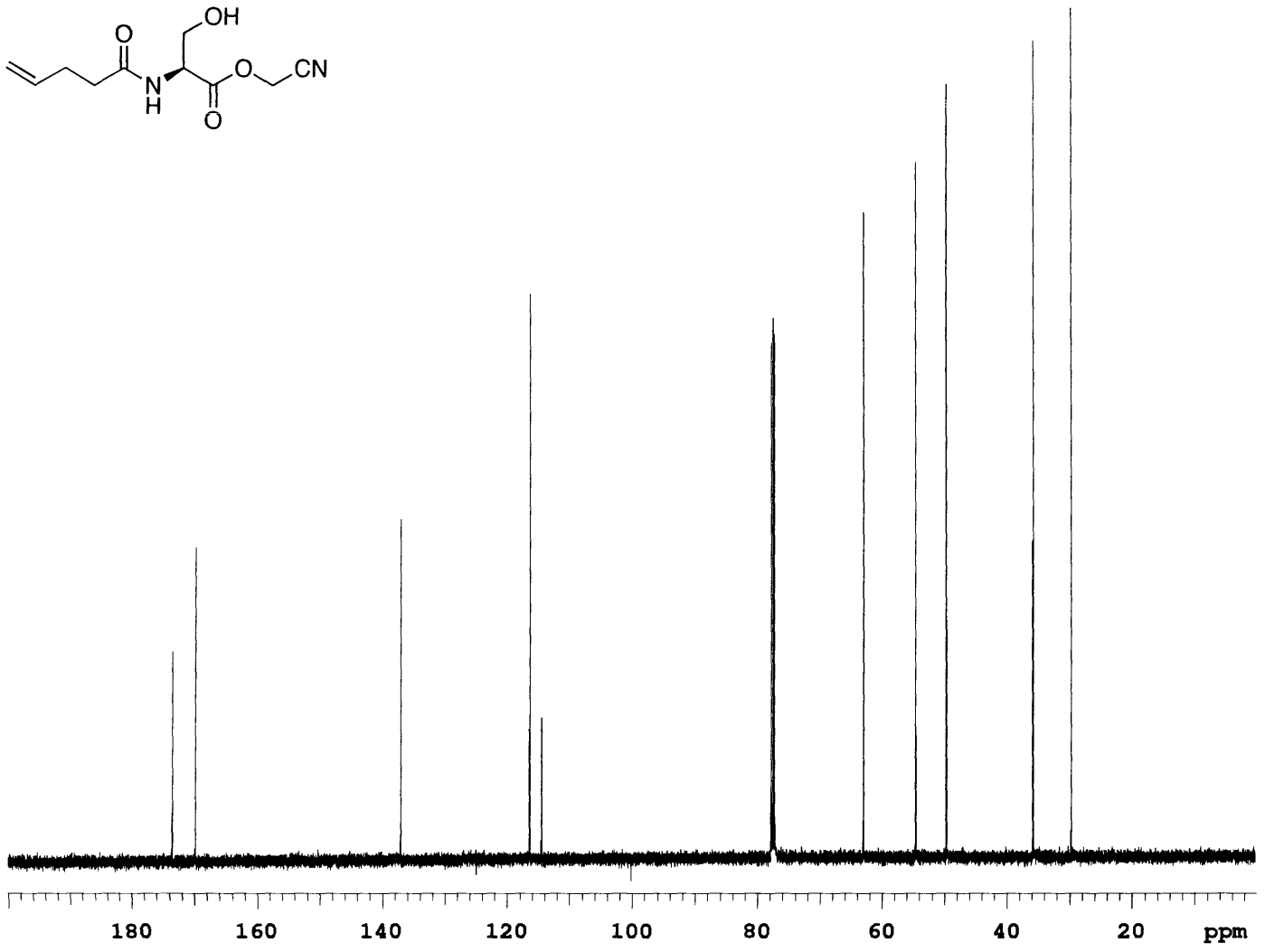

4.10 ^{1}H spectrum of N^{α}-4-pentenoyl-L-serine-OH, **34**.

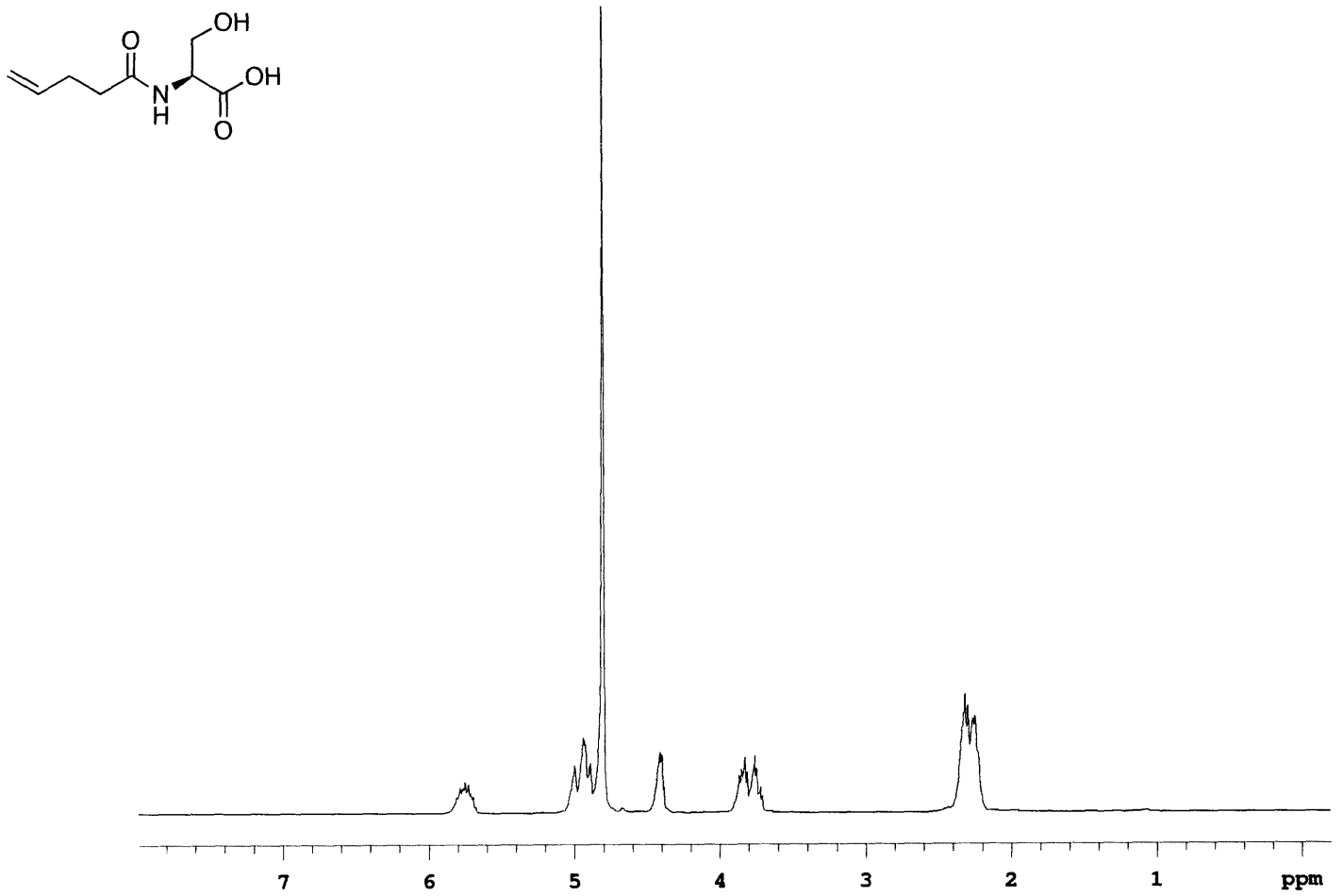

4.11 ^{1}H spectrum of N^{α}-4-pentenoyl-L-serine cyanomethyl ester, **30a**.

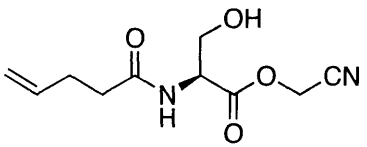

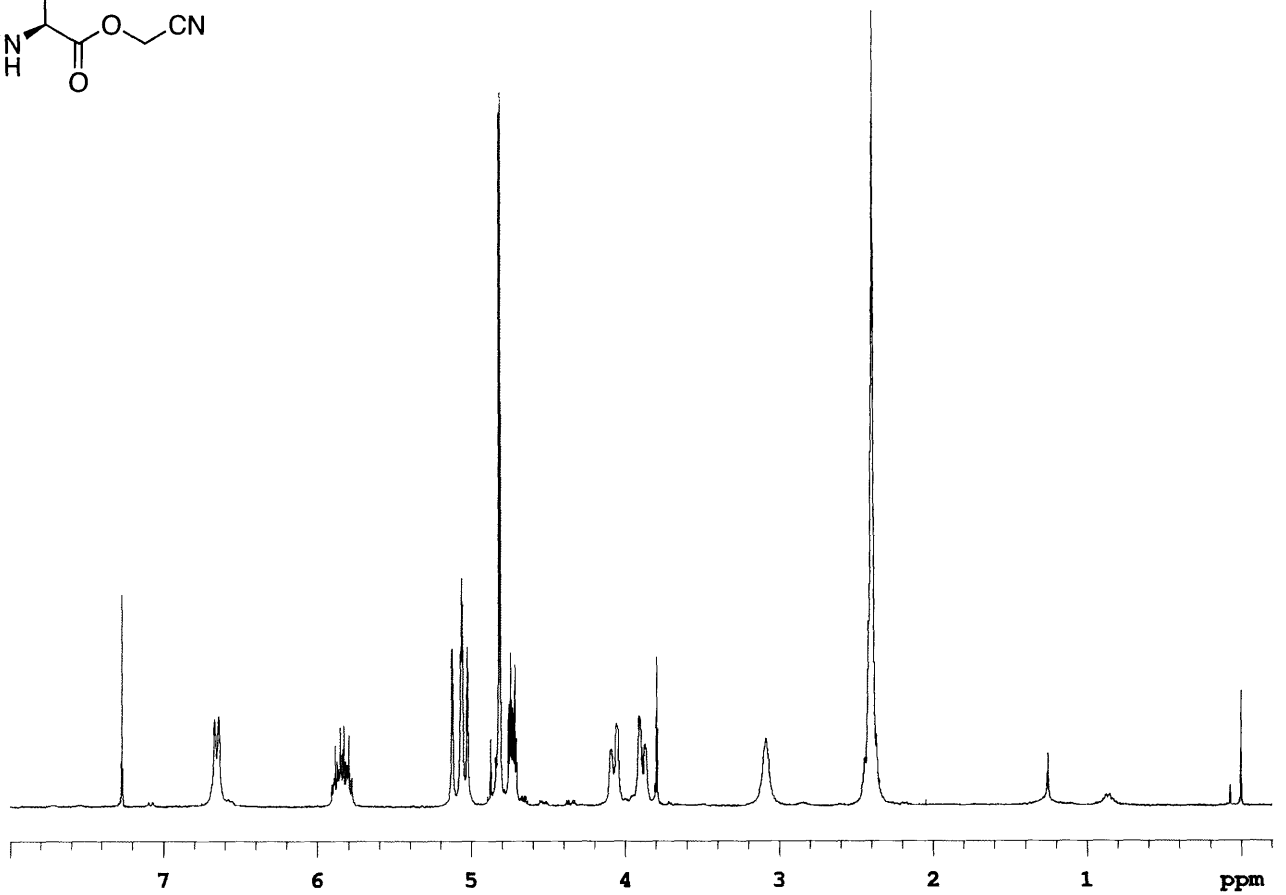

4.12 ^{1}H spectrum of N^{α}-4-pentenoyl-phospho(nitrophenylethyl)-L-serine cyanomethyl ester, **32a**.

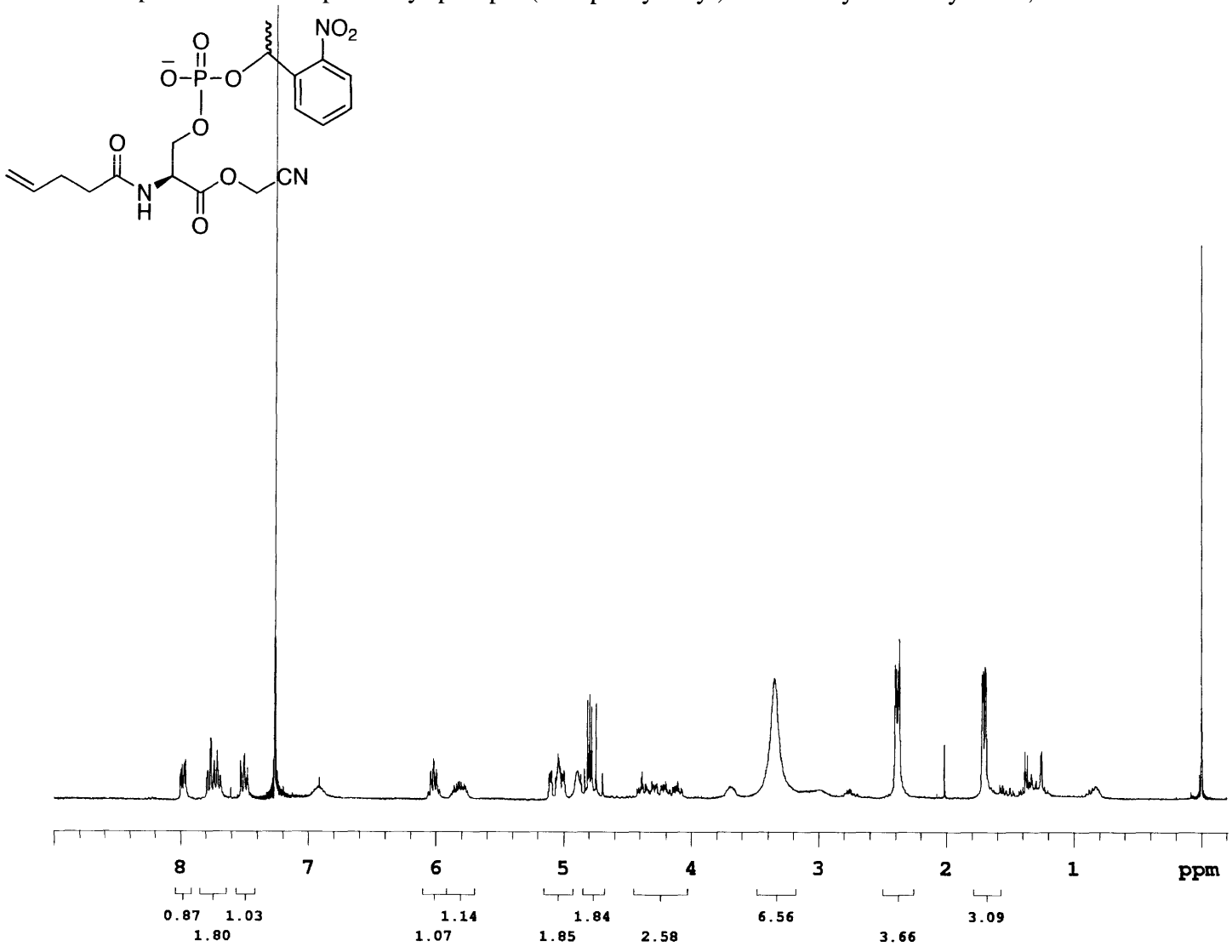

4.13 ^{13}C spectrum of N^{α}-4-pentenoyl-phospho(nitrophenylethyl)-L-serine cyanomethyl ester, **32a**.

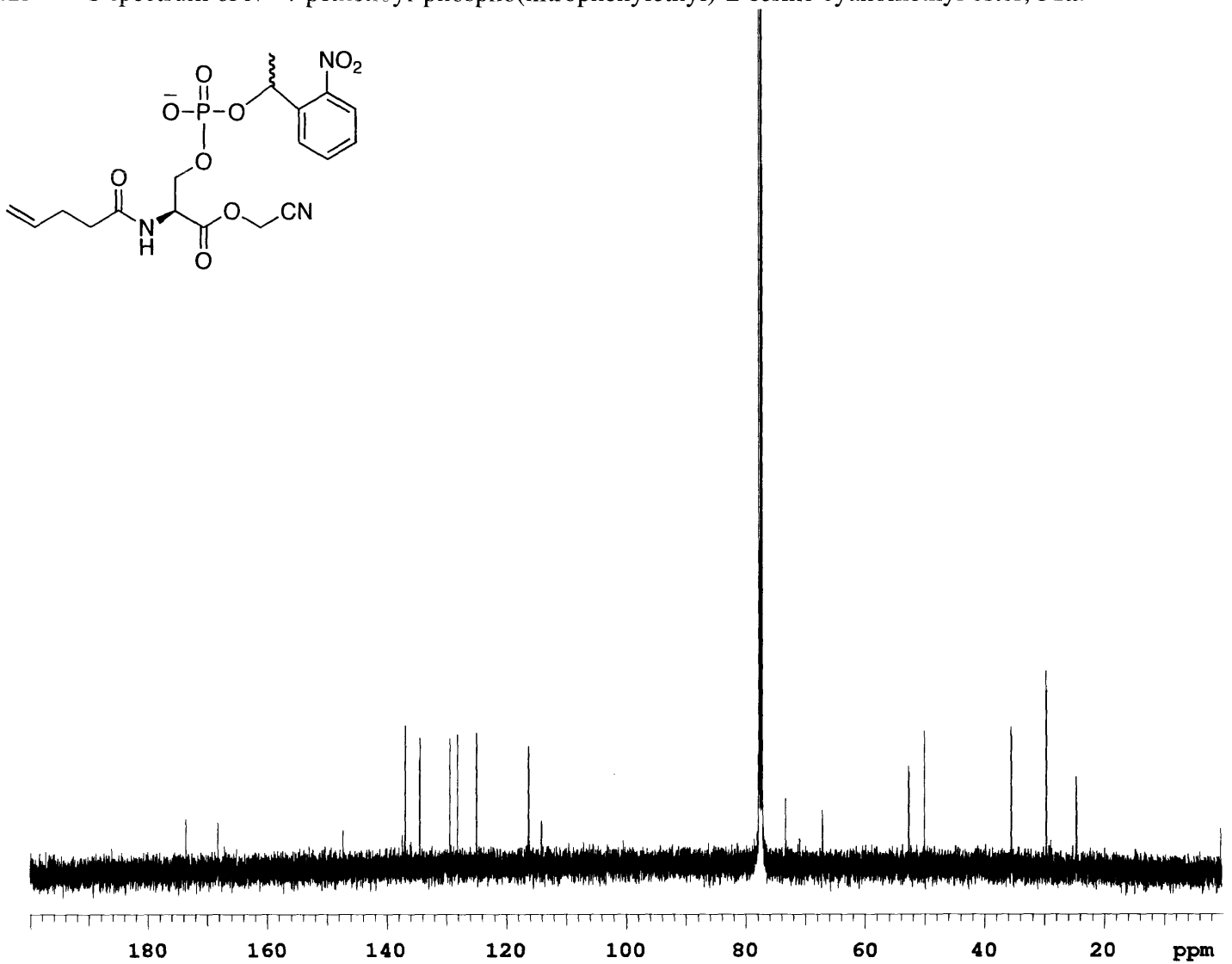

4.14 ^{31}P spectrum of N^{α}-4-pentenoyl-phospho(nitrophenylethyl)-L-serinc cyanomethyl ester, **32a**.

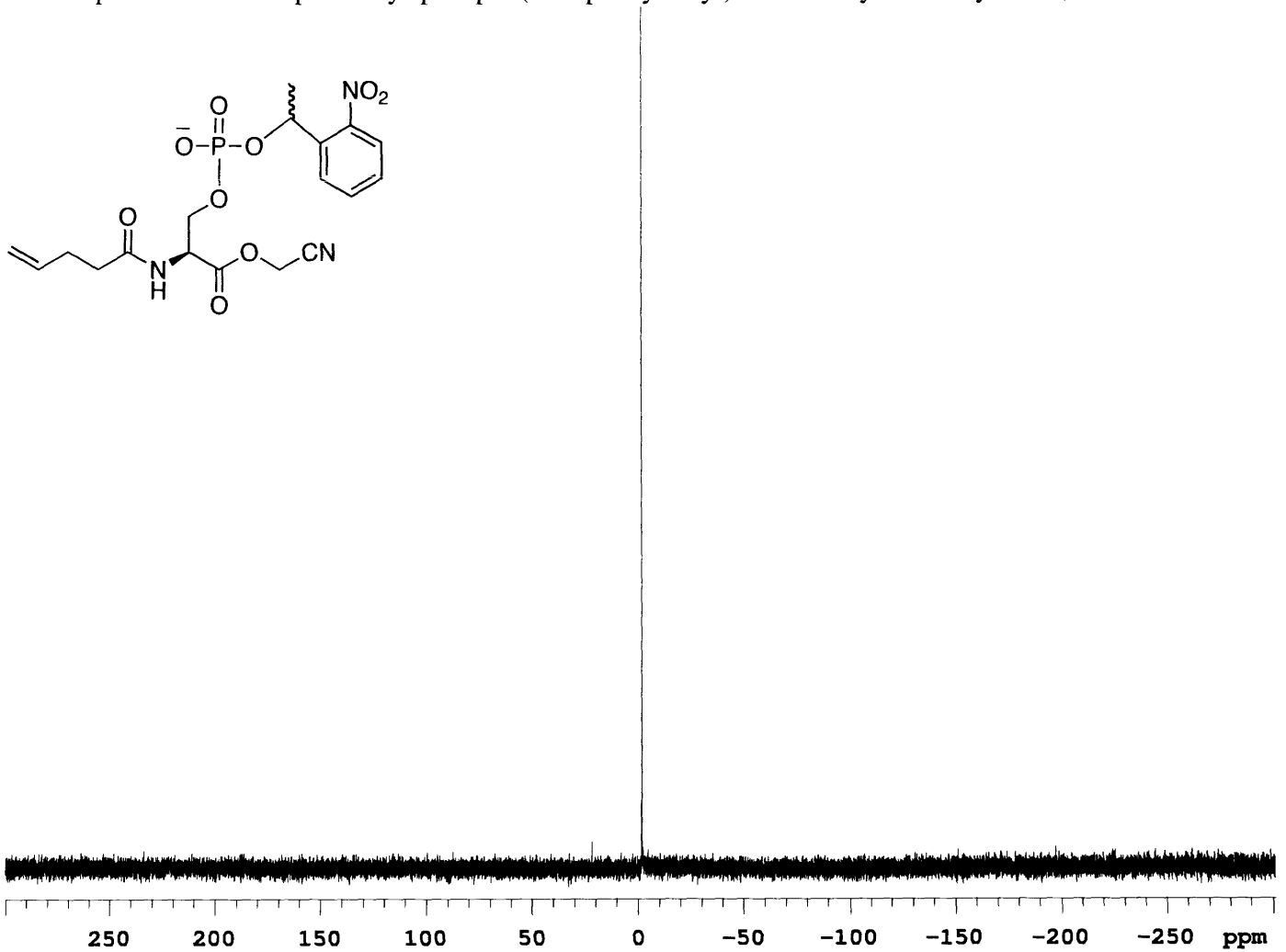

4.15 ^{1}H spectrum of N^{α}-4-pentenoyl-*O*-tert-butyl-L-threonine, **28b**.

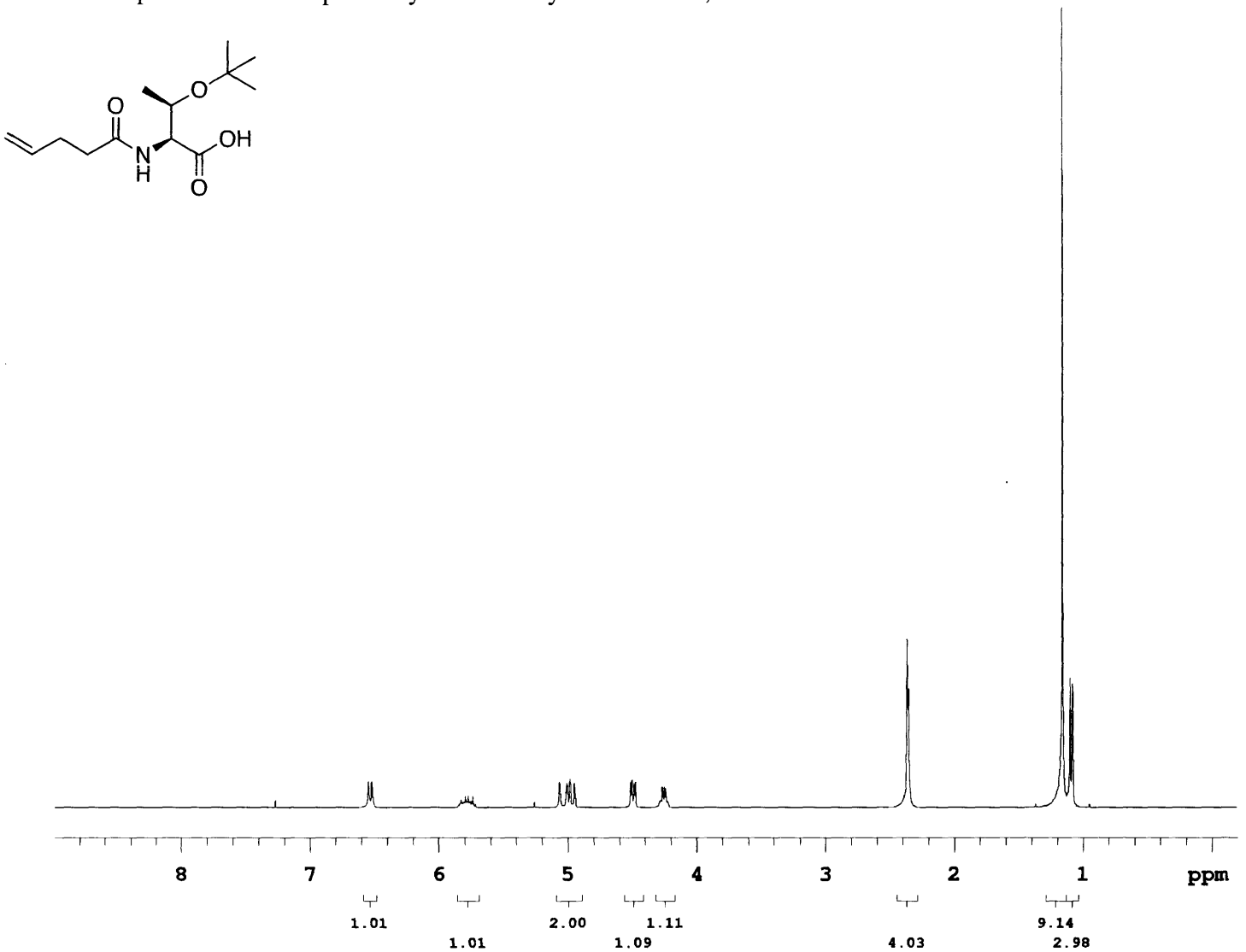

4.16 ^{13}C spectrum of N^{α}-4-pentenoyl-*O*-tert-butyl-L-threonine, **28b**.

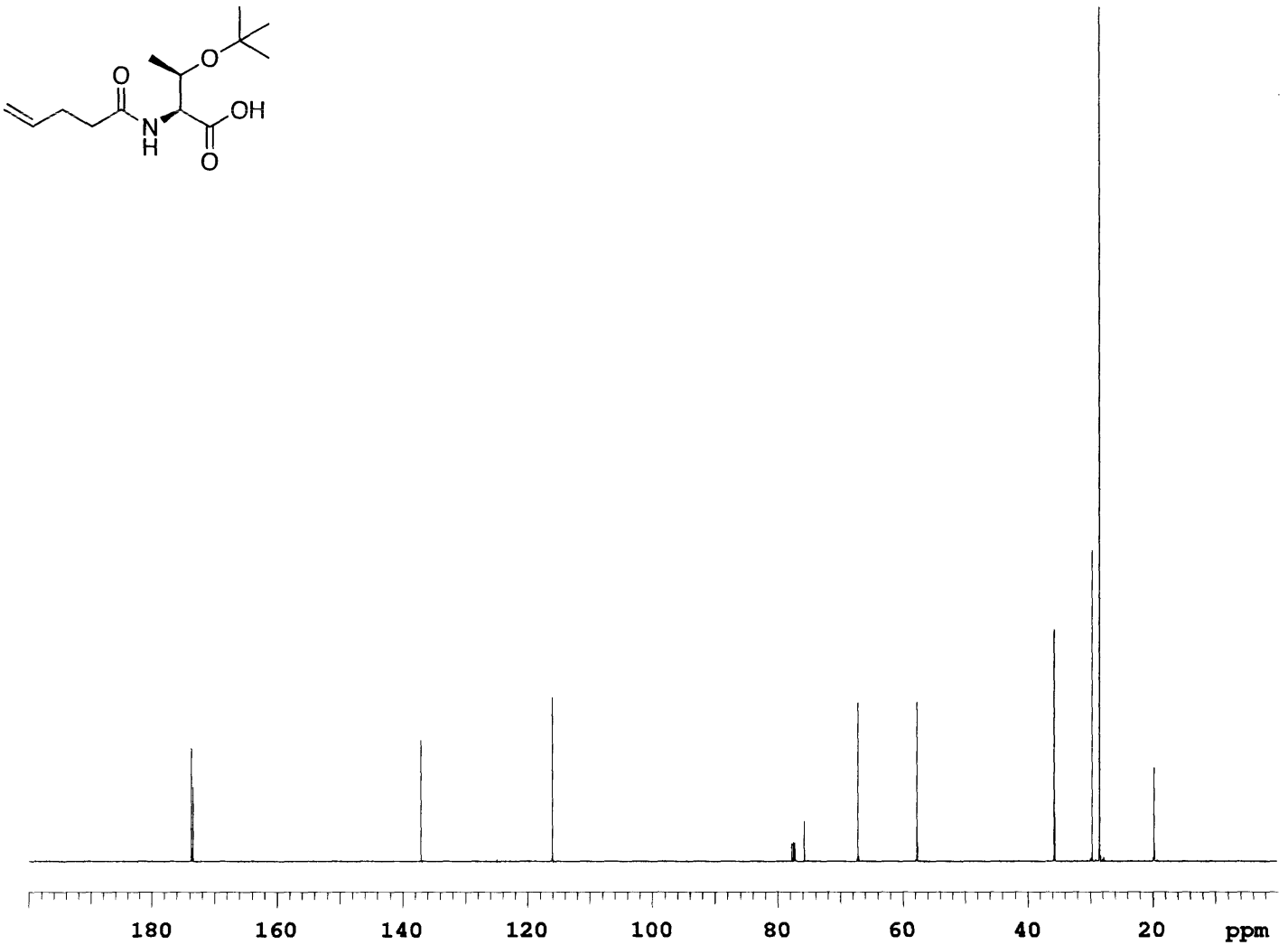

4.17 ^{1}H spectrum of N^{α}-4-pentenoyl-*O*-tert-butyl-L-threonine cyanomethyl ester, **29b**.

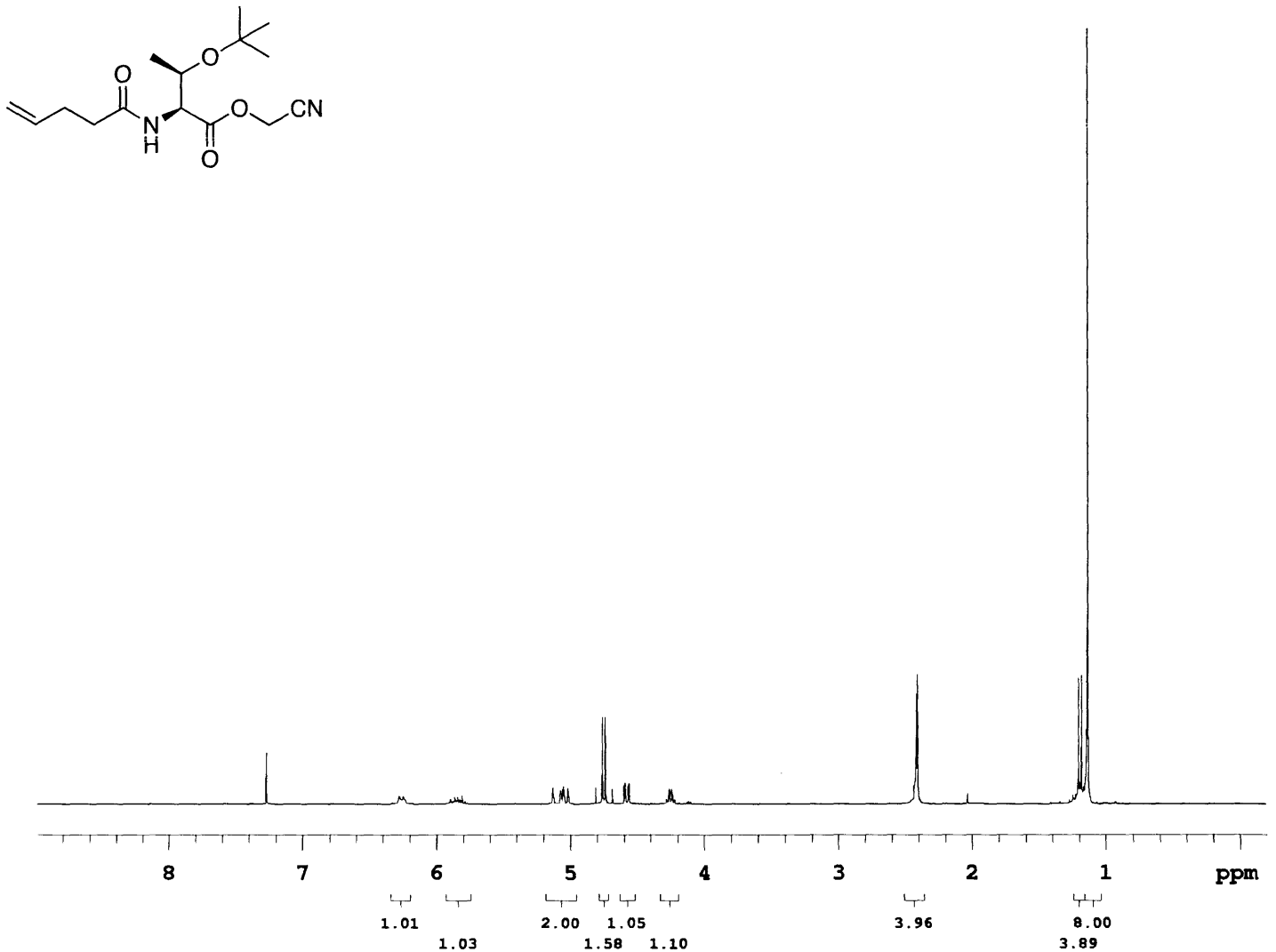

4.18 ^{13}C spectrum of N^{α}-4-pentenoyl-*O*-tert-butyl-L-threonine cyanomethyl ester, **29b**.

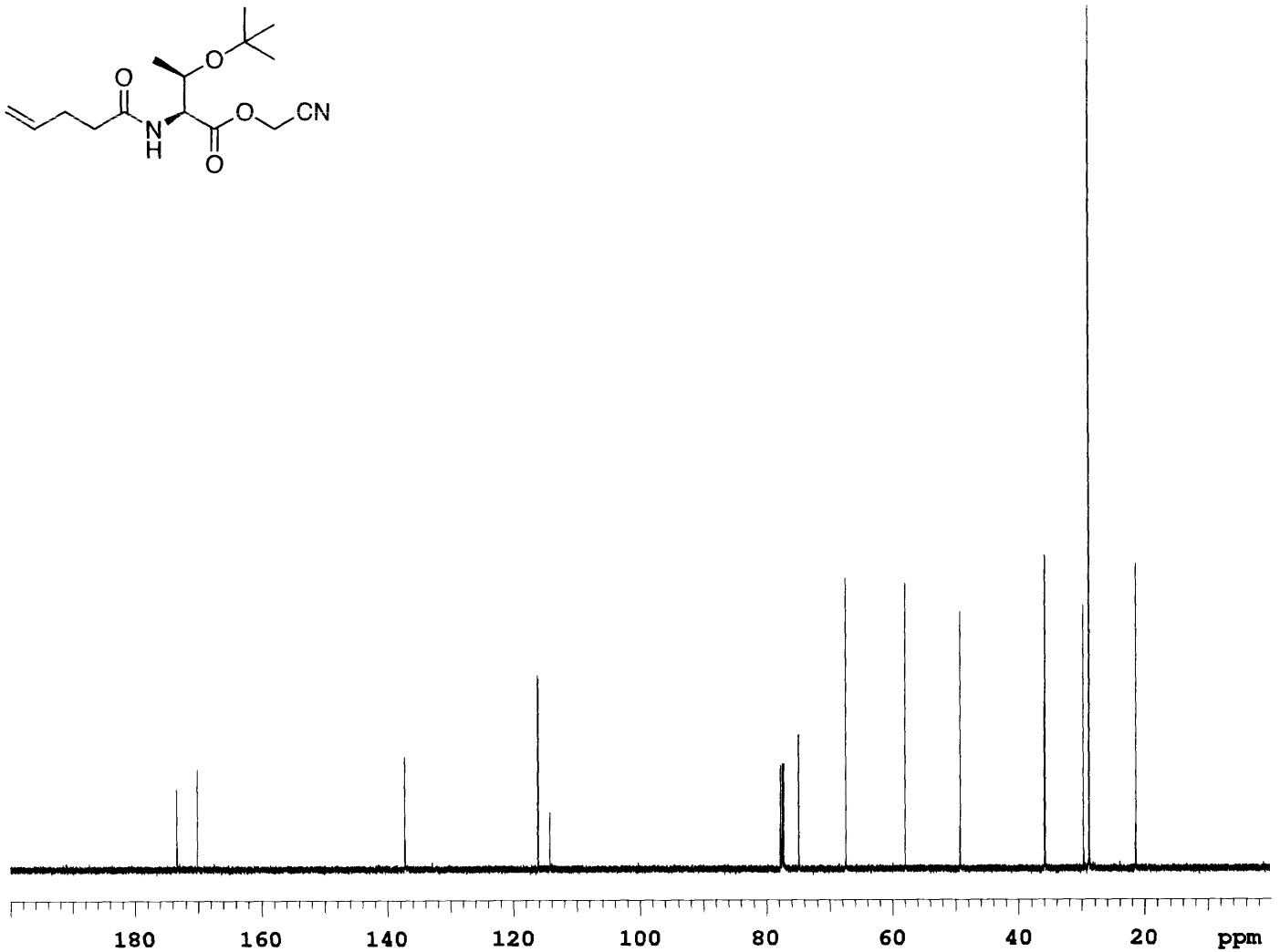

4.19 ^{1}H spectrum of N^{α}-4-pentenoyl-L-threonine cyanomethyl ester, **30b**.

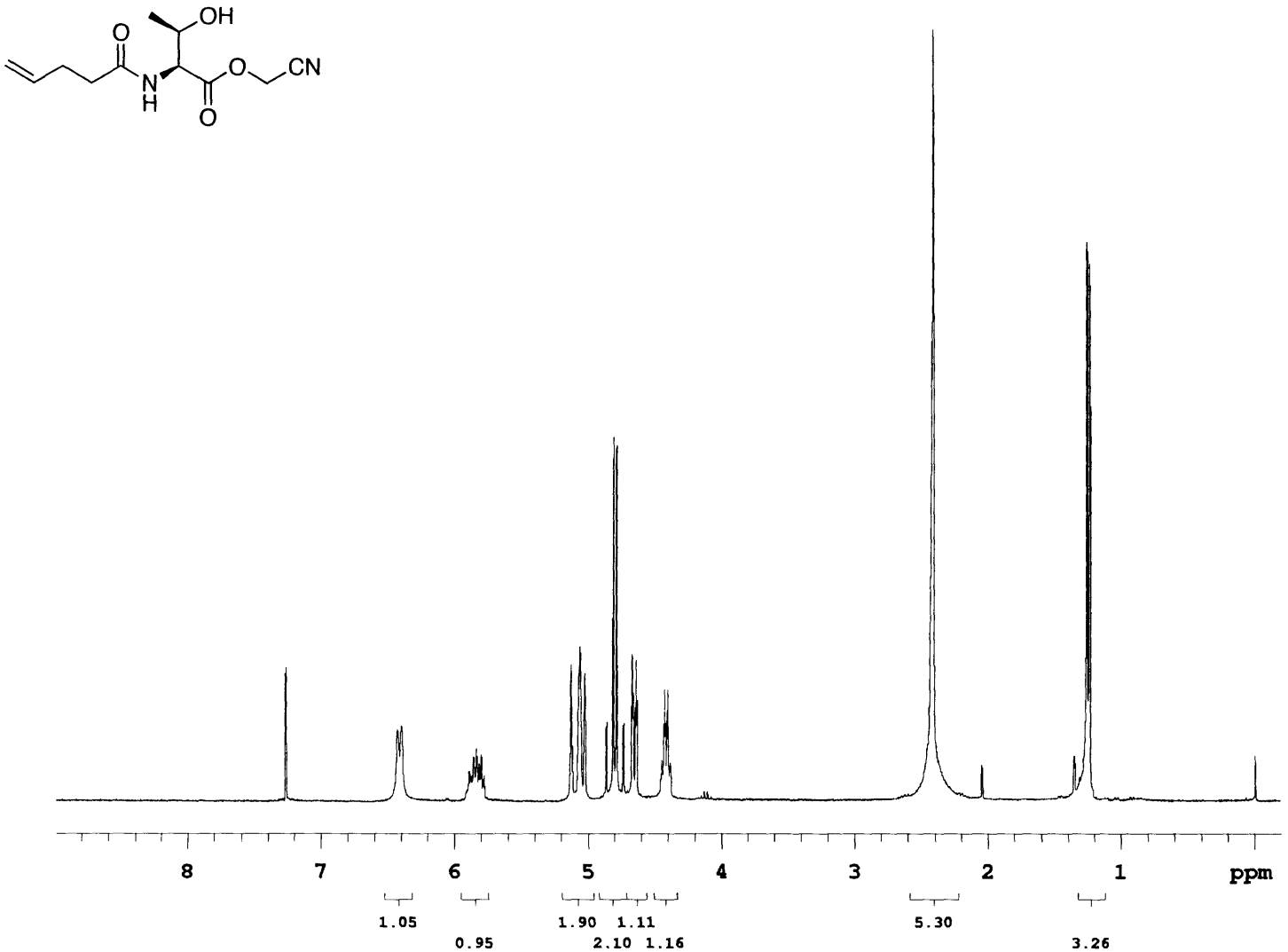

4.20 ^{13}C spectrum of N^{α}-4-pentenoyl-L-threonine cyanomethyl ester, **30b**.

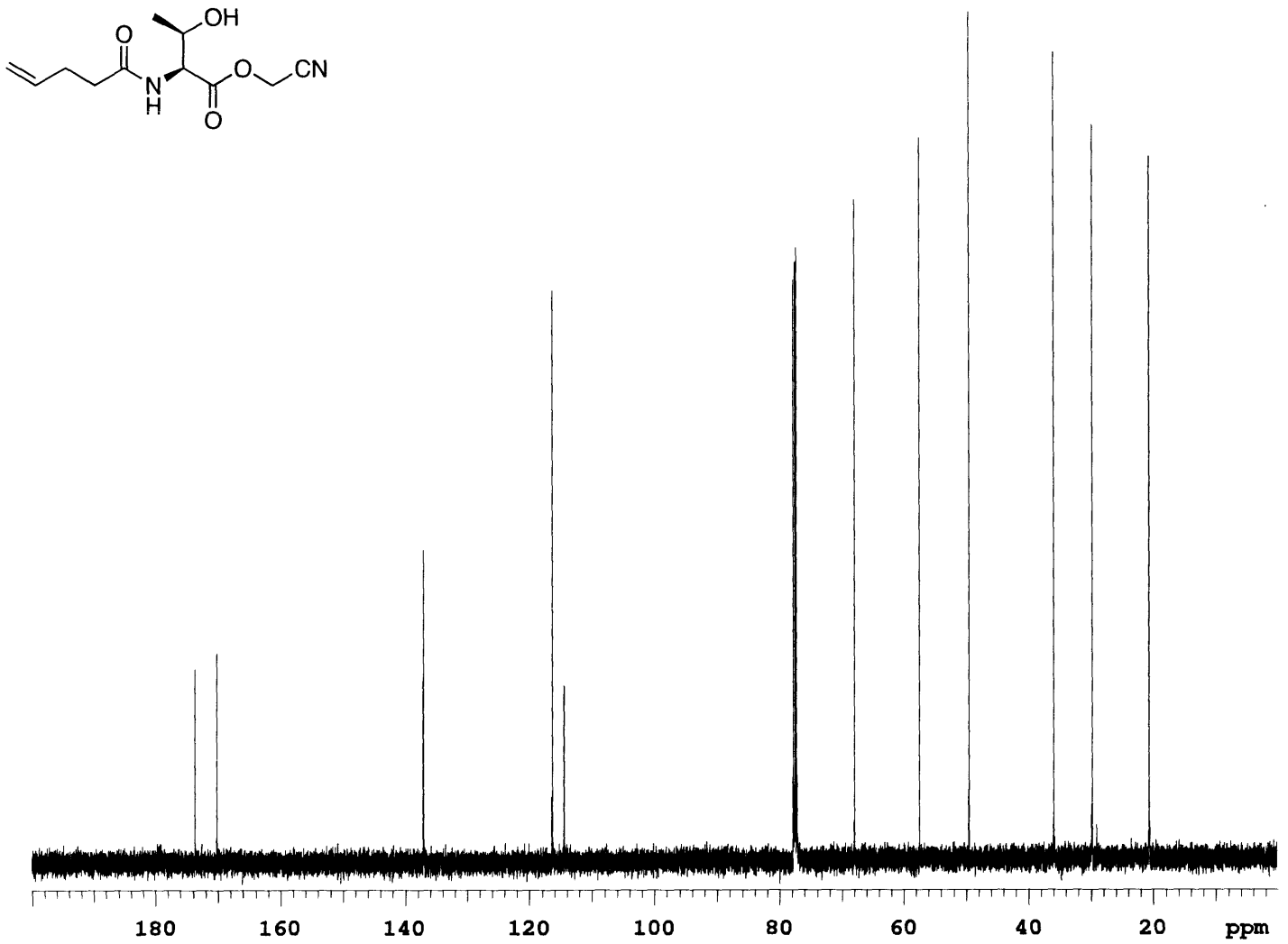

4.21 ^{1}H spectrum of N^{α}-4-pentenoyl-phospho(nitrophenylethyl)-L-threonine cyanomethyl ester, **32b**.

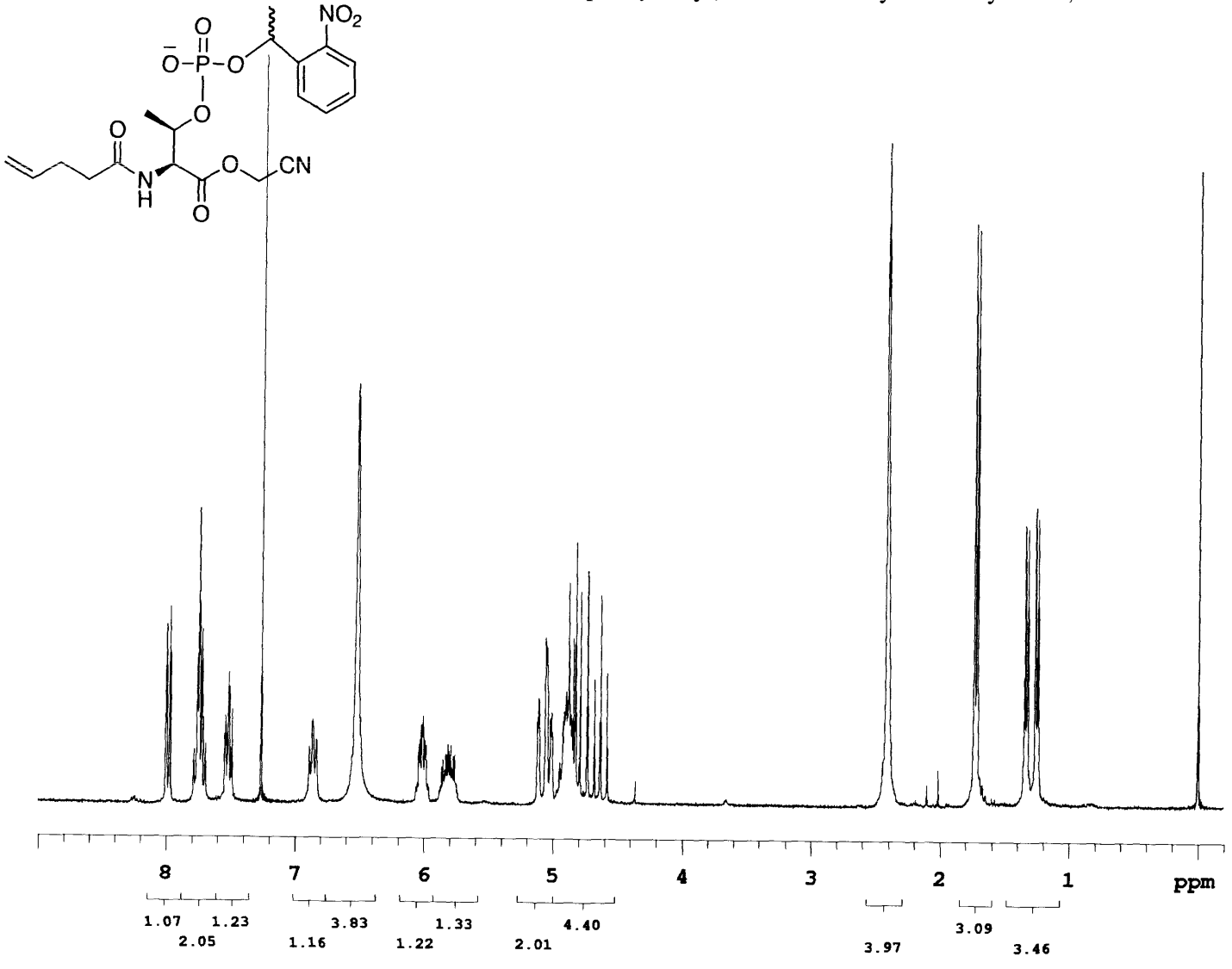

4.22 ^{13}C spectrum of N^{α}-4-pentenoyl-phospho(nitrophenylethyl)-L-threonine cyanomethyl ester, **32b**.

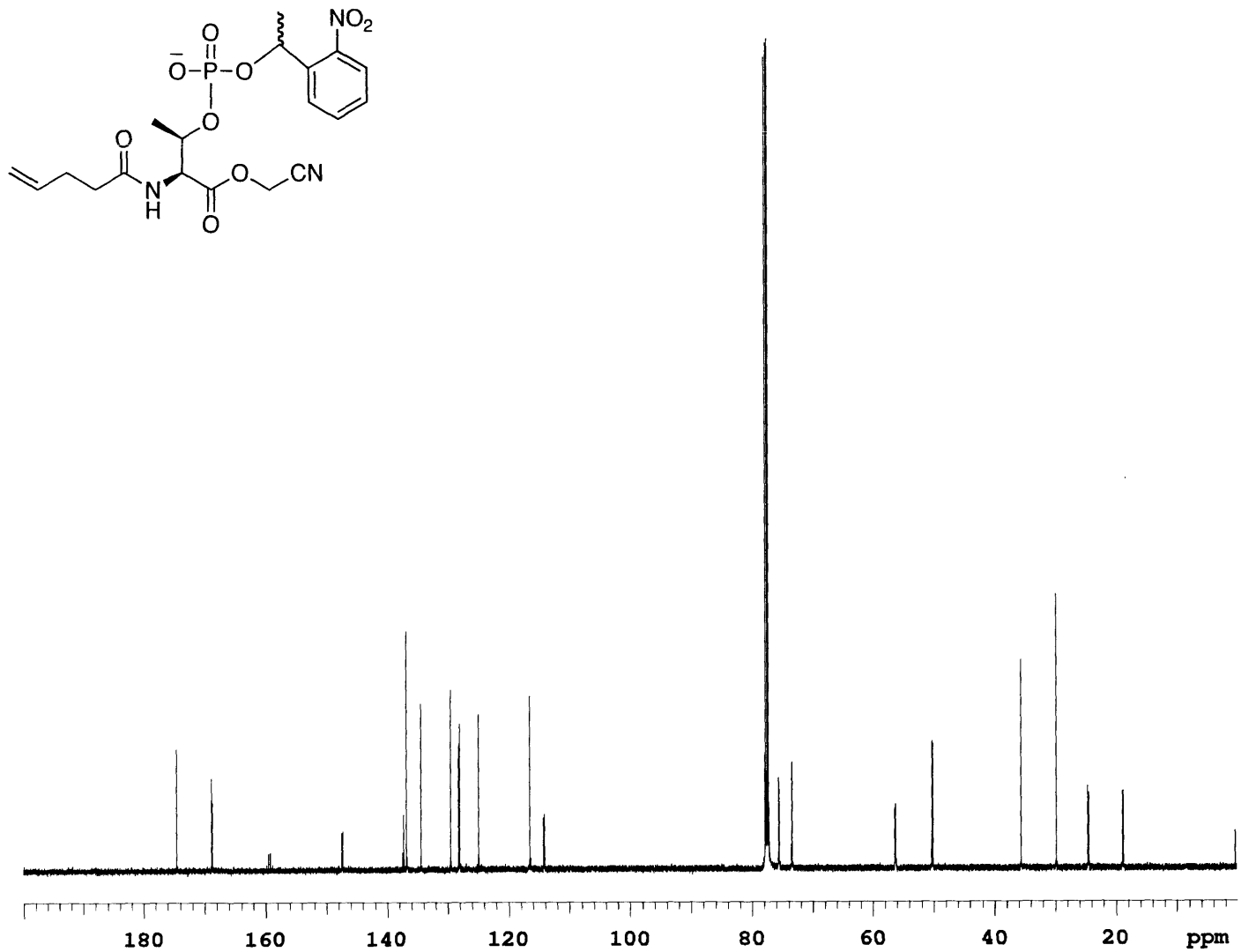

4.23 ^{31}P spectrum of N^{α}-4-pentenoyl-phospho(nitrophenylethyl)-L-threonine cyanomethyl ester, **32b**.

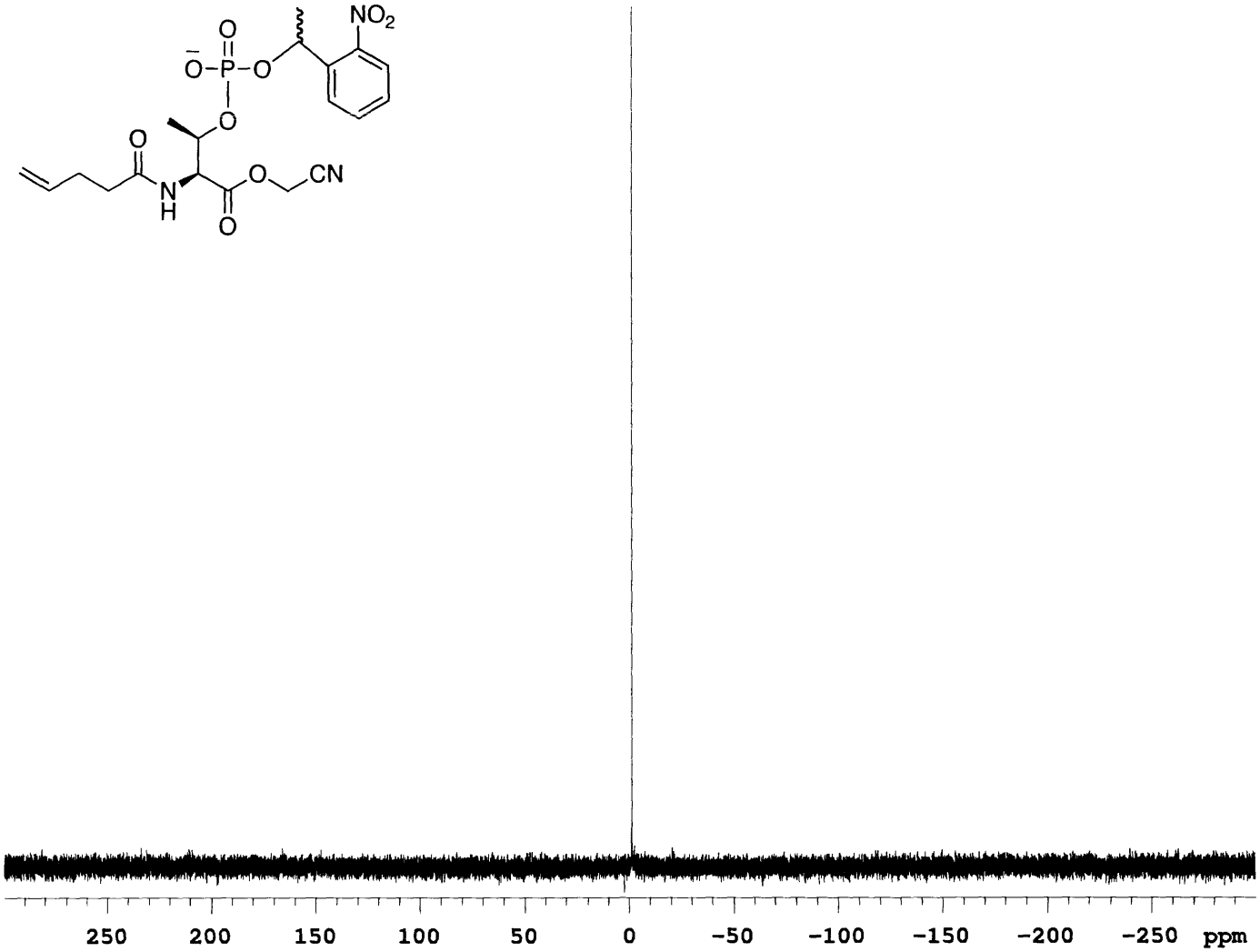

Deborah Maria Rothman

Education

2000-2005 — ***Massachusetts Institute of Technology*** — ***Cambridge, MA***

- Ph. D. candidate in Organic Chemistry, Spring 2005
- Advisor: Dr. Barbara Imperiali
- Thesis Title: "Caged Phosphopeptides and Phosphoproteins: Agents in Unraveling Complex Biological Pathways"

1996-2000 — ***University of Chicago*** — ***Chicago, IL***

- S. B. in Biochemistry, A. B. in Biology
- General Honors

Experience

2001-2005 — ***Research Assistant: Organic Chemistry***

Massachusetts Institute of Technology

- Developed chemical methods for the synthesis of caged phosphoserine peptides and proteins.
- Characterized these photochemical probes and used them in cell signaling assays.
- Instigated the caged phospho-amino acids project in the research group; established techniques specific to the project in the lab and instructed new colleagues.
- Collaborative effort with Dougherty Lab at *California Institute of Technology*, Fall 2003: Incorporated caged phospho-amino acids into full-length protein.

Spring 2001 — ***Teaching Assistant: Organic Chemistry***

- Intermediate organic chemistry lab, M. I. T., 5.32

Fall 2000 — ***Teaching Assistant: General Chemistry***

- Introductory chemistry lecture, M. I. T., 5.111

1998, 1999 — ***Summer Research Internship: Molecular Biology***

National Institutes of Health

- Determined the sub-cellular localization of FGFR-2 and Dachsund proteins in various mammalian cell lines.
- Guided project toward biochemical assays of protein interactions.

Honors and Affiliations

- Poster Prize awarded at M. I. T. Computational and Systems Biology Initiative Spring Workshop, *2003*
- Travel Grant for Summer 2004 awarded by M. I. T. Computational and Systems Biology Initiative, *2003*
- Poster Prize (1st place) awarded at M. I. T. Computational and Systems Biology Symposium, *2005*
- American Chemical Society, *2002-present*
- Computational and Systems Biology Initiative, M. I. T., *2002-present*
- American Peptide Society, *2005*

Deborah Maria Rothman

Publications

- Rothman, D. M., Petersson, E. J., Vázquez, M. E., Brandt, G. S., Dougherty, D. A., Imperiali, B. Caged Phosphoproteins. *Journal of the American Chemical Society*, **2005**, *127(3)*, 846-847.
- Nguyen, A.,* Rothman, D. M.,* Stehn, J., Imperiali, B., and Yaffe, M. B. Caged Phosphopeptides Reveal a Temporal Role for 14-3-3 in G1 Arrest and S-phase Checkpoint Function. *Nature Biotechnology*, **2004**, *22(8)*, 993-1000.
- Vázquez, M. E., Rothman, D. M., Imperiali, B. A New Environment-sensitive Fluorescent Amino Acid for Fmoc-based Solid Phase Peptide Synthesis. *Organic Biolmolecular Chemistry*, **2004**, *2*, 1965-1966.
- Rothman, D. M., Vázquez, M. E., Vogel, E. M., and Imperiali, B. Caged Phospho-Amino Acid Building Blocks For Solid Phase Peptide Synthesis. *Journal of Organic Chemistry*, **2003**, *68 (17)*, 6795-6798.
- Rothman, D. M., Vázquez, M. E., Vogel, E. M., and Imperiali, B. General Method for the Synthesis of Caged Phosphopeptides: Tools for the Exploration of Signal Transduction Pathways. *Organic Letters*, **2002**, *4(17)*, 2865-2868.

*These authors contributed equally to this work.

Presentations

- Rothman, D. M., Imperiali, B. "Caged Phosphoserine Peptides," Poster, 224th ACS National Meeting, Boston, MA, August 2002.
- Rothman, D. M., Imperiali, B. "Caged Phosphoserine Peptides and Proteins," Poster, CSBi Spring Workshop, Ogunquit, ME, April 2003.
- Rothman, D. M., Imperiali, B. "Caged Phosphoserine Peptides and Proteins," Poster, Northeast Student Chemistry Research Conference, Brookline, MA, April 2004.
- Rothman, D. M., Imperiali, B. "Caged Phosphoserine Peptides and Protiens," Poster, Gordon Research Conference in Bioorganic Chemistry, Andover, NH, June 2004.
- Rothman, D. M., Imperiali, B. "Caged Phosphoserine Peptides and Proteins," Poster, CSBi Symposium, Cambridge, MA, January 2005.
- Rothman, D. M., Imperiali, B. "Caged Phosphoserine Peptides and Proteins," Oral, Young Investigators' Mini-Symposium, American Peptide Society Symposium, San Diego, CA, June 2005.